Enhancement of alphavirus replication in mammalian cells at sub-physiological temperatures

Jinchao Guo

Submitted in accordance with requirements for the degree of Doctor of Philosophy

The University of Leeds

School of Molecular and Cellular Biology

Faculty of Biological Sciences

September 2021

The candidate confirms that the work submitted is his own and that appropriate credit has been given where reference has been made to the work of others.

Acknowledgement

I’d like to give biggest thanks to my dear supervisor Prof. Mark Harris for his excellent supervision in this project. Transferring to his laboratory is the most important and right choice I made in the past 4 years. His intelligence, knowledge, experience in virology, patience and kindness inspired me through my research and help me get through my four years PhD, especially in such a hard year of COVID-19. Without his scientific advice in this project and help in finance, this project will never be accomplished.

I would say thanks to all the past and present members of Garstang 8.61 and also the Virology research group for their support and advice. I would especially thank Yanni Gao, who is a former lab member and helped me start with my project quickly in this new laboratory. I would also want to thank Raymond Li, whom I asked a lot of questions and still happy to answer me patiently after he graduated. Thank you will also go to those who helped me in my project, which included but not limited to Carsten, Joe, Suki, Cayla, Anya, Seb and Upasana.

A big thank you to my family members, my mother, father and sister. Chatting with them helps me release the pressure from research, and they are forever supporting me whoever I am, I love them.

Finally I would like to acknowledge the Chinese Scholarship Council and the University of Leeds Scholarship for funding with this project and the hardship fund from the University of Leeds. I would also thank the Microbiology Society and Arbovirus meeting for providing me the opportunities to present my work there.

Abstract

Chikungunya virus (CHIKV) is a re-emerging Alphavirus that transmitted by mosquitoes and causes fever, rash, arthralgia. Currently there are no effective vaccines or antiviral agents against CHIKV, therefore it is important to understand the molecular details of CHIKV replication. In this regard the function of the Alphavirus unique domain (AUD) in the non-structural protein 3 (nsP3) remains enigmatic. Building on a previous study (Gao et al 2019), I generated a panel of mutants in a conserved and surface exposed cluster in the AUD and tested their replication phenotype in a CHIKV sub-genomic replicon (SGR) in mammalian and mosquito cells. Three AUD mutants were shown to replicate poorly in mammalian cells but no defect was detected in mosquito cells. These mutants were further demonstrated to be temperature-sensitive, rather than species-specific, as they exhibited no replication defect in mammalian cells at sub-physiological temperature (28°C). A similar phenotype was observed in the context of infectious CHIKV and a closely related virus: O'Nyong Nyong virus (ONNV).

Interestingly, the study also revealed a hitherto unrecognized enhancement of genome replication for the WT SGR at 28°C as compared to 37°C. This was not due to the previously reported impaired interferon responses at lower temperatures (Prow et al 2017), as this enhancement was also observed in Vero cells. Neither was this due to a defect in the phosphorylation of eIF2α, as treatment with ISRIB (an inhibitor of global translation attenuation) did not compensate for the replication defect of the AUD mutants at 37°C. This was also not due to the effect of cold shock proteins previously shown to interact with nsP3, as ablation of these cold shock proteins did not recover replication defect of the AUD mutants at 37°C. However, significant differences in the sizes and numbers of ONNV-induced G3BP-positive granules were observed. Considering that in mammalian hosts, cells in the periphery will be at sub-physiological temperatures and they will be the first cells infected via a mosquito bite, it is reasonable to propose that alphaviruses

have evolved mechanisms to limit antiviral responses and promote virus genome replication.

Table of contents

Table of figures

List of Tables

Abbreviations

A	Ala, alanine
ADP	Adenosine diphosphate
arbovirus	arthropod borne virus
AUD	Alphavirus unique domain
BCA	Bicinchoninic acid
BHK-21	Baby hamster kidney 21
bp	base pairs
BSA	bovine serum albumin
BSL3	Biosafety laboratory level 3
BUNV	Bunyamwera virus
C	Cys, cysteine
cDNA	complementary DNA
CHIKV	Chikungunya virus
CHIKV-D-Luc-SGR	Chikungunya virus dual luciferase sub-genomic replicon
CHIKV-FLuc-SGR	Chikungunya virus firefly luciferase sub-genomic replicon
CHIKV-nsP3-mCherry-FLuc-SGR	Chikungunya virus non-structural protein 3 mCherry firefly luciferase sub-genomic replicon
CHX	Chlorhexidine
CSD	Cold shock domains
CPE	Cytopathic effect
D	Asp

Da	Dalton
DAPI	4’, 6’-diamidino-2-phenylindole dihydrochloride
DENV	Dengue Fever virus
DEPC	Diethyl pyrocarbonate
DMEM	Dulbecco’s modified eagles medium
DMSO	Dimethyl sulfoxide
DNA	Deoxyribonucleic acid
dNTP	Deoxynucleotide
DRs	Direct repeats
dsRNA	Double stranded RNA
E.coli	Escherichia Coil
E1	Envelope 1 protein
E2	Envelope 2 protein
EDTA	Ethylenediamine tetraacetic acid
eIF2α	eukaryotic initiation factor
EM	Electron Microscopy
ER	Endoplasmic Reticulum
FBS	fetal bovine serum
FLuc	Firefly luciferase
G3BP	Ras-GTPase-activating protein-binding protein
GLB	Glo lysis buffer
h	hour

hpi	hours post infection
hpt	hours post transfection
HCV	Hepatitis C virus
Huh7	Human hepatocellular carcinoma cell line-7
Huh7.5	Human hepatocellular carcinoma cell line-7.5
HVD	Hypervariable domain
ICRES	ECSA strain
IF	immunofluorescence
IFN	interferon
kb	kilobase
kDa	kilodalton
LB	Luria Bertani
M	Molecular weight
m^7G	7-methylguanosine
min	minutes
MOI	Multiplicity of infection
mRNA	Message RNA
$NaAsO_2$	Sodium arsenite
NC	nucleocapsid
NEAA	Non-essential amino acids
NLuc	Nano luciferase
nsP	Non-structural protein

nsP1-4	Non-structural protein 1-4
nt	nucleotide
O/N	overnight
ORF	Open Reading Frame
ONNV	O’ Nyong Nyong virus
P	Pro, proline
PAGE	Polyacrylamide gel electrophoresis
PBS	Phosphate buffered saline
PCR	Polymerase chain reaction
PDB	Protein database
PFA	paraformaldehyde
PFU	Plaque forming units
PLB	Passive lysis buffer
prom	promoter
PVDF	Polyvinylidene fluoride
Q	Gln, glutamine
RdRp	RNA-dependent RNA polymerase
RLuc	Renila luciferase
RNA	Ribonucleic acid
RNAi	RNA interference
RRV	Ross River Virus
RSE	Repeat sequence element

RT	Room temperature
RT-PCR	Reverse transcriptase-polymerase chain reaction
SDS	Sodium dodecyl sulphate
SE	Standard Error
SFV	Semliki Forest Virus
SGR	Sub-genomic replicon
SGs	Stress granules
sgRNA	Sub-genomic RNA
SINV	Sindbis Virus
siRNA	Small interfering RNA
SRSF5	Serine and Arginine Rich Splicing Factor 5
T	Thr, threonine
TAE	Tris-Acetate-EDTA buffer
TBS	Tris-buffered saline
TC	Tissue culture
TEMED	Tetramethylrhodamine
TST	Twin-strep-tag
UNR	upstream of N-RAS
UTR	Untranslated region
V	Val, valine
v/v	Volume by volume
VEEV	Venezuelan Equine Encephalitis Virus

W	Trp, tryptophan
w/v	weight by volume
WEEV	West Equine Encephalitis Virus
WT	wildtype
Y	Tyr, tyrosine
YB1	Y-box-binding protein 1

Chapter 1: Introduction

1.1 Introduction to Chikungunya virus (CHIKV).

1.1.1 Identification and classification of CHIKV.

CHIKV was first isolated and recognized as a human pathogen during the outbreak of a polyarthralgia disease in 1952 in Tanzania (Lumsden 1955, Robinson 1955, Ross 1956). Chikungunya comes from the Kimakonde language that means “that which bends up”, which describes the stooped posture and rigid gait of people infected with CHIKV (Robinson 1955). Most of individuals infected with CHIKV develop fever, incapacitating polyarthralgia and arthritis, rash, myalgia and headache. For acute CHIKV disease, the symptoms resemble dengue virus (DENV), and retrospective reports indicate that CHIKV infection occurred as early as 1797, which was inaccurately attributed to DENV infection (Carey 1971, Halstead 2015). Chronic disease of CHIKV derived from acute symptom showed recurring musculoskeletal disease affecting peripheral joints that can persists and lasts from months to years, which is distinguishable from DENV (Couturier et al 2012, Hoarau et al 2010, Schilte et al 2013, Sissoko et al 2009). Subsequently, CHIKV was identified in Uganda and other countries in sub-Saharan Africa in mosquitoes as well as humans (Zeller et al 2016). Since 1960s, cases of CHIKV outbreaks were reported associated with DENV and hemorrhagic fevers in Asia (Hammon et al 1960, Weaver 2014). In 2005, CHIKV spread to the Indian subcontinent where millions of people were affected (Arankalle et al 2007). Since 2006, CHIKV has been imported into Europe and western hemisphere via international travelers (Arankalle et al 2007, Centers for Disease & Prevention 2007). CHIKV disease is often self-limiting and normally show low fatality rate (~0.1%) (Renault et al 2008), however, the substantial impact on quality of life for infected people as well as economic losses make it urgent to find antiviral drugs or vaccines (Couturier et al 2012, Gerardin et al 2008, Schilte et al 2013).

CHIKV is a re-emerging mosquito-borne enveloped alphavirus in *Togaviridae* family. The *Togaviridae* family consists of two genera: *Alphavirus* and *Rubivirus*. The sole member of *Rubivirus* is rubella *virus*, which is the causative agent of

rubella disease or “German measles” (Lambert et al 2015). Alphaviruses are positive-sense, single stranded RNA viruses that are transmitted by mosquitoes with two exceptions: salmon pancreatic disease virus (SPDV) and its subtype sleeping disease virus (SDV), which infect salmon and trout leading to death in farmed fishes (Weston et al 1999). Alphaviruses infection in mosquitoes can be long-term and persist while infection in mammalian hosts normally cause acute and severe disease. The *alphaviruses* include 29 species of RNA viruses and was organized into seven complexes according to antigenic relationships: Eastern equine encephalitis (EEE), Venezuelan equine encephalitis (VEE), and Western equine encephalitis (WEE), Barmah Forest (BF), Middelburg (MID), Ndumu (NDU), Semliki Forest (SF) (Weaver et al 2012) (Fig. 1.1). According to the geographic distribution, Alphaviruses can be divided into two clades: the New World virus and the Old World virus. The New World clade include the EEE and VEE complexes, while the Old World clade includes WEE, BF, MID, NDU, SF complexes. Most of the Old World Alphaviruses cause fever, rash and arthralgia while a vast majority of the New World Alphaviruses cause encephalitis. CHIKV belongs to the SF group of the Old World Alphaviruses which includes O’Nyong-Nyong virus (ONNV), Semliki Forest virus (SFV) and Ross River virus (RRV).

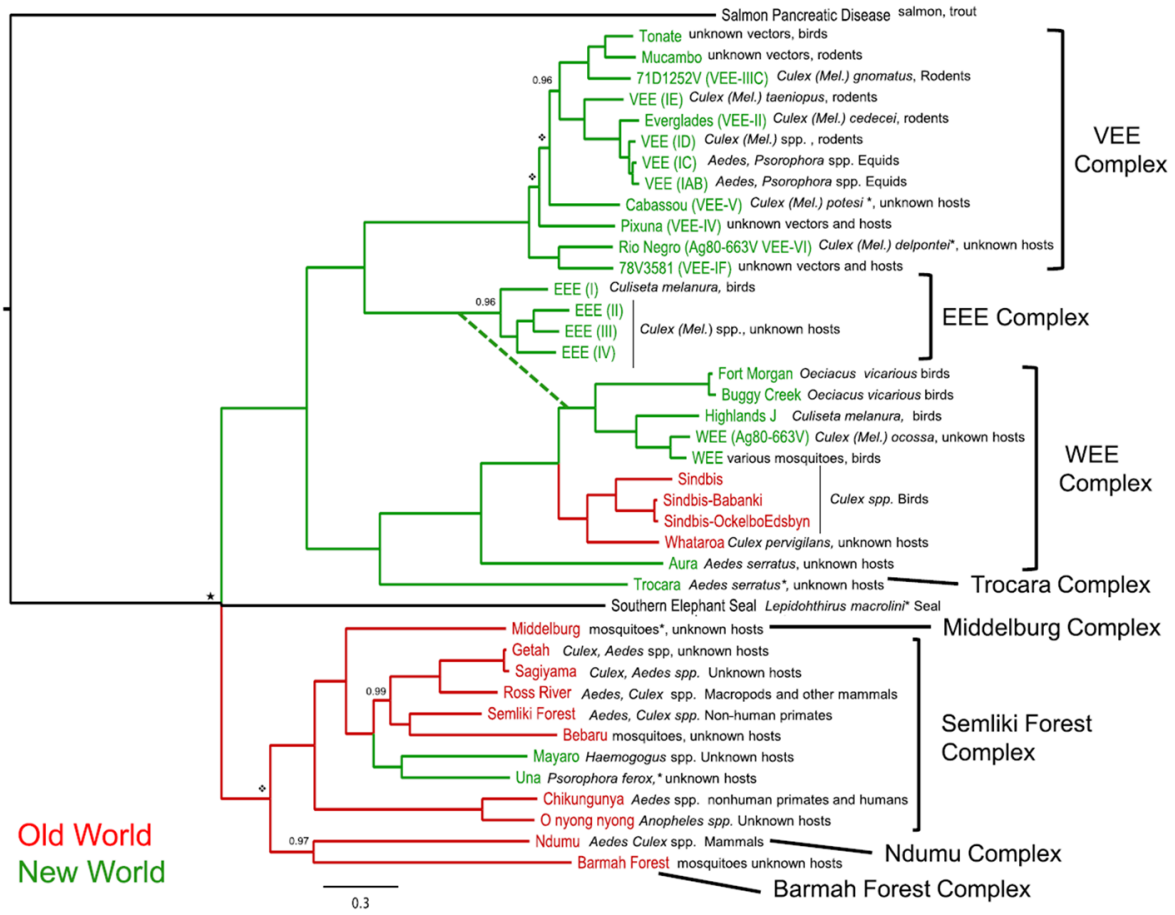

Figure 1.1 Phylogenetic tree of the alphaviruses produced using Bayesian methods and mid-point rooted.

Picture is taken from **(Weaver et al 2012)**.

CHIKV is divided into three geographically associated genotypes: West African (WAf), East/Central/South African (ECSA) and Asian genotypes (Powers et al 2000). Recent studies indicate that Indian Ocean and Indian strains form a monophyletic group within the ECSA lineage (Arankalle et al 2007, Cherian et al 2009, Dash et al 2007). The divergence of each distinct clade reflected the global transmission path way of CHIKV. CHIKV in Africa circulates primarily in a sylvatic/enzootic cycle and is transmitted mainly by Aedes aegypti, while in Asia the urban transmission is in a human-mosquito-human transmission circle mediated primarily by *Aedes aegypti* and *Aedes albopictus* (Weaver 2006). Many of the recent outbreaks in Indian Ocean and Southern Asia derived from the Indian

Ocean lineage contain the adaptative mutation E1-A226, which increases viral fitness *in Aedes albopictus* without affecting its replication in *Aedes aegypti*.

1.1.2 Pathology of CHIKV.

Among the RNA viruses, arthropod-borne viruses (arboviruses) are especially important as many induce severe diseases and deaths in humans and animals. Transmission of CHIKV normally occurs through mosquito bite, although cases have been reported by maternal-fetal transmission (Gerardin et al 2008). CHIKV first replicates in the skin and fibroblasts, then disseminates into lymphoid tissue, liver, muscle, joint and brain, presumably through the blood (Das et al 2010, Robin et al 2010, Staikowsky et al 2009) (Fig. 1.2). Chikungunya disease does not often lead to death, but the clinical symptoms can be serious. Initial infection of CHIKV observed between 2-7 days are characterized by chills and fever normally between 39°C and 40°C, with a certain proportion of people developing headache, persistent myalgia/arthralgia, maculopapular rash and headache. In addition, severe joint pain occurs in infected individuals and is often incapacitating (Mourya & Mishra 2006, Yazdani & Kaushik 2007). Rash is a common symptom in clinical signs of CHIKV infection across trunk, extremities, palms, soles and even face (Borgherini et al 2007). Infection without symptoms do occur but with only around 15% rate (Lemant et al 2008). The acute CHIKV disease normally lasts from a few days to a couple of weeks, while chronic phase typically with signs of recurrent joint pain and mild swelling that can lasts for months to years.

During CHIKV infection, tissues start with a marked infiltration of mononuclear cells including macrophages. However, apart from muscle and joints which are normally with strong pain, most tissues associated with CHIKV infection is subclinical (Dupuis-Maguiraga et al 2012, Robin et al 2010). Acute infection coincides with high titers of virus, which triggers activation of type I interferons (IFNs) (Fig. 1.3). Infected individuals clear the virus infection around one week and only then CHIKV-specific adaptive immunity can be detected (Schwartz & Albert 2010). Not all people have the abilities to clear the virus, with approximately 30% of individuals

suffer from long-term sequelae that include arthralgia or in less cases arthritis.

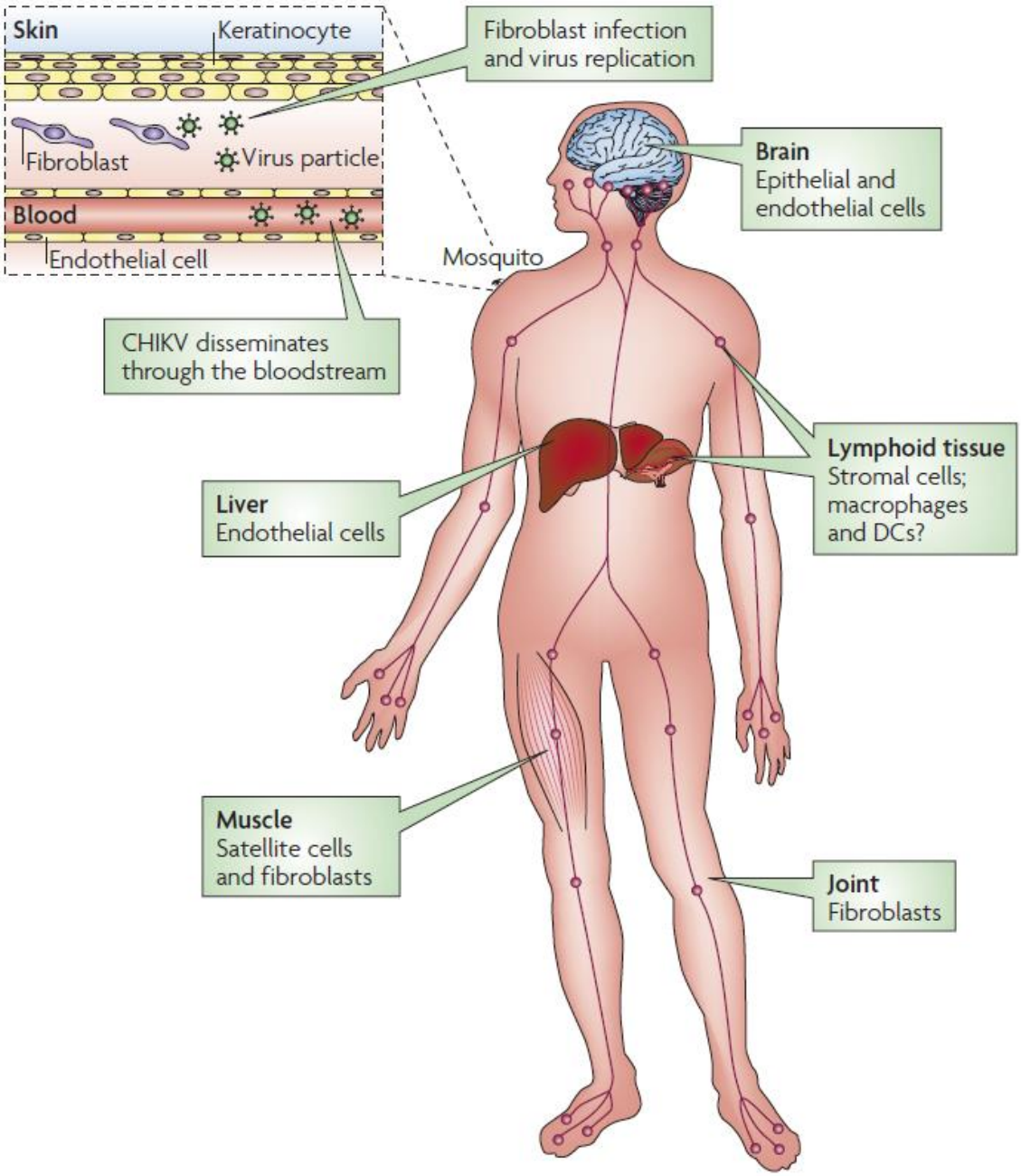

Figure 1.2 Dissemination of chikungunya virus (CHIKV) in vertebrates.

Picture is taken from **(Schwartz & Albert 2010)**.

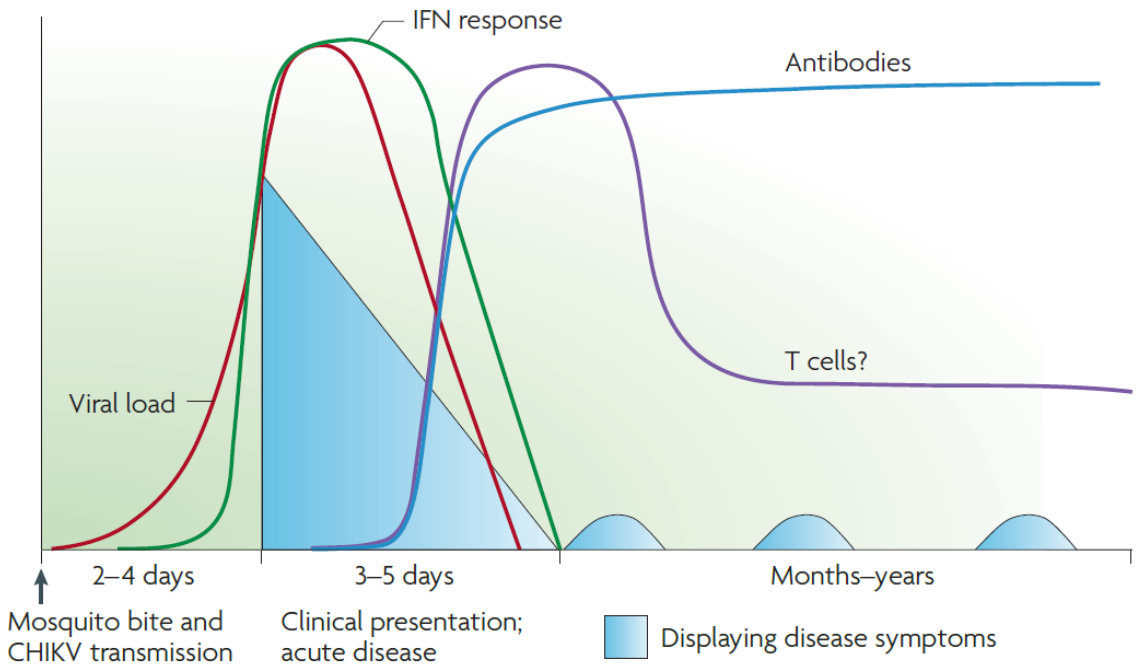

Figure 1.3 CHIKV pathogenesis.

Picture is taken from (Schwartz & Albert 2010).

Both vertebrate and mosquito cell culture systems have been used for the study of alphavirus replication and pathogenesis (Sourisseau et al 2007). CHIKV is able to infect a wide range of vertebrate cell and cell lines (Her et al 2010, Solignat et al 2009), and most of them show strong and apparent cytopathic effect (CPE) (Sourisseau et al 2007). However, CHIKV infection only induce light CPE and establish long-term persistent infection in mosquito cells (Li et al 2013). In Sindbis virus (SINV) infection, almost all vertebrate cells died whereas mosquito cell lines provide long-term persistent infection (Karpf et al 1997b). The mosquito cells establish long-term and persistent infection without being killed by alphavirus might be regulated by intracellular factors (Karpf et al 1997a).

1.1.3 Epidemiology of CHIKV.

Epidemic emergence of CHIKV in Africa involves both enzootic transmission from mosquito vectors to non-human primates and endemic cycle, however, in Asia, CHIKV only circulates in the endemic, urban cycle (Volk et al 2010). Since first

report of CHIKV infection in 1952 in Tanzania, subsequent epidemics of CHIKV occurred throughout the second half of the 20th century in sub-Saharan Africa and Asia (Powers et al 2000). Since the 1960s, CHIKV outbreaks were reported in Asia and Africa, with major events in 1960s to 1980s and then sporadic activities until 2004 (Zeller et al 2016). In 2004, a large epidemic outbreak on the coast of Kenya and then spread quickly to Indian Ocean, to India and to Southeast Asia (Powers & Logue 2007, Sergon et al 2008, WHO 2006). It is reported that a large epidemic outbreak during 2005 to 2006 with an overall attack rate of 35% (Renault et al 2007). Viral isolates from La Réunion showed a distinct clade within ECSA genotype with a mutation in the E1 glycoprotein (E1-A226), which was later confirmed to be responsible for the efficient dissemination rate in *Aedes albopictus* (Vazeille et al 2007). Position E1 226 is located closely to the peptide fusion region, mutation in this region induces a loss of dependence on cholesterol and enhances replication in mosquitoes infected with SFV, which is closely related with CHIKV (Schuffenecker et al 2006). Since 2005, resurgence of CHIKV transmission were reported in several countries in central and Western Africa and transmitted by *Ae. aegypti* and *Aedes albopictus*. Over 1.3 million people were infected with CHIKV in India during 2005-2006 (Arankalle et al 2007), and the ECSA genotype was shown to be the main causative agent and *Aedes albopictus* to be the main vector. The Pacific region has experienced a few outbreaks of CHIKV since 2011 (Aubry et al 2015). Since 2007, cases of CHIKV infection have been reported in Europe such as Italy and France with the ECSA genotype (Delisle et al 2015, Rezza et al 2007). CHIKV emerged in Caribbean and then spread to the neighboring islands in 2013. It then transmitted to Central, South and North America with more than 1.2 million cases reported (Zeller et al 2016).

CHIKV has become a global threat nowadays (Fig. 1.4). The presence of the large human population, the large existing mosquitoes of *Aedes aegypti* and *Aedes albopictus*, and the intensive movement of people globally all contribute to the rapid and wide spread of CHIKV, posing a huge threat to human health.

Precautionary measures should be taken in the future to help reduce and control the CHIKV infection and disease.

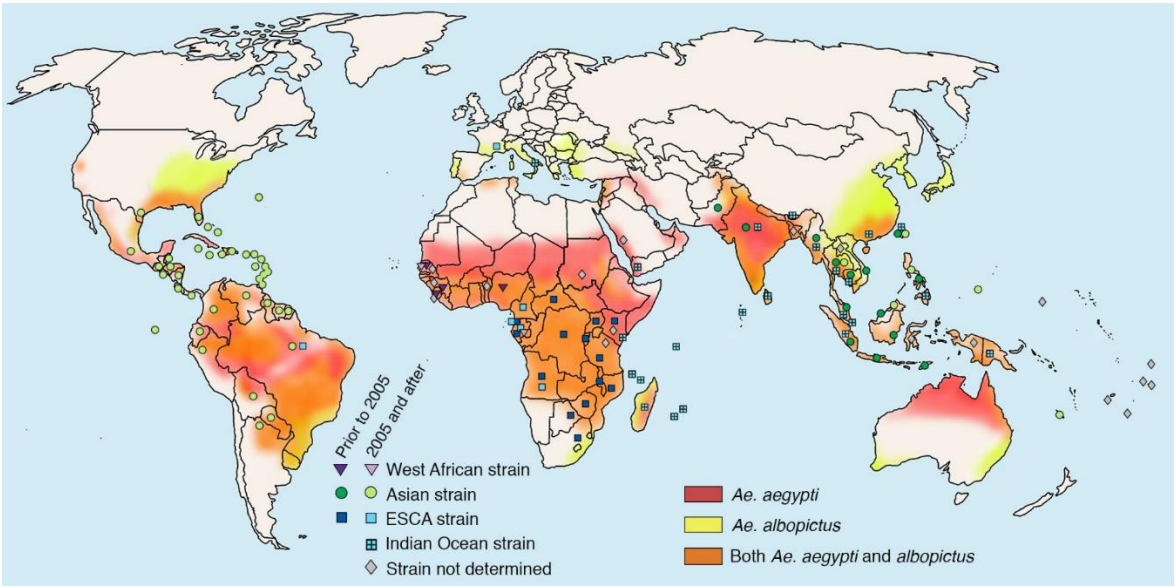

Figure 1.4 Global distribution of CHIKV and the mosquito vectors, Ae. aegypti and Ae. albopictus.

Picture is taken from (Silva & Dermody 2017).

1.1.4 Treatment of CHIKV.

Despite the re-emerging CHIKV disease has been documented in Asia, Europe, America and Africa, there is still no licensed antiviral drugs or vaccines available to prevent CHIKV infection. Nevertheless, therapeutic strategies aiming at inhibiting viral replication are still under evaluation and various vaccines are ongoing to fight the incapacitating disease. It has been reported that priming target cells with low doses of interferon before infection reduced CHIKV replication (Paucker & Boxaca 1967), while addition of actinomycin D (an inhibitor of interferon) enhanced CHIKV replication (Gifford & Heller 1963). However, it would be difficult to use interferon for treatment of CHIKV infection as in an epidemic episode. CHIKV enter into the cell cytoplasm by endocytosis in clathrin-coated vesicles before transfer to endosomes (in low pH) leading to a conformational re-arrange of E1-E2 heterodimer so that the fusion domain in E1 is exposed and fused with endosomal membrane. Chloroquine is previously tested for treatment of chronic CHIKV

arthritis due to raising endosomal pH (Brighton 1984). Although the anti-CHIKV effect of chloroquine has been confirmed *in vitro* by Sentinelles France's national disease surveillance network, the double blind placebo-controlled clinical trials on the island of La Reunion were not convincing enough to confirm the potential application of the drug in counteracting CHIKV infection (De Lamballerie et al 2008). Recent characterization and structure resolution in alphavirus nsP3 macro-domain showed structure conservation compared to macro-domain in bacteria (Malet et al 2009, Pehrson & Fuji 1998), which provides potential of available anti-bacterial compounds as antiviral compounds.

Vaccines are often used as therapeutic strategies in boosting immune responses against CHIKV infection. In the early 1970s, inactivated CHIKV by formalin fixation and ether extraction were both successful in stimulating the production of haemagglutination-inhibiting, complement-fixing and neutralizing antibodies (Eckels et al 1970, Harrison et al 1971). One important issue of early researches is the increasing potential interference from co-utilization of heterologous alphaviruses, as individuals vaccinated with Venezuelan equine encephalitis viruses (VEEV) showed poor neutralizing antibody to CHIKV vaccine (McClain et al 1998). A CHIKV live attenuated vaccine was developed at the U.S. Army Medical Research Institute of Infectious Diseases in Maryland, and vaccination showed 98% volunteers developed neutralizing antibody. However, 8% of infected volunteers developed transient arthralgia (Edelman et al 2000). The development of traditional vaccine using inactivated or live-attenuated viruses are under challenge due to the cost and safety concerns, thus new strategies of vaccines include virus-like particles (VLPs), replication deficient viral vectors and DNA vaccines are developed and researches are ongoing to find effective vaccines against CHIKV (Reyes-Sandoval 2019).

1.2 Molecular biology of CHIKV.

1.2.1 Structure and genome organization of CHIKV.

CHIKV is a small (~70 nm in diameter), spherical, enveloped virus with a positive sense, single-stranded RNA genome that belongs to *Alphavirus* genus, *Togaviridae* family (Powers et al 2001) (Fig. 1.5). CHIKV virion contains one copy of genome RNA, 240 copies of capsid in the form of 120 copies of dimers (Powers et al 2001). The virion is arranged in *T*=4 icosahedral capsid proteins and is enveloped by glycoproteins consisting of E1 and E2.

The CHIKV genome is approximately 11,800 nucleotides with a 5' 7-methylguanosine cap and a 3' poly-A tail (Khan et al 2002). It contains two open reading frames (ORFs) as well as 5' and 3'-untranslated regions (UTRs) with a noncoding junction between the two ORFs (Khan et al 2002) (Fig. 1.6). The ORF1 encodes non-structural polyproteins, which was further cleaved into nsP1, nsP2, nsP3 and nsP4, while ORF2 encodes 6K, E1, E2 and capsid.

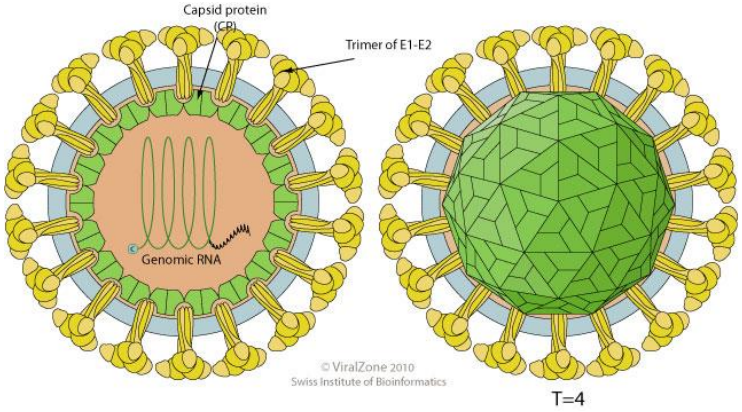

Figure 1.5 Structure of CHIKV.

The CHIKV is an enveloped, spherical and icosahedral virus. It shows a diameter of approximately 70 nm, and its capsid is composed of 240 monomers and arranged in *T*=4 lattice. The envelope contains 80 spikes with each spike as a trimer of E1/E2 proteins. Picture is taken from (ViralZone 2017).

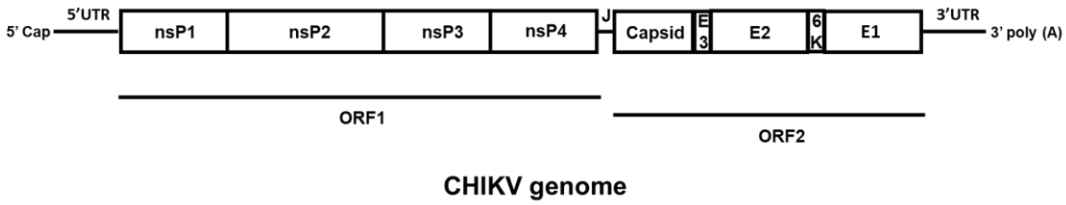

Figure 1.6 Structure of CHIKV genome.

The CHIKV genome is 5'capped and contains 3' poly A. It contains two open reading frames (ORFs), with ORF1 encoding non-structural proteins and ORF2 encoding structural proteins. The non-structural proteins include nsP1, nsP2, nsP3 and nsP4, while structural proteins include capsid, 6K, E1 and E2.

1.2.2 Non-encoding regions of CHIKV.

The CHIKV genome contains three UTRs, including the 5' UTR, 3' UTR and the junction region between them (Fig. 1.6). The junction region between nonstructural and structural ORFs forms 5' UTR of sub-genomic RNA. In alphavirus genomes, 5' and 3' UTR contain distinct core promoter elements in sequence and structure and are required for both negative- and positive-strand RNA synthesis (Hyde et al 2015). Shorter sequences within the 5' and 3' UTRs form cis-acting sequence elements and facilitate genome replication.

1.2.2.1 5' UTR of CHIKV.

The length of 5' UTR in CHIKV is conserved at 76-77 nt (Hyde et al 2015). The 5' termini at the 5' UTR of alphavirus genome is modified by addition of a 7-methylguanosine (m7G) cap structure (Cap 0), promoting RNA stability and protein translation. The RNA capping way of alphavirus is distinct from that of host cells (Ahola & Kaariainen 1995, Mi et al 1989) (Fig. 1.7). The main difference is that in cellular mRNA, the diphosphate mRNA is first capped by guanylyltransferase before methylated by methyltransferase, while in alphavirus genome it is conducted in one step by nsP1 with function of 7-methyl guanylyltransferase. mRNAs of Eukaryotes contain 2'-O-methylation in the Cap1 structure, which protects RNAs from decapping degradation (Picard-Jean et al 2018), and many viruses have utilized this mechanism to "steal" the cap from host mRNA, but alphavirus do not show 2'-O-methylaion in Cap1 (Hyde et al 2014). Recent

analysis on secondary structure of CHIKV 5' UTR and part of nsP1 identified a novel element, SL47, which is essential for efficient replication in mammalian and mosquito cells (Kendall et al 2019). During translation, host factors eIF4E and eIF4F function differentially with genomic 5' UTR to initiate translation. In replication, the alphavirus 5' UTR and its complementing sequence in the 3' UTR of the negative strand contain core promoter elements that are required for RNA synthesis, and they work together with other cis-acting elements in downstream to regulate RNA synthesis (Frolov et al 2001). The alphavirus 5' UTR forms stable secondary structures and studies have shown that both the structure and sequences modulate viral replication (Kulasegaran-Shylini et al 2009, Nickens & Hardy 2008). The AU dinucleotide at the very terminus of 5' UTR is required for genome replication, which does not rely on base pair (Kulasegaran-Shylini et al 2009). Disruption of the 5' UTRs of eastern equine encephalitis viruses (EEEV) and SINV lead to production of pseudo-revertant viruses containing AU rich sequences at the 5' terminus, which restore viral replication efficiency (Kulasegaran-Shylini et al 2009). Sequence and structural changes in alphaviruses 5' UTR also impact immune response and viral pathogenesis. It has been shown that alphaviruses use their specific secondary structure motifs within the 5' UTR to antagonizes the antiviral function of Ifit1, which is an Interferon (IFN)-stimulated gene that regulates protein synthesis (Hyde et al 2014). Thermodynamic stability of stem-loops in CHIKV 5' UTR contributes to Ifit1 antagonism, as SINV and VEEV mutants that contain less stable structures are more susceptible to Ifit1 restriction (Hyde et al 2015). Ifit1 competes with host translation factors eIF4E and eIF4F by binding with viral RNA, which restricts viral replication (Kumar et al 2014). In summary, the 5' UTRs of alphavirus RNAs show diverse roles in promoter function, translation initiation and shutoff as well as anti-innate immune mechanisms.

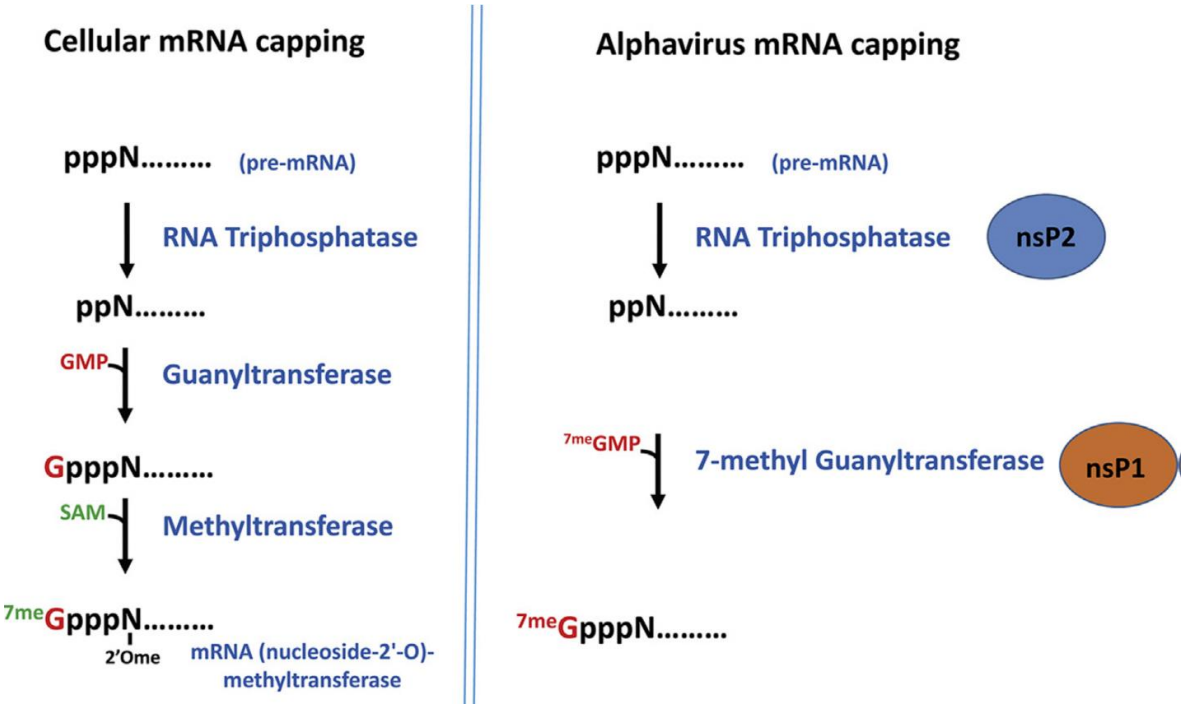

Figure 1.7 Comparison of capping mechanism between cellular mRNA and alphavirus genome RNA.

In cellular mRNA capping, 5'UTR of pre-mRNA is first dephosphorylated by triphosphatase activity. Then Guanosine monophosphate (GMP) is added to the treated pre-mRNA to form Gppp-mRNA. The methyl donor S-adenosyl methionine (SAM) bind to Gppp-mRNA with the function of methyltransferase. In contrast, in alphavirus genome capping, nsP2 functions as RNA Triphosphatase, followed by nsP1 functions as 7' methyl guanylyltransferase. To note, cellular contains a 2'-O-methyl modification on first nucleotide of N-7^{me}Gppp cap, while there is no modification in alphavirus at the same position. Picture is taken from (Hyde et al 2015).

1.2.2.2 Sub-genomic promoter of CHIKV.

The sub-genomic promoter of CHIKV, also named junction between two ORFs, comprises 65-66 nt (Hyde et al 2015). The sub-genomic promoter shares various similar functions with 5' UTR of CHIKV: (1) it is modified by capping at 5' terminus and show exact same capping mechanism with 5' UTR. (2) the structure and thermodynamic stability of sub-genomic RNA also contribute to Ifit1 antagonism and thus counteract host innate immunity. However, during host shut-off, sub-genomic RNA is still translated efficiently while genomic RNA is not. During host shut-off by viral infection, eIF4G is cleaved by host caspase-3 protein or viral

proteins (Marissen & Lloyd 1998), and eIF2α is phosphorylated by double-stranded RNA (dsRNA)-dependent protein kinase R (PKR) (Gorchakov et al 2004, Ryman et al 2002), which results in a global inhibition of mRNA translation. While translation of nonstructural proteins from genome is inhibited during host shut-off, the alphavirus sub-genomic RNA retains efficient translation due to the fact that the 5' UTR of sub-genomic RNA does not require eIF4G for translation (Castello et al 2006). In summary, the sequence and structure of alphavirus sub-genomic 5' UTR not only contribute to replication of ORF2 and anti-immune activity, but also facilitate translation without eIF4G, which is inactivated or absent during host transcriptional shut-off.

1.2.2.3 3' UTR of CHIKV.

The 3' UTR of CHIKV genome varies from 498 to 723 nt (Hyde et al 2015), which have a variety of functions in virus evolution, viral replication and polyadenylation, viral pathogenesis, cellular innate immunity and interaction with host proteins. Poor alignments of various alphavirus 3' UTRs suggest the fast evolution with point mutation, frequent insertions and deletion as well as sequence duplications are observed in alphavirus 3' UTRs. Despite the various differences, most alphavirus 3' UTRs share a common core structure, with short repeated sequence elements (RSEs) and a 19-24 nt conserved sequence elements (CSE) at the 3' end of the genome immediately adjacent to the poly(A) tail (Pfeffer et al 1998). The CHIKV 3' UTR contains a number of direct repeats (DRs 1, 2 and 3) that are distinct in lineage-specific patterns (Fig. 1.8). The 3' UTR of Asian endemic lineage is distinct from ECSA and WA lineages, as it shows point mutations, duplications and replacements of DR1 and DR2 regions, namely DR (1+2) and a duplication of DR3. Replication of CHIKV with longer 3' UTR resulted in lower replication in both mammalian and mosquito cells compared to ECSA strain (Chen et al 2013b), suggesting that its fixation in Asia is not due to directional selection. The finding suggests a population bottleneck that is resulted from a founder effect since CHIKV was introduced into Asia that has been detected since 2005 (Lanciotti et al 2007,

Panning et al 2008). Later accumulated mutations and insertions led to loss of structural/functional constraints and formation of duplication of DR (1+2) and DR3 (Chen et al 2013b), indicating the evolution pathway of CHIKV 3' UTR in Asia lineage.

As CHIKV is a positive sense RNA virus, synthesis of a negative-strand RNA is required for viral replication. The 19 nt CSE immediately to poly (A) tail serves as the promoter for negative strand RNA synthesis (Kuhn et al 1990, Ou et al 1981). Mutations in SINV CSE reduced viral plaque size as well as genome replication (George & Raju 2000). The cytosine at -1 nt (just prior to poly (A)) is identified as the initiation site for negative strand synthesis, and nucleotides -5 to -1 are required for initiation of negative strand RNA synthesis (Hardy & Rice 2005). The poly (A) tail functions in collaboration with the CSE in 3'UTR to produce negative strand RNA synthesis as well as efficient translation. Polyadenylation of cellular mRNA occurs in the nucleus immediately after transcription, while in alphavirus, this step occurs in the cytoplasm. The nsP4, apart from its RNA-dependent RNA polymerase (RdRp) function, contains a terminal adenylyltransferase activity that adds poly (A) to the end of viral RNA (Tomar et al 2006). A minimum of 11-12 residues in 3' UTR poly (A) is required for efficient negative strand RNA synthesis, as the necessary interaction between poly (A) and poly (A) binding protein (PABP) (Hardy & Rice 2005). In mammalian cells, PABP that previously utilized for binding with poly (A) interacts with translation initiation factors and binds to the cap structure in 5' UTR, which results in the circularization of mRNA and protein translation (Lemay et al 2010). MicroRNAs (MiRNAs) are small endogenous RNAs that regulate mRNA translation by degradation or inhibition of mRNA (Bartel 2004). In hematopoietic/myeloid cells, host miRNA binds to RSE in 3' UTR of EEEV and blocks viral protein translation by minimizing type I IFN and limiting prodromal disease (Trobaugh et al 2014). However, it allows EEEV to replicate under undetected condition by host defense response, which exacerbates the severity of the disease. Thus, while restricting virus replication in certain cells, miRNA provide a growth advantage in the mosquito vector or reservoir host. Most alphaviruses,

apart from CHIKV, ONNV and RRV, share a U-rich sequence (approximately 40 nt) preceding CSE, which is the interaction site with cellular protein HuR. In ONNV and RRV that lack a U-rich sequence in 3' UTR, HuR interacts with RSEs with high affinity (Dickson et al 2012). The interaction stabilizes viral RNA in cytoplasm and prevents deadenylation and decay of viral RNA (Dickson et al 2012, Gardner et al 2008).

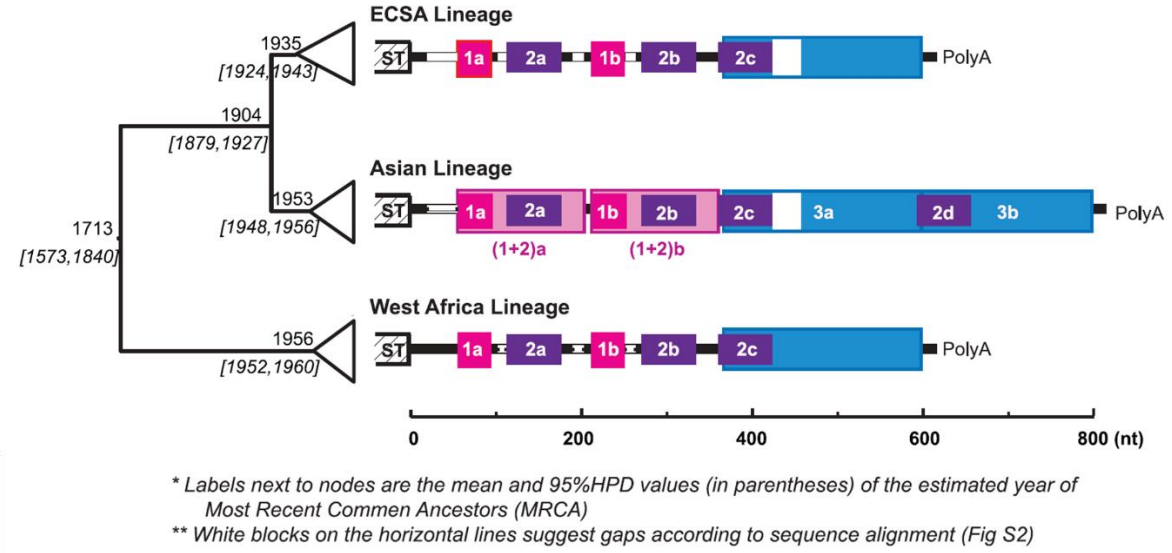

Figure 1.8 Evolutionary history and lineages-specific structures of the CHIKV 3' UTR.

Picture is taken from (Chen et al 2013b). On the left is the Maximum Clade Credibility based on the complete ORF sequences of different CHIKV strains. Estimated year of the most recent common ancestor of each clade is labeled to the node on the left side. 3'UTR structures of CHIKVs are shown next to each lineage. Different colored blocks represent direct repeats and each of them represents a different homologous sequence region. Sequence gaps are indicated by white blocks. In the Asian lineage, duplication of direct repeat (DR) 3 and duplication of DR (1+2) region are observed.

1.2.3 Non-structural proteins of CHIKV.

1.2.3.1 nsP1.

The CHIKV non-structural proteins include nsP1, nsP2, nsP3 and nsP4. The function of nsP1 is mainly characterized in two aspects. As described in Figure 1.7, nsP1 serves as a methyltransferase and guanylyltransferase-like enzyme, which is

necessary for the capping of viral positive strand genome and sub-genomic RNA (Martin & McMillan 2002, Rozanov et al 1992). Recent sequence and secondary structures demonstrated that the conserved capping domain contains over 400 amino acid (aa) residues (Ahola & Karlin 2015) (Fig. 1.9). The Rossman-like methyltransferase motif is in the N-terminal domain. Following its N-terminal is the amphipathic helix and palmitoylation domain, which both act to anchor the nsP1 as well as nsP1-containing non-structural polyproteins to the host membrane (Ahola et al 2000, Ahola et al 1999, Laakkonen et al 1996, Spuul et al 2007), although palmitoylation is not essential for enzymatic activity of the nsP1 protein (Laakkonen et al 1994, Mi & Stollar 1991). The nsP1 also show membrane and cytoskeletal rearrangements, the development of cell filopodia and cell-to-cell transmission (Karo-Astover et al 2010, Laakkonen et al 1998, Martinez et al 2014), which might be responsible for the lacking phenotype in tissue culture for infection with the de-palmitoylation (Ahola et al 2000). Recent study in structural elements of CHIKV nsP1 indicated that the RNA structures in nsP1 encoding region are required for efficient CHIKV genome replication in a host-dependent manner (Kendall et al 2019). nsP1 also counteracts the function of tetherin (BST-2), which is a virus restriction factor that retains viral particles on the cell surface (Jones et al 2013). Due to its unique features, nsP1 is an appealing target for antiviral target. However, due to the lack of specific structural information and characteristic of membrane association, it was not until recently specific inhibitors have been described (Delang et al 2016).

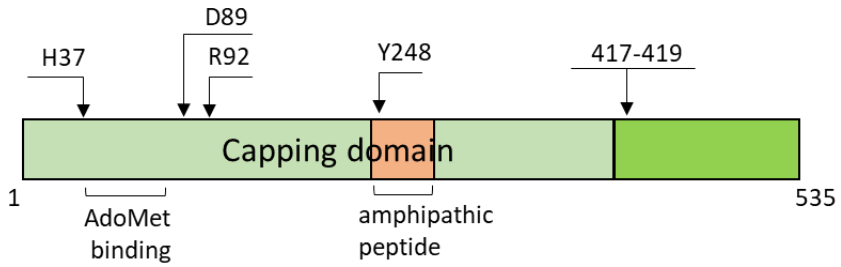

Figure 1.9 Schematic of the CHIKV nsP1 structure.

Capping domain and important residues related with membrane association are marked. Picture is originated from (Ahola & Merits 2016).

1.2.3.2 nsP2.

The ~90 kDa CHIKV nsP2 shows multiple functions during virus infection. Initially nsP2 was described mainly in two domains, a helicase domain at N-terminal and a protease domain at C-terminal (Fig. 1.10). However, crystallographic analyses of the nsP2 C-terminal of CHIKV and VEEV indicate an extra methyltransferase domain, although it is nonfunctional due to lack of crucial structural elements (Russo et al 2006, Shin et al 2012). As for the enzymatic functions, nsP2 is known for four enzymatic activities, namely protease, helicase, NTPase and 5' triphosphatase activities (Rupp et al 2015). CHIKV nsP2 protease is known in polyprotein processing, but the true cleavage requirements and efficiencies remains excusive. Recently, the actual protease of CHIKV nsP2 has been analyzed using full length nsP2 N-terminus as an enzyme and recombinant proteins containing different length of cleavage sites (Utt et al 2015). The result revealed that substrates representing 1/2 and 3/4 sites were efficiently cleaved but not for 2/3 sites until in an extended form (10 preceding and 170 following aa residues). Although essential for processing of the non-structural polyproteins, the alphavirus nsP2 protease domain is not entirely functionally independent, rather it is modulated by other domains of nsP2 and nsP2 containing polyproteins (Vasiljeva et al 2003). The NTPase and RNA 5'-triphosphatase activities of CHIKV nsP2 have been reported (Karpe et al 2011). The triphosphatase remove γ-phosphate from nascent RNA substrates, which is necessary for the subsequent capping activity mediated by nsP1. The NTPase activity not only depends on the intactness of nsP2 N-terminus but also depends on its C-terminal region, and can be stimulated by DNA and RNA oligonucleotides. For the helicase activity, only intact nsP2 of CHIKV is capable of acting as a helicase, and later it showed that nsP2 possess 5' to 3' RNA helicase activity (Das et al 2014). Furthermore, nsP2 is shown to have RNA strand annealing activity. However, both RNA helicase and RNA-strand annealing activities were dependent on the C-terminal region of nsP2, indicating the RNA-modulating activities of nsP2 depend on the communication between nsP2 N-terminal and C-terminal domains (Das et al 2014).

Alphavirus nsP2 is localized both to the cytoplasm and the infected cell nucleus (Peranen et al 1990), however, the exact mechanism remains exclusive. By infection of CHIKV, nsP2 exhibited a time-dependent nuclear localization: at early stage (4 h post infection) nsP2 show a nuclear prominent localization, while at later stage (12 h post infection) nsP2 is mostly located in the cytoplasm (Utt et al 2015). In SINV and CHIKV, the nuclear localization of nsP2 is required for the shutdown of host-cell transcription (Breakwell et al 2007), which is due to the ability of nsP2 to induce degradation of Rpb1 (Akhrymuk et al 2012). The ability of nsP2 to induce shutdown of cellular transcription and probably combined with other mechanisms that makes it highly cytotoxic, and mutations in nsP2 can suppress cytotoxic effect but also showed reduced viral replication (Utt et al 2015, Utt et al 2016). Alphavirus infections not only led to transcription shutoff, but also result in rapid translation shutoff, and it has been clearly identified that these two events are independent (Gorchakov et al 2005). Translation of viral genomic RNA is inhibited, however, translation of sub-genomic RNAs remains active, as described in sub-genomic promoter of CHIKV genome (Strauss & Strauss 1994). CHIKV also induce antiviral effect by inhibiting type I/type II IFN. The Pro718 to Ser mutation in CHIKV nsP2 significantly reduced IFN-induced JAK-STAT inhibition (Fros et al 2010). Internal domain-domain interactions in nsP2 was conserved (Das et al 2014), which support the previous conclusion that a functional interaction between N-terminal and C-terminal of nsP2 (Lulla et al 2012). Alphaviruses are sensitive to the effects of the unfolded protein response (UPR), which is triggered by Endoplasmic Reticulum (ER) Stress from alphavirus glycoproteins (Barry et al 2010). Indeed, the transient expression of nsP2 is sufficient to suppress UPR and mutations in nsP2 rendered the protein unable to suppress UPR (Fros et al 2015).

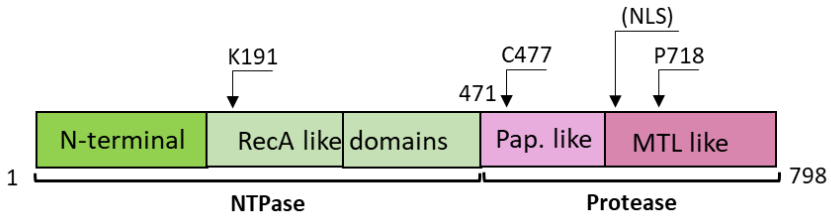

Figure 1.10 Schematic of the CHIKV nsP2 structure.

The nsP2 can be mainly characterized into two aspects: NTPase at N terminal and Protease at C terminal. The putative NLS and the conserved proline residue affecting cytotoxicity have been marked. Picture is originated from (Ahola & Merits 2016).

1.2.3.3 nsP3.

The nsP3 of CHIKV is ~60 kDa and consists of three domains: the macrodomain, the alphavirus unique domain (AUD) and the hypervariable domain (Fig. 1.11). The functional importance of nsP3 is clear as it is required for RNA synthesis, and mutations in nsP3 exhibited defects in the initiation of minus-strand synthesis or sub-genomic RNA synthesis (Lastarza et al 1994a, Rupp et al 2011, Wang et al 1994). Recently published paper in our laboratory indicated that the AUD of nsP3 is necessary for viral replication and one mutant P247A/V278A showed smaller plaque assay (Gao et al 2019). The P247A/V248A showed reduced binding affinity with CHIKV genomic RNA as well as sub-genomic promoter, which resulted in lower replication and less virus production (Gao et al 2019). Despite these discoveries, many of the important roles of nsP3 remains not clear. The detailed information of nsP3 will be provided in 1.3.

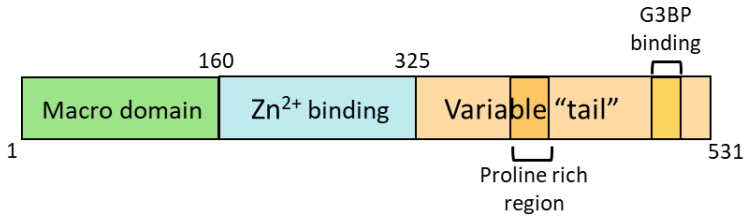

Figure 1.11 Schematic of the CHIKV nsP3 structure.

The three domains of nsP3 as well as the important motifs for association with host proteins are indicated. Picture is originated from (Ahola & Merits 2016).

1.2.3.4 nsP4.

The ~70 kDa nsP4 is the most conserved protein among alphaviruses, which shows common RdRp activity at C-terminal (Fig. 1.12). Mutations in the polymerase active site Gly-Asp-Asp (residues 465-467) completely abolish CHIKV RNA synthesis (Utt et al 2016). The disordered N terminus is sensitive to protease, which is induced by the N-terminal Tyr residue of nsP4 that has been shown to be crucial for enzymatic activity (Shirako & Strauss 1998). Inside infected cells, nsP4 concentration is the least among non-structural proteins and is highly regulated by readthrough of an opal termination codon, degradation of the ubiquitin-dependent nsP4 N-terminal rule pathway and proteinase processing (de Groot et al 1991). The opal 524R mutation did not impair viral replication kinetics *in vitro* or *in vivo*, but showed reduced pathogenesis significantly and delayed immune response in mouse models (Jones et al 2017). Until now there are still no reports of successful expression and purification of functional CHIKV nsP4 as a recombinant protein, this is hampered by instability of individual nsP4 in eukaryotic cells or insolubility of recombinant nsP4 in the bacterial system. A Δ97nsP4 mutant in SINV possesses terminal adenylyltransferase activity (Tomar et al 2006), which likely contribute to the synthesis of poly (A) tails of positive-strand RNAs. For host protein interaction, little information is available due to the low abundance and low stability of nsP4. One heat shock protein 90 alpha subunit (HSP-90α) interacts with nsP4, which is identified and confirmed by reverse pull-downs and proposed to be critical for assembly of the viral replication complex (Rathore et al 2014).

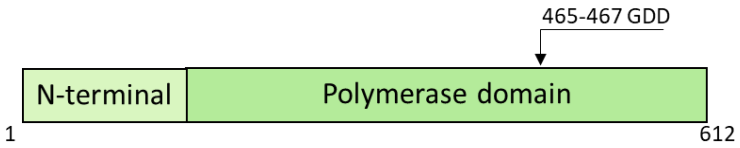

Figure 1.12 Schematic of the CHIKV nsP4 structure.

The nsP4 consists of the N-terminal domain and the polymerase domain at the C-terminus. The central polymerase motif Gly-Asp-Asp (GDD) is marked. Picture is originated from (Ahola & Merits 2016).

1.2.4 Structural proteins of CHIKV.

The 26S sub-genomic mRNA of CHIKV is transcribed from the remaining one-third of 3' template strand. The structural polyprotein is first synthesized and then cleaved into capsid, E1, 6K and p62 by capsid protease and host proteases. 240 copies of the capsid associate with a genomic RNA molecule and forms a nucleocapsid (NC) in host cellular cytoplasm (Melancon & Garoff 1987). The glycoproteins E1 and P62 interact with each other and form heterodimers before subsequently trimerize into viral spikes in the ER. Then glycoprotein p62 is then cleaved into E2 and E3 by cellular furin during transportation from the acidic Golgi environment and early endosomes to the neutral pH environment of cell surface, and E3 is released following transportation (Yap et al 2017). The mature alphavirus virions have envelope derived from host cell membrane, embedded with 80spikes in *T*=4 icosahedral symmetry.

1.2.4.1 Capsid.

The ~29 kDa capsid is a multi-functional protein consisting of two domains, the N-terminal RNA binding domain and the C-terminal protease domain (Choi et al 1991, Melancon & Garoff 1987). The N-terminal domain is less conserved and intrinsically disordered with high degree of positive charge, which is responsible for genome binding, capsid protein dimerization and host transcription off (Lulla et al 2013b, Owen & Kuhn 1996, Toribio et al 2016). Genetic and biochemical data showed a highly stable RNA hairpin loop located at the downstream of the AUG initiator codon in alphavirus 26S mRNA, which provides translational resistance to eIF2α phosphorylation by stalling the ribosomes on the correct site and obviating the participation of eIF2 (Toribio et al 2016, Ventoso et al 2006). The C-terminal protease domain is highly conserved and is a chymotrypsin-like serine protease, which possesses cis-proteolytic activity from the structural polyprotein (Choi et al 1991, Melancon & Garoff 1987). Structural studies revealed that the active sites and the catalytic triads are highly conserved among serine proteases including the capsid protein of alphaviruses, with CHIKV capsid protein at His139, Asp161 and

Ser213 (Aggarwal et al 2012, Choi et al 1991). The alphavirus capsid also contains nuclear localization signal (NLS) and nuclear export signal (NES) for nuclear-cytoplasmic trafficking (Thomas et al 2013).

1.2.4.2 E1.

The E1 envelope glycoprotein is involved in the formation of the icosahedral shell of the virus particle and membrane fusion during virus entry into the host cells. The SFV E1 ectodomain consists of three β barrel domain (Lescar et al 2001). While the domain I contains amino terminus and is spatially located between domains II and domain III, the domain III lies at C-terminus and the fusion peptide locates at the distal of domain II. E1 monomers of alphaviruses lie at the bae of surface spikes and forms trimer, resulting in the formation of lattice on viral surface (Zhang et al 2002). The resulting surface protein lattice is primed to cause membrane fusion when exposed to acidic environment of the endosome (Lescar et al 2001).

1.2.4.3 E2.

Alphavirus E2 has two functions: its cytoplasmic domains interact with NC and its ectodomain involves in receptor binding and cell entry (Mukhopadhyay et al 2006). The entry of alphaviruses into host cells via receptor mediated endocytosis involves the interactions of E2 glycoproteins with host cell receptors. Cryo-EM studies indicated that the N-liked glycosylation sites on E2 is responsible for binding to the heparin sulphate (Knight et al 2009, Ryman et al 2007). The alphavirus E2 consists of three domains, namely domain A, B and C (Kam et al 2012, Porta et al 2014). Domain A forms the tip of E1-E2 heterodimer spikes on viral surface, domains B is the key factor for neutralization (Weger-Lucarelli et al 2015a), domain C is critical to complete virus transmission (Weger-Lucarelli et al 2015b). The E1-E2 heterodimer self-assembles on the virus surface to form trimeric spikes (Mukhopadhyay et al 2006). Virus budding occurs at the cell membrane where the NC is enveloped by the glycoproteins E1-E2 on the plasma lipid membrane (Yap et al 2017).

1.2.4.4 E3.

The E3 of alphavirus is a small peptide cleaved from precursor of E2 (pE2) by cellular furin in Golgi. The E3 domain of the pE2 locates in the head of the spike and fills part of the space between them that like a bulky side protrusion (Wu et al 2008). The glycoprotein E3 facilitates E1-p62 heterodimerization and prevents the exposure of E1 fusion loops from premature fusogenic activation (Carleton et al 1997, Mulvey & Brown 1995). Mutant analysis revealed that the E3 domain mutant ($p62^{SQL}$) establishes a gripper over domain II of the fusion protein E1, with a cotter-like connection toward to a hydrophobic cluster in its central β-sheet. Cryo-EM have shown that E3 remains associated with mature virus of SFV (Mancini et al 2000), while SINV and CHIKV release E3 after budding (Paredes et al 1993, Sun et al 2013).

1.2.4.5 6K.

The 6K protein is a small, hydrophobic, cysteine-rich protein that involves in envelop protein processing, membrane permeabilization, virus budding and assembly (Lusa et al 1991, Strauss & Strauss 1994, Welch & Sefton 1979). Mutations in 6K reduced virion production greatly or showed deformed multi-cored virions, although the viruses are still viable (Gaedigk-Nitschko & Schlesinger 1991, McInerney et al 2004). Bioinformatic analyses identified a frameshift site within the 6K coding sequence and the synthesis of an extra trans-frame protein (TF) with a size of ~8 kDa (Firth et al 2008). Later the presence of TF in SFV was confirmed by mass spectrometry in SFV. Following studies showed that TF from SINV in infected cells in two palmitoylated states, basal and maximal (Ramsey et al 2019). Mutagenesis studies demonstrated that without palmitoylation, TF fails to incorporate into released virions, suggesting the important function of palmitoylation of TF in regulating virus assembly (Ramsey et al 2019).

1.3 nsP3 of CHIKV.

1.3.1 Macro-domain.

Macro-domain is a conserved protein fold that exists in the form of single protein or embedded in a larger protein, which have been identified in virus, bacteria, archaea and eukaryotes (Barkauskaite et al 2013, Feijs et al 2013, Rack et al 2016). The name of macro-domain derives from their similarity in C-terminal domain with the histone H2A, which was given the name MacroH2A (Pehrson & Fuji 1998). This domain typically contains 130-190 amino acids that adopt a distinct fold, consisting of a central β sheet and 4-6 helices surround it. In CHIKV, it contains a central twisted six-stranded surrounded by three helices on each side (Malet et al 2009). Many studies have demonstrated that most macro-domains have the ability to bind to monomeric ADP-ribose (MAR) and its derivatives, while a subset of them possess enzymatic activity to hydrolyze ADP-ribose derivatives (Leung et al 2018) (Fig. 1.13). In coronavirus infection, macro-domain is characterized to dephosphorylate ADP-ribose-1''-phosphate, a byproduct of cellular tRNA splicing (Putics et al 2005), and innate immunity is suppressed by macrodomain (Fehr et al 2016). Recent study showed that ADP-ribosylhydrolase activity of Chikungunya virus macrodomain is critical for viral replication and virulence (Abraham et al 2020, McPherson et al 2017), with mutations in macro-domain showed either reduced ADP-ribosyl-binding or hydrolase activities or both. Furthermore, CHIKV infection induced ADP ribosylation of cellular proteins, and nsP3 macro-domain ADP-ribose binding activity is required for initiation of alphavirus replication, while hydrolase activity facilitate amplification viral replication complexes (Abraham et al 2018).

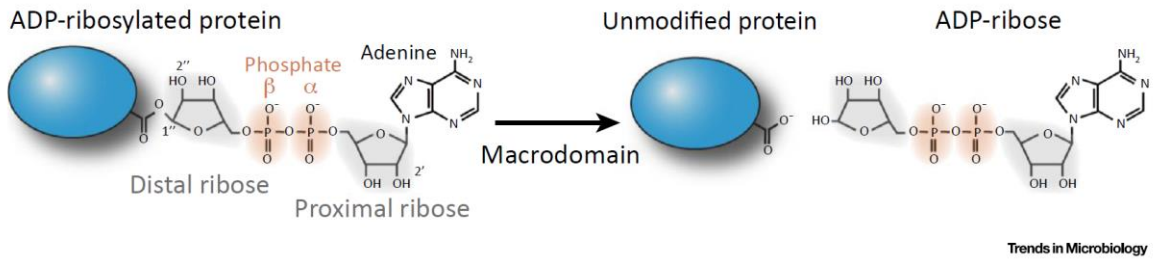

Figure 1.13 CHIKV nsP3 macro-domain functions in removal of ADP-Ribose from Protein.

A-Schematic representation of the de-ADP-ribosylation reaction. Distal and proximal ribose are shaded in gray, α and β phosphate groups are shaded in orange. Picture is taken from (Fehr et al 2018).

1.3.2 AUD.

The AUD is located in the central portion of nsP3, a region that shares a high sequence homology across the alphaviruses. The nsP2/nsP3 junction is the most well-defined structural data in alphavirus replication complexes, and crystal structure analysis in the region of SINV revealed the presence of a zinc coordination site within AUD (Shin et al 2012). The conserved nsP3 AUD contains an antiparallel α-helical bundle, two parallel β-strands as well as the zinc-coordination site (Fig. 1.14). The two cysteines in a loop between α-helices and the other two cysteines at the end of two parallel β-strands constitute the structural scaffold for zinc-ion coordination (Krishna et al 2003). All four SINV mutants in these cysteines failed to exhibit productive infection, supporting the structural role of the zinc ion (Shin et al 2012), and this is further verified by the observation that same mutants in CHIKV failed to produce viruses (Gao et al 2019). Previous study showed a F312S temperature sensitive mutant resulted in RNA synthesis defective at nonpermissive temperature (Hahn et al 1989b). This site is located in the hydrophobic core and surrounded by residues from nsP3 macro, AUD and nsP2 methyltransferase-like domain. Mutation of this residue is presumed to destabilize the core and disrupt domain interaction, which results in defective RNA phenotype at nonpermissive temperature (Shin et al 2012). Mutations within AUD were shown defects in minus-strand synthesis (LaStarza et al 1994b), poly-protein processing (De et al 2003), and neuro-virulence (Tuittila & Hinkkanen 2003). Recent research in our laboratory showed that AUD is required for CHIKV replication and assembly, and one mutant P247A/V248A exhibited a significant reduction in virus production and much smaller plaques compared to WT (Gao et al 2019). Further investigation showed that it is due to a block in transcription of the sub-genomic RNA, which is induced by reduced binding activities of mutant AUD to genomic RNA and sub-genomic promoter RNA. Despite these discoveries, the AUD functions in CHIKV

replication and infection as well as the mechanisms behind them remain largely enigmatic.

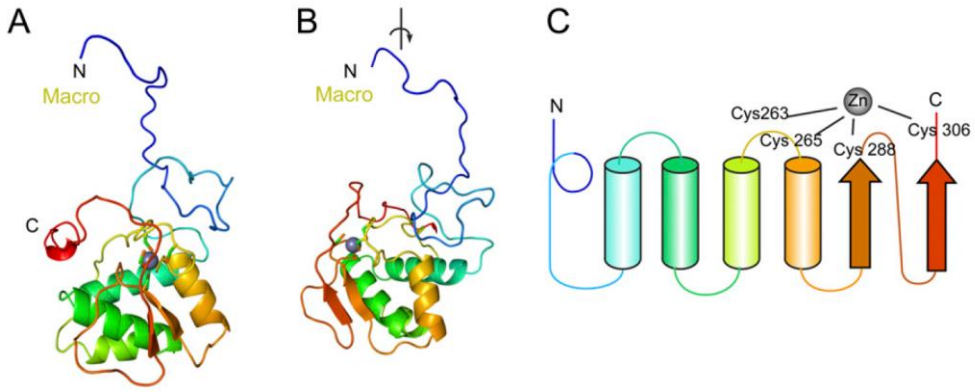

Figure 1.14 Alphavirus unique domain (AUD) of nsP3.

(A and B) Ribbon diagrams of nsP3 AUD. The polypeptide chain is rainbow colored starting from amino terminus (blue) to carboxyl terminus (red). The zinc atom is shown in a gray sphere that surrounded by four coordinating residues in stick format. B is rotated 90° from A. (C) Topology model of the nsP3 ZBD and liner, with the cysteine-coordinating residues highlighted. Picture is taken from (Shin et al 2012).

1.3.3 Hypervariable domain.

The C-terminal domain of nsP3 is characterized as being hypervariable, exhibiting poor conservation across alphaviruses in terms of sequence composition and length. In CHIKV, the length of hypervariable domain is ~205 aa. The hypervariable domain is heavily phosphorylated on serines and threonines (Vihinen et al 2001), and it is considered unstructured. Mutation of phosphorylation sites in SFV reduced viral replication and pathogenicity in mouse models (Vihinen et al 2001), while in VEEV viral replication was not affected but viral pathogenicity is attenuated in mouse models (Foy et al 2013b). Further investigation showed this domain is responsible for the formation of virus-species specific complexes in infected cells (Foy et al 2013a). Together these data suggest the hypervariable domain plays an important role in virus-host interactions and is important for pathogenesis by interaction with cell type specific factors. This region tolerates large deletions and insertions, and has been applied as an insertion site for marker proteins (Kummerer et al 2012, Pohjala et al 2011). Despite their variations, it still contains conserved elements in several or even all alphaviruses. A conserved

proline-rich element (PVAPPRRRR) binds to host protein SH3-domains, for example amphiphysin-1 and 2 in CHIKV, SFV, SINV and probably all Old World alphaviruses (Neuvonen et al 2011). The nsP3 of CHIKV and other Old World alphaviruses binds to GTPase-activatingprotein-1 (G3BP1) and G3BP2 directly, which are components of cellular stress granules (SGs). Recruitment of G3BPs by nsP3 prevents the formation of SG by altering the virus-induced granules, which are devoid of many SG components (Fros et al 2012, Panas et al 2014). Therefore, apart from replication complex, nsP3 mainly localized in granular cytoplasmic structures (Neuvonen et al 2011). G3BPs is also assumed function in facilitating the switch from ns-polyprotein translation to RNA replication, as depletion of G3BPs reduced CHIKV replication (Cristea et al 2010, Scholte et al 2015). It is interesting that recent results suggest that CHIKV nsP3 can be replaced by SFV nsP3 in a chimeric virus, which retains its infectivity but becomes temperature-sensitive and only replicates well at 28°C (Merits, unpublished). This highlights the essential functions of nsP3 are conserved and can be replaced by homologues, but more specific interactions maybe altered during different alphaviruses replication, which can be compromised in chimeras.

1.4 CHIKV lifecycle.

1.4.1 Viral Entry.

Infection inside cells starts with the attachment of virus to cell surface, followed by viral entry into cells. The binding of virus to cells concentrates viral particles on cell surface, but this does not often trigger conformational changes in envelope proteins, which indicates that attachment factors are usually non-specific and can be used by multiple types of viruses. In contrast, canonical viral receptors induce conformational change in viral envelope and promote viral entry by interaction with viral envelopes. The exact mechanisms of how alphaviruses enter host cells remains unclear, but as alphaviruses are transmitted by arthropod hosts, it is assumed that they use either conserved receptors or different entry mechanisms in insect and mammalian cells.

Several attachment factors have been described for CHIKV and other alphaviruses. Glycosaminoglycans (GAGs) are large complex carbohydrate molecules, which is an essential part of extracellular matrix and are ubiquitously expressed on the cell surface in a large variety of mammalian cells. GAGs include keratan sulfate, heparan sulfate, chondroitin sulfate and dermatan sulfate (Gandhi & Mancera 2008). The functional role of GAGs in CHIKV and SINV attachment have been discussed previously (Gardner et al 2012, Klimstra et al 1998, Weber et al 2017). Point mutations in E2 protein showed enhanced GAG dependency but reduced viral replication, and this enhancement is due to increased positive charge in domain A of E2 and thus facilitates binding affinity with virus (Ashbrook et al 2014). However, the GAGs are not absolutely required for CHIKV infection but they functions in promoting viral entry, as CHIKV entry into GAG-deficient cells is still possible, and soluble GAGs fail to fully block CHIKV entry (Weber et al 2017). The cell-surface glycoprotein T-cell immunoglobulin and mucin 1 (TIM-1) is also expressed on a large variety of cells, and has been demonstrated to be a viral receptor for alphaviruses (Moller-Tank et al 2013). TIM-1 binds to phosphatidylserine (PtdSer), which is believed to be involved in mediating virus internalization. CHIKV entry are moderately enhanced in TIM-1 overexpressing cells, and transduction of cells with CHIKV-pseudotyped vectors can be partially inhibited by PtdSer liposomes (Moller-Tank et al 2013). The C-type calcium-dependent lectin DC-SIGN (DC-specific intercellular adhesion molecule-3-grabbing non-integrin) that acts as an attachment factor has been shown to significantly enhance SFV and CHIKV infection (Prado Acosta et al 2019).

Alphaviruses have been reported to be taken up by clathrin-mediated endocytosis in mammalian and mosquito cells (Kielian et al 2010, Lee et al 2013, Smith & Helenius 2004). Endocytic vesicles coated with clathrin rapidly traverse the cell membrane and deliver cargoes into cytoplasm. The acidic pH in endosomes triggers virus penetration and uncoating (Kielian et al 2010). However, there is also evidence that CHIKV enter cells via a clathrin-independent, epidermal growth factor receptor substrate 15 (Eps15)-dependent pathway (Bernard et al 2010).

After entering into the endosomal compartment, fusion of CHIKV with host cell membrane relies on a low pH environment, as lysosomotropic agents chloroquine or bafilomycin A1 inhibited CHIKV infection at certain levels (Bernard et al 2010, Weber et al 2014). Recent study showed that micropinocytosis is an entry pathway for CHIKV into muscle cells, which is actin-dependent and is initiated by the stimulation of growth factor receptors of the virus (Lee et al 2019). Macropinosomes are large, uncoated vesicles that are involved in unspecific uptake of extracellular material. Formation of macropinosomes results in signal transduction and actin filament polarization, which pushes the membrane forward to form ruffles. A number of the ruffles fold inwards and fuse with cell membranes forming macropinosomes that take up bound viruses (Mercer & Helenius 2009) (Fig. 1.15).

A genome-wide CRISPR-Cas9 based screen identified cell adhesion protein Mxra8 as an entry mediator for multiple alphaviruses, including CHIKV, ONNV, Mayaro virus (MAYV) and RRV. CHIKV particles bind to Mxra8 led to enhanced virus attachment and internalization into cells, and Mxra8 directs the virus to low pH environment of the endosome, which additionally triggers the release of capsid into the cytoplasm. Fusion protein of Mxra8 and IgG-Fc fragment or anti-Mxra8 antibody were able to block CHIKV infection (Zhang et al 2018a). Mxra8-deficient mice showed decreased infection in musculoskeletal tissues with CHIKV, ONNV, RRV and MAYV (Zhang et al 2019), which demonstrates the importance of Mxra8 in pathogenesis of alphaviruses. However, CHIKV infection was also detectable in the absence of Mxra8, showing that it is not an exclusive alphavirus receptor (Zhang et al 2019, Zhang et al 2018a). Another study using mass spectroscopy led to the identification of prohibitin (PHB) proteins 1 and 2 (Wintachai et al 2012). Antibodies against PHB-1 or treatment of its downstream by siRNA slightly inhibited CHIKV infection. Since interference with PHB fail to inhibit CHIKV infection completely, it is possible that PHB-1 acts as an enhancement factor.

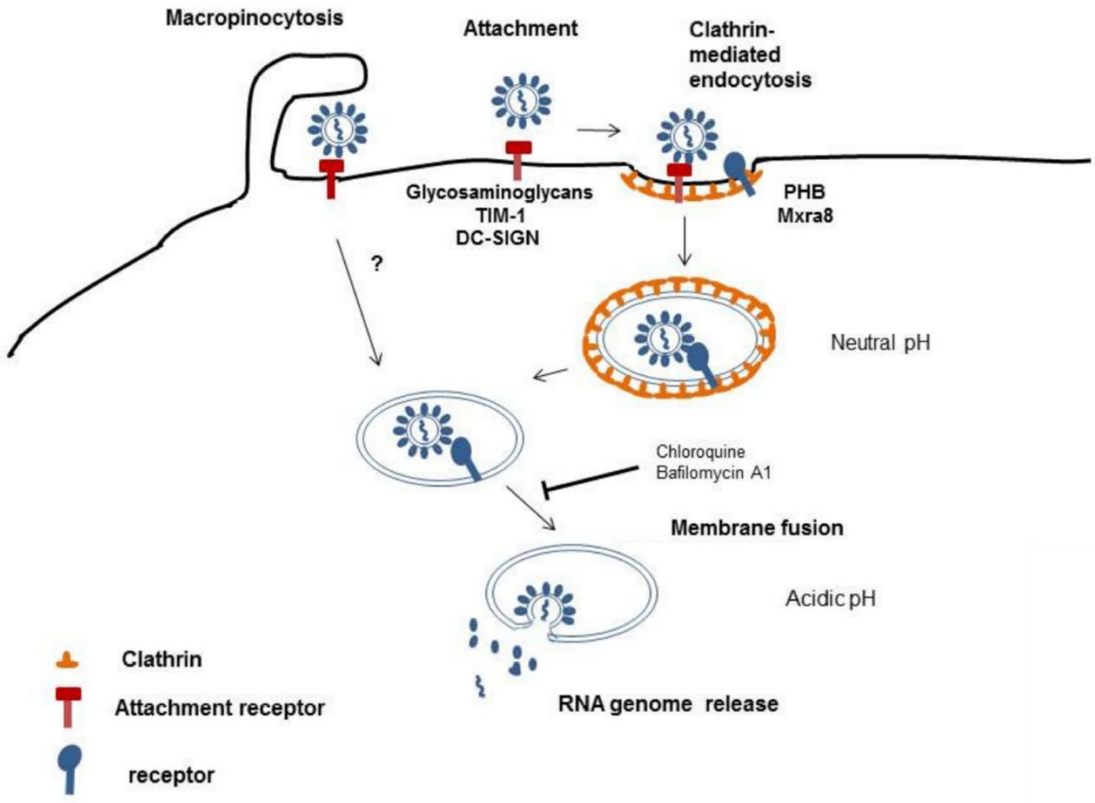

Figure 1.15 Schematic illustration of CHIKV cell entry.

Picture is taken from (Schnierle 2019).

1.4.2 Replication of CHIKV.

RNA replication of Alphaviruses take place in association with cellular membranes (Paul & Bartenschlager 2013, Salonen et al 2005). By modifying various membranes, the alphaviruses generate thousands of small membrane invaginations known as spherules (Spuul et al 2010). It is assumed that one spherule corresponds to one replication complex and thus contain one negative strand RNA. The spherules arise concomitantly with RNA synthesis, and it is interesting to note that the size of the spherules is determined by the size of the replicating RNAs, whereas the spherule size appears to be fixed by proteins involved in some other viruses (Kallio et al 2013). Those spherules are quite stable and can be active for several hours in producing multiple positive-strand genomic and sub-genomic RNAs (Sawicki et al 2006). The interior of spherules is connected to the cytoplasm, which allows the exit of RNAs and nucleotides entry (Fig. 1.16).

In mammalian cells, spherules from many alphaviruses are formed on the plasma membrane, while in some alphaviruses they are later endocytosed and large vacuolated lysosomes were formed on the cytoplasmic surfaces of endosomes, which is known as type-1 cytopathic vacuoles (CPVs) (Chen et al 2013a, Frolova et al 2010, Spuul et al 2010). Host proteins must be involved in the formation of spherules. It has been shown that ESCRT proteins generated structures resembling spherules, which is involved in making internal vesicles on multivesicular endosomal structures. ESCRT proteins function in spherule formation were shown in some virus (Barajas et al 2009), and recent work indicated that ESCRT factors are recruited during CHIKV infection and are required for intracellular viral replication cycle (Torii et al 2020).

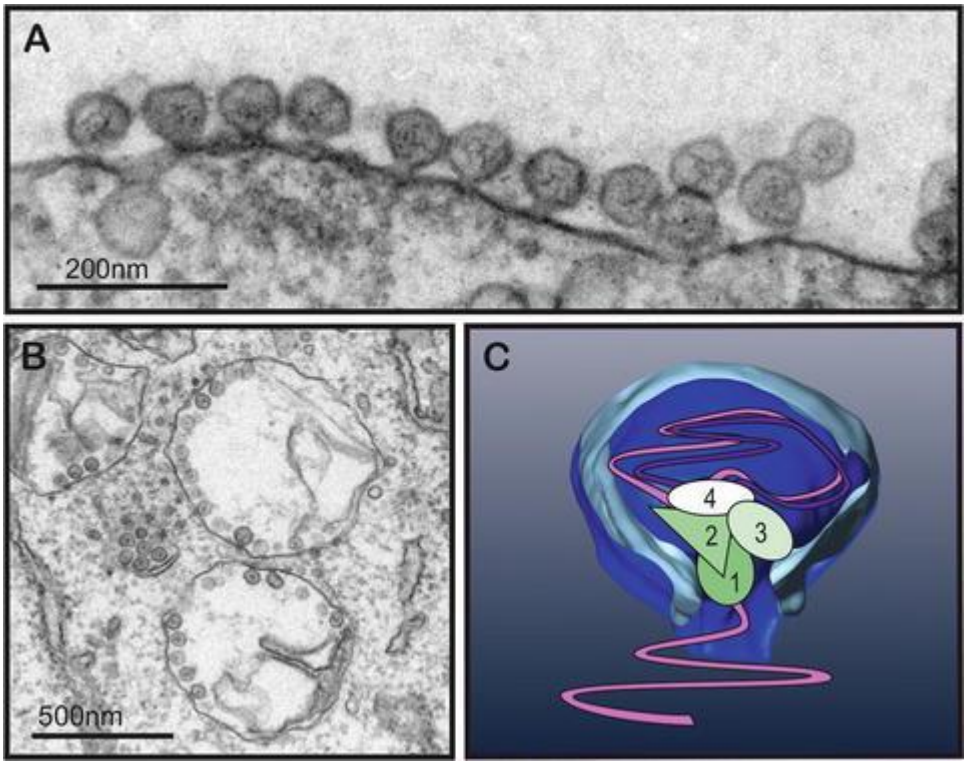

Figure 1.16 CHIKV RNA replication complex.

(A) CHIKV replication spherules at the plasma membrane. (B) CHIKV replication spherules on intracellular vacuoles. (C) Hypothetical model of a spherule. The dsRNA replicative intermediate is inside, and positive strand RNA is released to the cytoplasm through the neck. Picture is taken from (Ahola & Merits 2016).

Once alphaviruses enter the cells, translation of alphavirus genomic RNA resulted in the formation of non-structural polyproteins precursors (Strauss & Strauss 1994). The majority of the translation products is the P123 polyproteins, which can be up to ~90%, while less product of P1234 is produced due to readthrough of the opal stop codon at the junction region of nsP3 and nsP4 (Li & Rice 1993). However, some isolates of SFV and ONNV as well as laboratory-adapted CHIKV strains have an arginine codon in lien of the opal stop codon, which results in the only production of P1234. The avirulent SFV isolate with arginine codon mutation exist in the opal codon suggest the potential role in pathogenesis (Tuittila et al 2000). This is further supported by that disruption of the opal stop codon attenuates CHIKV arthritis and pathology (Jones et al 2017). The expression of non-structural polyproteins only occurs at the early stage of infection in mammalian cells before it is shut down 6-8 h post infection, due to global inhibition of cellular translation (Scholte et al 2013).

In order to generate functional replication complexes as well as non-structural proteins, the process of cleaving non-structural polyproteins is precise and highly regulated in a sequential manner (Fig. 1.17). The non-structural P1234 contains three cleavage sites, namely 1/2 (site between nsP1 and nsP2), 2/3 and 3/4 sites. All three cleavage sites are processed by protease activity in nsP2 or in polyproteins containing nsP2. For precise sequential cleavage, nsP2 must recognize each of the cleavage sites specifically, and previously it was thought that different affinities toward the three sites is responsible for the ordered cleavages (Lulla et al 2006). However, recent study of P1234 processing in SFV indicated a second mechanism, the cleavage sequences via long range interactions between different domains of P1234 play a major role in ordered cleavage (Lulla et al 2012, Lulla et al 2013a). Current data suggest that the cleavage patterns of P1234 in SFV and CHIKV are quite similar: to form functional replicase complexes, first 3/4 site is cleaved, followed by cleavage of 1/2 and finally by cleavage of 2/3 site (Vasiljeva et al 2003) (Fig. 1.17).

The P1234 is unable to initiate RNA synthesis until proteolytic processing at 3/4 site releases the nsP4 (Shirako & Strauss 1994). The P123 polyprotein in combination with nsP4 exhibit RNA synthetic activity resulting in the formation of negative strand RNA synthesis (Shirako & Strauss 1994) (Fig. 1.17). It is important and interesting to note that processed nsPs fail to assemble replication complexes and generate negative strand RNA, indicating the essential role of P123 as an intermediate. Assumptions have been made that each replicase complex make only one negative strand RNA before switching to positive-strand RNA synthesis. The switch from negative strand to positive strand RNA is connected to cleavage of 1/2 and 2/3 sites. Cleavage of the P123 into nsP1 and P23 efficiently witness the functional transition between the synthesis of negative sense to positive sense RNAs (Shirako & Strauss 1994). The final cleavage of 2/3 site may further facilitate the synthesis of sub-genomic RNAs. As a result, inhibition of minus-strand RNA synthesis is connected to overall viral nsPs shutoff as well as the rapid processing of the non-structural polyproteins. Positive sense RNA synthesis still occurs but is very inefficient if the two latter cleavages are blocked (Shirako & Strauss 1994), while it also indicated that cleavage of the P123 is not an absolute requirement for the transition from negative to positive-strand RNA synthesis. The synthesis of sub-genomic RNA is initiated from the sub-genomic promoter that is located on the negative-strand RNA. Mutations in nsP2 and nsP3 suggested that they might act as a transcription factor by binding to the sub-genomic RNA to recruit RNA synthesis complex (Gao et al 2019, Suopanki et al 1998). Although the template for positive-strand RNA synthesis is minus-strand RNA, evidences have shown that template remains double stranded (Kaariainen & Ahola 2002, Simmons & Strauss 1972a, Simmons & Strauss 1972b). This form of templating results in different dsRNA species, as when these dsRNAs were isolated by RNase treatment, three forms were released dubbed replicative forms (RFs). RFI, RFII and RFIII correspond to full-length genome, non-structural protein ORF and sub-genome respectively (Simmons & Strauss 1972a, Simmons & Strauss 1972b). As RFII is non-functional outside the intermediate, it is assumed that RFII is a paused genomic ternary complex, which can reactive and finish synthesis (Wielgosz &

Huang 1997). As a consequence of P1234 processing, only nsP1 show Met residue at N-terminal whereas N-terminal residues of nsP2, nsP3 and nsP4 of CHIKV are Gly, Ala and Tyr respectively (Ahola & Merits 2016). The native N-terminus indicates important requirements for functionality of nsP2 and nsP4, as some of their function can be abolished even by minor changes of a single N-terminal amino acid (Shirako & Strauss 1994, Vasiljeva et al 2003), and this is clearly the case for CHIKV nsP2 and presumably for nsP3 and nsP4 (Das et al 2014). This property indicates that nsPs have different functions or are involved in different interactions in their mature forms compared to the non-structural polyprotein form.

Although many of the enzymatic and nonenzymatic activities of nsPs have been characterized, it remains unclear how they function together as replication complexes to coordinate the polymerase, helicase and RNA capping activities. The issue is further complicated by how the recruitment and interaction of RNA template to the replication complexes. Overall, many of the replication mechanisms in CHIKV as well as other alphaviruses remain enigmatic, and new methods and technology are needed in the future to explore the multiple virus-host interactions involved in antiviral responses and viral replication mechanism including nsPs interactions with RNA.

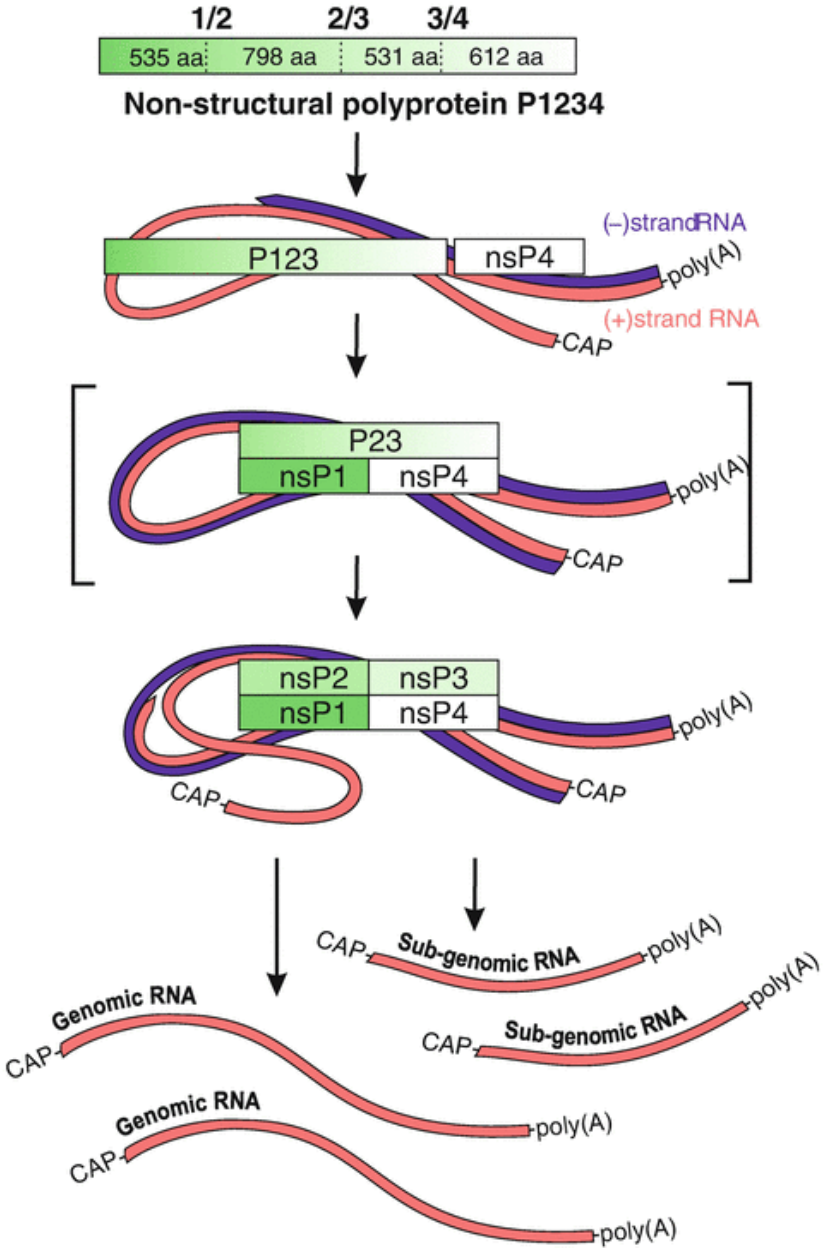

Figure 1.17 Processing of CHIKV non-structural polyproteins and synthesis of genomic RNA and sub-genomic RNA.

Top is shown with non-structural polyprotein P1234 and its cleavage sites as well as the size of each nsPs. The intermediate P123 plus nsP4 is required for synthesis of negative strand RNA, this is followed by the short lived nsP1+ P23 + nsP4 complex, then mature replication complexes are formed to produce genomic RNA and sub-genomic RNA. Picture is taken from (Ahola & Merits 2016).

1.4.3 Viral assembly, budding and maturation.

The assembly, budding and maturation steps of CHIKV remains largely unknown so far, and it is the same for other alphaviruses. Here data collected from previous studies provide a basic understanding of alphaviruses exist from cells. Virus assembly and budding require Capsid protein (Cp)-E2 binding, formation of E2/E1 heterodimer, pH protection of E2 by p62/E3-E2, and spike lattice assembly. Cp specifically packages the genomic RNA to assemble into NC into cytoplasm. Viral genomic RNA packing is favored over sub-genomic RNA and cellular RNA, even though the cellular RNA is present in molar excess over genomic RNA. The exact mechanism is not well understood, but studies in alphaviruses identified nucleotide sequences as packaging signals that promote genomic RNA packaging (Frolova et al 1997, White et al 1998). Previous study showed that SINV, EEEV, WEEV and VEEV have packaging signals that can be recognized by Cp, however, this does not apply to CHIKV and other viruses in SFV clade (Kim et al 2011). They contain packaging signals in nsP2 gene, but their capsid retains the ability to use nsP1-specific packaging signals of other alphaviruses.

Alphaviruses budding is temperature and pH dependent, with optimal budding at physiological temperatures and at a neutral to mildly alkaline pH (Lu et al 2001b, Lu & Kielian 2000). Alphaviruses bud through the plasma membrane in both mammalian and mosquito cells (Lu & Kielian 2000). Although not explicitly required, budding is significantly enhanced by 6K, TF, and cholesterol in unknown mechanisms (Lu & Kielian 2000). The p62/E1 heterodimer is acid resistant and protects E1 from prematurely fusing in the acidic environment of the trans-Golgi network (~pH 6.0) (Wahlberg et al 1989). During alphavirus budding, NC undergo a maturation event and it requires binding to E2 for appropriate targeting to cell membrane (Suomalainen et al 1992). Using RRV-SINV chimeras it showed that capsid-E2 interactions involved 33 aa residues of E2, which is also found in CHIKV (Lopez et al 1994). The NC, E1 and E2 glycoproteins are phosphorylated (Liu et al 1996). Previous study indicated that some of the phosphorylation might play a role

in assembly or post-assembly step, as addition of protein kinase or phosphatase inhibitors interfere with viral maturation (Liu & Brown 1993).

The whole life cycle of CHIKV is depicted in Figure 1.18.

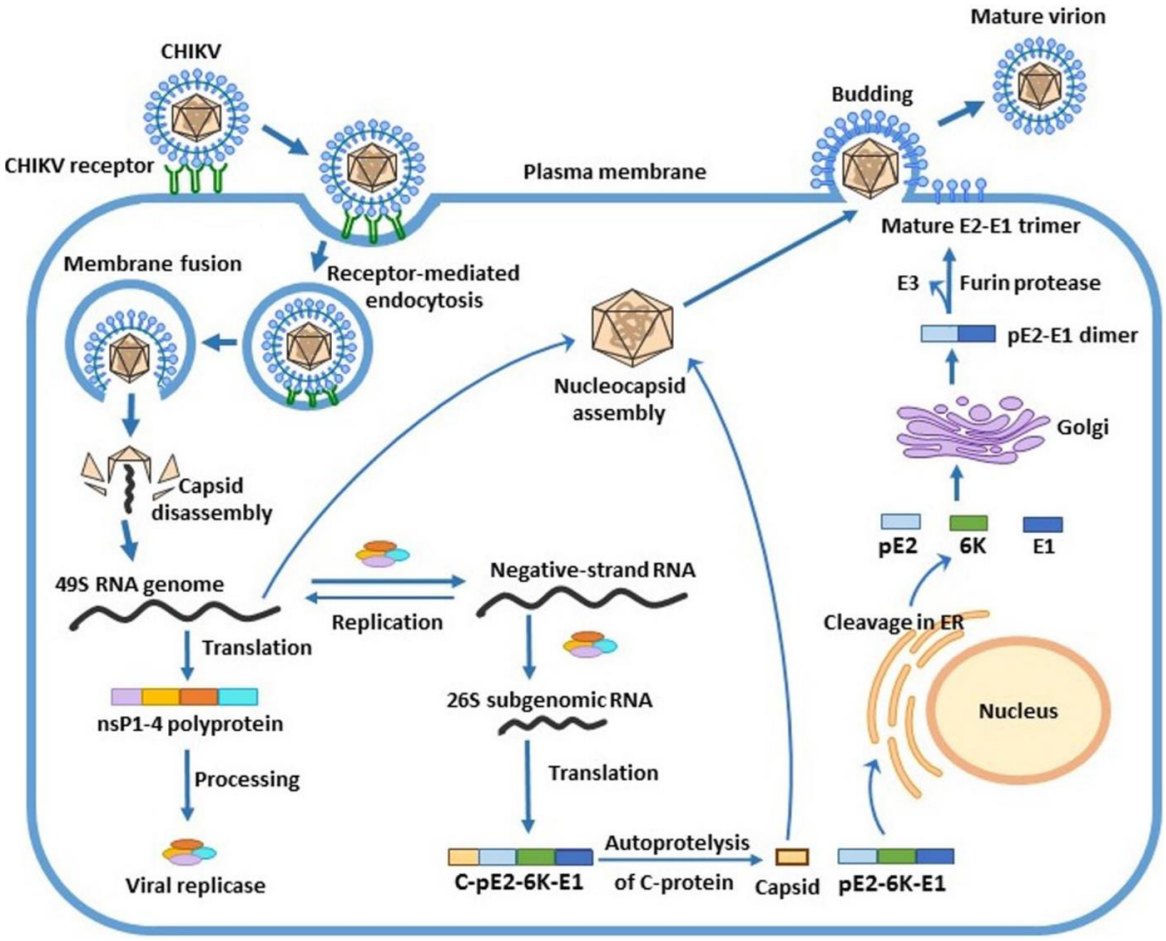

Figure 1.18 Schematic representation of CHIKV life cycle.

CHIKV enters the cells first by binding of E2 protein to receptors on cell surface, followed by endocytosis. Inside the endosome, low pH trigger fusion of viral envelope with endosome membrane, leading to nucleocapsid release into cytoplasm, followed by disassembly to liberate viral genome. The viral genome is then translated to produce non-structural proteins, which is processed and form replicase complexes to initiate RNA synthesis. The RNA synthesis includes the genome RNA and sub-genomic RNA using the newly synthesized minus-strand RNA as template. The sub-genomic RNA is translated into structural polyprotein (C-E3-E2-6K-E1), which is then cleaved to produce individual structural proteins. Those structural proteins assemble the viral with positive strand RNA as well as nsPs. The assembled virus particle is finally released by budding through the plasma membrane, where the envelope is embedded as viral glycoproteins. Picture is taken from (Abdelnabi et al 2015).

1.5 Cellular activity in response to stress and ONNV.

1.5.1 Type I IFNs and PKR.

Type I IFNs are polypeptides that are secreted by infected cells, which induce cells-intrinsic antiviral states in infected and neighboring cells, resulting in the limitation of viral pathogens (Ivashkiv & Donlin 2014). The PKR is an intracellular sensor of stress and activated by virus infection, specifically by recognizing cytosolic dsRNA (Rojas et al 2010) or 5'-triphosphorylated RNA (Nallagatla et al 2007). Following detection of dsRNA (or 5'-triphpsphorylated RNA), eIF2α kinase PKR dimerizes and auto-phosphorylates threonine residues and therefore stabilizing the dimers and increasing its kinase activity, which results in rapid inhibition of translational initiation (Garcia et al 2007, Nallagatla et al 2011). Upon translational arrest, eukaryotic cells continue synthesize antiviral factors, for example type I IFNs and IFN-stimulated genes (ISGs) that need to be induced and translated (Liu et al 2012). To note, cytosolic dsRNA and 5'-triphosphorylated RNA can also be recognized by melanoma differentiation-associated gene 5 (MDA5, also known as IFIH1) or retinoic acid-inducible gene I (RIG-I, also known as DDX58) (Reikine et al 2014). Upon binding to viral RNAs, these structural related DEAD-box helicases signal via the adaptor protein mitochondrial antiviral signaling protein (MAVS) to promote the transcription of antiviral cytokines. However, it is still not clear how these newly synthesized mRNAs maintain access to the translation machinery during global translation inhibition.

Type I IFN induction plays a crucial role in antiviral innate immune responses. Signaling via the type I IFN receptors results in protein translation encoded by ISGs and establish an antiviral state in both infected and uninfected cells (Teijaro 2016). Among the ISG-encoded proteins, PKR is most closely related with translation arrest and stress granule (SG) formation. Although in uninfected cells, PKR is constitutively expressed, however, upon type I IFN treatment it is further induced (Garcia et al 2007) and the activity of PKR is increased (Nallagatla et al 2007).

1.5.2 Stress granules (SGs) and its antiviral effects.

SGs are large cytoplasmic foci that are nucleated by the accumulation of stalled 48S translation initiation complexes in response to stress (Kimball et al 2003), which contain translationally-stalled mRNAs, pre-initiation factors and RNA binding proteins. Many signaling proteins are also transiently recruited to SGs and influence their assembly (Kedersha et al 2013). The most known pathway of SG formation initiates with phosphorylation of eIF2α by four eIF2 kinases, including PKR (Srivastava et al 1998), PKR-like endoplasmic reticulum (ER) kinase (PERK) (Harding et al 2000a, Harding et al 2000b), heme-regulated inhibitor (HRI) (McEwen et al 2005) and general control non-depressible protein 2 (GCN2) (Wek et al 1995). Other alternative pathways include inhibition of eIF4A RNA helicase (Dang et al 2006, Kim et al 2007, Mazroui et al 2006) and viral infection (Mazroui et al 2006). As described before, PKR is a component of IFN response and can be activated by RNA viruses producing double-stranded RNA replication intermediates and PERK is activated by ER stress associated with viruses that many express glycoproteins. HRI is activated by heme deprivation and oxidative stress; GCN2 is activated by nutrient starvation and not commonly linked to virus infection, although GCN2 binding to SINV induces its activation (Berlanga et al 2006). SGs, the transient, non-membrane-bound organelles, are hubs of stalled translation initiation machinery, including 40S ribosome subunits and subunits of eIF4F complexes (Kedersha et al 2002, Mazroui et al 2006). SGs also contain many RNA-binding proteins, some of them are markers of SGs such as T-cell restricted intracellular antigen 1 (TIA-1), TIA-1 related protein (TIAR) and RasGAP SH3-domain binding protein 1 (G3BP1) (Kedersha et al 1999, Tourriere et al 2003). Most SG components exhibit short residence times (seconds) whereas SGs themselves persist for minutes to hours, fusing with each other or other RNA granules (Kedersha et al 2013).

SG formation is a manifestation of robust translation arrest, however, the formation of SGs themselves are not required for translation arrest (Ohn et al 2008). Recently, SG have been shown to be signaling platforms and their transient

existence alters multiple signaling pathways by intercepting and sequestering signaling components. For example, as described before, cytosolic dsRNA and 5'-triphosphorylated RNA can also be recognized by MDA5 and RIG-I apart from PKR. The PKR (Reineke et al 2015), RIG-I (Onomoto et al 2012), MDA5 (Langereis et al 2013), polyubiquitin chains (Kwon et al 2007), ubiquitin ligases TRIM25 (Sanchez-Aparicio et al 2017) and TRAF2 (Kim et al 2005) are recruited to SG that are formed in response to eIF2α phosphorylation.

Inactive PKR was shown to be specifically recruited to SG by interaction with G3BP1 and cell cycle-associated protein 1 (CAPRIN1) (Schulte et al 2016). This recruitment results in PKR activation independent of sensing dsRNA, creating a positive amplification loop of PKR activation. In another study, knockdown of G3BP1 or PKR in HeLa cells that were infected with influenza A virus lacking NS1 inhibited SG formation and also suppressed the IFNβ mRNA induction (Onomoto et al 2012). As type I IFN induction in response to virus infection is mediated mainly by RIG-I, diminished type I IFN induction in the absence of SG formation suggests that SG might be important for RIG-I signaling. DHX36, a protein that may link SG formation and RIG-I signaling, augments eIF2α phosphorylation, SG formation and IRF3 activation in virus-infected or poly(I:C)-transfected cells (Yoo et al 2014). TRAF2, one of the first signaling molecules, was unable to relay signals to induce apoptosis following tumor necrosis factor receptor activation upon recruitment to SG (Kim et al 2005). Thus it is proposed that SG may promote cell survival under stress via suppressing pro-apoptotic signaling cascade. G3BP1 also has a positive effect on the activation of NF-kB and the kinase of JUN N-terminal (JNK) pathway that, together with IRF3, are required for the induction of type I IFNs and other cytokines (Reineke & Lloyd 2015). It was also proposed that the concentration of cytoplasmic viral RNA sensors, along with their signaling cofactors and viral RNA ligands, might be able to increase virus recognition by innate immune sensors and may even be required for their full activation (Onomoto et al 2012).

In general, most viruses antagonize SG formation during infection, although in a few cases some viruses induce and exploit portions of SG responses during their infectious cycle. Viruses that first induce then inhibit SG include mammalian orthoreovirus (MRV) (Qin et al 2009), SFV (McInerney et al 2005), Poliovirus (Mazroui et al 2006, White et al 2007), hepatitis C virus (HCV) (Ariumi et al 2011), etc. MRV induce SG formation via an eIF2α phosphorylation dependent mechanism. At early time points, SG are triggered by viral entry; viral gene expression then led to the inhibition of SG as infection progressed (Qin et al 2009). The ability of MRV to translate under stress was by exogenous stressors correlated with the absence of SG. Similar to MRV, SFV induced SG at early times during infection in an eIF2α dependent manner and prevent SG formation by exogenous stressors at late times post infection, but the induction of SG required viral replication (McInerney et al 2005). Viruses that inhibit SG formation include Rotaviruses (Montero et al 2008), West Nile and dengue virus (Emara & Brinton 2007), Herpes simplex 1 virus (Esclatine et al 2004), HIV-1 (Abrahamyan et al 2010). West Nile virus and dengue virus inhibit SG formation in response to exogenous stress by sequestering TIA-1 and TIAR and inhibiting their binding to the minus strand 3'-terminal stem-loop structure (Emara & Brinton 2007), which is shown to be required for viral replication (Li et al 2002). Viruses that tolerate or exploit SG include Respiratory syncytial virus (Lindquist et al 2010), mouse hepatitis coronavirus (Smith et al 2006), vaccinia virus (Katsafanas & Moss 2007), etc. Vaccinia virus is a DNA virus that may utilize aspects of SG response by subverting SG components into novel aggregates forming SG-like structure, which share properties with SG but crucially different as they don't contain translationally silenced mRNAs (Katsafanas & Moss 2007).

1.5.3 Cold shock proteins.

Cold shock proteins are multifunctional RNA/DNA binding proteins, which are characterized by the presence of the one or more cold shock domains (CSD). The nucleic acid binding properties endows these proteins with pleiotropic functions, for

example, regulating cellular transcription, translation and splicing (Brandt et al 2012, Lindquist et al 2014).

Cold shock proteins were first discovered in bacteria, with a sudden temperature drop from 37°C to 10°C induced a 200-fold increase in cold shock protein A expression, and this was independent of transcriptional activity (Gottesman 2018, Jones & Inouye 1994). A recent study using genome-wide methods to analyse the global changes occurring in bacteria during the cold shock response supported the observation (Zhang et al 2018b). They identified RNase R and cold shock protein A to be the major players. Cold shock protein A melts double-stranded RNAs while RNase R degrades misfolded RNA to enable translation.

In humans, the predominant group of cold shock proteins is the Y-box protein family. The prototypic member is the Y-box binding protein-1 (YB1), also known as DNA binding protein B, which is encoded by YBX1 gene. Two additional family members are DNA binding protein A and C, encoded by YBX3 and 2 genes, respectively. Another member of the cold shock proteins family is upstream of N-RAS (UNR) (Anderson & Catnaigh 2015, Ray et al 2015), UNR was initially identified as a regulator of N-Ras expression (Jeffers et al 1990), but later it turned out that UNR encodes a proteins with 5 CSD, which undergoes alternative splicing (Boussadia et al 1993, Doniger et al 1992, Jacquemin-Sablon et al 1994), an then it was renamed CSD containing E1 (CSDE1). UNR works together with the polypyrimidine-tract-binding protein to regulate translation and mRNA stability (Mitchell et al 2001, Sawicka et al 2008). In Dengue virus infections, YB1 inhibits virus production by binding to 3’ untranslated region and suppresses viral RNA translation (Paranjape & Harris 2007). YB1 was shown to be associated with nsP3 of SINV and the complexes locates on both endosomal membranes as well as nucleus (Gorchakov et al 2008). However, the importance of this interaction remains to be determined.

1.5.4 ONNV biology and disease.

ONNV is a mosquito-borne virus, belonging to *Alphavirus* genus, *Togaviridae* family. It was first isolated in Uganda in 1959 (Williams & Woodall 1961). Unlike other members of the *Alphavirus* genus, ONNV is primarily transmitted by anopheline mosquitoes (Corbet et al 1961). CHIKV and ONNV diverged from a common ancestor thousands of years ago (Powers et al 2000), and thus ONNV is genetically and serologically related to CHIKV (Williams & Woodall 1961), although ONNV infection is restricted to African continent. Infection of ONNV in humans is self-limiting, with clinic signs of low grade-fever, headache, rash and more distinct signs of lymphadenopathy and joint pain without effusions (Rwaguma et al 1997).

1.6 Aims and objectives.

CHIKV is an arthropod-borne positive sense RNA virus that transmitted from mosquitoes to humans and other livestock, which causes economic loss and public health concern. The recent outbreaks of CHIKV epidemic led to CHIKV infection with wider epidemic ranges and more severe public health issue. Until now, there are still no safe and effective vaccines or antiviral therapies. To find efficient antiviral targets or attenuated vaccine, a deep understanding of the mechanism of how CHIKV replicate in both the vertebrate host and the vector is required. Previous work in our laboratory identified AUD in virus assembly by binding to sub-genomic promoter (Gao et al 2019). This project aims to explore other functions of AUD in alphavirus replication.

The first step was to identify critical residues in the AUD that are required for CHIKV genome replication in mammalian or mosquito cells. To do this, conserved and surface exposed residues in the AUD were identified based on sequence alignment of different alphaviruses and the three-dimensional structure of SINV. These residues were mutated by a mutagenic strategy and introduced into a CHIKV dual-luciferase reporter system. The critical residues were further exploited in the context of infectious alphavirus virus.

Secondly, to explore the mechanism that induce the different replication phenotypes in mammalian and mosquito cells, temperature variance was studied. The investigation was based on the luciferase reporter system, protein expression and virus production. The effect of temperature variance was also investigated in other arboviruses.

Thirdly, to explore the mechanism behind temperature variance that regulates alphavirus replication, a number of anti-viral cellular responses were studied, including eIF2α phosphorylation, SG formation. The effect of cold shock proteins was also investigated in response to alphavirus replication.

The results shown in this study shed light on a hitherto unrecognized enhancement of alphavirus genome replication in mammalian cells at sub-physiological temperature, which reveal a role in the early stages of transmission of virus to mammalian via a mosquito bite. The discoveries of the temperature-sensitive mutants of AUD might also have the potential as vaccine candidate.

Chapter 2: Material and Methods

2.1 General materials

2.1.1 Bacterial strains

Escherichia coli (E.coli) DH5α: Genotype F-Φ80lacZ△(lacZYA-argF)U169recA1 endA1 hsdR17 (rk-, mk-) phoA supE44λ-thi-1 gyrA96 relA1 were used for molecular cloning. XL10-Gold® Ultracompetent cells: Tet^{r}D(*mcrA*)*183*△(*mcrCB-hsdSMR-mrr*)*173 endA1 supE44 thi-1 recA1 gyrA96 relA1 lac* Hte [F´ *proAB lacI^{q}Z△M15* Tn*10* (Tet^r) Amy Cam^r].

2.1.2 Cell lines

Mammalian cell lines include: C2C12 cells (mouse muscle myoblast cells), BHK-21 cells (baby hamster kidney cells), *Vero* cells (African green monkey kidney epithelial cells), RD cells (human muscle rhabdomyosarcoma cells), Huh7 cells (human hepatoma cells), Huh7.5cells (human hepatoma cells with defective in RIG-1 induced IFN antiviral signal), 293FT cells (human embryonal kidney cells transformed with the SV40 large T antigen). Two mosquito cell lines were applied: U4.4 (*Aedes albopictus* mosquito cells) and C6/36 cells (*Aedes albopictus* mosquito cells with a mutation in Dicer-2 gene and is RNAi defective) (Morazzani et al 2012).

2.1.3 Plasmids and viral constructs

All plasmids and CHIKV constructs generated are listed in Appendix Table 8.1. The CHIKV sub-genomic replicon with dual-luciferase reporter (CHIKV-D-Luc-SGR, donated by Prof Andres Merits), CHIKV SGR with mCherry fused within nsP3 and firefly luciferase (FLuc) replaced structural components (CHIKV-nsP3-Mcherry-FLuc-SGR), CHIKV SGR with FLuc replaced structural components (CHIKV-FLuc-SGR) were utilized. ONNV-2SG-ZsGreen (kind gifts from Prof Andres Merits) and full length CHIKV virus ECSA strain from an infectious clone (Tsetsarkin et al 2006) were used in the experiments. pcDNA3.1 (+) was used for subcloning of the ONNV nsP3 AUD mutants. Lentivirus vectors pCAG-HIVgp, pCMV-VSV-G-RSV-rev, pLKO.1-TRC cloning vector were used for ablation of cold shock proteins in RD cells.

2.1.4 Oligonucleotide primers

DNA oligonucleotides were ordered from Integrated DNA technologies and were resuspended in DEPC H_2O at the concentrations of 100 µM before stored at -20°C. Those primers are listed in the Appendix Table 8.2.

2.1.5 Antibodies

Primary antibodies include: rabbit anti-nsP3, rabbit anti-nsP1 (kind gifts from Prof Andres Merits, University of Tartu), J2 mouse anti-dsRNA antibody (Scisons), rabbit anti-G3BP antibody (Abcam), mouse anti-G3BP antibody (Proteintech), rabbit anti-TIA1 antibody (Thermo Fisher), rabbit anti-eIF4G antibody (Invitrogen), mouse anti-β-actin (Sigma Aldrich), rabbit anti-eIF2α (Cell Signaling) and rabbit anti-phosphorylated eIF2α (Invitrogen), rabbit anti-YB1 (Cambridge Bioscience), rabbit anti-UNR (Cambridge Bioscience), rabbit anti-SRSF5 (Thermo Fisher).

Secondary antibodies include: donkey anti-mouse (700 nm) (Li-Cor) and donkey anti-rabbit (800 nm), which were used for western blotting. Alexa Fluor chicken anti-rabbit (594 nm) (Thermo Fisher) and Alexa Fluor Goat anti-Mouse (647 nm) (Thermo Fisher) were used for immunofluorescence at a dilution of 1:500.

DAPI nucleic acid staining (Sigma).

2.2 Molecular Biology methods

2.2.1 Preparation of plasmids from *E.coli* cells

The CHIKV-D-Luc-SGR derived from an ECSA strain was gifted by Prof Andres Merit (University of Tartu). The dual luciferase include a Renila luciferase (RLuc) fused with nsP3 and a FLuc that replaced the structural components. In principle, 100 ng plasmid or 10 µl ligated products was mixed with 50 µl chemically competent DH5α *E.coli* cells. The mixture was kept on ice for 30 min, followed by addition of 950 µl Luria broth (LB) and incubated at 37°C for 1 h at 180 rpm. After 1 h, 100 µl of the mixture (or the resuspended pellet by centrifuge from ligation products) were coated onto the agar plates with appropriate antibiotics (ampicillin

100 µg/ml) and incubated at 37°C overnight. The next day, single colonies were picked from the plates and were added into 5 ml LB with the corresponding antibiotics and incubated at 37°C overnight at 180rpm. The following day, bacterial cultures were centrifuged at 4000 x g for 20 min at 4°C, then pellets were resuspended and plasmids were extracted using commercial Miniprep Kit following manufacturer's instructions (Qiagen). The purified plasmids were stored at -20°C freezer, and the plasmids in bacterial were stored in glycerol stock (25%) at -80°C freezer.

For transformation of WT and mutant ONNV, each plasmid was mixed with XL10 cells, followed by cultured in Tryptic soy broth (TSB) and coated onto the TSA plates with kanamycin 50 µg/ml at 37°C overnight. The next day, single colonies were picked from the plates and were added into 5 ml TSB with the corresponding antibiotics and incubated at 37°C overnight at 180rpm. Plasmids were extracted using commercial Miniprep Kit following manufacturer's instructions (Qiagen).

2.2.2 Amplification of DNA fragments by PCR

DNA fragments was amplified by PCR. The PCR reaction was performed in a total of 50 µl, including 10X Thermo® reaction buffer 5 µl, 10 mM dNTP 1 µl, 10 mM forward primer 2.5 µl, 10 mM reverse primer 2.5 µl, Vent® DNA polymerase 0.5 µl (NEB), template 1 µl (100 ng), nuclease-free water 37.5 µl. The PCR reactions started with an initial denaturation step at 95°C for 5 min followed by 30 cycles of a second denaturation step at 95°C for 30 s, annealing step at suggested Tm value for 30 s and extension step at 72°C for 1 min/kb. The final step was an extra extension at 72°C for 5 min.

2.2.3 DNA and RNA agarose gel electrophoresis

To purify and separate DNA fragments from PCR, DNA agarose gels were made with 1% (w/v) agarose diluted in 1X TAE buffer (40 mM Tris, 20 mM Acetic acid and 1 mM EDTA), the mixture were heated by microwave to completely dissolve agarose and then cooled down to ~50°C and SYBR® safe DNA gel Stain (Invitrogen) was added (1:20000). After the gels were set, they were immersed

with 1X TAE, DNA ladder was then added together with DNA samples (mixed with 5X gel loading buffer (NEB)) to each well of the gels, followed by electrophoresed at a voltage of 80 V with corresponding time (60-120 min depending on the DNA length). DNA samples were visualized by ultraviolet illumination with Gene Genius bio-imaging system (Syngene).

To verify the quality of RNA samples, RNA gels were made with 0.3 g 1% (w/v) agarose diluted in 28.6 ml 1X MOPS buffer (2 mM sodium acetate, 1mM EDTA and 20 mM MOPS). After the mixture were heated by microwave and cooled down, 1.4 ml paraformaldehyde (37%) and 1.5 µl SYBR® safe DNA gel Stain (Invitrogen) were added. After RNA gels were set, ssRNA ladder and RNA samples (mixed with 2X RNA gel loading dye (Invitrogen)) were added to each well of RNA gel, which was immersed in 1X MOPS buffer. Gels were run at 70 V for 60 min to 90 min before visualized with UV light using the Gene GENIUS Bioimaging system (Syngene).

2.2.4 DNA purification from DNA agarose gel

After gel electrophoresis, DNA bands were visualized with blue-light excitation. The desired bands were then cut out with knife blades and placed into 1.5 ml microtubes. The purification procedure was performed following the instructions of Monarch® DNA Gel Extraction Kit (NEB).

2.2.5 DNA and RNA quantification

Purity of plasmids, DNA fragments and RNAs were measured using a NanoDrop 1000 Spectrophotometer (Invitrogen). Absorbance at 260 nm was used to measure the concentration. The ratio of A260/A280 is used to determine protein contamination with DNA between 1.8 and 2.0 while RNA between 2.0 and 2.5. The ratio of A260/A230 is used to determine salt contamination and phenol contamination with purified value at 2.0.

2.2.6 Endonuclease digestion with restriction enzymes

For linearization of WT and AUD mutants in CHIKV-D-Luc-SGR or ONNV-2SG-ZsGreen, plasmids were performed in 50 µl mixtures including 10 µg plasmid DNA,

1 µl NotI-HF (CHIKV-D-Luc-SGR) or PmeI-HF (ONNV-2SG-ZsGreen), 5 µl 10X Cut smart buffer (NEB), and nuclease-free water, followed by incubation at 37°C overnight. For other DNA fragments or plasmids, DNA fragments or plasmids were digested for 2 h at 37°C, including DNA 2 µg, restriction enzyme 1µl, 5 µl 10X corresponding buffer (NEB or Thermo fisher) and nuclease-free water. For the purification of DNA fragments or plasmids vectors, they were separated by DNA agarose gel (see 2.2.3) and purified by gel purification kit (see 2.2.4).

2.2.7 Ligation

After digestion with restriction enzymes and DNA purification, DNA fragments and vectors were ligated with T4 DNA ligase following the manufacturer's instructions (NEB). The mixtures were incubated at 16°C overnight, followed by transformation into DH5α or XL10 cells (ONNV plasmids).

2.2.8 Site-directed mutagenesis

In order to generate AUD mutants in CHIKV-D-Luc-SGR, Q5 Site-Directed Mutagenesis kit was used following the protocol: Q5 Hot Start High Fidelity 2X Master Mix 12.5 µl, 10 µM Forward Primer 1.25 µl, 10 µM Reverse Primer 1.25 µl, Template DNA (25 ng/µl) 1 µl, Nuclease-free water 9.0 µl. The reaction started with initial denaturation at 98°C for 30 s, followed by 25 cycles of denaturation at 98°C for 10 s, annealing at 68°C for 30 s and extension at 72°C for 7 min, the final extension is at 72°C for 2 min. The second step is KLD reaction (Kinase, ligase and DpnI treatment), which include 1 µl of the PCR product, 5 µl of 2X KLD Reaction Buffer, 1 µl of 10X KLD Enzyme Mix and 3 µl of nuclease-free water. The mixture was incubated at 37°C for 30 min. 5 µl of the mixture was then transformed into DH5α or XL10 cells (described in 2.2.1). The plasmids were then sent for sequencing (Fig. 2.1).

As for the mutants of ONNV-2SG-ZsGreen, due to its large sequence, the ONNV-2SG-ZsGreen was first digested by XmaI and NheI separately (see 2.2.6) followed by purification of ONNV nsP2/3 fragment (detail in 2.2.4). The ONNV nsP2/3 was then ligated with the pcDNA3.1 vector (digested by XmaI and NheI) followed by

transformation and sequencing analysis. Following the generation of pcDNA3.1-ONNV-nsP2/3, Q5 site directed mutagenesis were performed as described. A schematic is shown for the generation of mutants from pcDNA3.1-ONNV-nsP2/3 (Fig. 2.2).

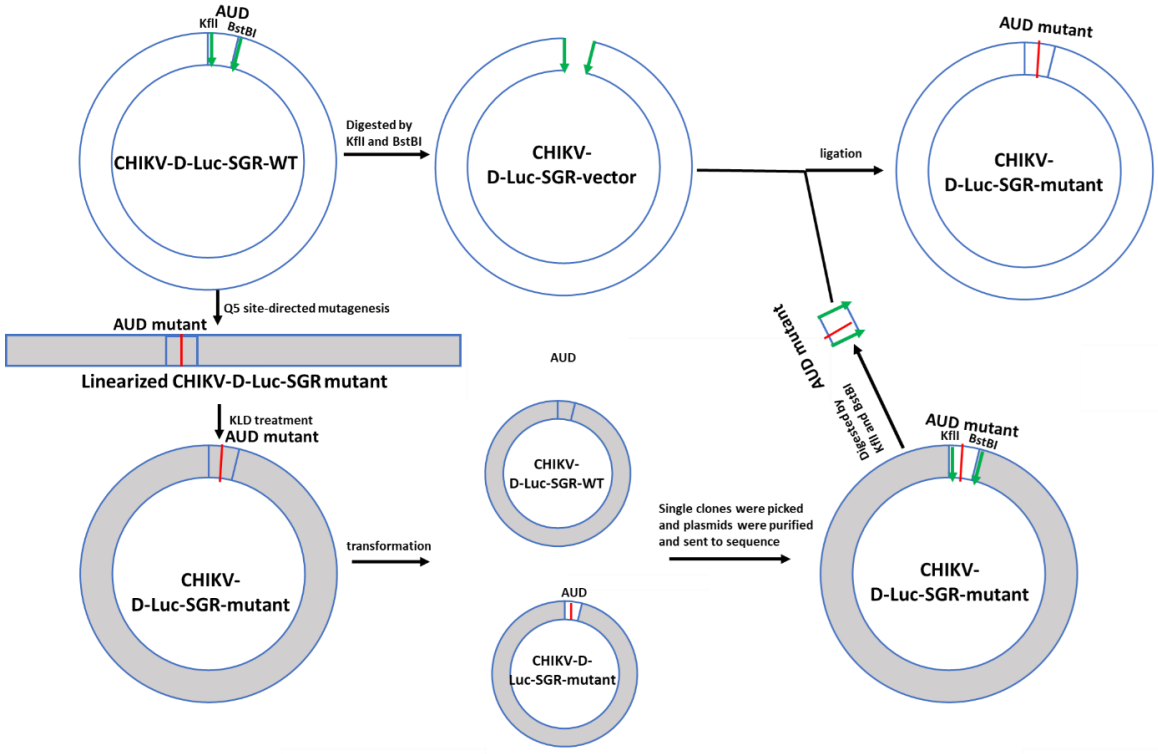

Figure 2.1 Schematic of construction of CHIKV-D-Luc-SGR mutants.

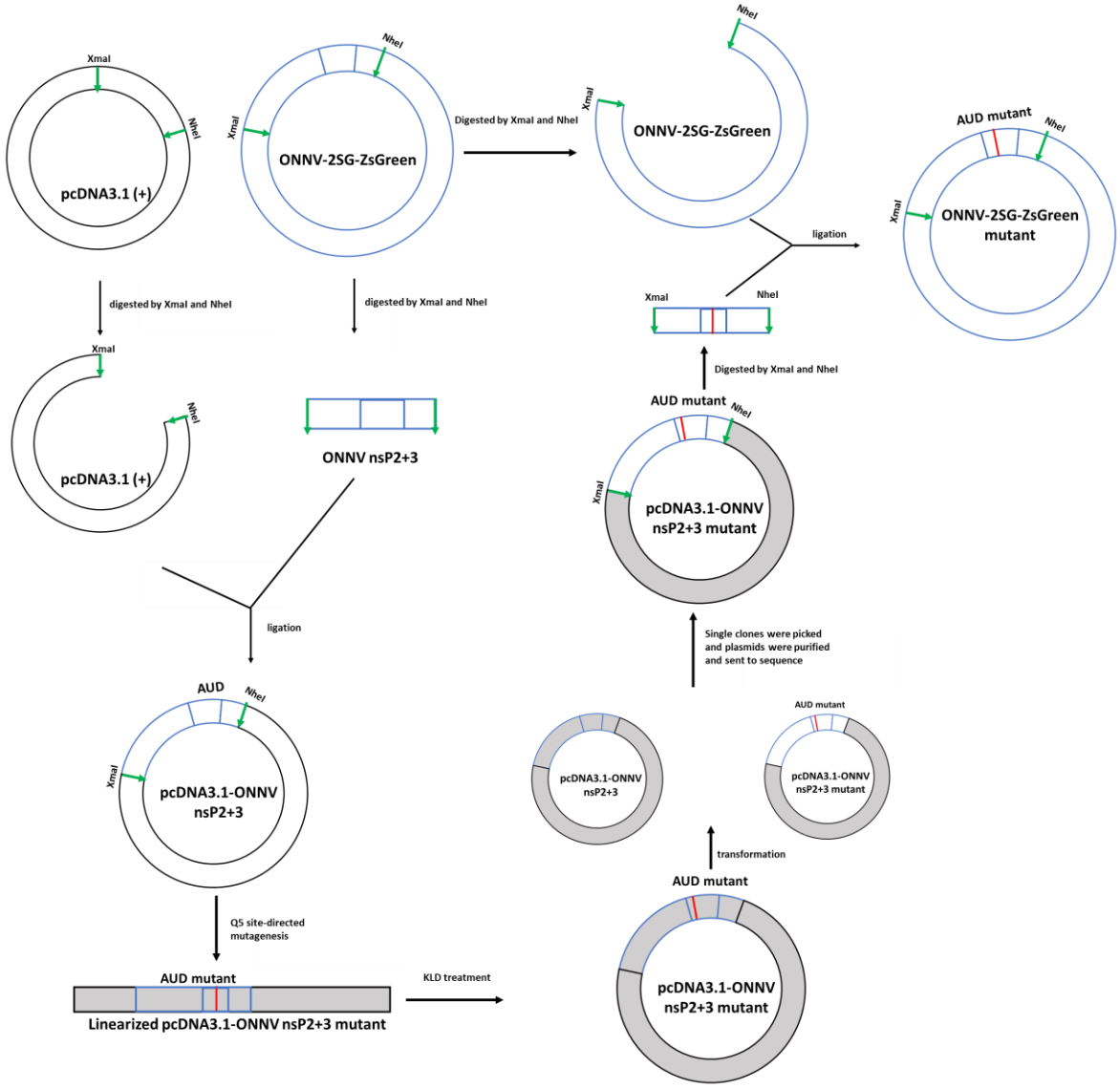

Figure 2.2 Schematic of construction of ONNV-2SG-ZsGreen mutants.

2.2.9 Construction of the AUD mutants in the context of CHIKV-D-Luc-SGR, ICRES-CHIKV and ONNV-2SG-ZsGreen

To generate the mutant constructs of CHIKV-D-Luc-SGR, the plasmids with expected mutations were digested by KflI and BstBI and DNA fragments of AUD mutants were purified, followed by ligation with the backbone of CHIKV-D-Luc-SGR or the backbone of ICRES-CHIKV infectious clone (Tsetsarkin et al 2006). The mixtures were transformed separately into DH5α cells following the protocols, the plasmids were then extracted and sequenced.

For mutant constructs of ONNV-2SG-ZsGreen, the plasmids with expected mutations were digested by XmaI and NheI separately, and DNA fragments of ONNV nsP2/3 mutants were purified, followed by ligation with the backbone of ONNV-2SG-ZsGreen. The mixtures were transformed separately into XL10 cells (details in 2.2.1). The plasmids were then extracted and sequenced.

2.2.10 Purification of linearized plasmid DNA

As described in 2.2.6, linearized plasmids were confirmed by gel electrophoresis. Following this, the linearized plasmids were purified by phenol: chloroform mixture and were used as templates for RNA transcription. Protocol as follows: first nucleus-free water was added to restriction enzyme mixture in a final volume of 200 µl, then equal volume of phenol: chloroform: isoamyl alcohol (25:24:1), mixture was added. Each of the samples was vortexed thoroughly for 1 min before being centrifuged at 13, 000 rpm for 5 min. The upper aqueous phase layer was transferred into a fresh Eppendorf tube (170 µl) and mixed with equal volume of chloroform by vortexing for 1 min, which was followed by centrifugation at 13, 000 rpm for 5 min. Upper aqueous phase layer was transferred into new Eppendorf tubes (each tube 130 µl), and two volumes of ethanol and 0.1 volume of 3 M Sodium Acetate (pH 5.2) were added to precipitate the DNA. The mixture was stored at -20°C overnight. The next day, the mixture was centrifuged at 13, 000 rpm for 20 min at 4°C. The pellet was washed with 70% ethanol once and air-dried before resuspended with 20 µl nuclease-free water. The DNA concentration was measured before being used as a template for RNA transcription.

2.2.11 *In vitro* RNA transcription and purification

To generate RNA, linearized plasmids of WT and mutants in the context of CHIKV-D-Luc-SGR or ONNV-2SG-ZsGreen were used as templates for RNA transcription. For each *in vitro* transcription, 1 µg of DNA template was added to fresh PCR tubes, followed by 2X NTP/CAP solution 10 µl, 10X Reaction Buffer 2 µl (room temperature (RT)), SP6 Enzyme Mix 2 µl, nucleus-free water to a total of 20 µl (mMACHINE™ SP6 Transcription Kit (Thermo Fisher)). The mixture was mixed properly and incubated at 37°C for 2 h, and then treated with 1 µl of Turbo DNase

and incubated at 37°C for 15 min. To purify RNA after *in vitro* transcription, RNA was immediately stored on ice and mixed with 30 µl of Lithium Chloride and 30 µl nucleus-free water and transferred to -20°C freezer overnight. The next day, the unpurified RNA was centrifuged at 13, 000 rpm for 20 min at 4°C. The RNA pellet was washed with 70% ethanol (in DEPC water) once and air-dried on ice before resuspended with 40 µl nuclease free water. The RNA concentration was measured and its quality was verified by gel electrophoresis (detail in 2.2.3). Then RNA was stored at -80°C freezer.

2.2.12 Protein quantification

For those protein samples lysed by 1X Passive Lysis Buffer (PLB) (from Luciferase Kit, Promega) or 1X Glo Lysis Buffer (GLB, made in our laboratory), protein concentrations were measured using Pierce™ BCA Protein Assay Kit (Thermo Fisher). For the preparation of BSA standard samples, 2 mg Bovine serum albumin (BSA) was first dissolved in 1 mL of 1X PLB or 1X GLB, and gradient dilution samples were made as standard curves following the manufacturer's instructions. At the meantime, Cell lysate samples were diluted 5 times in 1X PLB or 1X GLB and transferred into 96 well plates together with gradient BSA dilutions. Each of the samples was mixed with 200 µl of BCA solution (prepared following manufacturer's instructions). The samples in 96 well plate was then covered with foil and incubated at 37°C for 30 min. After 30 min, the absorbance of the samples was measured at 570 nm with Infinite F50 plate reader and software Magellan For 50 (Tecan). Protein concentrations were then converted using linear regression equation.

2.2.13 Sodium dodecyl sulfate–polyacrylamide gel electrophoresis (SDS-PAGE)

SDS-PAGE was prepared consisting of separation gel and stacking gel. Separation gel was made with 10% (v/v) including acrylamide (30%), 1.5 M Tris pH 8.8, 10% (w/v) SDS, 10% (w/v) ammonium persulphate (APS), tetramethylethylenediamine (TEMED) and nucleus-free water. Stacking gels were made with 6% (v/v) including

acrylamide (30%), 0.5 M Tris pH 6.8, 10% (w/v) SDS, 10% (w/v) APS, TEMED and nucleus-free water. The protocols can be found on website https://www.cytographica.com/lab/acryl2.html. After gels were set, protein samples were mixed with SDS-PAGE loading buffer (62.5 mM Tris-HCl, pH 6.8, 10% (v/v) Glycerol, 2% (w/v) SDS, 0.01 % (w/v) Bromophenol blue, 5% (v/v) β-mercaptoethanol), and then were heated at 95°C for 5 mins and stored on ice. Each of the protein samples as well as protein ladder (Prestained Protein Standard, 11-245 kDa, Thermo Fisher) were loaded into empty wells immersed with 1X SDS-PAGE running buffer (25 mM Tris, 192 mM Glycine, 0.01(w/v) SDS). Gels were run in 1X SDS-PAGE running buffer at 180 V for 60 min.

2.2.14 Western Blotting

After protein samples were separated by SDS-PAGE, the gels were transferred onto polyvinylidene fluoride (PVDF) membrane (Immobilon®-FL PVDF membrane) pre-soaked with 100% methanol. Western Blotting Filter Papers (BOSTER) were pre-soaked in 1X transfer buffer (25 mM Tris, 192 mM Glycine, 20% (v/v) methanol). The order from bottom to top as follows: filter paper, PVDF membranes, gel, filter paper. Protein transfer was performed at 15 V for 1 h. After protein transfer, PVDF membrane was blocked with 50% (v/v) Odyssey blocking buffer (Li-Cor) diluted in 1X TBST ((25 mM Tris-HCl, pH7.4, 137 mM NaCl, 0.1% Tween-20) for 1 h at RT. After blocking, PVDF membrane was incubated with primary antibodies (1:1000 dilution in TBS with 25% (v/v) of Odyssey blocking buffer) and incubated at 4°C overnight. After primary incubation, PVDF membrane was washed 3 times with 1X TBST with 5 min for each wash, followed by secondary antibody incubation at RT for 1 h and 3-time washes with 1X TBST. Membranes were dried with new filter paper and then imaged through Li-Cor Odyssey Sa Imager (Li-cor).

2.3 Tissue culture work

2.3.1 Cells passaging

Of the mammalian cells used in the experiments, RD cells, *Vero* cells (typically don't secret IFNα/β), BHK-21 cells, Huh7 and Huh7.5 cells were cultured in Dulbecco's Modified Eagles Media (DMEM, Sigma) supplemented with 10 % (v/v) fetal bovine serum (FBS), 100 µg/ml streptomycin, 100 IU penicillin/ml, and 1 % non-essential amino acids (NEAA) (Lonza) in flasks or plates. RD-shCTL cells, RD-shYB1 cells, RD-shUNR cells, RD-shSRSF5 cells were cultured in complete media contains 3 µg/mL puromycin. C2C12 cells was cultured in the complete media with 20% FBS. Those flasks or plates were incubated in a humidified incubator at 37°C, 32°C or 28°C with 5% CO_2. When cells grew into confluency, cell media were removed and cells were washed with phosphate buffered saline (PBS) before trypsinized with trypsin-EDTA solution by incubation at 37°C for 3 min. Then cells were mixed with complete media to inactivate trypsin and diluted for next passage or other experiments.

For the two mosquito cell lines U4.4 and C6/36, they were cultured in Leibovitz's L-15 supplemented with 10% FBS, 10% tryptose phosphate broth (TPB) in flasks or plates in incubator at 28°C. When cells grew into confluency, media were removed and cells were washed with PBS. The mosquito cells were scraped off by scrapers with complete media for next passage or other experiments.

2.3.2 Transfection of Nucleic acid by lipofectamine 2000

Mammalian cells were seeded at 5X 10^4 per well in 24 well plate or 1X 10^5 per well in 12 well plate or 3X 10^5 per well in 6 well plate. The next day before transfection, media was removed and washed with PBS before replaced with opti-MEM™ (Thermo Fisher). Transfection reagent lipofectamine 2000 (Invirtogen) was mixed with plasmids or RNA following the manufacturer's instruction. In brief, 1 µg RNA was mixed with 100 µl opti-MEM and incubated in the tissue culture (TC) hood for 5 min, meanwhile 2 µl of lipofectamine was mixed with another 100 µl opti-MEM and incubated for 5 min. Then RNA and lipofectamine 2000 were mixed and

incubated at RT for 20 min before transferred to the cells. Each well was loaded with 50 µl of the mixture (24 well pate) or 100 µl of the mixture (12 well plate) or 200 µl of the mixture (6 well plate). The plates were incubated at 37°C, 32°C or 28°C for 4 h before washed with PBS and then replaced with fresh complete media.

2.3.3 MTT assay

To determine cell metabolic activity or the effect of ISRIB on CHIKV-D-Luc-SGR replication, MTT assay was performed. In brief, 48.6 mg of MTT was dissolved into 10 ml of PBS to a concentration of 12 mM. MTT was then filtered by 0.22 µm syringe filter and transferred to new tubes. The sterilised MTT was diluted to 6 mM with Phenol red free DMEM media (Doug). For cells at indicated time points, cell media was replaced with 150 µl phenol-red free DMEM media and filled with 30 µl 6mM MTT solution. Then cells were incubated at 37°C for 2 h in cell incubator and then cell media was replaced with 100 µl of DMSO. Cells with DMSO were wrapped with foil and mixed with an orbital shaker for 15 mins until MTT granules dissolved completely. Finally, cell absorbance was measured at 570 nm with Infinite F50 plate reader and software Magellan For 50 (Tecan).

2.3.4 Generation of cold shock protein ablated RD cell lines

To generate cold shock protein ablated RD cell lines, each of the shRNAs targeting human YB1, UNR and SRSF5 gene or a control shRNA (RD-shCTL) was designed on website (https://portals.broadinstitute.org/gpp/public/seq/search). The phosphorylated primers of shRNA were annealed to each other following the protocol (95°C 4 min, 70°C 10 min, then slowly cooled down to RT in 2 h). Then each of the annealed shRNAs was diluted to 1 ng/µl. The vector for shRNA insertion pLKO.1-TRC was digested with AgeI and EcoRI separately before being ligated with diluted shRNA. After transformation and amplification of plasmids from *E. coli* cells, plasmids were extracted and sent for sequencing. The successful generation of pLKO.1-TRC-shYB1, shUNR, shSRSF5 and shCTL were confirmed by sequencing analysis.

To generate lentiviruses that contain human shYB1, or shUNR, or shSRSF5 or shCTL, three plasmids pCAG-HIVgp, pCMV-VSV-G-RSV-rev and pLKO.1-TRC-shYB1, or shUNR, or shSRSF5 or shCTL were co-transfected into 293T cells in 10 cm dishes at a ratio of 1 µg: 1 µg: 1.5 µg. Lentiviruses from supernatants at 48 pht and 72 hpt were collected and stored at -80°C freezer. The lentiviruses were then mixed, filtered by 0.45 µm filter and aliquoted into 1 ml each.

To generate cold shock protein ablated cell lines in RD cells, RD cells were transduced with 1 ml of each of the lentiviruses containing shYB1, or shUNR, or shSRSF5 or shCTL as well as 1 ml of media (a negative control) in the presence of 8 µg/ml polybrene in 6 well plate. The supernatant in each well was replaced with complete media 6 h post-transduction. Cells were selected with puromycin (3.5 µg/ml) 72 h post-transduction until mock transduced cells were completely dead. The cold shock protein ablated RD cell lines were maintained in 2.5 µg/ml puromycin for passage.

2.4 Sub-genomic replicon work of CHIKV and other arboviruses

2.4.1 Dual luciferase assay

At 4, 12, 24, 48 or 72 hpt, cells transfected with CHIKV-D-Luc-SGR RNAs in 24 well plates were washed with PBS for 3 times and lysed with 100 µl of 1X PLB. Then each 50 µl of the lysed cell sample was transferred into white 96 well plate and dual luciferase activity were measured using the BMG plate reader which automatically added LARII and Stop & Glo reagents (Promega) into each well followed by the measurement of dual luciferase activity.

2.4.2 Single luciferase assay

Based on the CHIKV-D-Luc-SGR construct, CHIKV-nsP3-Mcherry-FLuc-SGR and CHIKV-nsP3-FLuc-SGR were generated by SpeI restriction digestion and ligation. At 4, 12, 24 or 48 hpt, cells were washed with PBS for 3 times and lysed with 100 µl of 1X PLB. Then each 50 µl of lysed samples was transferred to white 96 well

plate, and equal volume of LARI (Promega) was added to the plates and measured by the BMG plate Reader.

2.4.3 Mutant reversion sequencing

After transfection of CHIKV-D-Luc-SGR RNA, total cellular RNAs were extracted by TRIzol reagent at 24 hpt. Each of the cDNA was synthesized using SuperScript IV (Invitrogen) following manufacturer's instructions. 1 µl of cDNA were used as template for amplifying nsP3 encompassing AUD mutants by PCR. After DNA fragments were purified by gel electrophoresis, DNA fragments were sent for sequencing. All primers used were shown in Appendix Table 8.2.

2.4.4 Replication of BUNV and Zika virus SGRs at 28°C or 37°C

BHK-21 cells were transfected with Zika virus SGR and incubated at 28°C or 37°C. Cells were collected at indicated time points and Nano luciferase activities were measured and normalized to their respective 4 h values. BSR-T7 cells supplied with G418 were transfected with BUNV mini-genome and incubated at 28°C or 37°C. Cells were collected at indicated time points and RLuc activities were measured and normalized to their respective 4 h values.

2.4.5 Temperature shift assay of CHIKV-D-Luc-SGR

Cells were transfected with WT CHIKV-D-Luc-SGR and incubated at 37°C or 28°C. At 12 hpt, cells were either incubated at their temperatures or shifted from 37°C to 28°C or 28°C to 37°C. Cells were then lysed at indicated time points with 1X PLB and measured by dual luciferase kit (Promega), protein expression of nsP1, eIF2α and P-eIF2α were also detected by western blotting. Along with the temperature shift assay, cells growth number was counted and cell metabolic activity was determined by MTT assay. To verify the growth speed of C2C12 cells at 37°C or 28°C, cells were seeded into 24 well plates with 5×10^4 per well. At 4, 12 and 24 hpt, cell numbers were enumerated by trypsin digestion and resuspended in 1 ml fresh DMEM.

2.4.6 Replication of WT CHIKV-D-Luc-SGR with ISRIB at different temperatures

Previous report showed that 200 nM ISRIB works efficiently inside cells (Carmela et al, 2013). To determine the effect of ISRIB on WT CHIKV-D-Luc-SGR replication, C2C12 cells were transfected with WT CHIKV-D-Luc-SGR RNA, cells were then treated with 200 nM ISRIB at 2 hpt and incubated at 28°C, 32°C or 37°C. Cells were collected at indicated time points and dual luciferase activity were measured. Protein expression of nsP1, eIF2α and P-eIF2α were detected by western blotting.

2.4.7 Replication of WT and the mutants in the context of CHIKV-D-Luc-SGR in RD cold shock protein ablated RD cell lines at different temperatures

To determine replication of WT and mutant CHIKV-D-Luc-SGR in cold shock protein ablated RD cells, RD-shCTL, RD-shYB1, RD-shUNR and RD-shSRSF5 cells were seeded into 24 well plates. The cells in 24 well plates were not selected with puromycin as puromycin might also affect cellular translation. The next day, each of the cell lines was transfected with WT, W220A, R243A/K245A and GAA CHIKV-D-Luc-SGR RNAs and incubated at 37°C or 28°C. Cells were harvested at 4, 12 and 24 hpt and dual luciferase activities were measured.

2.5 Phenotype of WT and the mutants in the context ICRES-CHIKV

2.5.1 Virus production of WT and the mutants in the context of ICRES-CHIKV at 28°C or 37°C

WT and mutant ICRES-CHIKV RNAs were transfected into C2C12 cells and incubated at 37°C or 28°C. Supernatants were collected at 48 h post infection (hpi) and stored at -80°C. The cells were either washed with PBS and then fixed with 4% formaldehyde or treated with TRIzol reagent for total cellular RNA exaction. Mutant reversion sequencing was conducted to determine whether these mutants have reverted back to WT or showed other compensatory mutation sites. All the ICRES-CHIKV experiments were conducted in BSL3.

2.5.2 Plaque assays of WT and the mutants in the context of ICRES-CHIKV

To determine virus titers of WT and mutants ICRES-CHIKV, plaque assay was conducted on BHK-21 cells. In brief, virus from -80°C freezer was defrozen at RT and diluted in FBS-free media (from 10^{-1} to 10^{-6}). 200 µl of dilutions from WT and mutant viruses were spreaded onto cells in each well of 12 well plates. Cells were incubated at 37°C for 1 h. Then dilutions were removed and cells were washed with PBS, followed by replaced with 1 ml of 0.8% Methylcellulose (MC) (1:1 in complete media) and incubated at 37°C (as 28°C failed to form detectable plaques). After 48 h, MC was removed and cells were washed by PBS before deactivated with 4% formaldehyde for 30 min. The 4% formaldehyde was then discarded and cells were stained with crystal violet dye (0.25% (w/v) crystal violet, 10% ethanol, 35 mM Tris, 0.5% (w/v) $CaCl_2$ and 90% dH_2O) by incubated for 30 min at RT. The crystal violet was then discarded and viral titers were determined by counting plaque numbers. Meanwhile, plaque sizes were also determined. The experiments were repeated independently for 3 times.

2.5.3 Mutant reversion sequencing of ICRES-CHIKV mutants

Cells transfected with ICRES-CHIKV mutant RNAs from 37°C or 28°C were extracted by TRIzol reagent at 48 hpi, followed by phenol-chloroform purification (detail in 2.4.3). The total cellular RNA from mutants were extracted and their concentrations were measured. cDNAs of mutants were synthesized using a LunaScript8482 RT SuperMix Kit (NEB) following manufacturer's instructions. Protocols as follows: 5X NEB reverse transcription buffer 4 µl, total RNA 1 µg, Reverse transcription enzyme 4 µl, nucleus-free water added to a total of 20 µl. The mixture was incubated at 25°C for 5 min followed by 42°C for 10 min. The DNA fragments encompassing the AUD mutants or all the non-structural components were synthesized by PCR using Vent polymerase, followed by purification and sequencing analysis.

2.6 ONNV-2SG-ZsGreen work

2.6.1 Production of WT and the mutants in the context of ONNV by transfection

To produce WT and mutant ONNV, WT and mutant ONNV RNAs were transfected into C2C12 cells and incubated at 37°C or 28°C. The supernatants were collected and stored at -80°C freezer 48 hpi. Cells were then washed with PBS, fixed with 4% paraformaldehyde, scanned by EVOS microscopy (Nikon) and quantified by ImageJ or scanned and quantified by IncuCyte.

WT and the mutants ONNV were then titrated by plaque assays on BHK-21 cells at 28°C or 37°C. The details can be found in 2.5.2. Cells incubated at 37°C were fixed with 4% paraformaldehyde at 72 hpi whereas at 28°C it was fixed at 96 hpi. The plaques were determined from ZsGreen-positive cells scanned by EVOS microscopy.

2.6.2 Mutant reversion sequencing of AUD mutants in ONNV

Mutant reversion sequencing was similar as that of ICRES-CHIKV mutants. In brief, total cellular RNA from cells were extracted using TRIzol reagent and purified, followed by cDNA synthesis and PCR. As for sequencing, all of the non-structural proteins were sequenced for all the mutants incubating at 37°C, and nsP2-nsP3 proteins were sequenced for all the mutants from 28°C incubation. Then all of the non-structural proteins were sequenced for W220A and R243A/K245A incubating at 28°C.

2.6.3 Infection of WT and W220A ONNV in Vero cells

Vero cells were infected with WT and W220A ONNV at MOI 0.1 and incubated at 28°C or 37°C. Supernatants were collected at 48 hpi, cells were lysed with 1X GLB or fixed with 4% paraformaldehyde and scanned by IncuCyte. Protein expression of nsP1, P-eIF2α and eIF2α were determined by western blotting with each sample 20 µg. Virus titres of WT and W220A were titrated by plaque assay on BHK-21 cells at 28°C. Cells were fixed at 96 hpi and plaques were numerated by ZsGreen positive cells scanned by EVOS microscopy.

2.6.4 Temperature shift assay in the context of ONNV

C2C12 cells were infected with WT and W220A ONNV at an MOI of 0.2 and incubated at 37°C or 28°C, with and without a temperature shift assay from 37°C to 28°C or 28°C to 37°C. Cells were fixed with 4% paraformaldehyde at 48 hpi. ZsGreen expression and cells confluency were quantified by IncuCyte. Protein expression of nsP1, P-eIF2α and eIF2α were determined by western blotting with each sample 20 µg.

2.6.5 Infection of WT and W220A ONNV with and without ISRIB at different temperatures

C2C12 cells were infected with WT and W220A ONNV at MOI 0.1. After incubation at 37°C for 1 h, cells were replaced with complete media containing 200 nM ISRIB and incubated at 37°C, 32°C or 28°C. Cells were either fixed with 4% paraformaldehyde at 48 hpi, followed by ZsGreen scanned by EVOS microscopy, or lysed in 1X GLB. ZsGreen expression representing ONNV genome replication was quantified by ImageJ.

2.6.6 Infection of WT and mutants ONNV in cold shock protein ablated RD cell lines at different temperatures

RD-shCTL, RD-shYB1, RD-shUNR and RD-shSRSF5 cells were seeded into 24 well plates. The cells in 24 well plates were not selected with puromycin as puromycin might also affect cellular translation. The next day, each of the cell lines was infected with WT, W220A, R243A/K245A ONNV at an MOI of 0.1 and was incubated at 37°C or 28°C. Cells were fixed with 4% paraformaldehyde at 48 hpi and ZsGreen expression was scanned and quantified by IncuCyte.

2.6.7 One-step growth curve of WT and W220A ONNV in cold shock protein ablated RD cell lines at different temperatures

RD-shCTL, RD-shYB1, RD-shUNR and RD-shSRSF5 cells were seeded into 24 well plates. The cells in 24 well plates were not selected with puromycin. The next day, each of the cell lines was infected with WT ONNV at an MOI of 0.1 and was incubated at 37°C or 28°C. Cells were fixed with 4 % paraformaldehyde at 12, 24,

36 and 48 hpi and ZsGreen expression of all time points were scanned and quantified by IncuCyte. Virus titres at indicated time points from 28°C or 37°C were determined by plaque assays at 28°C.

2.6.8 SG formation by Immunofluorescence assay (IFA)

The day before infection, 19 mm glass coverslips were transferred into each well of 12 well plates followed by sterilized by 70% ethanol for 30 mins and washed with PBS for 3 times to remove ethanol residue. C2C12 cells were seeded into each well of 12 well plates at a density of 1X 10^5 per well. The next day, cells were mock infected or infected with WT ONNV at an MOI of 5 and incubated at 37°C or 28°C. 7 h later, mock infected cells were treated with 0.5 mM sodium arsenite ($NaAsO_2$). Cells were either fixed with 4% formaldehyde at 8 hpi, or treated with 100 µg/ml cycloheximide (CHX) in $NaAsO_2$ treated cells or ONNV infected cells or for 45 min prior to fixation. The coverslips were then stored at 4°C

For RD-shCTL, RD-shYB1, RD-shUNR, or RD-shSRSF5 cells, the next day each of them was mock infected or infected with WT ONNV at an MOI of 5 and incubated at 37°C or 28°C. 7 h later, mock infected cells were treated with 0.5 mM $NaAsO_2$ for 1 h. Cells were fixed with 4% paraformaldehyde at 8 hpi. The coverslips were stored at 4°C.

The next day, cells were washed twice with PBS, permeabilized with ice-cold methanol at -20 °C for 10 min. Permeabilized cells were again washed with PBS for 3 times with each time 5 min, then cells were blocked with 2% BSA in PBS for 1 h at RT. Then primary antibody G3BP (Abcam), TIA-1 (Thermo Fisher), eIF4G (Invitrogen) or G3BP (Proteintech) and P-eIF2α (Invitrogen) in 2% BSA in PBS was added to cells at a dilution of 1:200 and incubated at 4°C overnight. The next day, cells infected with ONNV (except incubated with G3BP and P-eIF2α primary antibodies) were washed once with DEPC-PBS, incubated with J2 dsRNA antibody (Scicons) for 1 h at RT at a dilution of 1:100. Cells were washed by DEPC-PBS for 3 times with each time 5 min. Then Alexa Fluor-594 chicken anti-rabbit secondary antibody and Alexa Fluor-647 goat anti-mouse secondary antibody diluted in 2%

BSA DEPC-PBS at a dilution of 1:500 were applied to cells at RT for 1 h in a dark environment. Cells were then washed with DPEC-PBS 3 times with each time 5 min to remove unbounded secondary antibody. Then coverslips were mounted onto glass microscope slides by Prolong Gold antifade reagent (Invitrogen, Molecular Probes) containing the 4', 6'-diamidino-2-phenylindole dihydrochloride (DAPI) and sealed with nail varnish. Slides were then stored in dark for over 24 h. Confocal microscopy images were then acquired using the Zeiss LSM880 microscope. Post-acquisition analysis of images was performed using Zen software (Zen version 2018 black edition 2.3, Zeiss) or Fiji (v1.49) software.

2.7 Statistical analysis

Statistical analysis of all data was carried out using the One-way ANOVA followed by Dunnett's post hoc test. Error bars presented in all graphs represent the Standard Error (SE) of the Mean from three experimental replicates.

Chapter 3: Different replication phenotypes of the CHIKV AUD mutants in mammalian and mosquito cells

3.1 Introduction

The AUD is the central domain in CHIKV nsP3, and is uniquely present in the alphaviruses. The high identity of AUD sequence in alphaviruses suggests that this domain plays a key role in the virus lifecycle. However, although AUD is essential for alphavirus replication, its function in detail remains unclear. In this regard, our laboratory recently demonstrated that AUD is required for both genome replication and alphavirus assembly, the latter could be further explained by AUD binding to sub-genomic RNA promoter as disrupted by the P247A/V248A mutant (Gao et al 2019). To further investigate other functions of AUD in alphavirus replication, site-directed mutagenesis of surface exposed and conserved residues was performed based on the structure of SINV AUD (Shin et al 2012). As CHIKV AUD shows a high identity in different alphaviruses, AUD residues from different alphaviruses were aligned and conserved amino acid residues exposed on the structure surface were identified and mutated into the CHIKV-D-Luc-SGR (Fig. 3.1C). As a control, one mutant Y324A at the end of AUD was also generated, which I initially thought would have no effect on viral replication. The effect of AUD mutations on genome replication as well as translation were reflected by the dual luciferase reporter. Due to differences in evolutionary origins, structures and substrates between firefly luciferase (FLuc) and renila luciferase (RLuc), it is possible to selectively discriminate their respective bioluminescent signals. In the structure of CHIKV-D-Luc-SGR, RLuc is fused within the nsP3 hypervariable domain in ORF1 and FLuc replaces structural components in ORF2 (Fig. 3.1C). RLuc activity is thus a marker of ORF1 translation from the full-length RNA, and early time points of ORF1 represents input translation and allows assessment of transfection efficiency. As ORF2 is translated from a sub-genomic RNA which is templated from the negative strand replicative intermediate, FLuc activity thus represents genomic replication. CHIKV is an arbovirus and is transmitted by mosquitoes, mainly by *Aedes aegypti* and *Ae. albopictus* (Chen et al 2018a), thus it is able to infect both mammalian and mosquito cells. While CHIKV infection induces strong and apparent CPE in a variety of mammalian cell lines (Her et al 2010, Solignat et al 2009), it only lead to

very light CPE in mosquito cells (Li et al 2013). The varied CPEs in mammalian and mosquito cells suggest different mechanisms in virus replication and assembly, so this chapter will focus on the impact of AUD mutants on replication of CHIKV-D-Luc-SGR in both mammalian and mosquito cells.

As described before, five mammalian cell lines and two mosquito cell lines were used in this chapter. Mammalian cells include C2C12, BHK-21, RD (rhabdomyosarcoma), Huh7 and Huh7.5 cells. C2C12 is an immortalized mouse myoblast cell line and is one of the most important cell lines used for CHIKV. Huh7.5 cells is defective in RIG-I induced IFN antiviral response compared to Huh7 cells due to a mutation in one copy of the RIG-I gene, which results in expression of a dominant negative form of RIG-I (Sumpter et al 2005), therefore both Huh7.5 and Huh7 cell lines were used to detect function of host IFN activity in response to CHIKV replication. Two mosquito cell lines U4.4 and C6.36 cells, both from *Ae. albopictus*, were used to explore replication of AUD mutants in mosquito cells. In C6/36 cells, there is a single nucleotide mutation in Dicer-2 (Dcr2) gene which leads to a truncated Dcr2 protein and results in defective RNAi response (Morazzani et al 2012). Replication phenotype of AUD mutants in C6/36 and U4.4 thus indicates AUD function with Dcr2 induced RNAi antiviral response.

As CHIKV is an RNA virus and its replication relies on error-prone RNA-dependent RNA polymerase (lack proofreading), it is likely to be unstable during replication (Holland et al 1982). Previous work showed that the general mutation rates of RNA viruses ranging from 10^{-3} to 10^{-5} substitution per nucleotide copied (Domingo 1997, Drake 1993). In this case, CHIKV-D-Luc-SGR is likely to mutate and revert under selective pressure for adaptation and evolution. In accordance with this assumption, R243A/K245A in AUD of CHIKV nsP3 showed replication defects in mammalian cells but exhibited similar replication levels compared to WT in mosquito cells, this was due to reversion to WT with ongoing replication (Gao et al 2019). Therefore it was considered necessary to sequence the AUD mutants that showed efficient replication, which might provide an explanation for the replication phenotype.

3.2 Results

3.2.1 Construction of AUD mutants in the context of CHIKV-D-Luc-SGR

CHIKV nsP3 consists of three domains: the macro domain, the AUD and the hypervariable domain (Fig. 3.1A). AUD is a unique domain that shares high identity in alphaviruses. To explore other functions of nsP3 AUD in alphavirus replication, amino acid sequences of AUD in different CHIKV species and a range of both Old World and New World alphaviruses were aligned (Fig. 3.2). Following the confirmation of conserved residues in AUD, a panel of surface exposed residues in the CHIKV nsP3 AUD were selected and mutations were designed based on the protein structure of SINV nsP2/nsP3 (PDB ID code 4GGUA) (Fig. 3.1B), which shares high identity between CHIKV and SINV AUD sequence (118 out of 243 residues are identical). Of the mutants, five were mutated to alanine and three were mutated to glutamine (due to the existence of alanine at the same position in other alphaviruses). The mutants were T218Q, M219Q, W220A, P221A, C246A, D249A, A251Q and Y324A. These mutants were generated in the context of CHIKV-D-Luc-SGR.

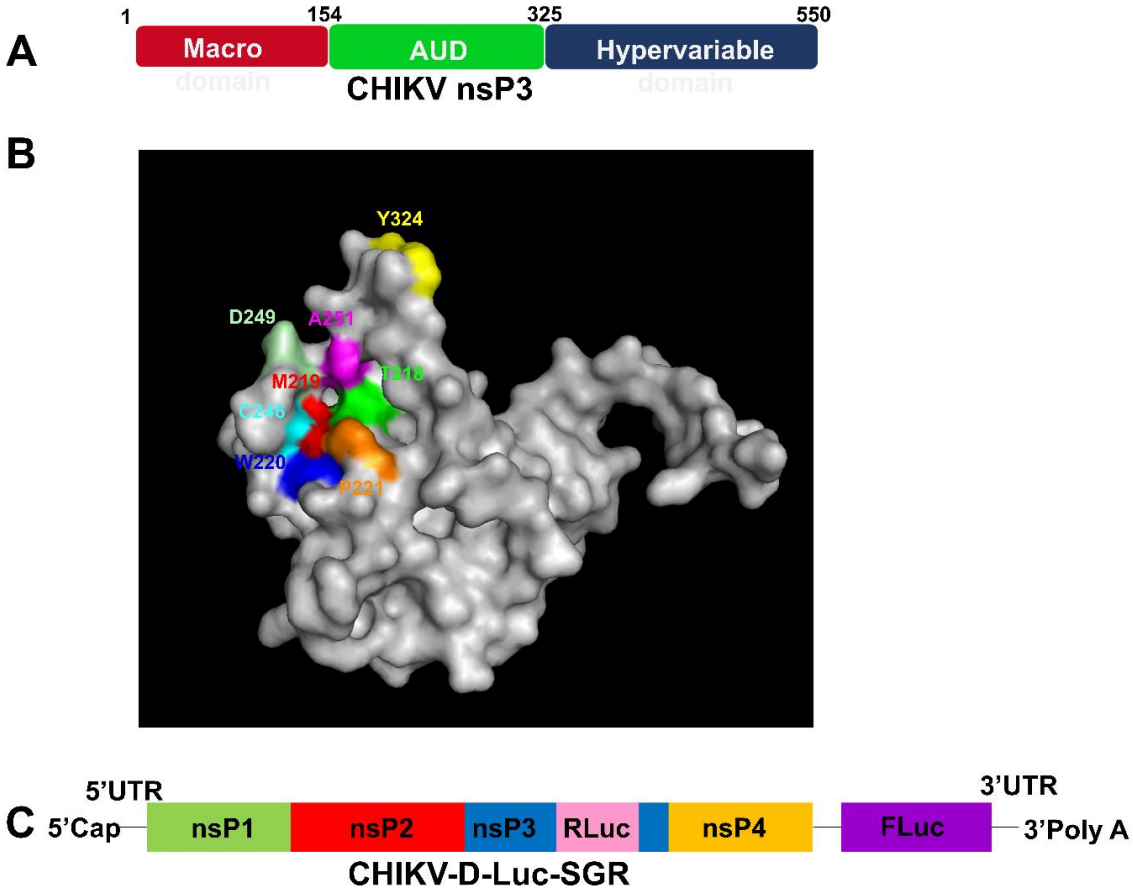

Figure 3.1 Selection of AUD mutants in CHIKV-D-Luc-SGR.

(A) Structure of CHIKV nsP3. nsP3 comprises of three domains: Macro-domain, AUD (alphavirus unique domain), HVD (hypervariable domain). (B) Three-dimensional structure of the SINV (Sindbis virus) AUD (Shin et al 2012). Conserved and surface exposed residues targeted for mutagenesis are highlighted in corresponding colors. (C) Structure of the CHIKV-D-Luc-SGR. RLuc (Renilla luciferase) is expressed as a fusion protein within nsP3, FLuc (firefly luciferase) is expressed from the sub-genomic promoter (sg-prom).

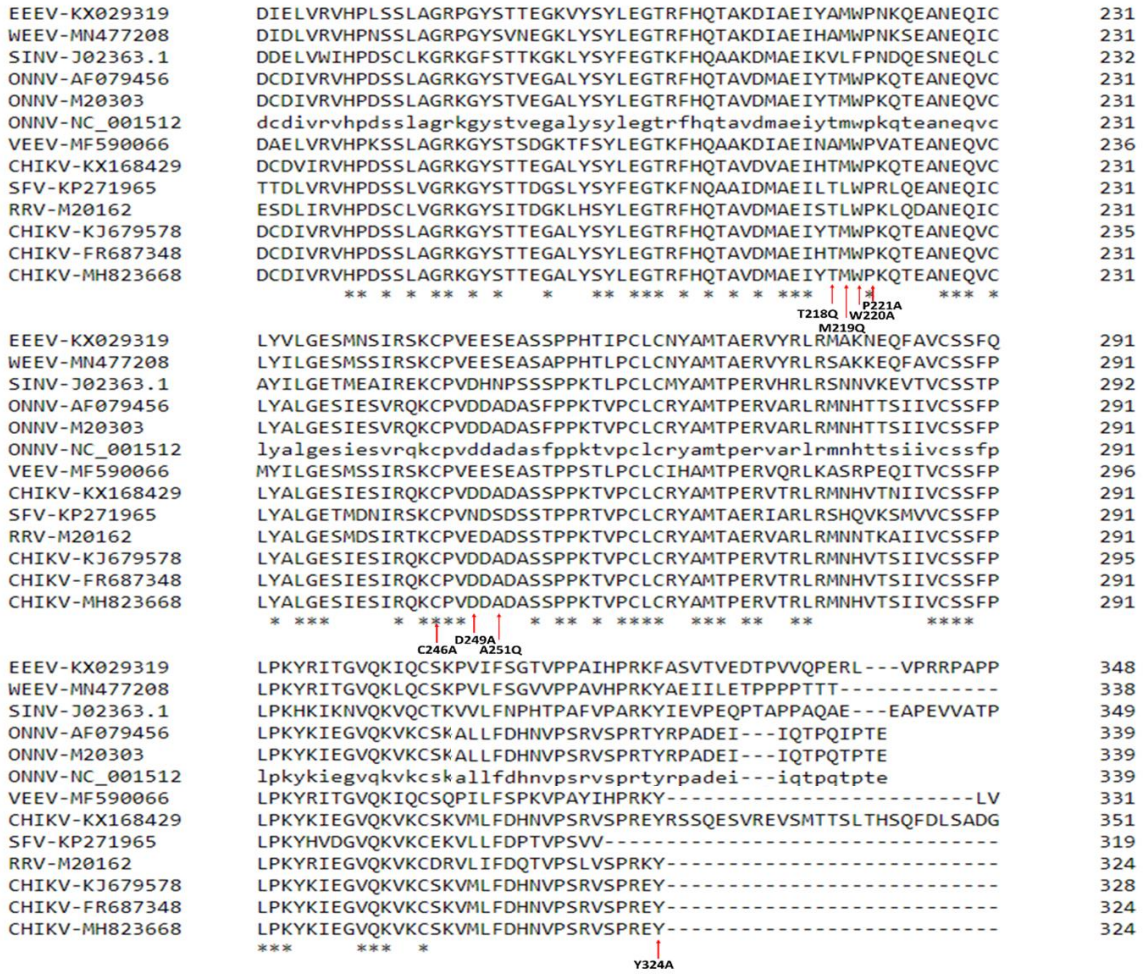

Figure 3.2 Sequence alignment of AUD fragment from multiple alphaviruses with mutants indicated.

The alphaviruses aligned include different strains of CHIKV, other Old World alphaviruses including SINV, Ross River virus (RRV), and O'Nyong-Nyong virus (ONNV), Semliki Forest virus (SFV), as well as some of the New World Alphaviruses including Venezuelan, eastern and western equine encephalitis viruses (VEEV, EEEV, and WEEV). * indicate absolute conserved amino acid residues.

3.2.2 Replication of the AUD mutants in mammalian C2C12 cells

CHIKV mainly induces arthritis and joint pain (Schwartz & Albert 2010) and infect muscle cells. To evaluate replication of the AUD mutants in mammalian cells, I first transfected WT and mutant CHIKV-D-Luc-SGR RNA into C2C12, an immortalized mouse myoblast cell line widely used in the study of CHIKV (Roberts et al 2017). As expected, WT CHIKV-D-Luc-SGR exhibited very high level of genome replication in C2C12 cells, with FLuc level peaking at 12 h post transfection (hpt) and increasing over 1000-fold between 4-24 hpt (Fig. 3.3A). Similarly, AUD

mutants T218Q, M219Q, P221A, C246A and A251Q showed as efficient replication as WT. However, the three AUD mutants (W220A, D249A and Y324A) showed significant lower levels of replication compared to WT CHIKV-D-Luc-SGR, ranging from 10-200 fold reduction in replication. A polymerase-inactive mutant (GDD-GAA in nsP4) was used as a negative control. In accordance with genome replication, the three AUD mutants (W220A, D249A and Y324A) showed defects in translation (Fig. 3.3B). The results confirmed replication defects of the three AUD mutants (W220A, D249A and Y324A) in mammalian C2C12 cells.

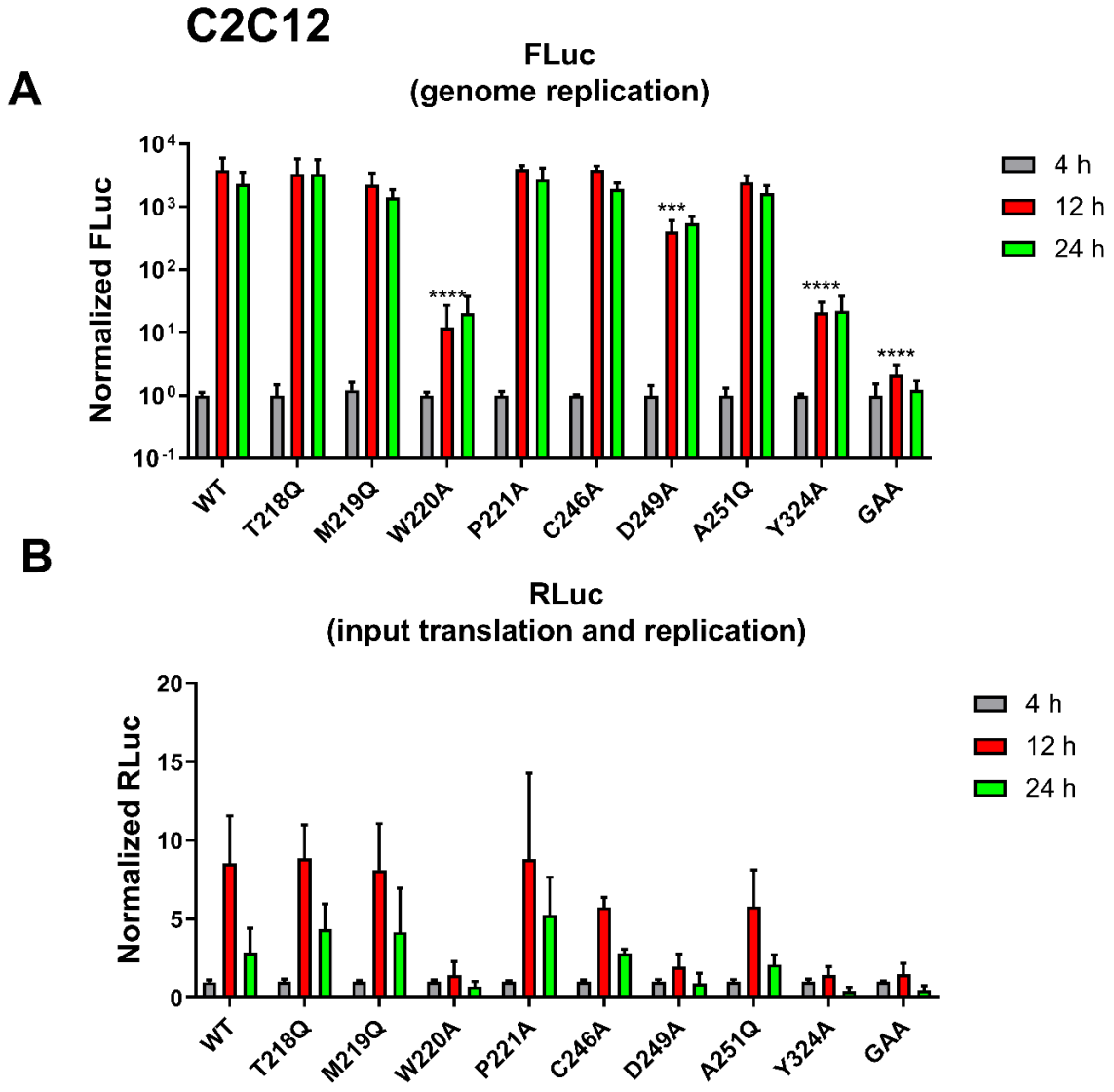

Figure 3.3 Replication and translation of WT and mutant CHIKV-D-Luc-SGR in C2C12 cells.

C2C12 cells were transfected with WT and mutant CHIKV-D-Luc-SGR RNAs and incubated at 37°C. Cells were collected at 4, 12 and 24 h post transfection (hpt). Firefly luciferase (FLuc) (A) and Renilla luciferase (RLuc) (B) activities were detected and normalized to their respective 4 h values and thus values represent fold-change compared to those 4 h values. GAA: nsP4 polymerase inactive mutant. *** (P<0.001), **** (P<0.0001) compared to WT replication at 12 hpt. Data are displayed as the means ±S.E. of three experimental replicates.

3.2.3 Replication of the AUD mutants in mosquito cells

CHIKV are transmitted by mosquitoes, mainly by *Ae. albopictus* and *Ae. aegypti*. Here two cell lines C6/36 and U4.4, both from *Ae. albopictus* were used to evaluate replication capacities of AUD mutants in CHIKV-D-Luc-SGR. C6/36 harbors a frame shift mutation in Dcr2 gene, which results in a truncated Dcr2 protein and thus is defective in RNAi response (Morazzani et al 2012). Consistent with this, although robust replication for WT CHIKV-D-Luc-SGR in both cell lines were observed, C6/36 supported higher levels of replication than U4.4 (Fig. 3.4A and 3.5A), increasing ~10,000-fold in C6/36 cells and ~100-fold in U4.4 cells between 4-48 hpt respectively. In agreement with more efficient replication in C6/36 cells, WT CHIKV-D-Luc-SGR showed higher levels of translation in C6/36 cells than U4.4 cells, increasing ~100-fold in C6/36 cells and ~10-fold in U4.4 cells between 4-48 hpt (Fig. 3.4B and 3.5B). However, unlike the replication defects of the three AUD mutants in mammalian C2C12 cells, all AUD mutants showed similar replication levels compared to WT in C6/36 cells or U4.4 cells. The results indicated that the replication phenotype of AUD mutants was not related with RNAi response and all AUD mutants replicated efficient in mosquito cells.

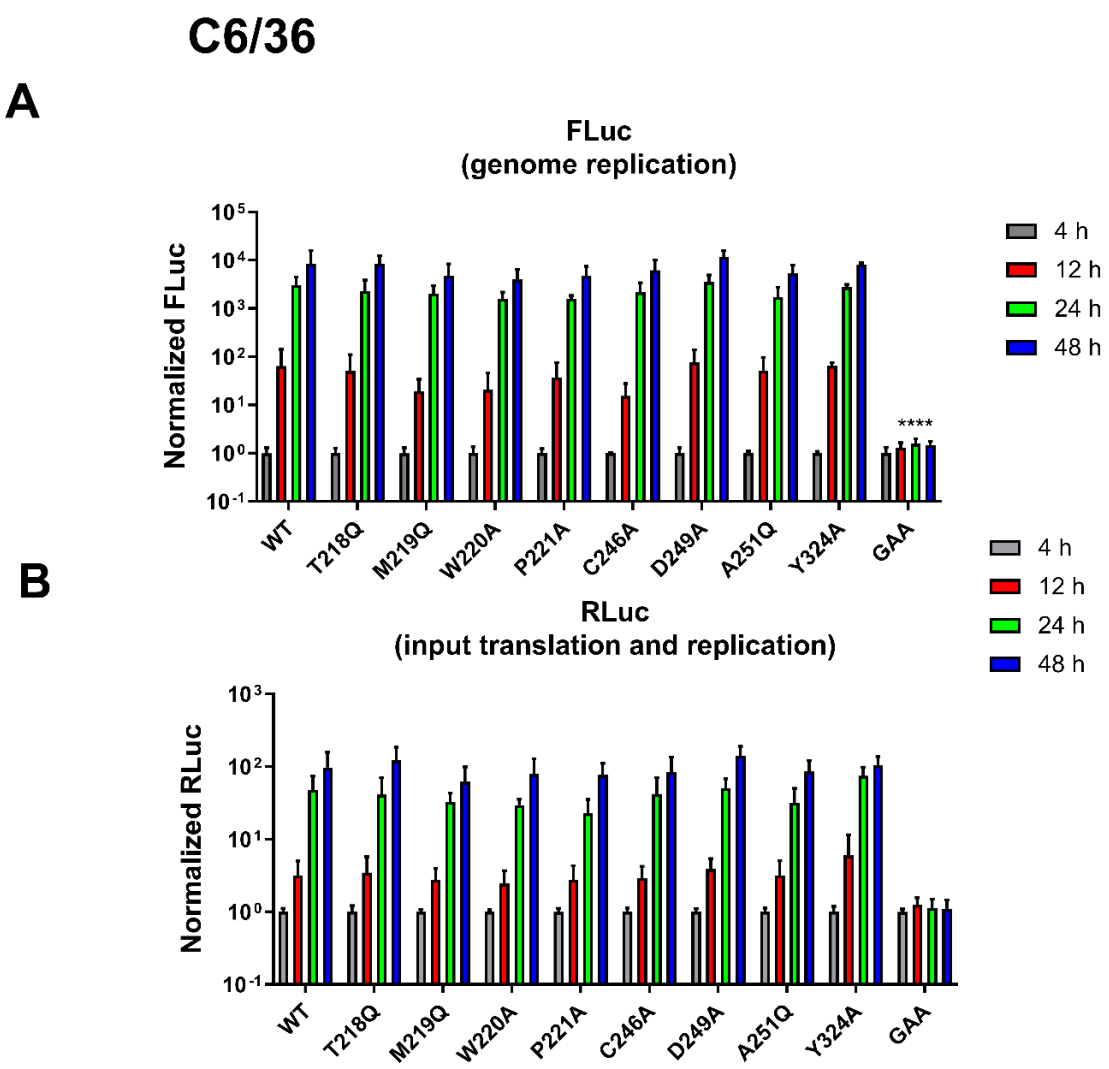

Figure 3.4 Replication and translation of WT and mutant CHIKV-D-Luc-SGR in C6/36 cells.

C6/36 cells were transfected with WT and mutant CHIKV-D-Luc-SGR RNAs and incubated at 28°C. Cells were collected at indicated time points. FLuc (A) and RLuc (B) levels were detected and normalized to their respective 4 h values and thus values represent fold-change compared to those 4 h values. **** (P<0.0001) compared to WT replication at 48 hpt. Data are displayed as the means ±S.E. of three experimental replicates.

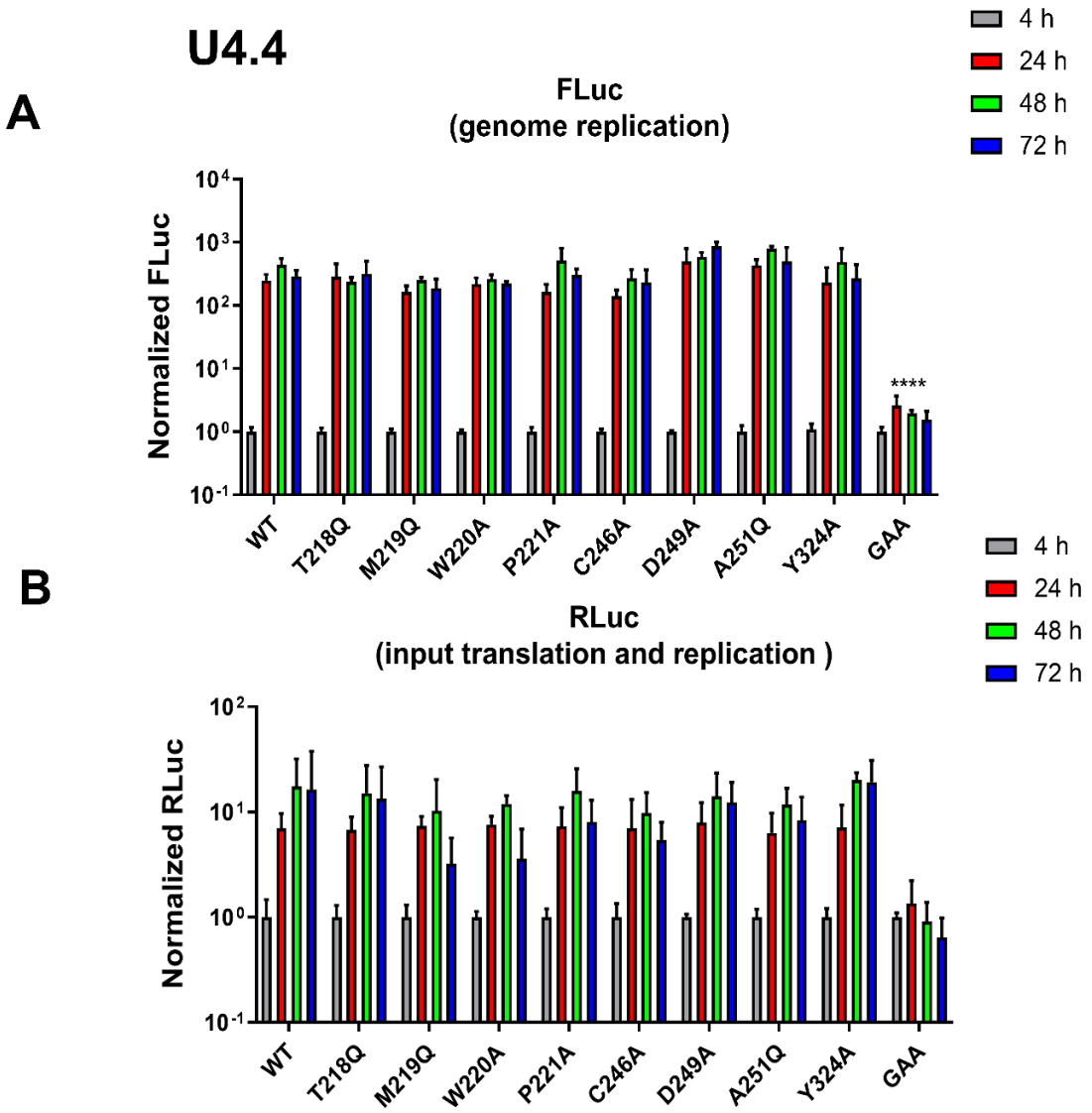

Figure 3.5 Replication and translation of WT and mutant CHIKV-D-Luc-SGR in U4.4 cells.

U4.4 cells were transfected with WT and mutant CHIKV-D-Luc-SGR RNAs and incubated at 28°C. Cells were collected at indicated time points. FLuc (A) and RLuc (B) levels were detected and normalized to their respective 4 h values and thus values represent fold-change compared to those 4 h values. **** (P<0.0001) compared to WT replication at 48 hpt. Data are displayed as the means ±S.E. of three experimental replicates.

3.2.4 Sequencing analysis of AUD mutants in mosquito cells

The three AUD mutants showed low replication in mammalian C2C12 cells but replicated as efficient as WT in mosquito cells. The striking phenotypic differences between mammalian and mosquito cell lines for the three AUD mutants led us to investigate further. A simple explanation might be that these AUD mutants had

reverted to WT with ongoing replication, as we had previously observed this reversion for the AUD mutant R243A/K245A (Gao et al 2019). This AUD mutant replicated poorly in C2C12 cells but replicated efficiently in mosquito cells, and this was due to the fact that R243A/K245A gradually reverted to WT in C6/36 or U4.4 cells. To test this assumption, total RNA from transfected C6/36 and U4.4 cells at 72 hpt were extracted, nsP3 fragments encompassing mutations were amplified by RT-PCR and then sequenced. To our surprise, none of the three AUD mutants had reverted to WT or showed compensatory mutations and they retained the same sequence as input RNA (Fig. 3.6). The results indicated that the ability to replicate efficiently in mosquito cells for the three AUD mutants was not due to mutation reversion.

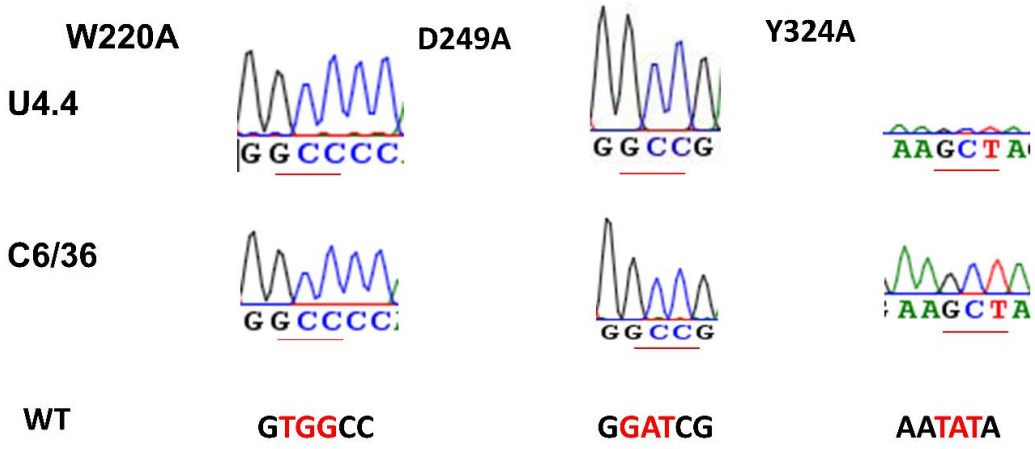

Figure 3.6 Sequencing analysis of AUD mutants in mosquito cells.

Cells were lysed by TRizol at 72 hpt and total RNA were extracted and purified by phenol-chloroform. The cDNAs were synthesized by reverse transcription and nsP3 fragments encompassing the mutations were amplified by PCR. Amino acid sequence of W220, D249 and Y324 from WT were indicated and labelled as red.

3.2.5 Replication of the three AUD mutants in other mammalian cells

To confirm the replication defects of the three AUD mutants was not specific to C2C12 cells, replication of the three AUD mutants were further investigated in RD, BHK-21, Huh7 and Huh7.5 cells. Reassuringly, replication levels of the three AUD mutants were lower compared to WT in all mammalian cells, although the

magnitude of the replication defects varied between different cell lines (Fig. 3.7 and 3.8).

In RD cells, WT showed over 100-fold increase in replication between 4-12 hpt, however, W220A and Y324A showed only 3 to 5-fold increase whereas D249A increased ~20-fold in replication between 4-12 hpt (Fig. 3.7A left panel). Consistent with defects in replication, the AUD mutants exhibited no increase in translation, while WT showed a 2-fold increase in translation (Fig. 3.7A right panel).

In BHK-21 cells, WT showed ~300-fold increase in replication between 4-12 hpt, however, W220A and D249A only showed ~10-fold increase whereas D249A increased ~100-fold in replication between 4-12 hpt (Fig. 3.7B left panel). Consistent with defects in replication, the three AUD mutants showed lower translation levels compared to WT (Fig. 3.7B right panel). Interestingly, the replication defects were less pronounced in BHK-21 cells, which is consistent with our observation of other mutants in nsP3 (Roberts et al 2019).

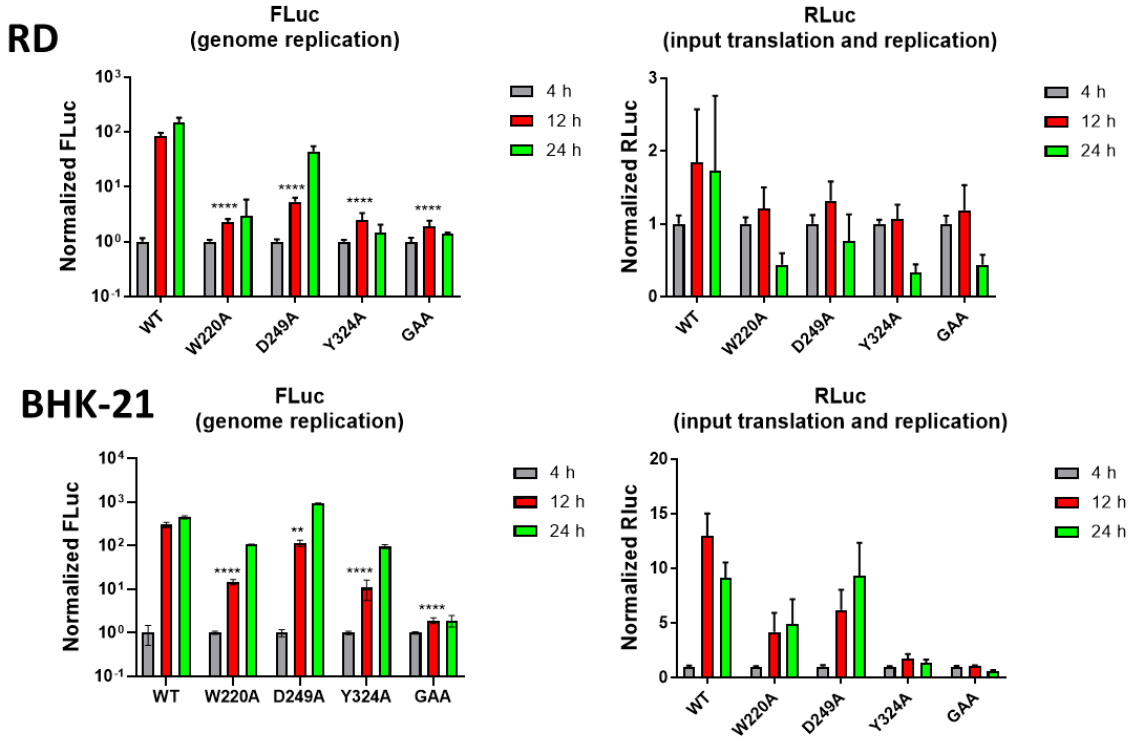

Figure 3.7 Replication and translation of WT and mutant CHIKV-D-Luc-SGR in RD and BHK-21 cells.

RD (A) and BHK-21 (B) cells were transfected with WT and mutant CHIKV-D-Luc-SGR RNAs and incubated at 37°C. Cells were collected at indicated time points. FLuc and RLuc levels were detected and normalized to their respective 4 h values. ** (P<0.01), **** (P<0.0001) compared to WT replication at 12 hpt. Data are displayed as the means ±S.E. of three experimental replicates.

Apart from RD and BHK-21 cell lines, two human hepatoma cell lines Huh7 and Huh7.5 were utilized to evaluate replication levels of the three AUD mutants. Huh7.5 is defective in the RIG-I induced IFN antiviral response. In Huh7 cells, WT showed ~30-fold of increase in replication between 4-24 hpt, mutants W220A, D249A and Y324A showed ~4-fold replication increases between 4-24 hpt (Fig. 3.8A left panel). Consistent with defects in RIG-I induced IFN activity, WT showed ~100-fold of increase in replication between 4-24 hpt in Huh7.5 cells, mutants W220A, D249A and Y324A showed ~10-fold of increase in replication (Fig. 3.8B left panel). Unlike translation increase of WT in other mammalian cells, no increase in translation for WT and the AUD mutants in both Huh7 and Huh7.5 cells (Fig. 3.8 A and B, right panel) were observed. The results demonstrated the replication defects of the three AUD mutants in human hepatoma cells, and the replication phenotype of AUD mutants was not due to the RIG-I induced IFN response.

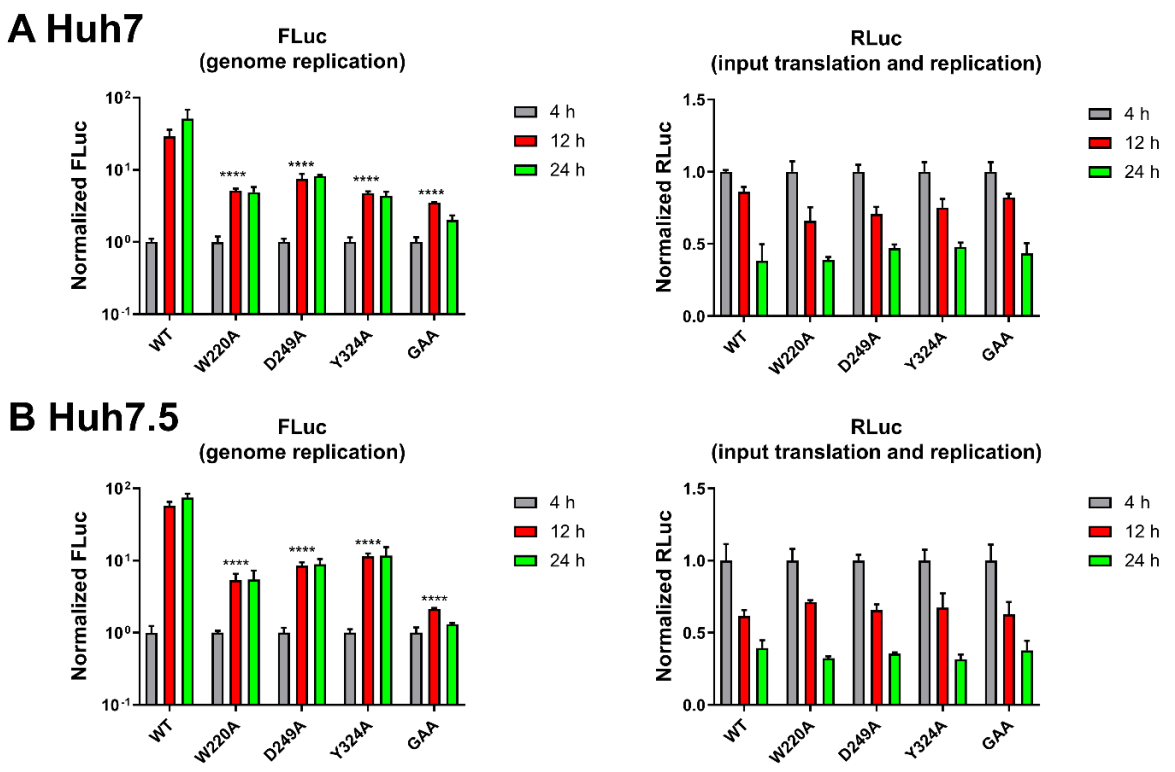

Figure 3.8 Replication of WT and mutant CHIKV-D-Luc-SGR in Huh7 and Huh7.5 cells.

Huh7 (A) or Huh7.5 (B) cells were transfected with WT and mutant CHIKV-D-Luc-SGR RNA and incubated at 37°C. Cells were collected at indicated time points. FLuc and RLuc levels were detected and normalized to their respective 4 h values. GAA: inactive mutant of nsP4 polymerase. **** (P<0.0001) compared to WT FLuc at 12 hpt. Data are displayed as the means ±S.E. of three experimental replicates.

Interestingly, although the replication defects were not due to RIG-I induced IFN activity, a several-fold increase in replication for WT CHIKV-D-Luc-SGR but not for mutant CHIKV-D-Luc-SGR at 4 hpt in IFN defective Huh7.5 and BHK-21 cells (Fig. 3.9) was observed. Therefore, by normalization with 4 h RLuc, a more pronounced replication defects for the three AUD mutants compared to these replication defects of the AUD mutants normalized with 4 h FLuc (Fig. 3.9) was observed.

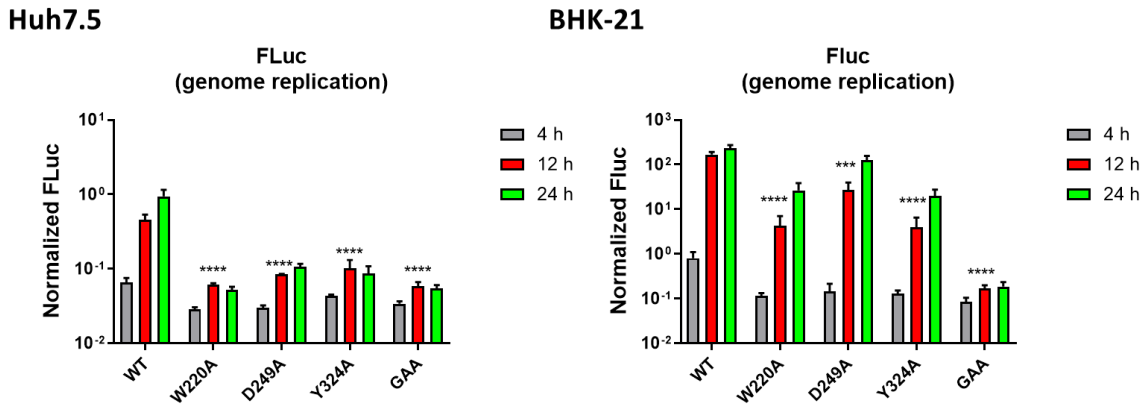

Figure 3.9 Replication of WT and mutant CHIKV-D-Luc-SGR in Huh7.5 and BHK-21 cells (normalized to 4 h RLuc).

FLuc levels were normalized to their respective 4 h RLuc values. *** (P<0.001), **** (P<0.0001) compared to WT replication at 12 hpt. Data are displayed as the means ±S.E. of three experimental replicates.

3.3 Discussion

CHIKV contains four non-structural proteins, however, nsP3 remains the least understood in promoting RNA replication or in viral production (Rupp et al 2015). CHIKV nsP3 consists of three domains – the macro domain, the AUD and the hypervariable domain. The macro domain at the N terminus exhibits ADP-ribose, RNA binding and ADP-ribosylhydrolase activity (Eckei et al 2017, Luscher et al 2018). The hypervariable domain at the C terminus shares low sequence identity among different alphaviruses and is intrinsically disordered, which functions in virus-host interactions with different cell types (Foy et al 2013a). The hypervariable domain of CHIKV nsP3 was reported to interact with G3BP, and although the proline-rich sequences in hypervariable domain of nsP3 were dispensable for binding to G3BP (Panas et al 2014) , the two conserved FGDF motifs can be sufficient for binding to G3BP (Panas et al 2014, Panas et al 2015, Panas et al 2012).

The role of AUD in CHIKV replication, however, remains unclear. The conserved amino acids sequence of AUD in different alphaviruses suggests its fundamental role in viral lifecycle. Recently, our laboratory published a paper showing that AUD

is necessary for viral assembly and replication, and one mutant P247A/V248A reduced virus production significantly by reducing AUD binding affinity to sub-genomic RNA promoter (Gao et al 2019). To further explore the function of AUD in CHIKV replication, I selected a panel of surface exposed and conserved residues in the AUD domain and mutated them in the CHIKV-D-Luc-SGR. However, protein structure of CHIKV nsP3 is still unavailable, therefore the closest structure I can use for protein prediction is the SINV nsP2/nsP3 precursor, which includes the nsP2 protease and methyltransferase-like domains in the C terminal and nsP3 macro domain and AUD (Shin et al 2012).

Among the mutants generated, T218Q, M219Q, P221A, C246A and A251Q CHIKV-D-Luc-SGR showed similar levels of replication compared to WT in mammalian C2C12 cells, indicating that these amino acid residues are not required for viral replication (Fig. 3.3). However, I cannot rule out an effect of the five mutants on virus assembly, as this was not evaluated in this study. The three mutants W220A, D249A and Y324A CHIKV-D-Luc-SGR showed replication defects compared to WT, suggesting the importance of these residues for replication (Fig. 3.3). Surprisingly, in mosquito cells C6/36 and U4.4 (*Ae. albopictus*), AUD mutants showed similar replication as WT (Fig. 3.4 and 3.5), indicating a possibility that the replication defects of the three AUD mutants was recovered in mosquito cells. As C6/36 is defective in RNAi response due to inactive Dcr2 protein, the highly efficient replication of all the AUD mutants in both cell lines suggest that the replication defect of the AUD mutants was not due to RNAi in mosquito cells. I postulate that instead of exhibiting efficient replication in mosquito cells, the three AUD mutants might had reverted to WT in both C6/36 and U4.4 cells. This assumption comes from our previous work, the R243A/K245A in AUD showed replication defects in mammalian cells but replicated efficiently in mosquito cells, and later sequence analysis revealed that it had reverted to WT with ongoing replication (Gao et al 2019). In order to initiate reverted mutations, the R243A/K245A must be able to replicate in mosquito cells, even at a low level, therefore providing replication complexes factors for mutation. However, contrary to our expectations, sequencing analysis indicated that none of the three AUD

mutants had reverted to WT, and all three AUD mutants retained the same sequence as the input RNA (Fig. 3.6). These results demonstrated different replication phenotypes for the three AUD mutants in mammalian C2C12 and mosquito cells.

To confirm the replication defects of the three AUD mutants was not specific to C2C12, replication levels of the three mutants were then further evaluated in other mammalian cells, including RD, BHK-21, Huh7 and Huh7.5 cells. As expected, I confirmed the replication defects of the AUD mutants were retained in all four mammalian cells (Fig. 3.7 and 3.8). Interestingly, the replication defects of the AUD mutants were less pronounced in BHK-21 cells, this is consistent with previous observations of mutants in nsP3 macro domain (Roberts et al 2019). Replication defects of the three AUD mutants in both Huh7 and Huh7.5 cells suggest this replication phenotype due to mutations in AUD is not related with RIG-I induced IFN response. However, I did observe a replication difference in IFN defective cells (Huh7.5 and BHK-21 cells) compared to those mammalian cells (C2C12, RD and Huh7 cells) with normal IFN activities. In mammalian cells with normal IFN activities, similar levels of genome replication for WT CHIKV-D-Luc-SGR compared to mutants and the negative control GAA at 4 hpt were observed, suggesting that they haven't initiated replication at this time point. However, in these IFN defective mammalian cells, WT exhibited a several-fold increase in replication at an early time point (4 hpt), whereas these mutants showed no sign of increase in replication (Fig. 3.9). The results indicated that WT CHIKV-D-Luc-SGR was able to initiate replication earlier in IFN defective cells compared to cells with normal IFN activities, suggesting the IFN response suppress virus replication. Intriguingly, the three AUD mutants failed to show increase in replication at 4 hpt, suggesting a role of AUD in counteracting IFN activities at early time points. However, as the AUD mutants retained replication defects in IFN defective mammalian cells, I determined that IFN activity was not the key factor in regulating the replication phenotype of the AUD mutants.

The replication of WT CHIKV-D-Luc-SGR also showed variable susceptibility in different cell lines. C2C12 and RD allowed higher levels of replication than Huh7 and Huh7.5 cells, which suggest that muscle cells were more susceptible for CHIKV infection than liver cells, and this correlates with CHIKV pathogenicity. A possible explanation is that the translation of non-structural proteins for WT CHIKV-D-Luc-SGR in Huh7 or Huh7.5 cells was inhibited, as no increase in RLuc activity (Fig. 3.8 A and B right panel) was observed, whereas in C2C12 or RD cells translation of non-structural proteins is supported at a certain level, showing an increase of 2 or 5-fold in RLuc activity (Fig. 3.3 B and 3.7 A right panel). Although BHK-21 cell is not the target cell for CHIKV, WT CHIKV-D-Luc-SGR also replicated more efficiently in BHK-21 cells than in RD cells, which could attribute to that BHK-21 cells lack of type 1 IFN response (Truant & Hallum 1977) or is defective in NF-κB activity (Roberts et al 2019).

In summary, I identified three AUD mutants that replicated poorly in mammalian cells but replicated efficiently in mosquito cells, and the replication phenotype is not due to mutation reversion in mosquito cells or related with RIG-I induced IFN response.

Chapter 4: AUD mutants exhibit a temperature-sensitive phenotype and reveal that CHIKV genome replication is enhanced at sub-physiological temperature

4.1 Introduction

Use of the dual luciferase reporter system in CHIKV SGR demonstrated replication defects of the three AUD mutants in mammalian but not in mosquito cells. Transmission of CHIKV from mosquitoes to humans is largely affected by temperature. Previous work showed the survival rate of the two mosquito species (*Ae. albopictus* and *Ae. aegypti*) are affected by upper and lower temperature thresholds (Brady et al 2013). Experimental models and human cases showed that transmission occurs between 18°C and 34°C with a maximum transmission at a temperature range of 26°C-29°C (Mordecai et al 2017). Despite the fact that mosquitoes (*Ae. albopictus* and *Ae. aegypti*) are the natural reservoir of CHIKV, CHIKV replicates efficiently in human body, with a temperature jump from human sub-physiological temperatures to physiological temperature. In accordance with this, mosquito cell lines are cultured at 28°C and mammalian cells are cultured at 37°C (Zhu et al 1984). Therefore, temperature variance might be the key factor that regulates replication defects of the AUD mutants. To test this, I initially transfected the AUD mutants in the context of CHIKV-D-Luc-SGR into C2C12 cells, an immortalized mouse myoblast cell lines widely used in the study of CHIKV (Roberts et al 2017) and incubated cells at 28°C or 37°C. Apart from C2C12 cells, this assumption was also investigated in Huh7 and Vero cells to confirm the relationship between temperature variance and replication phenotype of the AUD mutants.

Previous studies have used luciferase reporter systems to detect alphavirus replication (Pohjala et al 2008) or infection (Steel et al 2013). The application of luciferase reporter system allows rapid assessment of genome replication or non-structural protein translation. However, not all the infectious clones of SFV RLuc were positive (21 of 23 were positive) (Pohjala et al 2008). Therefore I also exploited replication phenotype of the CHIKV-FLuc-SGR (CHIKV SGR without RLuc thus expressing WT nsP3) and the CHIKV-nsP3-mCherry-FLuc-SGR (CHIKV SGR RLuc replaced with mCherry) at 28°C or 37°C, to determine whether it is a factor that affects the replication phenotype. As an arbovirus, CHIKV transmitting

from mosquitoes to humans undergoes a temperature jump, thereof the relationship between temperature variance and replication phenotype was also investigated in other arboviruses. To test it, I used SGRs from Bunyamwera virus (BUNV) (Leonard et al 2006) and Zika virus (Malone et al 2016) and investigated their replication at 28°C or 37°C. This would help identify whether temperature variance affect replication phenotype of other arboviruses.

Our previous work showed that AUD functions in virus replication and assembly, the later can be further explained by AUD binding to sub-genomic promoter, as shown by the P247A/V248A mutant (Gao et al 2019). Thereof, I also explored replication phenotype of the AUD mutants in the context of CHIKV using a ICRES-CHIKV infectious clone (Tsetsarkin et al 2006) at 28°C or 37°C. The consistency of the relationship between temperature variance and replication phenotype of the AUD mutants in CHIKV SGR and CHIKV would confirm the role of temperature in determining replication phenotype of the AUD mutants.

4.2 Results

4.2.1 Temperature plays a key role in determining replication phenotype of the AUD mutants in CHIKV-D-Luc-SGR

To investigate whether temperature plays a key role in determining replication phenotype of the AUD mutants, C2C12 cells were transfected with WT and mutant CHIKV-D-Luc-SGR RNA and incubated at 37°C or 28°C, harvested at indicated time points and assayed for RLuc and FLuc activities. Results showed that while AUD mutants exhibited similar levels of replication compared to WT at 28°C (increased ~10,000-fold) between 4-24 hpt, they exhibited significant lower levels of replication (5-20 fold increase) compared to WT (increased ~100-fold) at 37°C between 4-24 hpt (Fig. 4.1). Intriguingly, WT CHIKV-D-Luc-SGR showed similar levels of replication (increased ~100-fold) at both temperatures between 4-12 hpt. However, replication then increased ~100-fold at 28°C but reduced slightly at 37°C from 12-24 hpt (Fig. 4.1).

For translation, RLuc levels of WT and mutant CHIKV-D-Luc-SGR increased ~200-fold from 4-24 hpt at 28°C but only increased modestly for WT (3-5 fold) and AUD mutants (1-2 fold) at 37°C, indicating much more efficient translation at 28°C compared to 37°C (Fig. 4.1). The optimal temperature for FLuc activity is between 22°C to 28°C (Zhu et al 1984). In order to confirm that these observations were not due to the varied activities of luciferase at physiological and sub-physiological temperatures, nsP1 expression was detected by western blotting. As expected, protein expression of nsP1 at 28°C was high and similar for WT and mutant CHIKV-D-Luc-SGR, while GAA showed no protein expression (Fig. 4.2 left). However, WT CHIKV-D-Luc-SGR only showed a weak nsP1 band whereas no nsP1 can be detected for the AUD mutants and GAA at 37°C (Fig. 4.2 right). The high and similar levels of nsP1 for WT and the AUD mutants at 28°C and only a low level of nsP1 for WT but no nsP1 can be detected for the AUD mutants at 37°C further supported high levels of genome replication for CHIKV SGR at sub-physiological temperature.

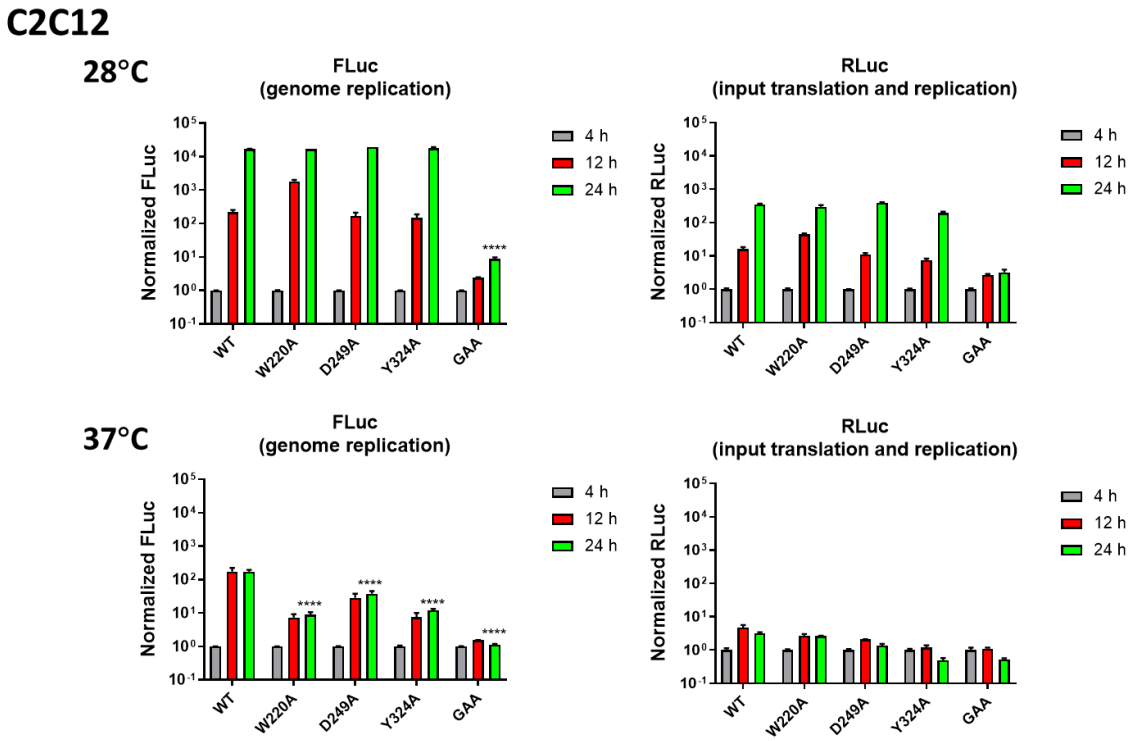

Figure 4.1 Replication and translation of WT and mutant CHIKV-D-Luc-SGR in C2C12 cells at 28°C or 37°C.

C2C12 cells were transfected with WT and mutant CHIKV-D-Luc-SGR RNA and incubated at 37°C or 28°C, cells were then lysed at indicated time points. GAA: nsP4 polymerase inactive mutant. RLuc and FLuc were detected and normalized to their respective 4 h values. Significant differences denoted by **** (P<0.0001) compared to WT replication at 24 hpt at their respective temperatures. Data are displayed as the means ±S.E. of three experimental replicates.

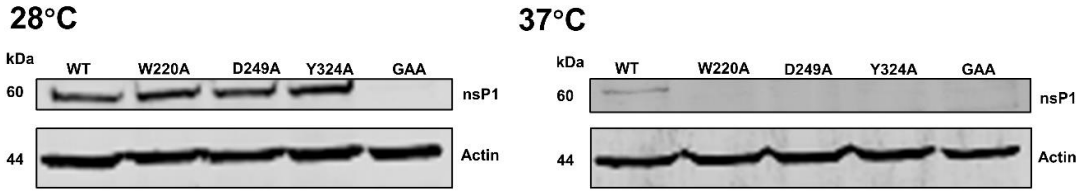

Figure 4.2 Protein expression of nsP1 for the WT and mutant CHIKV-D-Luc-SGR in C2C12 cells at 28°C or 37°C.

C2C12 cells were transfected with WT and mutant CHIKV-D-Luc-SGR RNAs and incubated at 37°C or 28°C. Cells were lysed at 24 hpt by 1X passive lysis buffer (PLB). Protein concentrations were determined by BCA assay, then 20 µg of each sample was loaded and analysed by western blot. Actin was also detected by western blot as a loading control.

To confirm that the temperature dependent replication phenotype of the AUD mutants was not specific to C2C12 cells, I further investigated this in Huh7 cells. Similar to C2C12, genome replication of WT and mutant CHIKV-D-Luc-SGR increased ~10,000-fold at 28°C between 4-24 hpt, however, replication only increased 5-fold for WT and 2-fold for AUD mutants between 4-12 hpt at 37°C (Fig. 4.3). Combining the data from C2C12 and Huh7, results indicated that AUD mutants exhibited a temperature sensitive, rather than a cell-type specific replication phenotype.

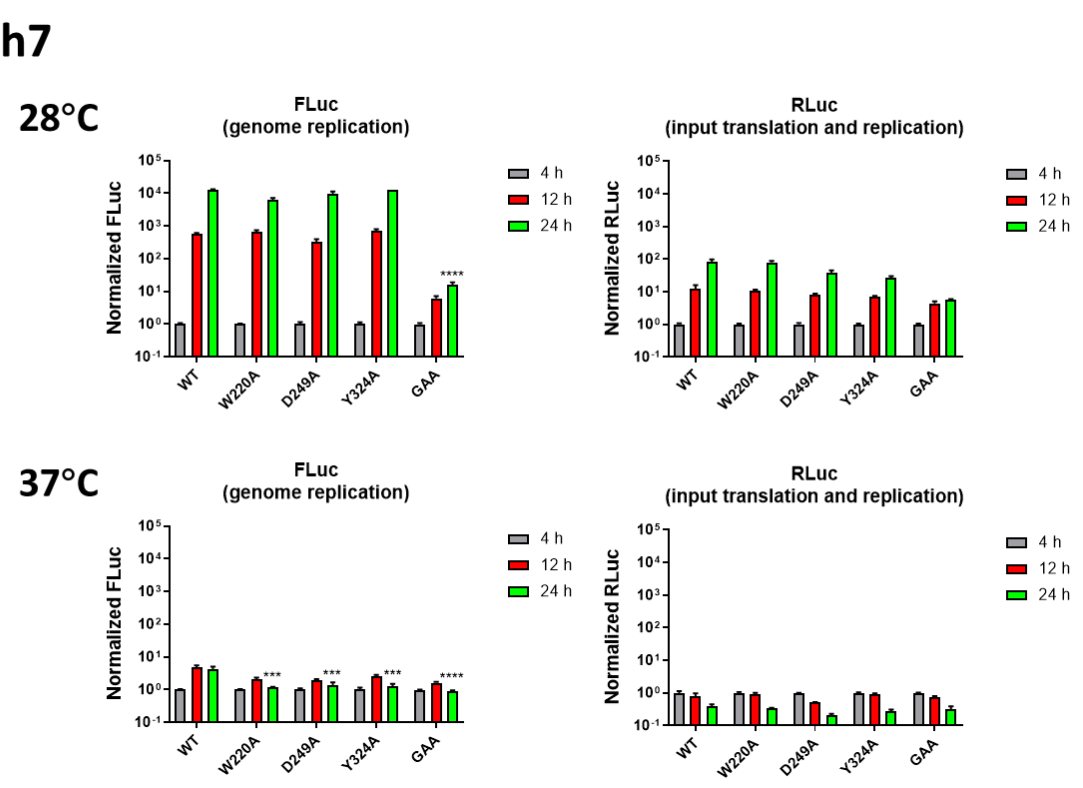

Figure 4.3 Replication of WT and mutant CHIKV-D-Luc-SGR in Huh7 cells at 28°C or 37°C.

Huh7 cells were transfected with WT and mutant CHIKV-D-Luc-SGR RNAs and incubated at 37°C or 28°C, cells were then harvested at indicated time points. RLuc and FLuc were detected and normalized to their respective 4 h values. Significant differences denoted by **(P<0.01), *** (P<0.001), **** (P<0.0001) compared to WT replication at 24 hpt at their respective temperatures. Data are displayed as the means ±S.E. of three experimental replicates.

4.2.2 Antiviral IFNα/β response is not responsible for the temperature sensitive replication phenotype of the AUD mutants

Recently, it was shown that IFNα/β activities were reduced at lower temperature, which resulted in higher levels of virus replication and production (Prow et al 2017). To investigate if the temperature sensitive replication phenotype of the AUD mutants at physiological and sub-physiological temperatures could be explained by differences in IFNα/β activities, Vero cells were used as they cannot produce IFNα/β but they can respond to exogenous IFNα/β. As shown in Figure 4.4, WT and mutant CHIKV-D-Luc-SGR showed ~1000-fold increase in genome replication at 28°C, although WT exhibited higher level of replication at 4 pht compared to

mutants at 37°C (data normalized to 4 h RLuc). However, AUD mutants failed to replicate at 37°C while WT only showed a several-fold increase in replication (Fig 4.4). As Vero cells failed to produce IFNα/β, thus the differences of IFNα/β response at various temperatures in Vero cells can be ignored. Therefore, I conclude that the temperature sensitive replication phenotype for the AUD mutants in mammalian cells is not due to the previously documented reduced activity of the IFN antiviral response at lower temperature (Prow et al 2017).

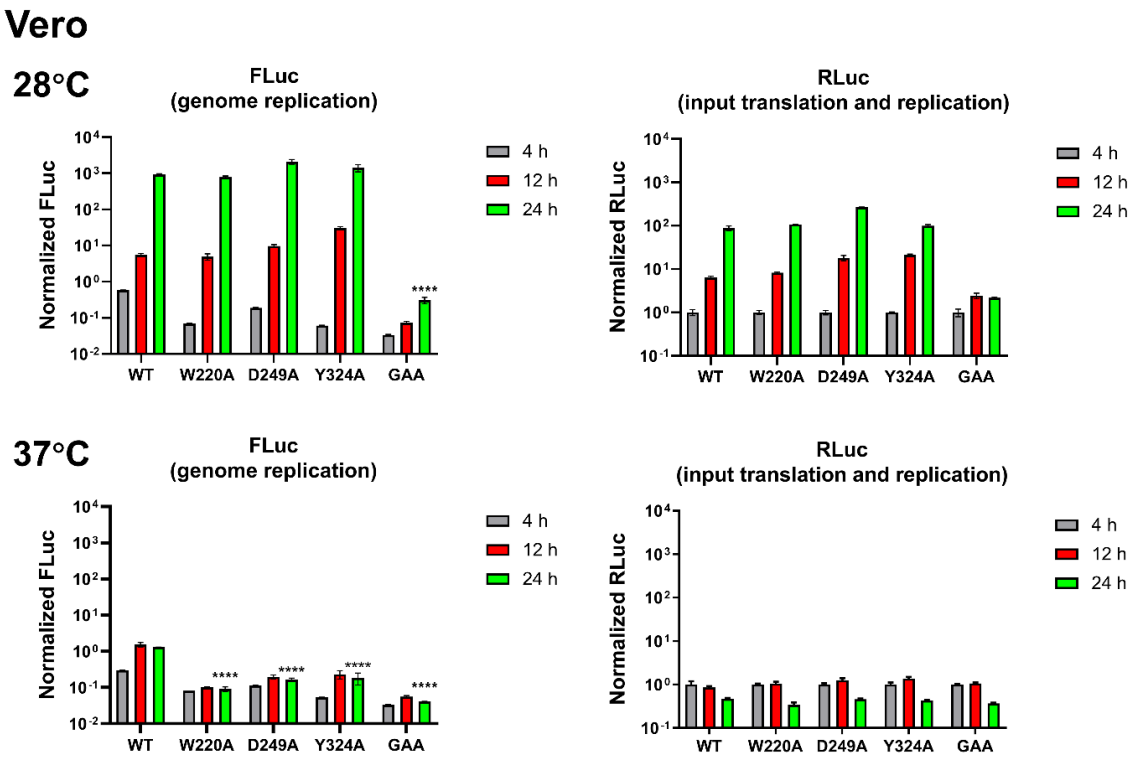

Figure 4.4 Replication of CHIKV-D-Luc-SGR mutants in Vero cells at different temperatures.

Vero cells were transfected with WT and mutant CHIKV-D-Luc-SGR RNAs and incubated at 37°C or 28°C, cells were then lysed at indicated time points. RLuc and FLuc were detected and normalized to their respective 4 h values. Significant differences denoted by **** (P<0.0001) compared to WT replication at 24 hpt at their respective temperatures. Data are displayed as the means ±S.E. of three experimental replicates.

4.2.3 Enhanced genome replication at sub-physiological temperature is not dependent on the nature of fused-nsP3 reporter proteins

Although I have shown that AUD mutants exhibited temperature sensitive replication phenotype, showing much higher levels of genome replication at sub-

physiological temperature, there is a concern that the replication phenotype might be affected by the nature of fused nsP3-reporter proteins. Previous work also showed that not all the fused luciferase reporter system are positive for luciferase activity (Pohjala et al 2008). To test this, two alternative CHIKV SGRs were generated, namely CHIKV-nsP3-mCherry-FLuc-SGR (in which the RLuc reporter was replaced with mCherry) and CHIKV-FLuc-SGR (RLuc removed and thus expressing unfused nsP3) (Fig. 4.5A). The three CHIKV SGRs were then tested in C2C12, Huh7 and Vero cells at 28°C or 37°C.

As shown in Figure 4.5B, replication of the three CHIKV SGRs showed higher genome replication at 28°C compared to 37°C in C2C12 cells. In detail, WT CHIKV-D-Luc-SGR showed ~500-fold increase in replication at both temperatures between 2-12 hpt, however, replication continued to increase over 20-fold at 28°C but reduced slightly at 37°C (Fig. 4.5B top left panel). Genome replication of WT CHIKV-FLuc-SGR also showed similar levels of increase compared to WT CHIKV-D-Luc-SGR at either 28°C or 37°C (Fig. 4.5B bottom left panel), suggesting that the nature of fused nsP3-RLuc reporter protein does not interfere with the replication phenotype. Interestingly, a slight reduction at 37°C and a significant reduction at 28°C in replication was observed for CHIKV-nsP3-mCherry-FLuc-SGR compared to CHIKV-FLuc-SGR between 2-12 hpt (Fig. 4.5B right panel). However, replication continued to increase over 50-fold at 28°C whereas it only increased 2-fold at 37°C between 12-24 hpt. The reduced genome replication of CHIKV-nsP3-mCherry-FLuc-SGR indicated a negative effect of the fused nsP3-mCherry reporter protein at early stage of replication.

In Huh7 and Vero cells, the three CHIKV SGRs showed much higher levels of genome replication at 28°C compared to 37°C between 2-24 hpt, although the increase in genome replication varied (50-500 fold for Huh7 cells and 10-200 fold for Vero cells) at 28°C from 2-12 hpt (Fig. 4.6A and B). Interestingly, unlike in C2C12 cells, replication of WT CHIKV-D-Luc-SGR and WT CHIKV-nsP3-mCherry-FLuc-SGR showed significant lower levels of replication compared to WT CHIKV-FLuc-SGR at 37°C in Huh7 or Vero cells (Fig. 4.6A and B). In detail, WT CHIKV-D-

Luc-SGR showed ~30-fold increase and WT CHIKV-nsP3-mCherry-FLuc-SGR showed ~100-fold increase in replication at 37°C whereas WT CHIKV-FLuc-SGR increased ~300-fold at 37°C in Huh7 cells (Fig. 4.6A). In Vero cells, WT CHIKV-D-Luc-SGR showed ~15-fold increase and WT CHIKV-nsP3-mCherry-FLuc-SGR showed ~40-fold increase in replication, whereas WT CHIKV-FLuc-SGR increased ~150-fold at 37°C (Fig. 4.6B).

The replication phenotype from three CHIKV SGRs in C2C12, Huh7 or Vero cells at 28°C and 37°C indicated that the replication phenotype of CHIKV SGR regulated by temperature variance is not dependent on the nature of fused nsP3-reporter protein. However, the nature of fused nsP3-reporter protein did have a negative effect on genome replication in a cell type-specific way at 37°C, which can be overcome at sub-physiological temperature.

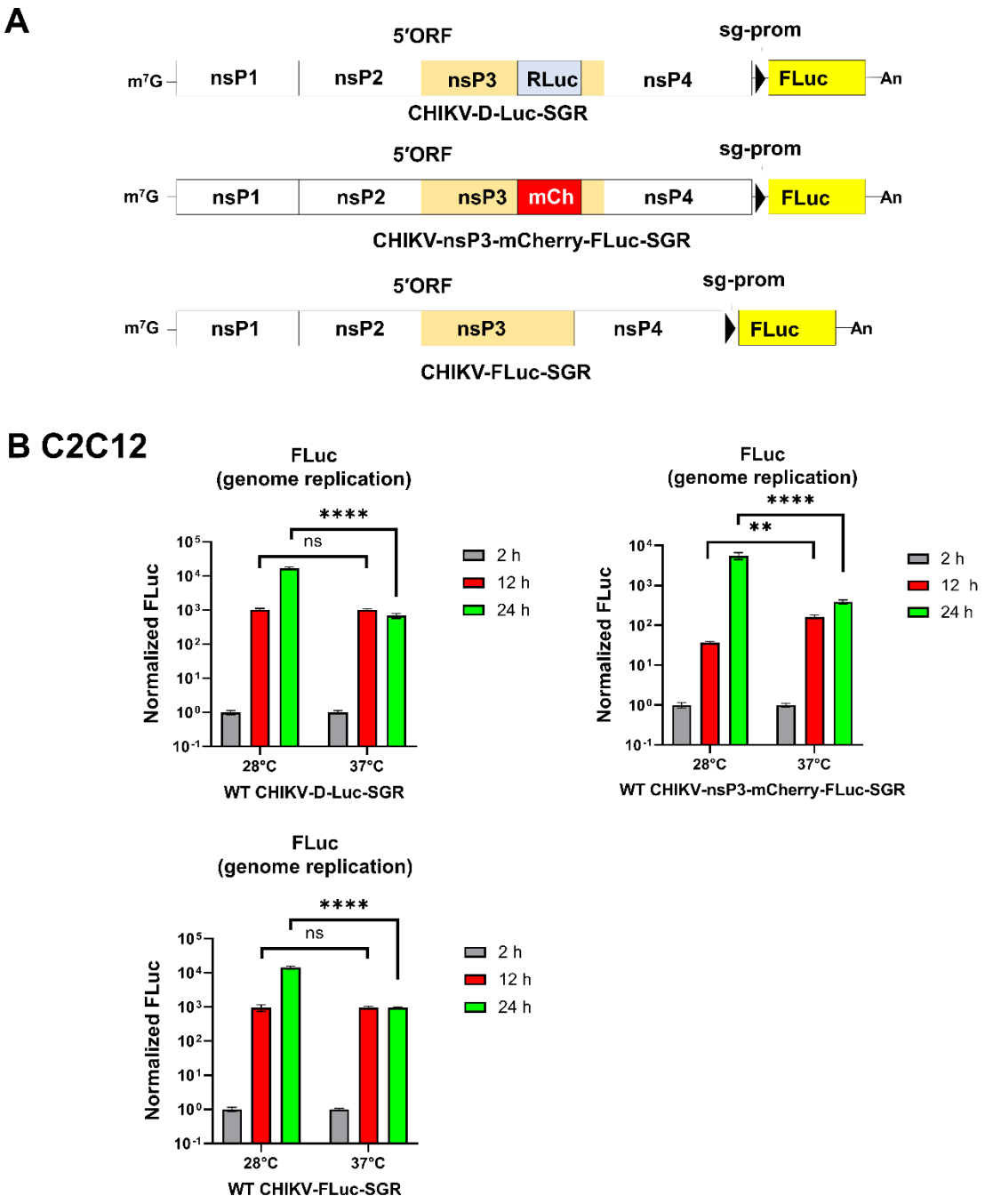

Figure 4.5 Replication of three CHIKV SGRs in C2C12 cells at 28°C or 37°C.

(A) Schematic the three CHIKV SGRs. (B) The three CHIKV SGRs were transfected into C2C12 cells and cultured at 28°C or 37°C. Cells were then harvested at indicated time points. FLuc were detected and normalized to their respective 2 h values. Significant differences denoted by ns (P>0.05), **(P<0.01), **** (P<0.0001) compared to replication of WT CHIKV-FLuc-SGR at 24 hpt at their respective temperatures. Data are displayed as the means ±S.E. of three experimental replicates.

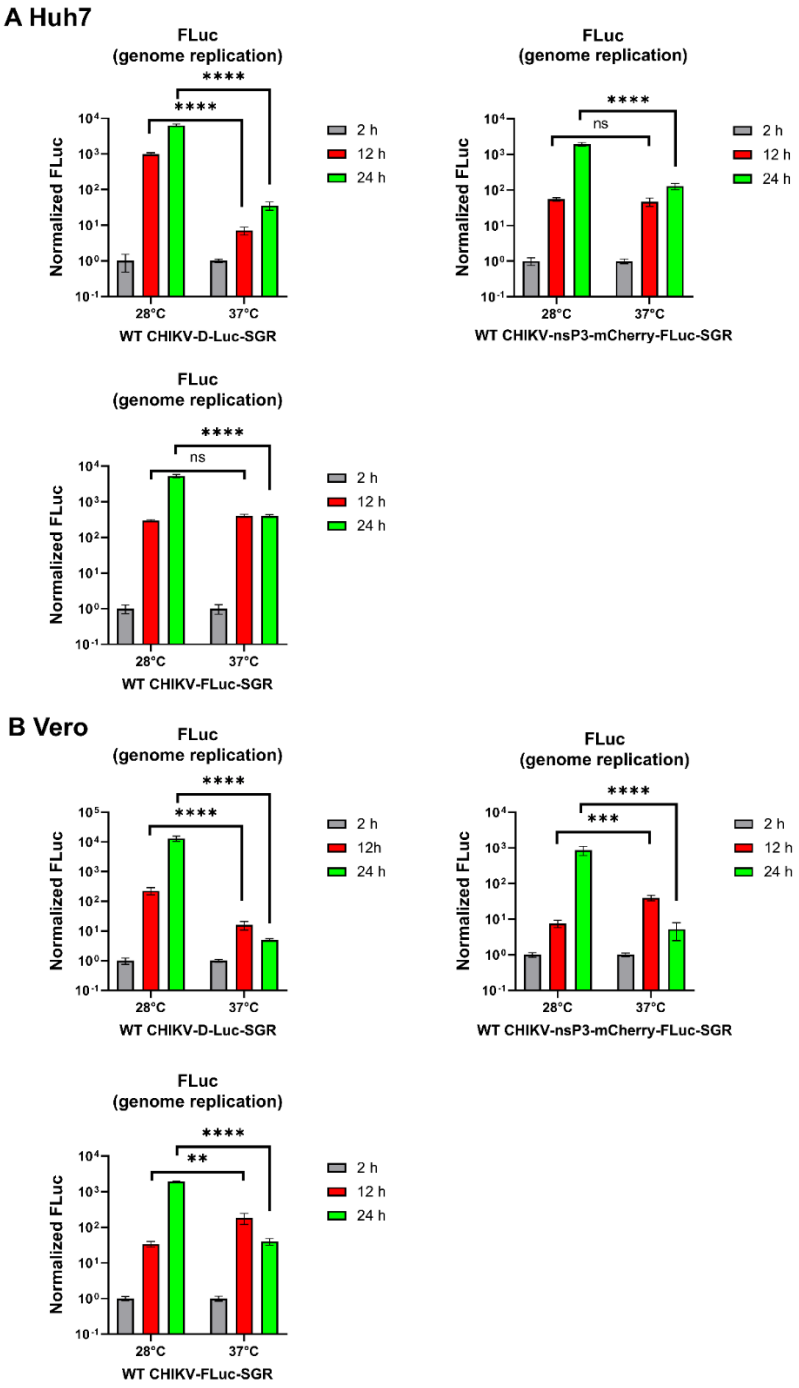

Figure 4.6 Replication of three CHIKV SGRs in Huh7 or Vero cells at 28°C or 37°C.

Huh7 cells (A) and Vero cells (B) were transfected with the three CHIKV SGRs and cultured at 28°C or 37°C. Cells were then harvested at indicated time points. FLuc were detected and normalized to their respective 2 h values. Significant differences denoted by ns (P>0.05), **(P<0.01), *** (P<0.001), **** (P<0.0001) compared to replication of WT CHIKV-FLuc-SGR at 24 hpt at their respective temperatures. Data are displayed as the means ±S.E. of three experimental replicates.

4.2.4 Enhanced genome replication in mammalian cells at sub-physiological temperature is not exhibited by Zika virus and bunyamwera virus (BUNV).

Transmission from mosquitoes to humans undergoes a temperature jump from sub-physiological temperatures to physiological temperature (37°C) (Alto et al 2018). Although CHIKV replicates efficiently in mammalian cells (Roberts et al 2017), replication of CHIKV SGR suggest a more efficient replication at sub-physiological temperature (28°C). Thus this might be a common feature in other arboviruses that share a mode of transmission from mosquitoes to humans via a peripheral bite. Therefore, replication of SGRs from BUNV (Weber et al 2001) and Zika virus (Malone et al 2016) was tested. BUNV is negative-sense, single-stranded RNA virus, belonging to the Bunyaviridae family, and Zika virus is a positive-sense, single stranded RNA virus in the Flaviviridae family. A schematic of the BUNV and Zika virus replicons is shown in Figure 4.7A. A ~20-fold increase in genome replication for BUNV replicon at 37°C or 28°C from 4-24 hpt, and a ~2-fold increase in Zika virus replication at 28°C or 37°C from 4-12 hpt (Fig. 4.6B) was observed. The results indicated that the enhanced genome replication at sub-physiological temperature is not a feature exhibited byBUNV and Zika virus.

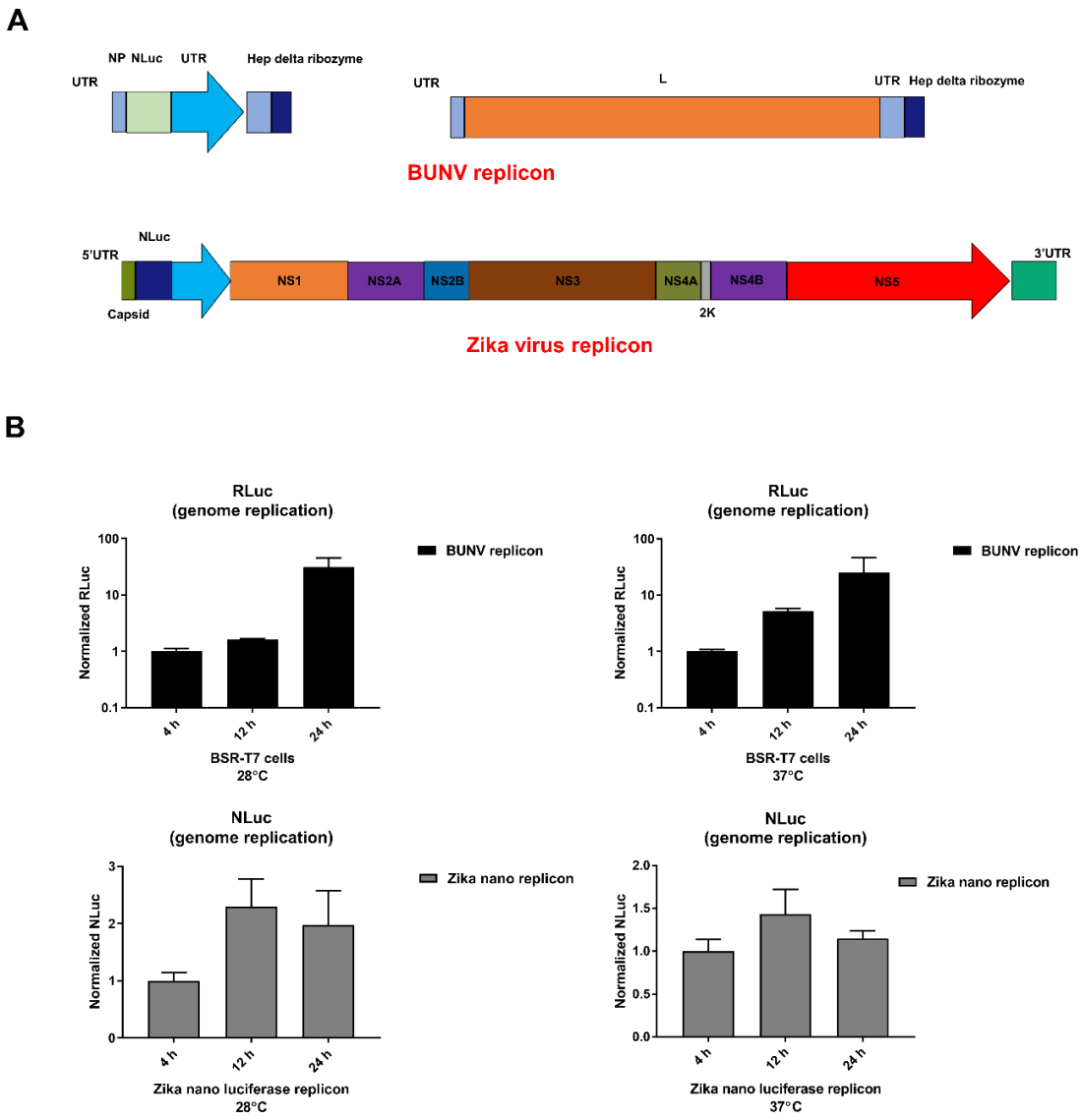

Figure 4.7 Replication of Zika virus SGR and Bunyamwera virus (BUNV) mini-genome at 28°C or 37°C.

(A) Schematic of the BUNV mini-genome (Weber et al 2001) and Zika virus SGR (Malone et al 2016). (B) Replication of Zika virus SGR and BUNV mini-genome at 28°C or 37°C. The BSR-T7 cells supplied with 200 µg/ml G418 were transfected with BUNV mini-genome RNA and incubated at 28°C or 37°C. BHK-21 cells were transfected with Zika virus SGR RNA and incubated at 28°C or 37°C. Cells were harvested at indicated time points and RLuc activities or Nano luciferase (NLuc) were measured and normalized to their respective 4 h values. Data are displayed as the means ±S.E. of three experimental replicates.

4.2.5 The AUD mutants retained the temperature sensitive replication phenotype in the context of infectious CHIKV

Previously we identified a novel function of the CHIKV AUD in promoting virus assembly (Gao et al 2019), Here I wished to determine whether the phenotype in the context of CHIKV SGR was also seen in infectious CHIKV. Therefore, the three AUD mutations (W220A, D249A and Y324A) were generated in the backbone of the ICRES-CHIKV infectious clone (Tsetsarkin et al 2006). In vitro transcribed RNA for each mutant was transfected into C2C12 cells and released viruses were harvested from supernatant at 48 h post infection (hpi) and titrated by plaque assay on BHK-21 cells at 37°C. As shown in Figure 4.8 right panel, the AUD mutants produced much less infectious viruses than WT at 37°C, which showed ~10,000-fold reduction in virus titre. However, unlike the CHIKV SGR data where the AUD mutants exhibited indistinguishable replication from WT at 28°C, the AUD mutants also showed significantly less virus titres compared to WT (between 5-50 fold reduction) at 28°C (Fig. 4.8 left panel), although the reduction was much less pronounced compared to at 37°C. Sequencing analysis work of the ICRES-CHIKV AUD mutants at 37°C or 28°C indicated no reversion had occurred at either 28°C or 37°C. To note, unlike the marked differences in genome replication using CHIKV SGRs, WT ICRES-CHIKV only showed 2-fold increase in virus production at 28°C than 37°C (Fig. 4.8). The data indicated that higher levels of alphavirus genome replication did not lead to a concomitant increase in assembly and release of the infectious virus.

Plaque size of W220A produced at 37°C was much smaller, while D249A and Y324A at 37°C showed similar sizes compared to WT (Fig. 4.9). Interestingly, plaque size of W220A produced at 28°C was also much smaller than WT (Fig. 4.9), suggesting a possible growth defect of W220A (produced from 28°C) at 37°C.

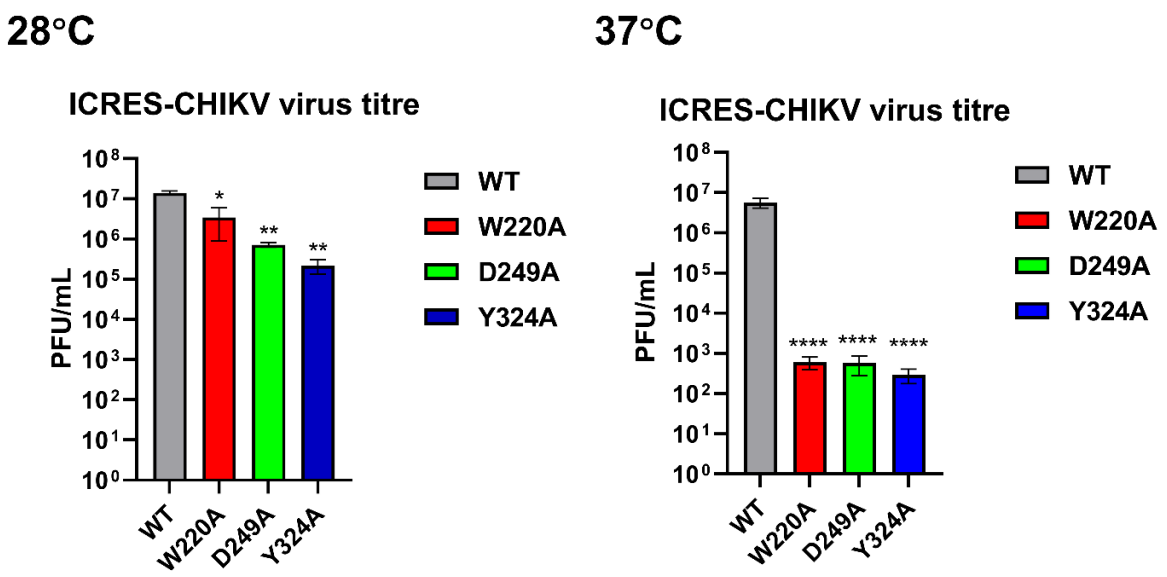

Figure 4.8 Phenotype of WT and the AUD mutants in the context of ICRES-CHIKV production at 28°C or 37°C.

C2C12 cells were transfected with WT and mutant ICRES-CHIKV RNAs and incubated at 28°C or 37°C. Supernatants were collected and titrated by plaque assay at 48 h post infection (hpi) and cells were fixed with 4% paraformaldehyde. Plaque assays were performed on BHK-21 cells at 37°C. BHK-21 cells were fixed with 4% paraformaldehyde at 48 hpi and stained with 0.05% crystal violet. Data are displayed as the means ±S.E. of three experimental replicates.

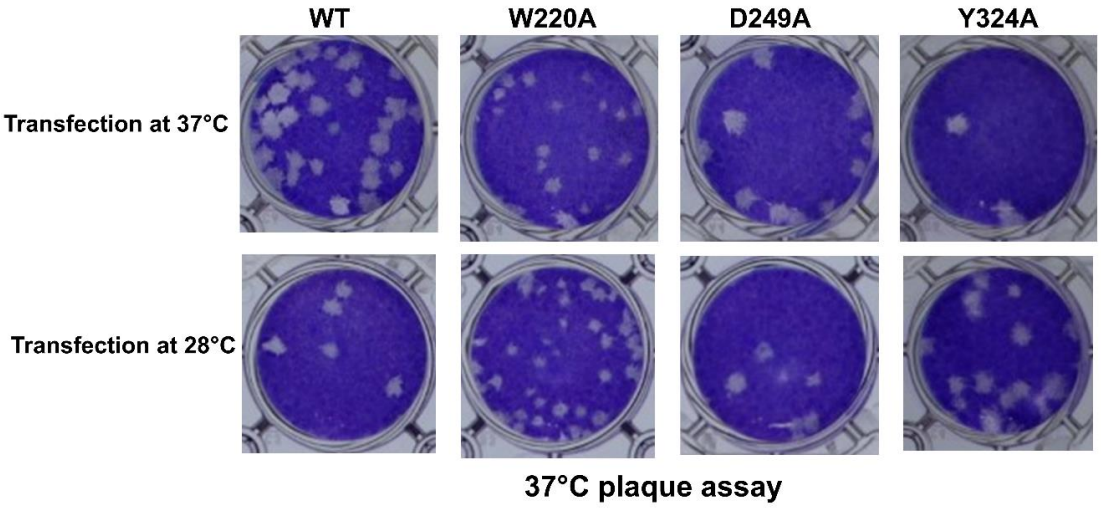

Figure 4.9 Plaque sizes of WT and mutant ICRES-CHIKV harvested from 28°C or 37°C.

The plaque assay was conducted at 37°C on BHK-21 cells.

4.3 Discussion

Previous work identified the phenotypic replication defects of the three CHIKV AUD mutants in mammalian cells but not in mosquito cells. Mosquito cells are cultured at 28°C and mammalian cells are cultured at 37°C. Transmission of CHIKV from mosquitoes to humans undergoes a temperature jump and is thus largely affected by temperature. It was proposed that temperature variance might be the key regulator that determine replication phenotype of the AUD mutants. Unfortunately, most mosquito cells fail to survive over 33°C (Kuno & Oliver 1989), therefore I tested replication of WT and mutant CHIKV-D-Luc-SGR in mammalian cells at 37°C or 28°C. I confirmed that temperature plays a key role in the replication phenotype of the AUD mutants as replication defects of the AUD mutants at 37°C was completely recovered at 28°C (Fig. 4.1 and 4.2). Intriguingly, replication of WT CHIKV-D-Luc-SGR at 28°C was significantly higher (approximately 100-fold) than at 37°C. This was further supported by the protein expression of nsP1 at 28°C or 37°C (Fig. 4.2), rather than the varied activities of FLuc at different temperatures (Mehrabi et al 2008).

Previous work showed that CHIKV infection was enhanced at lower temperatures, which was correlated with reduced IFN activities (Lane et al 2018, Prow et al 2017). However, unlike the ~100-fold increase in genome replication at sub-physiological temperature (28°C), the CHIKV titres only increased a few-fold at lower temperatures (Lane et al 2018). As Vero cells are defective in IFNα/β activities, my data indicated that the enhanced replication at 28°C is not due to the previously documented reduced IFN response at sub-physiological temperature (Lane et al 2018, Suopanki et al 1998), other mechanisms unknown affected by temperature play a more important role in the replication phenotype.

There was also a concern on the nature of the fused nsP3-reporter protein, as it might have a negative effect on replication of the CHIKV SGR at 37°C, which results in a pseudo phenotype of enhanced genome replication at sub-physiological temperature. My data using three CHIKV SGRs in C2C12, Huh7 and

Vero cells at 28°C or 37°C demonstrated that the replication phenotype of enhanced genome replication for CHIKV SGR at lower temperature is not due to the nature of the fused nsP3-reporter protein (Fig. 4.5 and 4.6). To note, consistent with low levels of replication for WT CHIKV-D-Luc-SGR in Huh7 or Vero cells at 37°C (Fig. 4.3), significant lower levels of replication for WT CHIKV-D-Luc-SGR and WT CHIKV-nsP3-mCherry-FLuc-SGR compared to WT CHIKV-FLuc-SGR in Huh7 or Vero cells at 37°C (Fig. 4.6) were observed. This suggested that the nature of the fused nsP3-reporter protein did suppress replication of CHIKV SGR at 37°C, but in a cell-type specific way, and the defects can be compensated at sub-physiological temperature. Previous work identified luciferase reporter system as a useful tool to detect alphavirus replication (Pohjala et al 2011) or production (Steel et al 2013). However, some luciferase proteins fused with alphavirus non-structural proteins showed a negative effect on replication (Pohjala et al 2011). Further work needs to be conducted to investigate how the nature of the fused nsP3-reporter proteins suppress alphavirus replication and why it was ablated at lower temperature.

As the first cells infected by CHIKV via a mosquito bite would be in the periphery and thus not at 37°C, it is reasonable to assume that the enhanced genome replication for CHIKV SGR at sub-physiological temperature supports CHIKV replication. However, my data indicated that it was not the case for BUNV and Zika virus replicons (Fig. 4.7). This suggested that this phenotype is alphavirus specific. In further explaining this, we noticed both nsP3 macrodomain and the AUD does not have functional homologues in bunyaviruses or flaviviruses. Therefore the function of nsP3 macrodomain and the AUD therefore might potentially responsible for the enhanced replication phenotype at sub-physiological temperatures, further evidence and research are needed to support this assumption.

I extended the replication phenotype of the AUD mutants in the context of CHIKV-D-Luc-SGR to infectious CHIKV. As expected, the AUD mutants showed much higher levels of virus production (over 1000-fold) at 28°C than at 37°C, supporting the temperature-sensitive phenotype of the AUD mutants (Fig. 4.8). Unlike the

indistinguishable replication for WT and mutant CHIKV-D-Luc-SGR at 28°C, the AUD mutants in the context of ICRES-CHIKV showed significant reduction (5-50 fold) in virus titers compared to WT at 28°C (Fig. 4.8). This might be explained by that viruses of the AUD mutants produced at 28°C still have growth defects at 37°C, as the plaque size of W220A (harvested from 28°C) was still smaller compared to WT when plaque assay was conducted at 37°C. However, plaques failed to form in BHK-21 cells at 28°C by crystal violet, so this cannot be confirmed further. Unlike significant higher levels of replication for CHIKV SGR at sub-physiological temperature, there was only a modest increase (2-fold) in virus production for WT ICRES-CHIKV at 28°C compared to at 37°C, indicating a defect in virus assembly or release from cells at lower temperature. Indeed, previous work demonstrated alphavirus budding is temperature dependent, with the optimal budding occurring at physiological temperatures (Lu & Kielian 2000).

Previously a number of studies focused on temperature sensitive mutants (ts mutants) of alphaviruses (Balistreri et al 2007, Barton et al 1988, Lulla et al 2008, Sawicki & Sawicki 1985, Sawicki & Sawicki 1993, Sawicki et al 1981, Wang et al 1991). Two ts mutants in SFV nsP1 (D119N and E529D) showed defects in synthesis of negative strand RNA at 39°C, indicating the role of nsP1 in negative-strand RNA synthesis (Lulla et al 2008). SINV nsP3 F312S (a ts mutant) destabilized the hydrophobic core, which is surrounded by the macro, AUD and nsP2 MT-like domain, and disrupted domain interaction at the non-permissive temperature 40°C (Hahn et al 1989a). Several ts mutants in nsP2 identified this protein as a regulator of sub-genomic RNA through the protease and the helicase domain by recognizing the sub-genomic promoter (Balistreri et al 2007, Suopanki et al 1998). Therefore, assumptions of enhanced genome replication at sub-physiological temperature can be explained by the enhanced proteinase activity (for cleaving non-structural proteins) at sub-physiological temperature (Balistreri et al 2007), or reduced degradation of non-structural proteins/ proteins involved in replication complexes, as temperature down-shift decreased expression of genes involved in ERAD (Torres et al 2021). Another possible explanation is that although the three AUD mutants are distal from each other, their side chain protrusions are

adjacent to each other in spatial structure, whereas mutations of these residues removed these protrusions. It is possible that that losing of these protrusions might be lethal to virus replication at 37°C but not at 28°C, which can be further explained in RNA folding or RNA-protein interaction differently at 28°C or 37°C. Other possible mechanisms might be related with cell response, which is ablated or blunted at sub-physiological temperatures, I will discuss this further in the next chapter.

Chapter 5: Enhancement of genome replication correlates with differences in the size and number of G3BP-positive granules

5.1 Introduction

The activity of eIF2α is a key regulator of protein synthesis in mammalian cells (Dever 2002). Upon phosphorylation, eIF2α binds to eIF2B more tightly, which prevents eIF2B-mediated guanine nucleotide exchange on eIF2α and the regeneration of the active GTP-bound state, resulting in a global translation arrest (Harding et al 2002). In mammalian cells, there are four kinases that phosphorylate eIF2α, each of which is activated by distinct types of stress. The HRI is activated by oxidative stress (McEwen et al 2005) or heat shock (Lu et al 2001a), GCN2 is activated by amino acid deprivation (Wek et al 1995) or UV light-induced damage (Deng et al 2002); PKR is specifically activated by sensing dsRNA (Srivastava et al 1998) and PERK is activated by ER stress (Harding et al 2000a, Harding et al 2000b). Treated by sodium arsneite ($NaAsO_2$), one of the oxidative stresses, the cells exhibited similar levels of phosphorylation of eIF2α at different temperatures (33°C, 35°C and 37°C) (Wheeler et al 2016). CHIKV has been reported to suppress eIF2α phosphorylation by nsP4 protein (Rathore et al 2013).

Phosphorylation of eIF2α blocks the recognition of the initiation codon and the recruitment of large ribosomal subunit, resulting in the accumulation of stalled 48S messenger RNA ribonucleoprotein particles (mRNPs) (Jackson et al 2010). SG are the discrete foci in the cytoplasm, which results from the accumulation of the stalled 48S ribosomal complexes. Experimentally, $NaASO_2$ is typically used for SG induction, and the formation of SG is regarded as an adaptation step for cells exposed to environmental stress (Kedersha & Anderson 2002). SG are sites of mRNA storage, as they are disassembled along with the release of mRNA when the stress is removed. In the assembly of SG, it is assumed that there is a balance between polysome-bound (translated) mRNA and non-translated mRNA, and the SG assemble is due to an excess of non-translated mRNA in the cytoplasm (Kedersha et al 2000). Treatment of CHX reduces the levels of non-translated mRNA by stabilizing polysomes, in which the SG induced by $NaAsO_2$ is dispersed by CHX. The structure of SG is highly dynamic and the components of SG keep rapid change with some proteins shutting in and out in seconds (Kedersha et al

2005). The composition of SG is thus variable, with over a hundred different components. The main components of SG contain stalled mRNAs, translation initiation factors, small ribosomal subunits, and various mRNA binding proteins. Despite varied compositions (Kedersha & Anderson 2007), certain components including the Ras GTP-activating protein-binding protein G3BP1/2, are required for all SG formation (Kedersha et al 2016, Matsuki et al 2013, Tourriere et al 2003). SG formation was postulated as hubs for regulating multiple signaling activities upon recruitment of signaling proteins (Hetz 2012, Kedersha et al 2013, Kim et al 2005) and promote antiviral responses (Arimoto et al 2008). RIG-I (Onomoto et al 2012) and MDA5 (Langereis et al 2013), for example, are recruited to SG. These RIG-I-like receptors were recognized as some of the most potent antiviral cytoplasmic pathogen recognition receptors (Randall & Goodbourn 2008, Yoneyama et al 2005). A specific interaction between PxxP domain of G3BP within SG and PKR was shown to activate PKR, suggesting a strong antiviral role of SG and G3BP (Reineke & Lloyd 2015). In SFV infection, TIA-1/R positive granules are formed transiently, but later disassembled with viral ongoing replication (McInerney et al 2005). Two FGDF repeats in the CHIKV nsP3 hypervariable domain have been shown to bind to G3BP (Panas et al 2015, Schulte et al 2016), and depletion of G3BP reduced CHIKV replication and infection (Scholte et al 2015). Recent work showed the assembly and disassembly of SG was determined by the ADP-ribosylhydrolase activity of CHIKV nsP3 macro domain (Jayabalan et al 2021), rather than the previously expected nsP3 hypervariable domain. Disassembly of translation initiation factors and other stress-related proteins from SG results in the formation of another type of membranous granules (Jayabalan et al 2021).

To investigate the mechanism behind temperature variance, I used an ONNV construct for infection (kind gift from Prof. Andres Merits, University of Tartu) (Fig. 5.1A). ONNV is an arbovirus and the only known reservoir is human (Vanlandingham et al 2005). CHIKV is closely related to ONNV, as they probably diverged from a common ancestor thousands of years ago (Powers et al 2000). Unlike CHIKV, which requires BSL3 containment, work with infectious ONNV can be conducted at BSL2. The ZsGreen, expressed from a second copy of sub-

genomic promoter in ONNV-2SG-ZsGreen (Fig 5.1A), allows rapid assessment of genome replication. Similar to CHIKV, I tested the replication phenotype of WT and AUD mutants in the context of infectious ONNV by transfection at 28°C or 37°C. Confirmation of the replication phenotype of the AUD mutants in ONNV would facilitate the use of ONNV to investigate the mechanism in temperature variance without requiring BSL3 containment. I also tested the phosphorylation of eIF2α by infection with ONNV at an MOI of 5 and incubated at 28°C or 37°C. The data would provide direct evidence on phosphorylation of eIF2α in response to ONNV infection at both temperatures.

Previous studies have investigated temperature-sensitive mutants of alphaviruses by use of a temperature shift assay (Kaariainen et al 1978, Saraste et al 1977, Suopanki et al 1998). In order to investigate how temperature variance affects replication of WT and the AUD mutants and if the effect of eIF2α phosphorylation was affected by temperature variance, temperature shift assay was performed using WT CHIKV-D-Luc-SGR by transfection or WT and mutant ONNV by infection. ISRIB was first reported to enhance cognitive memory via reversing the effect of eIF2α phosphorylation (Sidrauski et al 2013). Therefore, I tested replication of WT and mutant in the context of CHIKV-D-Luc-SGR or ONNV with ISRIB, to determine if inhibition of the effect of eIF2α phosphorylation at 37°C was able to recapitulate the replication phenotype at sub-physiological temperatures.

Previous work showed that SG formation at lower temperature was suppressed and delayed (Wheeler et al 2016). To further explain why alphavirus genome replication was enhanced in mammalian cells at sub-physiological temperatures, my attention focused on the formation of SG. I first tested this by treatment with $NaAsO_2$ at two temperatures. As I was only able to detect visible granules in response to ONNV infection at 8 hpi, and they might be different from bona fide SG, hereafter they were termed G3BP-positive granules. The formation of G3BP-positive granules at 28°C or 37°C in response to ONNV infection was evaluated. The data from G3BP-positive granules formation in response to ONNV infection at

different temperatures would potentially shed light on the enhanced genome replication of alphavirus in mammalian cells at sub-physiological temperature.

5.2 Results

5.2.1 The replication phenotype of the AUD mutants was retained in the context of infectious ONNV

To explore the mechanism behind temperature variance that determine the replication phenotype, I extended this analysis to ONNV, which can be propagated at BSL2. As expected, the three AUD mutants exhibited a similar temperature dependent phenotype in the context of infectious ONNV (Fig. 5.1B). At 37°C, the three AUD mutants showed a significant reduction in ZsGreen expression per cell, whereas the levels of ZsGreen expression per cell was indistinguishable between WT and the three AUD mutants at 28°C. In contrast to the CHIKV AUD mutants, sequence analysis revealed that at 37°C, ONNV W220A and D249A had reverted to WT and Y324A exhibited two compensatory pseudo-revertant mutations (nsP2 R768Q and nsP3 C173Y). However, no reversion was detected for the ONNV AUD mutants at 28°C. In agreement with the CHIKV production at 37°C or 28°C (Fig. 4.7), I only observed 2-fold increase in ZsGreen per cell for WT ONNV at 28°C compared to 37°C (Fig. 5.1B).

Interestingly, a significant difference in virus production was shown by plaque assays conducted at 28°C or 37°C (Fig. 5.1C). Due to the fact that the AUD mutants harvested from 37°C had reverted, WT and the AUD mutants showed similar virus production at 28°C compared to 37°C. However, when supernatants were harvested from 28°C, significant differences were observed. The AUD mutants exhibited similar virus production compared to WT by titration at 28°C, whereas they still showed significant lower virus production with virus titrated at 37°C, indicating that viruses of the AUD mutants produced from 28°C still exhibited growth defects at 37°C.

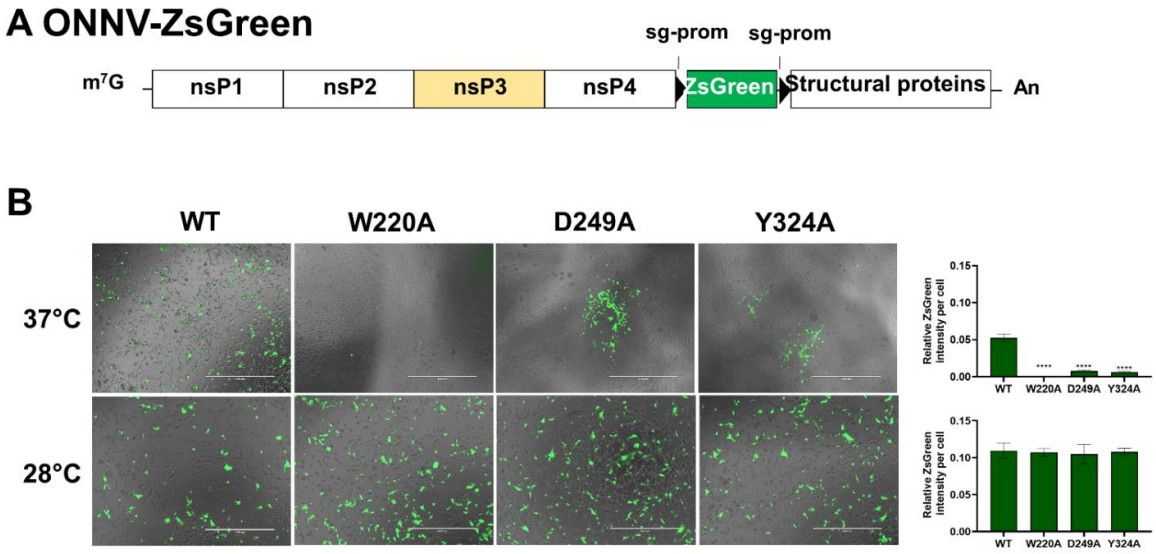
A ONNV-ZsGreen
sg-prom
sg-prom
m7G
nsP1
nsP2
nsP3
nsP4
ZsGreen
Structural proteins
An
B
WT
W220A
D249A
Y324A
37°C
28°C
Relative ZsGreen intensity per cell
0.15
0.10
0.05
0.00
****
WT
W220A
D249A
Y324A

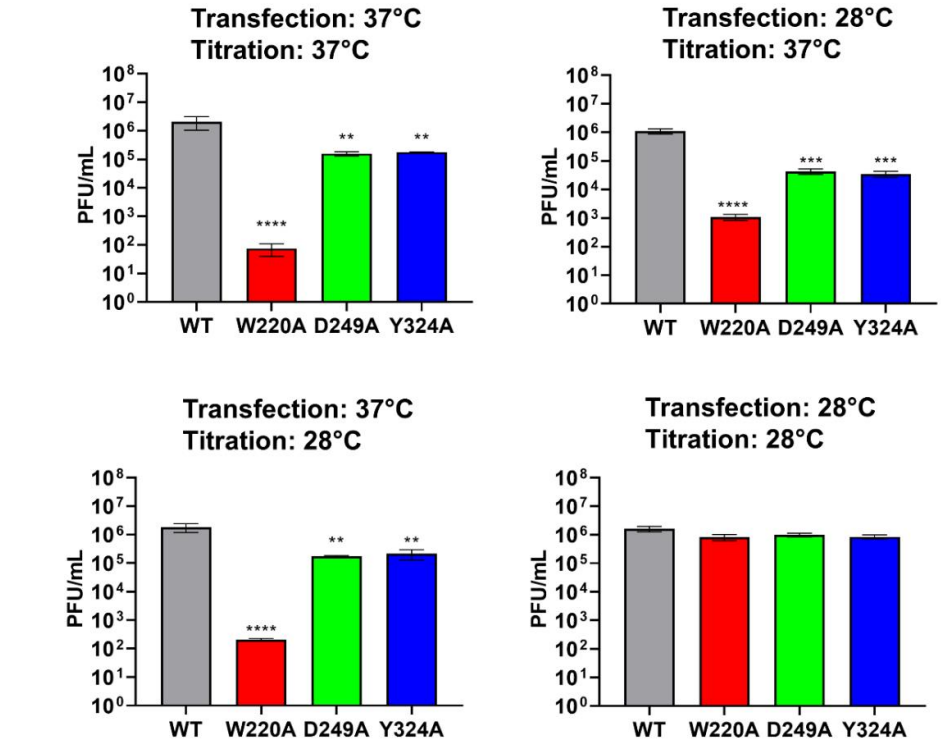
C ONNV-ZsGreen virus titre
Transfection: 37°C
Titration: 37°C
Transfection: 28°C
Titration: 37°C
Transfection: 37°C
Titration: 28°C
Transfection: 28°C
Titration: 28°C
PFU/mL
WT
W220A
D249A
Y324A

Figure 5.1 Replication and virus production of WT and AUD mutants in the context of ONNV at 28°C or 37°C.

(A) Schematic of ONNV-2SG-ZsGreen (kind gift from Prof. Andres Merits, University of Tartu). (B) Genome replication of WT and mutant ONNV at 28°C or 37°C. C2C12 cells were transfected with WT and mutant ONNV RNA and incubated at 28°C or 37°C. Cells were fixed with 4% formaldehyde at 48 hpi, scanned and normalized by EVOS microscopy. (C) Virus production of WT and mutant ONNV harvested from 28°C or 37°C. Supernatants harvested from 28°C or 37°C were titrated by plaque assay on BHK-21 cells at 28°C or 37°C. The BHK-21 cells were fixed with 4% formaldehyde at 72 hpi (37°C) or 96 hpi (28°C) The ZsGreen-positive cells were scanned by EVOS microscopy and counted.

5.2.2 ONNV infection induced eIF2α phosphorylation in cells at 28°C or 37°C

In order to investigate whether ONNV infection was able to induce eIF2α phosphorylation at both physiological and sub-physiological temperatures, RD cells were infected with ONNV and cells were stained with G3BP and P-eIF2α (phosphorylated eIF2α) primary antibodies. As seen from Figure 5.2A, ONNV infection induced eIF2α phosphorylation in cells at 28°C or 37°C, along with aggregation of G3BP and formation of bona fide SG. Surprisingly, rather than high levels of P-eIF2α in infected cells, low levels of P-eIF2α in those high-ZsGreen cells and high levels of P-eIF2α in those low-ZsGreen cells at 28°C or 37°C (Fig. 5.2B) were observed, indicating that cells in response to ONNV infection activated eIF2α phosphorylation, whereas ONNV specifically inhibited eIF2α phosphorylation at both temperatures.

Previous work showed that eIF2α phosphorylation is sufficient to induce SG in uninfected cells, however, some compounds that had no effect on eIF2α phosphorylation still stimulated SG formation by inhibiting translation initiation in a way that interacts with eIF4A (Bordeleau et al 2005, Dang et al 2006, Low et al 2005). In consistent with this, most of the SGs were dispersed at 37°C or 28°C by treatment with CHX, whereas phosphorylation of eIF2α was not affected at both temperatures (Fig. 5.3). The results suggested that CHX treatment only functioned at downstream of eIF2α phosphorylation rather than affecting eIF2α phosphorylation at 28°C or 37°C.

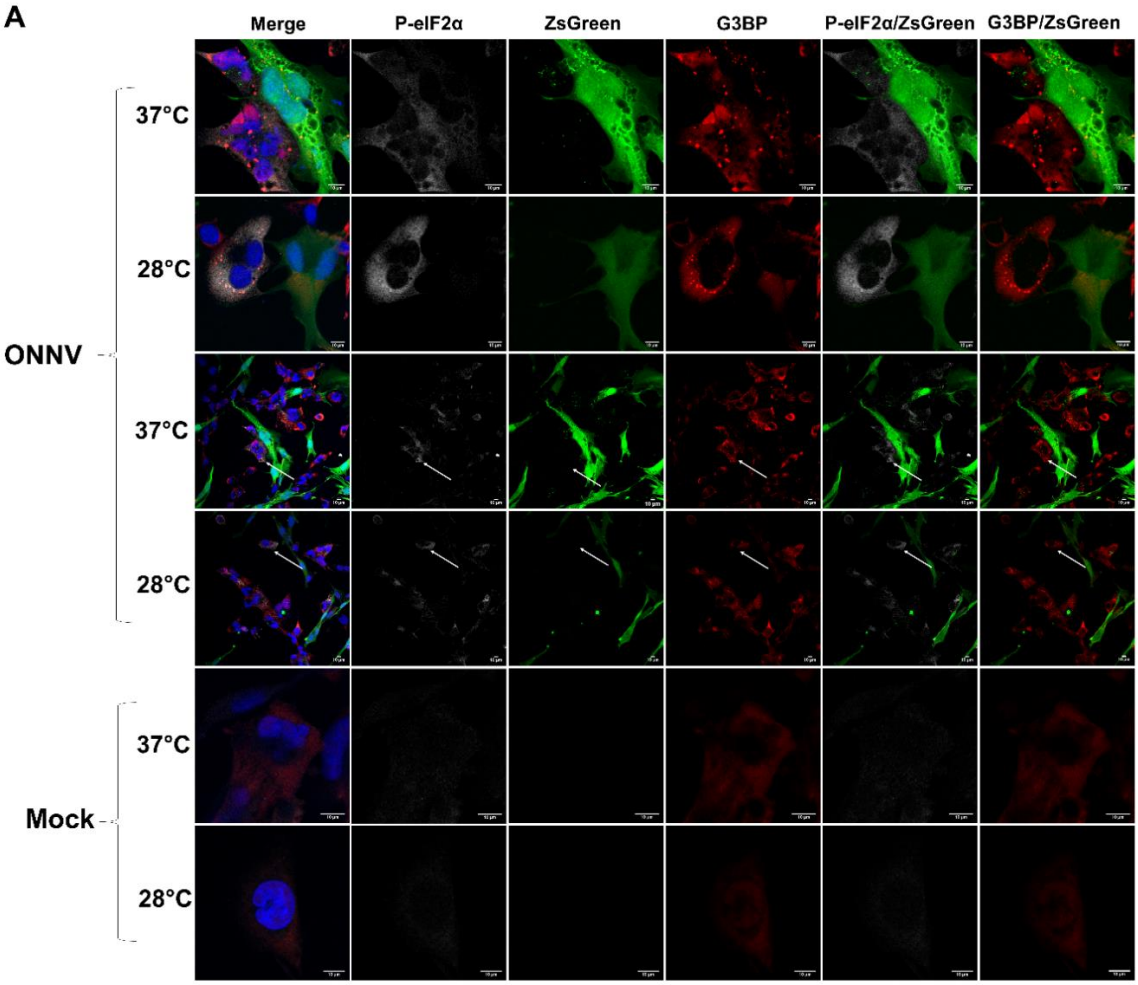
A
Merge
P-eIF2α
ZsGreen
G3BP
P-eIF2α/ZsGreen
G3BP/ZsGreen
ONNV
37°C
28°C
37°C
28°C
Mock
37°C
28°C

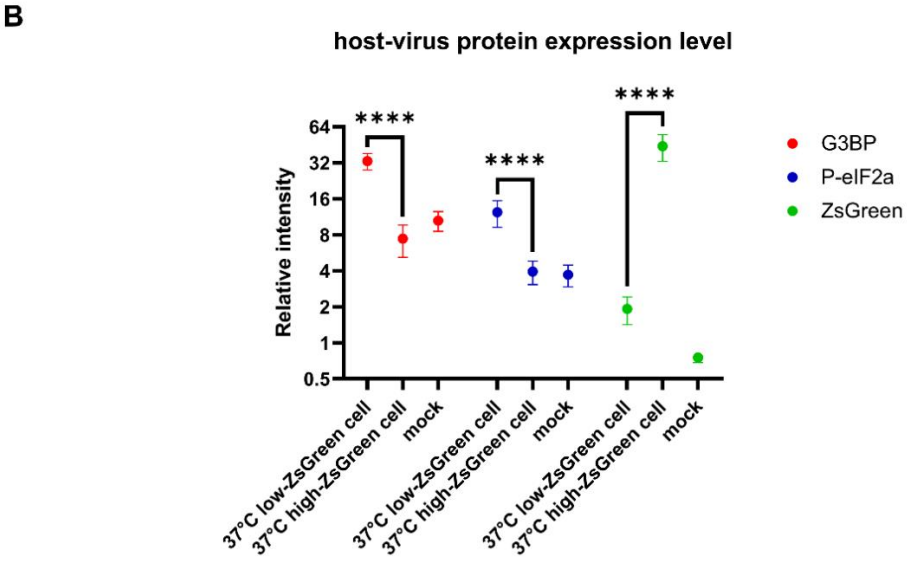
B
host-virus protein expression level
Relative intensity
64
32
16
8
4
2
1
0.5
****
****
****
G3BP
P-eIF2a
ZsGreen
37°C low-ZsGreen cell
37°C high-ZsGreen cell
mock
37°C low-ZsGreen cell
37°C high-ZsGreen cell
mock
37°C low-ZsGreen cell
37°C high-ZsGreen cell
mock

Figure 5.2 ONNV infection induced eIF2α phosphorylation in mammalian cells at either 28°C or 37°C.

(A) Phosphorylation of eIF2α at 28°C or 37°C in response to ONNV infection. RD cells were infected with WT ONNV at an MOI of 5 and incubated at 28°C or 37°C. Cells were fixed with 4% formaldehyde at 8 hpi and stained with phosphorylated eIF2α (P-eIF2α) antibody. White arrows indicate cells expressing high levels of P-eIF2α but low levels of ZsGreen. (B) Quantification of the levels of G3BP, P-eIF2α and ZsGreen in low-ZsGreen and high-ZsGreen cells at 28°C or 37°C. The relative intensities quantified by Fiji imageJ was determined for 10 cells.

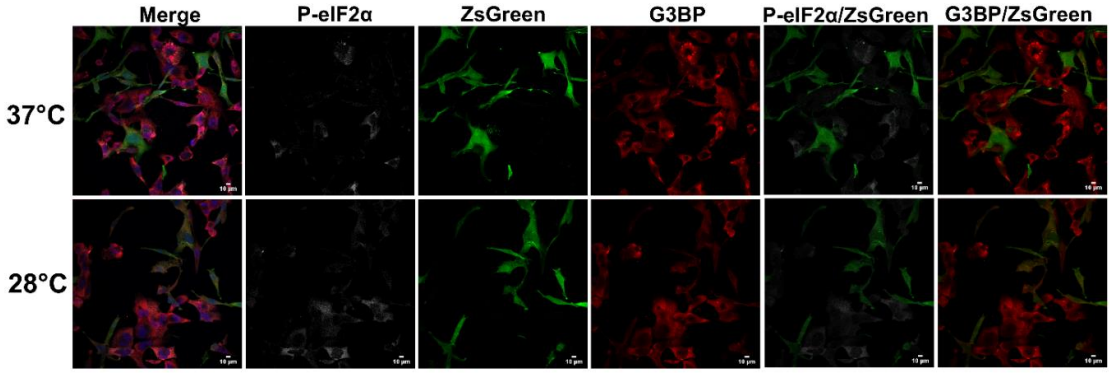

Figure 5.3 Treatment of CHX didn't reverse eIF2α phosphorylation in cells at either 28°C or 37°C.

RD cells infected with ONNV at an MOI of 5 were incubated at 37°C or 28°C for 8 h, cells were then treated with 100 µg/ml CHX for 45 min prior fixation with 4% formaldehyde and stained with P-eIF2α and G3BP antibodies.

5.2.3 Temperature shift assay of CHIKV-D-Luc-SGR

Previous studies have investigated the temperature-sensitive mutants of alphaviruses by use of a temperature shift assay (Kaariainen et al 1978, Saraste et al 1977, Suopanki et al 1998). Here I used temperature shift assay to investigate if eIF2α phosphorylation was ablated at sub-physiological temperature. A schematic of the temperature shift assay was shown in Figure 5.4A, the WT D-Luc-SGR RNA was transfected into C2C12 cells and incubated at 28°C or 37°C for 12 h, with and without a temperature shift from 12-24 hpt (37°C to 28°C (designated S#) or 28°C to 37°C (designated S*)). Similar as shown in Figure 4.1, replication of WT CHIKV-D-Luc-SGR increased ~100-fold between 12-24 hpt at 28°C, however, it only increased ~20-fold when the temperature was shifted from 28°C to 37°C between 12-24 hpt (Fig. 5.4B left panel). When the transfected cells were first incubated at 37°C, an opposite effect was observed: replication of WT CHIKV-D-Luc-SGR did

not increase between 12-24 hpt, while it increased 5-fold between 12-24 hpt when the temperature was shifted from 37°C to 28°C (Fig. 5.4 B right panel). Western blotting for nsP1 confirmed the high levels of translation at 28°C (Fig. 5.4C). Interestingly, while there was more genome replication at 28°C than 37°C at 24 hpt, lower levels of P-eIF2α at 28°C compared to 37°C was observed. As PKR senses dsRNA and induces eIF2α phosphorylation, the results indicated a defect in the PKR induced eIF2α phosphorylation at sub-physiological temperature.

To note, both cell growth assay accessed by quantification of variable cells and cell metabolic activity accessed by MTT assay showed more cell numbers and higher cell metabolic activity at 37°C, which is in contrary to the enhanced genome replication at sub-physiological temperature (Fig. 5.5). These data demonstrated the reduced levels of eIF2α phosphorylation in cells along with the enhanced genome replication for CHIKV SGR at sub-physiological temperature, which cannot be explained by increased cell growth and metabolic activity at lower temperature.

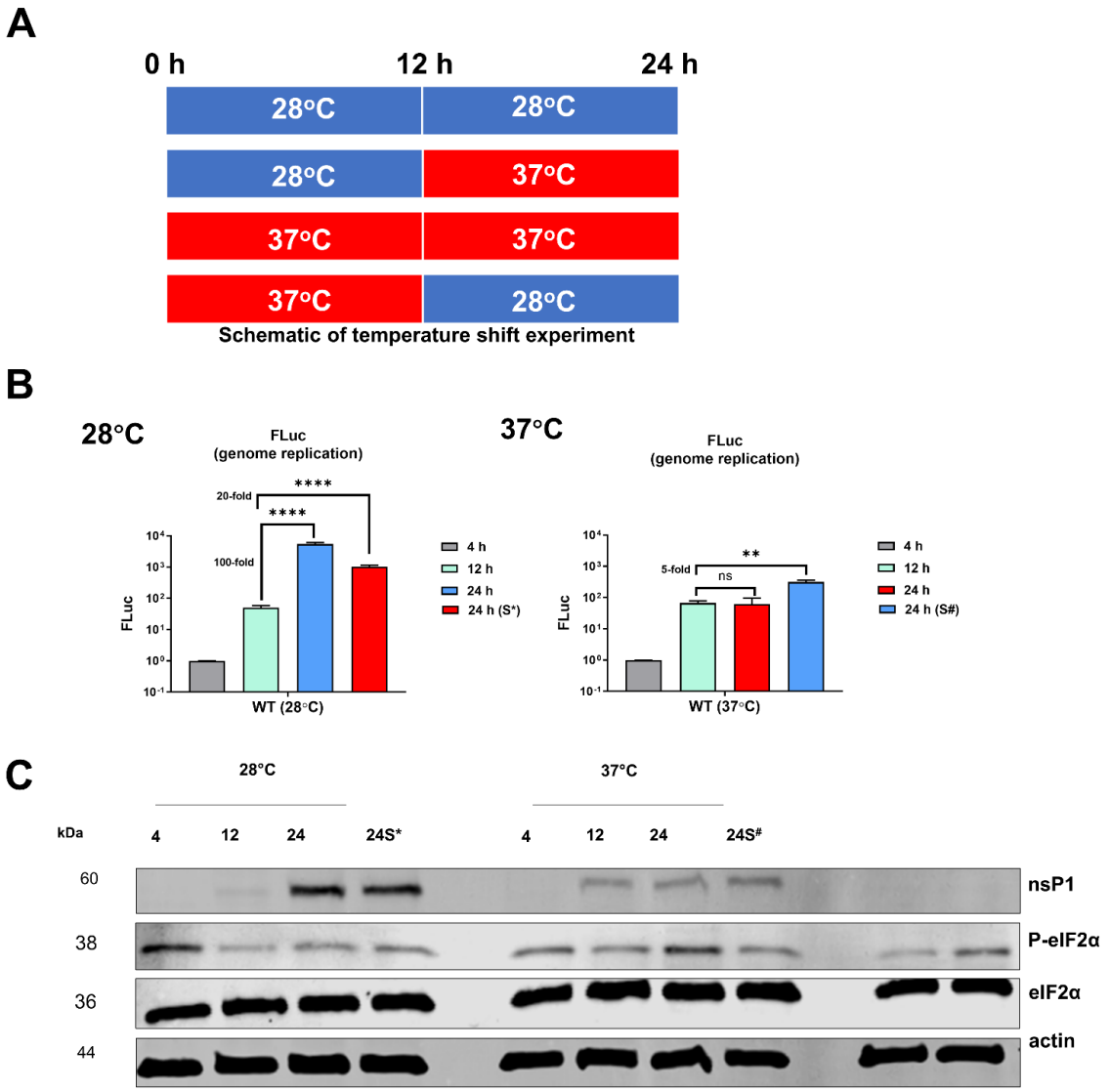

Figure 5.4 Temperature shift assay of WT CHIKV-D-Luc-SGR.

(A) Schematic of temperature shift assay. Transfected cells were incubated at 28°C or 37°C prior to a temperature shift between 12-24 hpt (28°C to 37°C (designated 24 h S#) and 37°C to 28°C (designated 24 h S*) respectively). Control cells maintained the same temperature between 0-24 hpt. (B) Replication of WT CHIKV-D-Luc-SGR at 28°C or 37°C. C2C12 cells were transfected with WT CHIKV-D-Luc-SGR RNA and incubated at 37°C or 28°C. Cells were collected at indicated time points and FLuc activities were measured and normalized to their respective 4 h values. Significant differences denoted by ns (P>0.05), ** (P<0.01), **** (P<0.0001) compared to replication at 12 hpt. (C) Protein expressions of nsP1 at different temperatures. 10 µg of each sample was loaded and analysed by western blotting. Actin was detected by western blotting as a loading control.

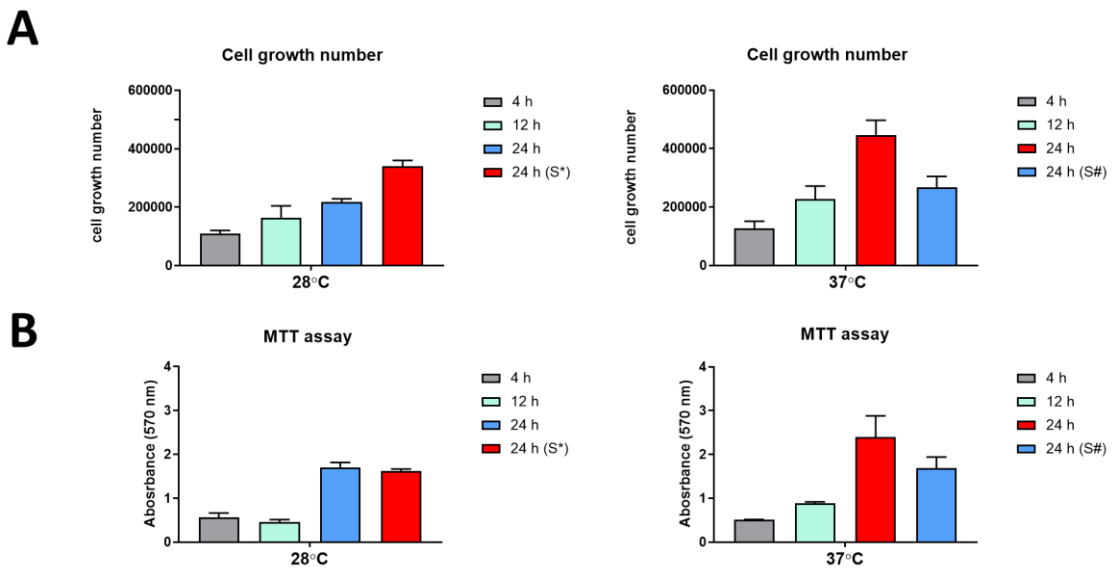

Figure 5.5 Cell growth number and cell viability assay during temperature shift assay.

Cell growth number was enumerated at each collection time by trypsin digestion and dilution into 1 ml DMEM. Cell metabolic activity was determined by MTT assay during temperature shift assay at either 37°C or 28°C.

5.2.4 Temperature shift assay of ONNV

I also used a temperature shift assay with WT and mutant ONNV to investigate the relationship between eIF2α phosphorylation and ONNV replication at 28°C or 37°C. In brief, C2C12 cells were infected with WT and W220A ONNV and incubated at 28°C or 37°C, with and without a temperature shift between 24-48 hpi (28°C to 37°C (designated S*) or 37°C to 28°C (designated S#)). Consistent with the results from temperature shift assay of CHIKV SGR, W220A ONNV showed poor replication at 37°C but exhibited similar levels of genome replication as compared to WT at 28°C (Fig. 5.6A). Indeed, shifting temperature from 28°C to 37°C reduced genome replication of W220A ONNV whereas temperature shifting from 37°C to 28°C allowed the W220A ONNV to replicate (Fig. 5.6A). As shown before (Fig. 5.1 B), unlike much more significant increase in replication at 28°C in CHIKV SGR, WT ONNV only showed 2-fold increase in replication at 28°C than 37°C at 48 hpi (Fig. 5.6B). Interestingly, replication of WT ONNV was reduced when temperature was shifted from 28°C to 37°C, but when temperature was shifted from 37°C to 28°C, replication of WT ONNV was also reduced (Fig. 5.6B).

Analysis of P-eIF2α and nsP1 by western blotting showed reduced level of P-eIF2α at 48 hpi (compared to 28°C 48 hpi) when temperature was shifted from 28°C to 37°C along with more nsP1 expression, whereas when temperature was shifted from 37°C to 28°C increased level of P-eIF2α at 48 hpi (compared to 37°C 48 hpi) along with reduced nsP1 expression (Fig. 5.6C) was observed. The results suggested that phosphorylation of eIF2α in response to ONNV infection and CHIKV SGR was different and phosphorylation of eIF2α inhibited ONNV translation at both temperatures, which was consistent with the IFA data.

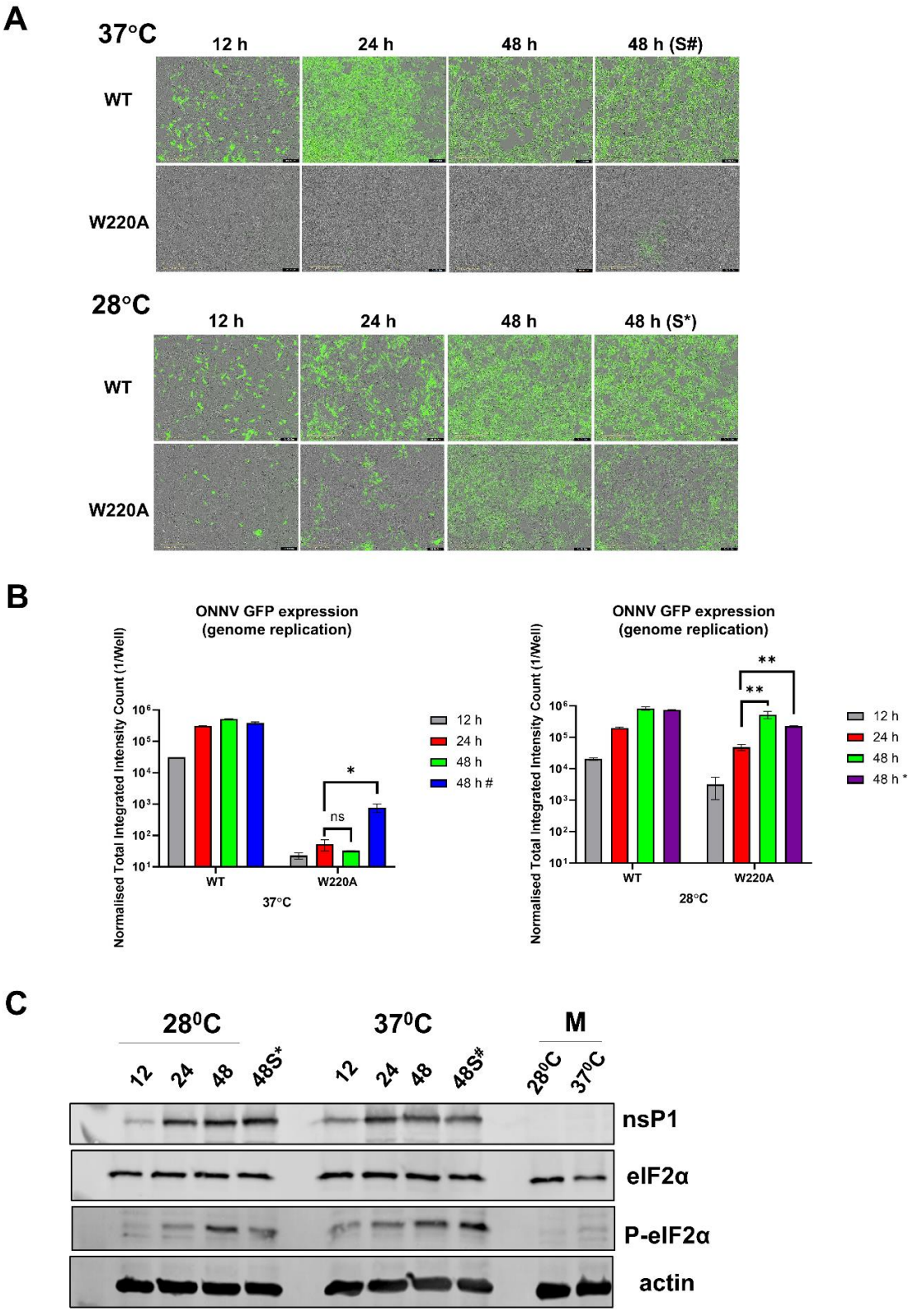
A
37°C
12 h
24 h
48 h
48 h (S#)
WT
W220A
28°C
12 h
24 h
48 h
48 h (S*)
WT
W220A
B
ONNV GFP expression
(genome replication)
Normalised Total Integrated Intensity Count (1/Well)
12 h
24 h
48 h
48 h #
*
ns
WT
W220A
37°C
ONNV GFP expression
(genome replication)
Normalised Total Integrated Intensity Count (1/Well)
12 h
24 h
48 h
48 h *
**
**
WT
W220A
28°C
C
28⁰C
37⁰C
M
12
24
48
48S*
12
24
48
48S#
28⁰C
37⁰C
nsP1
eIF2α
P-eIF2α
actin

Figure 5.6 Temperature shift assay of ONNV.

(A) C2C12 cells were infected with WT and W220A ONNV at an MOI of 0.2 and incubated at 28°C or 37°C prior to a temperature shift from 24-48 hpi (28°C to 37°C (designated 48 h S#) and 37°C to 28°C (designated 48 h S*) respectively. Cells were fixed with 4% formaldehyde at 48 hpi, ZsGreen expression and cell confluency were determined by IncyCyte. Significant differences denoted by ns (P>0.05), ** (P<0.01), compared to replication at 12 hpi (W220A) at their respective temperatures. Data are displayed as the means ±S.E. of three experimental replicates. (B) Protein expressions of nsP1, eIF2α and P-eIF2α at 28°C or 37°C. 20 µg of each sample was loaded and analysed by western blotting. Actin was detected by western blotting as a loading control.

5.2.5 eIF2α phosphorylation is positively correlated with the level of infection

In chapter 4, significant lower levels of replication for CHIKV-D-Luc-SGR and CHIKV-nsP3-mCherry-FLuc-SGR compared to CHIKV-FLuc-SGR (expressing WT nsP3) at 24 hpt at 37°C in Huh7 and Vero cells, but not in C2C12 cells (Fig. 4.5) was observed. Therefore, I also tested the replication of WT and mutant ONNV and eIF2α phosphorylation in Vero cells at28°C or 37°C. Unlike in C2C12 cells which showed similar levels of replication at 28°C, W220A ONNV also showed significant lower replication and virus titers (30-fold reduction) compared to WT ONNV at 28°C (Fig. 5.7A and B). In agreement with replication defects of the AUD mutants, I did not detect any ZsGreen expression for W220A ONNV at 37°C in Vero cells (Fig. 5.7A). Interestingly, a significant reduction in replication and virus production (3000-fold) for WT ONNV at 37°C than 28°C (Fig. 5.7A and B) was also observed. This reduction in replication showed the similar phenotype as results in CHIKV SGR with fused nsP3-reporter protein at two temperatures in Huh7 or Vero cells.

The levels of nsP1 for WT ONNV and the levels of eIF2α and P-eIF2α from cells were also detected by western blotting (Fig. 5.7C). In agreement with replication and virus production for WT ONNV, only nsP1 expressed at 28°C was detectable. Corresponding with replication, enhanced levels of P-eIF2α at 28°C but no increase in P-eIF2α at 37°C was observed. The results indicated that the levels of P-eIF2α is dependent on the level of infection, and the insertion of ZsGreen in ONNV might hampered ONNV replication in a cell-type specific manner, which can be overcome at sub-physiological temperature.

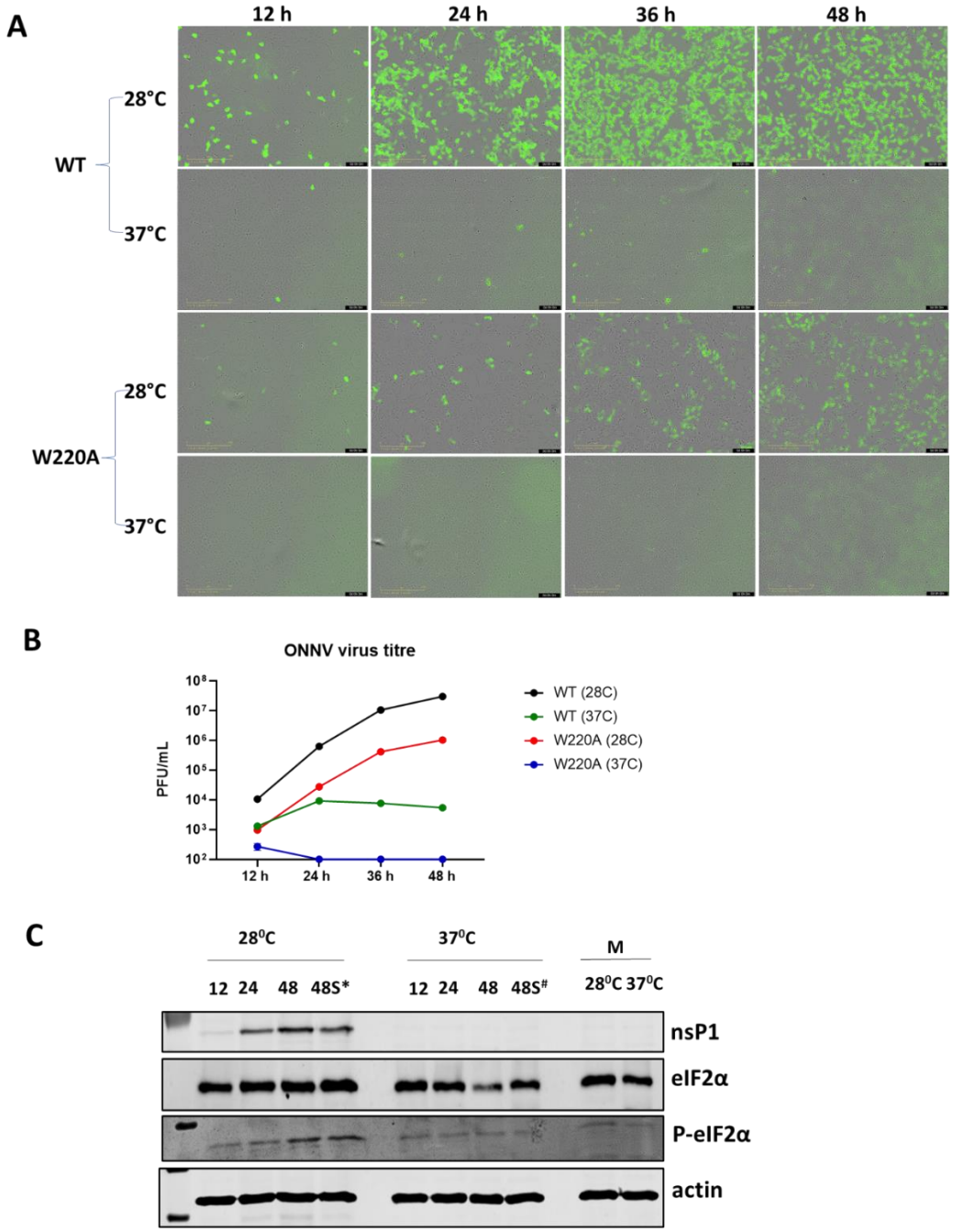

Figure 5.7 Replication, virus production of WT and mutant ONNV and eIF2α phosphorylation in Vero cells at 28°C or 37°C.

(A and B) Replication and virus production of WT and W220A ONNV in Vero cells at 28°C or 37°C. Vero cells were infected with WT or W220A ONNV at an MOI of 0.1 and incubated at 28°C or 37°C. Cells were fixed with 4% formaldehyde and supernatants were collected at indicated time points. The fixed cells were scanned by IncuCyte and viruses from supernatants were titrated on BHK-21 cells at 28°C. (C) Protein expression of nsP1, P-eIF2α and eIF2α for WT ONNV at 48 hpi at 28°C or 37°C. Cells were lysed in 1X GLB and proteins were detected by western blotting.

5.2.6 Pharmacological inhibition of the effect of eIF2α phosphorylation did not recover the replication defects of the AUD mutants

Following the effect of eIF2α phosphorylation on CHIKV SGR and ONNV infection, my next assumption was whether interfering with the effects of eIF2α phosphorylation will enhance replication and recover replication defects of the AUD mutants. As when humans are infected with CHIKV or ONNV, the first cells will be at sub-physiological temperatures (a few degrees lower than 37°C), therefore I also tested replication at 32°C apart from 28°C. To perform these assays I exploited the recently identified small molecule inhibitor, ISRIB, which has been shown to enhance cognitive memory and reverse the effect of eIF2α phosphorylation (Rabouw et al 2019, Sidrauski et al 2015). It should be noted that ISRIB does not block eIF2α phosphorylation but inhibits the downstream consequences of this phosphorylation event. To test the assumption, cells were treated with 200 nM ISRIB at 2 hpt and incubated at 28°C, 32°C or 37°C. Results showed that at sub-physiological temperatures (28°C or 32°C), replication of W220A CHIKV-D-SGR exhibited similar replication compared to WT CHIKV-D-Luc-SGR, whereas at 37°C it failed to replicate (Fig. 5.8A). Inhibition of the effect of eIF2α phosphorylation by treatment of ISRIB enhanced replication of WT and W220A CHIKV-D-Luc-SGR at sub-physiological temperatures (28°C or 32°C) (Fig. 5.8A). However, while it showed 3-fold increase in replication for WT and W220A CHIKV-D-Luc-SGR at 37°C, the replication defect of W220A was not recovered by ISRIB (Fig. 5.8A).

Protein expression of nsP1, eIF2α and P-eIF2α at 28°C, 32°C or 37°C was detected by western blotting (Fig. 5.8B). As expected, higher levels of nsP1 was expressed when cells were treated with ISRIB, which reassured the translation enhancement by inhibition of the effects of eIF2α phosphorylation.

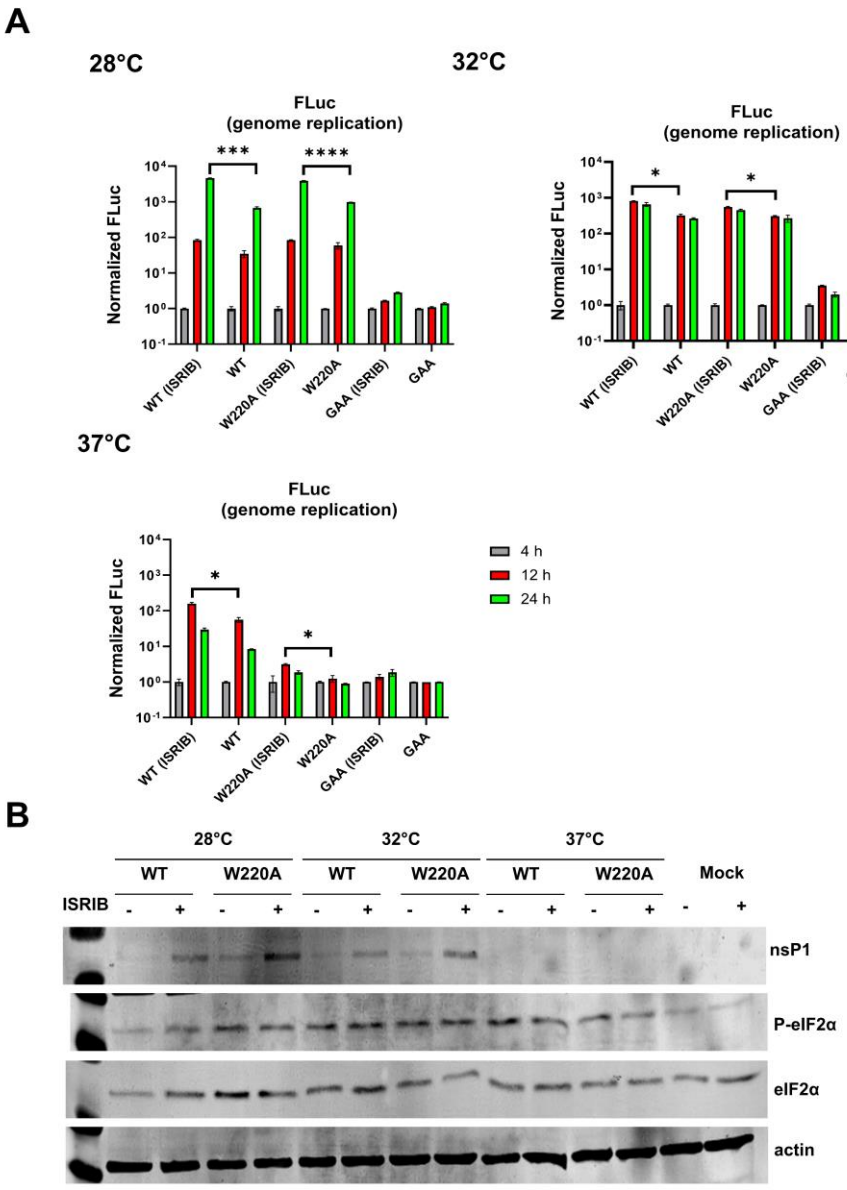

Figure 5.8 ISRIB treatment did not recover the replication defects of the AUD mutants in CHIKV-D-Luc-SGR at 37°C.

(A) Replication of WT and W220A CHIKV-D-Luc-SGR at 28°C, 32°C or 37°C with and without ISRIB. Cells were transfected with WT and W220A CHIKV-D-Luc-SGR RNA at 28°C, 32°C or 37°C. Cells were then treated with ISRIB (200 nM) at 2 hpt, harvested at indicated time points, measured by dual luciferase system. Significant differences denoted by * (P<0.05), *** (P<0.001), **** (P<0.0001) compared to replication without ISRIB at 24 hpt (28°C) or at 12 hpt (32°C or 37°C). Data are displayed as the means ±S.E. of three experimental replicates. (B) Protein expressions of nsP1, P-eIF2α and eIF2α at 24 hpt at different temperatures. 10 µg of each sample was loaded and analysed by western blotting. Actin was detected by western blotting as a loading control.

To investigate if inhibition of the effect of eIF2α phosphorylation was able to recover replication defects of the AUD mutants in the context of ONNV, I tested the replication of WT and W220A ONNV with and without ISRIB at 28°C, 32°C or 37°C. Similar as the results from CHIKV-D-Luc-SGR, enhanced ZsGreen expression for WT and W220A ONNV with ISRIB than those without ISRIB at 28°C or 32°C, as well as WT ONNV with ISRIB than it without ISRIB at 37°C (Fig 5.9A) were observed. However, no ZsGreen can be detected for W220A ONNV at 37°C with or without ISRIB (Fig. 5.9A), indicating that the replication defects of ONNV AUD mutants at 37°C cannot be recovered by inhibition of the effect of eIF2α phosphorylation.

Taken together, the results from CHIKV SGR and ONNV using ISRIB demonstrated that inhibition of the effect of eIF2α phosphorylation was not able to recover replication defects of the AUD mutants.

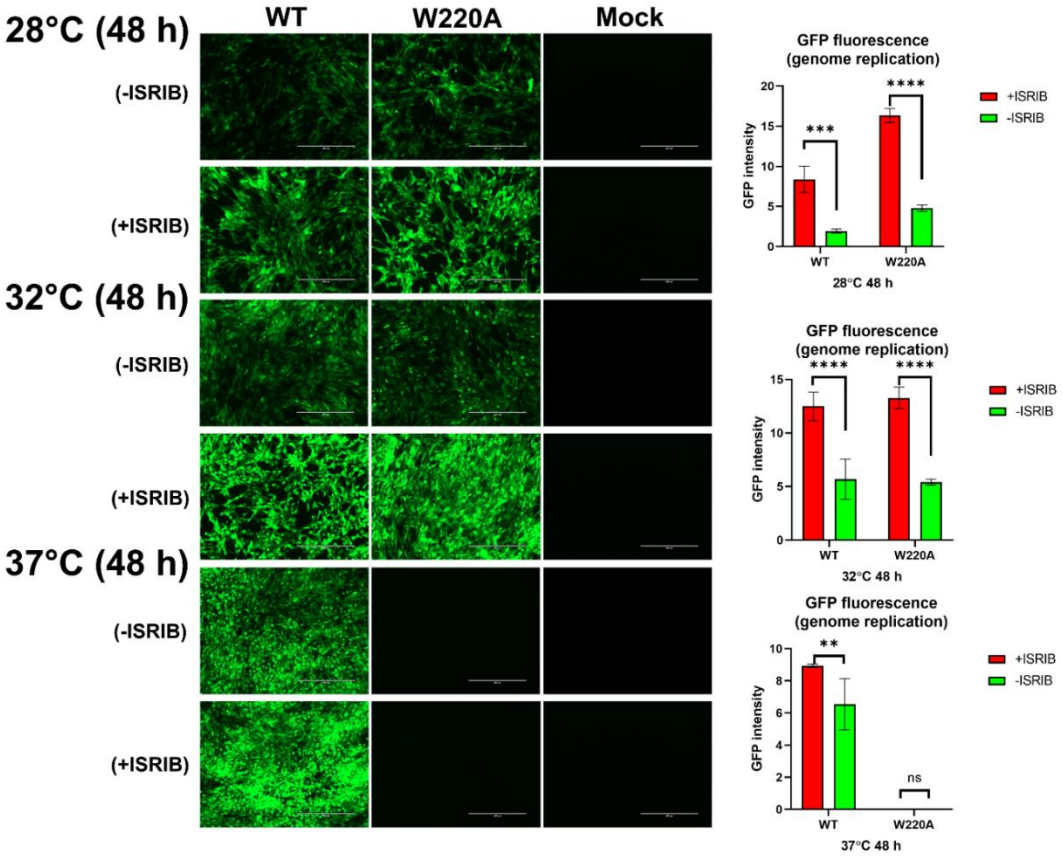

Figure 5.9 ISRIB treatment did not recover the replication defects of the AUD mutants in ONNV at 37°C.

C2C12 cells were infected with WT and W220A ONNV at an MOI of 0.1 with and without ISRIB (200 nM) and incubated at 28°C, 32°C or 37°C. Cells were fixed with 4% formaldehyde at 48 hpi and ZsGreen was scanned by EVOS microscopy. Significant differences denoted by ns (P>0.05), ** (P<0.01), *** (P<0.001), **** (P<0.0001) compared to replication of WT or W220A at 48 hpi without ISRIB. Data are displayed as the means ±S.E. of three experimental replicates.

5.2.7 SG induced by $NaAsO_2$ at 28°C or 37°C

Following phosphorylation of eIF2α in cells, the accumulation and aggregation of stalled 48S mRNPs resulted in the formation of SG (Jackson et al 2010, Kedersha et al 2002, Kedersha et al 1999). Although SG have been shown to be antiviral, alphavirus infection has been reported to induce SG and nsP3 has been shown to co-localize with components of SG, in particular G3BP1/2, to modulate their composition (Fros et al 2012, Scholte et al 2015). SG formation can be induced by $NaAsO_2$ treatment, which results in oxidative stress, and they can be dispersed by CHX. Previous work showed an inhibition and delay in the formation of SG in response to $NaAsO_2$ at sub-physiological temperatures (Wheeler et al 2016). I assumed that the differences in SG induction at 28°C or 37°C might be similar in response to ONNV infection, and might explain the replication phenotype that was observed before. Therefore the differences in SG formation was first tested by treating mock infected cells with $NaAsO_2$ or $NaAsO_2$ + CHX at 28°C or 37°C and stained with G3BP, a known indicator of SG (Kedersha et al 2016, Matsuki et al 2013). As expected, typical SG formation at 37°C but no SG formation at 28°C was observed, and treatment with CHX dispersed the SG induced by $NaAsO_2$ at 37°C (Fig. 5.10A and C). Interestingly, by quantification on levels of G3BPs at different temperatures, a slight lower level of G3BP expression at 28°C than 37°C, and increased levels of G3BP at 28°C or 37°C in response to $NaAsO_2$ stress (Fig. 5.10B) were observed. The result confirmed the inhibition of SG formation at sub-physiological temperature.

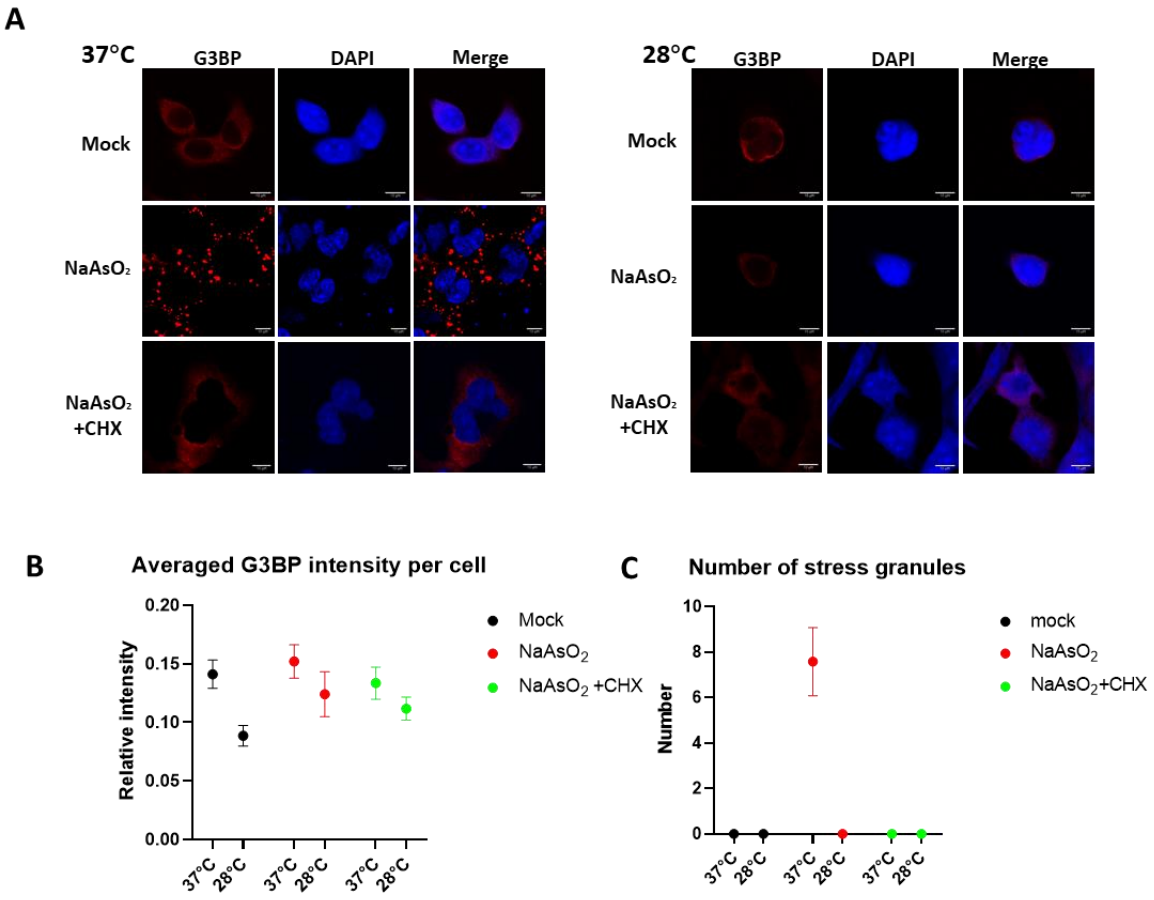

Figure 5.10 Stress granule (SG) induced by sodium arsenite ($NaAsO_2$) at 28°C or 37°C.

(A) RD cells were incubated at 28°C or 37°C. Cells were either mock treated or treated with 0.5 mM $NaASO_2$ for 1 h. Cells were either fixed with 4% formaldehyde or treated with 100 µg/ml cycloheximide (CHX) (on cells treated with $NaASO_2$) for 45 min prior to fixation. Cells from both temperatures were stained with G3BP antibody (red). (B) Quantification of G3BP expression from mock, $NaASO_2$ and $NaASO_2$ + CHX treated cells at 28°C or 37°C. The levels of protein expression were determined for 10 cells and calculated by Fiji imageJ. (C) The number of SG were determined for 10 cells.

5.2.8 Different sizes and numbers of SGs/G3BP-positive granules induced by $NaAsO_2$ or ONNV infection at 28°C or 37°C

The formation of SG by treatment with $NaAsO_2$ was inhibited at lower temperature (Wheeler et al 2016), and the sizes of SG by $NaAsO_2$ treatment was much larger than CHIKV infection (Jayabalan et al 2021). Therefore, I next investigated if the G3BP-positive granules were the case in ONNV infection at 28°C or 37°C. Surprisingly, in contrast to the inability of $NaAsO_2$ to induce SG at 28°C, ONNV

infection was able to induce G3BP-positive granules at both temperatures. Intriguingly, the G3BP-positive granules induced by ONNV differed significantly in sizes and numbers at 28°C or 37°C (Fig. 5.11 A and B). The average cross-sectional area of G3BP-positive granules at 28°C was much smaller than at 37°C (0.5 μm^2 compared to 1.6 μm^2), and both of these were much smaller than the average cross-sectional area of SG induced by $NaAsO_2$ at 37°C (4.5 μm^2). In addition, CHX treatment reduced the average size of ONNV-induced G3BP-positive granules from ~1.6 μm^2 to ~0.8 μm^2 at 37°C, whereas at 28°C CHX treatment showed no effect on the sizes of ONNV-induced G3BP-positive granules (Fig. 5.11B). In contrast, a larger number of ONNV-induced G3BP-positive granules at 28°C (~65/cell) than 37°C (~30/cell), and more G3BP-positive granules compared to $NaAsO_2$ induced SG (~7/cell) (Fig. 5.11B) were observed.

I also analysed the levels of dsRNA in ONNV-infected cells as an indicator of genome replication using the dsRNA specific antibody J2. Consistent with previous results using CHIKV SGR (Fig. 5.2B), a higher level of dsRNA in infected cells at 28°C than 37°C (Fig. 5.11 C) was observed, indicating enhanced genome replication at sub-physiological temperature. However, by quantification of ZsGreen expression in individual cells, lower levels of ZsGreen translation at 28°C compared to 37°C was observed, supporting that the elevated genome replication at sub-physiological temperature was not directly correlated with increased translation from sgRNA.

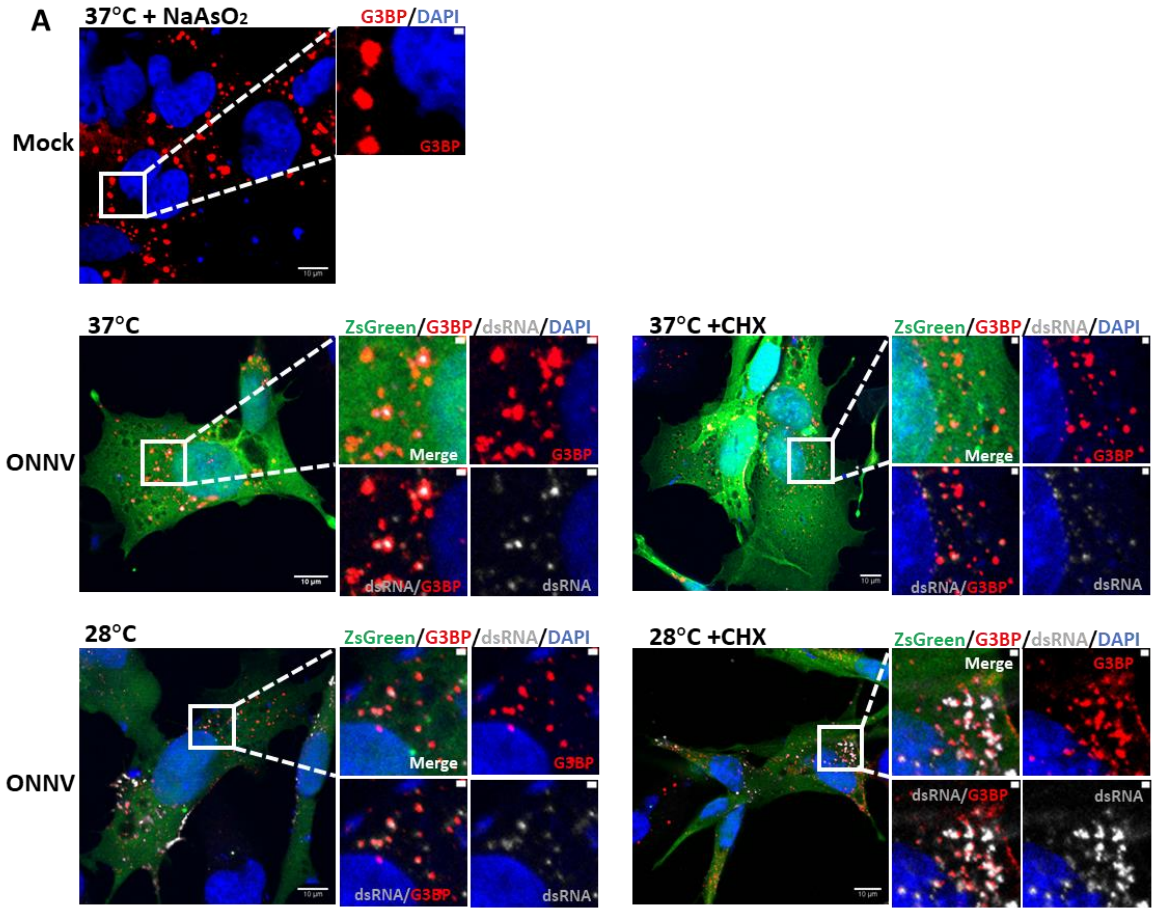
A
37°C + NaAsO2
G3BP/DAPI
Mock
G3BP
37°C
ZsGreen/G3BP/dsRNA/DAPI
37°C +CHX
ONNV
Merge
G3BP
dsRNA/G3BP
dsRNA
28°C
28°C +CHX
ONNV

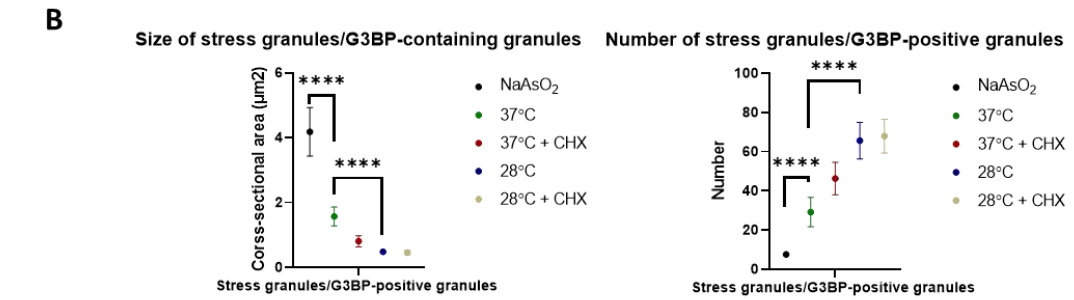
B
Size of stress granules/G3BP-containing granules
Corss-sectional area (μm2)
Stress granules/G3BP-positive granules
Number of stress granules/G3BP-positive granules
Number
NaAsO2
37°C
37°C + CHX
28°C
28°C + CHX
****

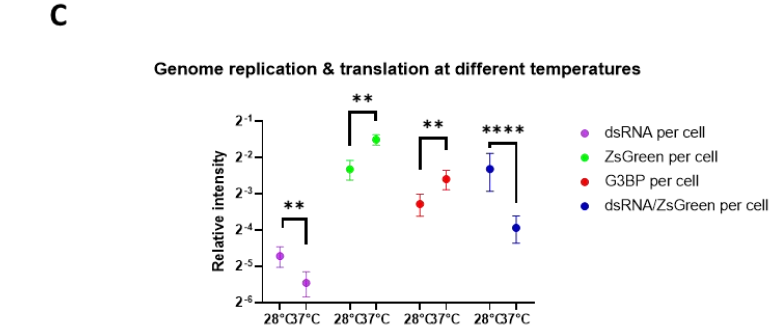
C
Genome replication & translation at different temperatures
Relative intensity
28°C37°C
dsRNA per cell
ZsGreen per cell
G3BP per cell
dsRNA/ZsGreen per cell
**
****

Figure 5.11 Different size and number of SGs/G3BP-positive granules induced by $NaAsO_2$ or ONNV infection at 28°C or 37°C.

(A) RD cells were mock infected or infected with WT ONNV at an MOI of 5 and incubated at 28°C or 37°C. 7 h later, mock infected cells were treated with 0.5 mM $NaAsO_2$ for 1 h. Cells were either fixed with 4% paraformaldehyde or treated with 100 µg/ml CHX for 45 min prior to fixation. (B) Quantification of the sizes and numbers of SGs/G3BP-positive granules induced by $NaAsO_2$ or ONNV infection at 28°C or 37°C. The sizes and numbers of SGs/G3BP-positive granules were determined for 10 cells and calculated by Fiji imageJ. Significant differences denoted by **** ($P<0.0001$), compared the sizes of those at 37°C. (C) Quantification of the overall dsRNA, ZsGreen, G3BP and dsRNA/ZsGreen expression in ONNV infection at 28°C or 37°C. The protein expressions were determined for 10 cells and calculated by Fiji imageJ. Significant differences denoted by ** ($P<0.01$), **** ($P<0.0001$), compared their respective proteins expression at 37°C.

5.2.9 TIA-1, but not eIF4G is a component of SGs/G3BP-positive granules induced by both $NaAsO_2$ and ONNV at 28°C or 37°C

The differences in the sizes of SGs/G3BP-positive granules induced by $NaAsO_2$ or ONNV infection at 28°C or 37°C led me to investigate if there were any differences in their compositions. Therefore, cells treated with $NaAsO_2$ or infected with ONNV were analysed for two other well-characterized SG components: the mRNA binding protein TIA-1 (Jayabalan et al 2021, McInerney et al 2005) and the translation initiation factor eIF4G (Suzuki et al 2009). As seen from Figure 5.12A and Figure 5.13A, I confirmed that the SG induction by $NaAsO_2$ contained TIA-1 and eIF4G, but neither TIA-1 or eIF4G accumulated into SG at 28°C. In contrast to this, TIA-1 accumulated in ONNV-induced G3BP-positive granules at both temperatures (Fig. 5.13) whereas no eIF4G accumulated into G3BP-positive granules at 28°C or 37°C. These results are consistent with previous work showing that G3BP-positive granules induced by CHIKV are compositionally distinct from those induced by oxidative stress. However, they do not explain the different compositions in ONNV-induced G3BP-positive granules at physiological and sub-physiological temperatures.

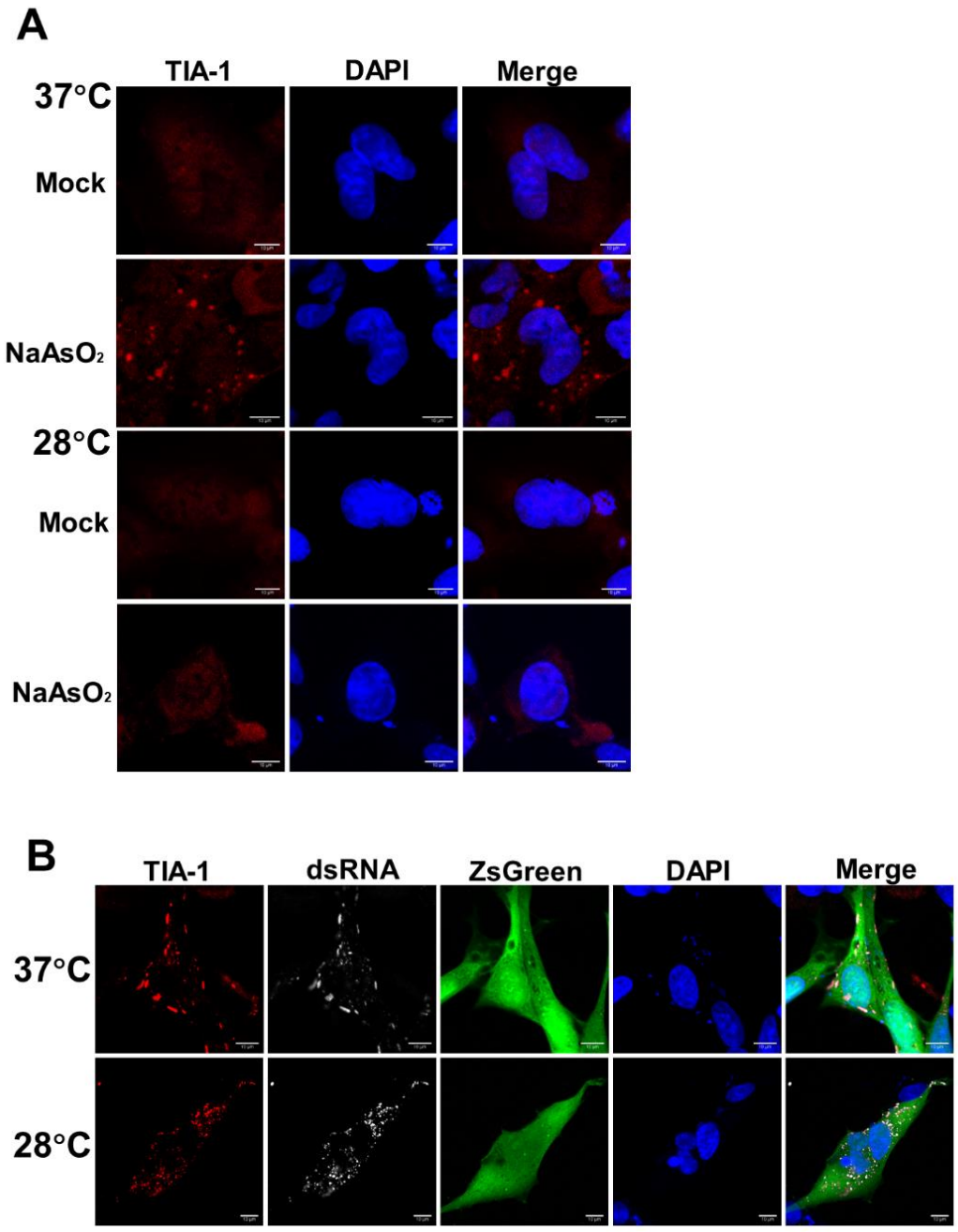

Figure 5.12 TIA-1 is a component of SGs/G3BP-positive granules induced by $NaAsO_2$ or ONNV infection at 28°C or 37°C.

(A) TIA-1 is a component of SG induced by $NaAsO_2$ at 37°C. RD cells were incubated at 28°C or 37°C and then treated with 0.5 mM $NaAsO_2$ for 1 h. Cells were stained with TIA-1 primary antibody. (B) TIA-1 is a component of G3BP-positive granules induced by ONNV at 37°C or 28°C. RD cells were infected with WT ONNNV at an MOI of 5 and incubated at 28°C or 37°C for 8 h. Cells were fixed with 4% paraformaldehyde and stained with TIA-1 and dsRNA primary antibodies.

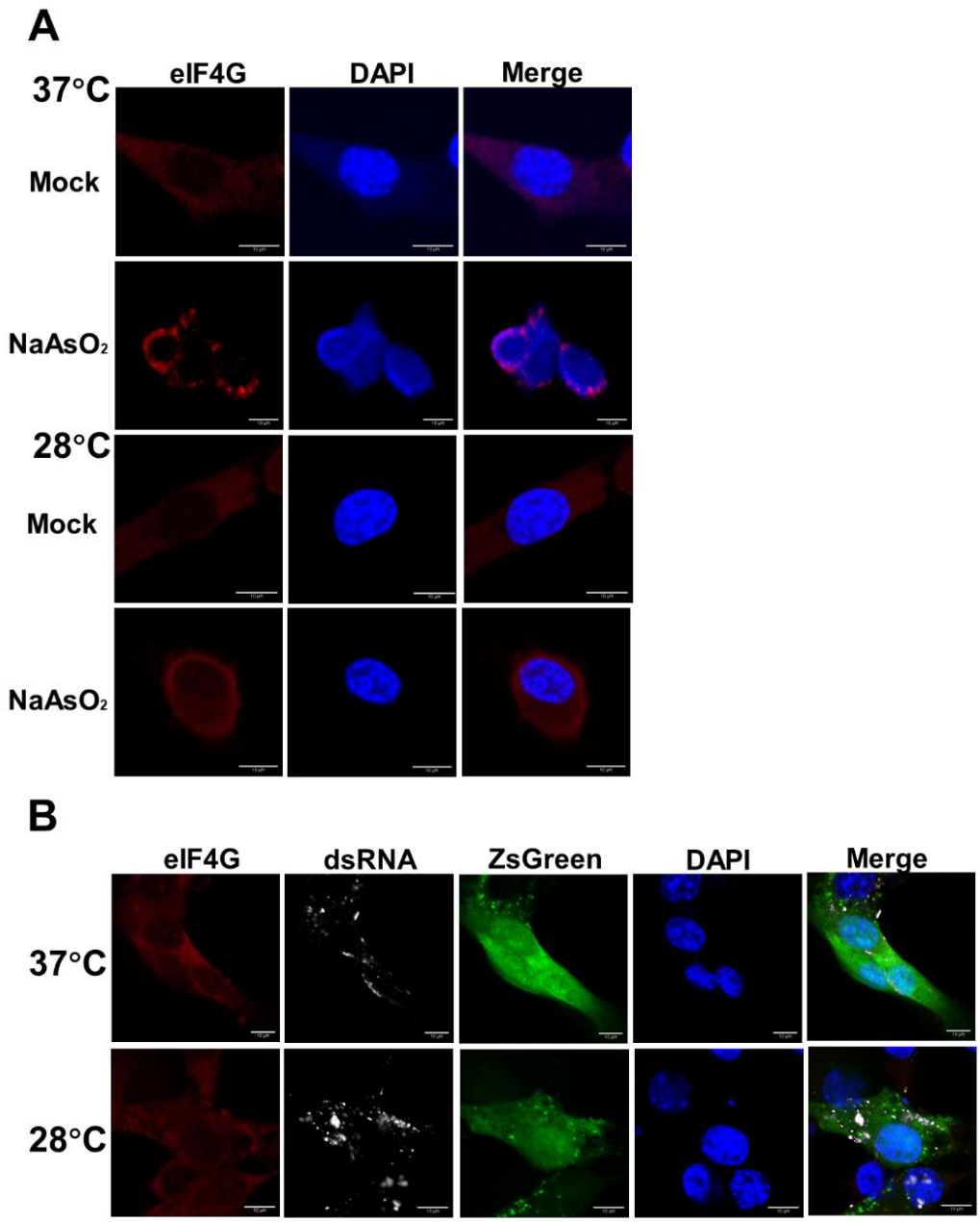

Figure 5.13 eIF4G is not a component of G3BP-positive granules induced by ONNV infection at 28°C or 37°C.

(A) eIF4G is a component of SG induced by $NaAsO_2$ at 37°C. RD cells were incubated at 28°C or 37°C and then treated with 0.5 mM $NaAsO_2$ for 1 h. Cells were stained with eIF4G primary antibody. (B) eIF4G is not a component of G3BP-positive granules induced by ONNV at 37°C or 28°C. RD cells were infected with WT ONNNV at an MOI of 5 and incubated at 28°C or 37°C for 8 h. Cells were fixed with 4% paraformaldehyde and stained with eIF4G and dsRNA primary antibodies.

5.3 Discussion

CHIKV is an arbovirus that transmitted from mosquitoes to humans (Schwartz & Albert 2010). The body internal temperature of mosquitoes is not constant and depends on the environmental temperature, therefore mosquitoes can only survive and reproduce in suitable environments that depend on the ecological characteristics of the mosquito species. CHIKV is transmitted by the mosquito species *Ae. aegypti* and *Ae. albopictus*, showing higher transmission rates at sub-physiological temperatures ranging from 18°C to 32°C (Heitmann et al 2018, Mbaika et al 2016, Wimalasiri-Yapa et al 2019). The enhanced genome replication of CHIKV at sub-physiological temperature might shed light on the efficient replication and apparent CPE in mammalian cells but only light CPE in mosquitoes (Endy et al 2011).

The high and similar levels of replication for the AUD mutants compared to WT CHIKV SGR at sub-physiological temperature led me to explore the mechanisms behind temperature change. Translational shutoff is a key downstream component of the innate immune in response to infection by many viruses, among which eIF2α phosphorylation has been shown to play a crucial role in this process (Wek 1994). Here I confirmed that the phosphorylation of eIF2α can be induced at both 28°C and 37°C by using ONNV infection with a ZsGreen reporter (Fig. 5.2). However, to my surprise, most of the cells that exhibited high levels of P-eIF2α had little ZsGreen expression, indicating that they were not infected by ONNV at 28°C or 37°C. In contrast, those cells that exhibited high levels of ZsGreen expression showed low levels of P-eIF2α, suggesting that ONNV infection can efficiently inhibit eIF2α phosphorylation, which supports the previous conclusion that CHIKV infection suppresses eIF2α phosphorylation (Rathore et al 2013). In considering why the uninfected cells exhibited high levels of eIF2α phosphorylation, it is assumed that the release of IFN from infected cells activated neighboring cells to respond to virus infection by phosphorylating eIF2α and reducing viral protein translation (LibreTexts 2021).

In defining a relationship between ONNV infection and overall eIF2α phosphorylation, I tested replication of ONNV in Vero cells at 28°C or 37°C. The data demonstrated that eIF2α phosphorylation was positively correlated with the level of infection, although it was still not clear why the ONNV virus replicated poorly in Vero cells at 37°C. I previously also observed that ONNV replicated poorly in Huh7 cells at 37°C (data not shown). These data were consistent with what I have observed in chapter 4 Figure 4.6, showing that the nature of nsP3-fused reporter proteins hampered CHIKV SGR replication at 37°C. To confirm this, a direct comparison between ONNV (with ZsGreen) and ONNV infection in Vero cells at 37°C is needed. The efficient replication of ONNV (with ZsGreen) in C2C12 cells but not in Huh7 or Vero cells might indicate novel cellular protein involved in alphavirus replication at 37°C but not at 28°C. Overall, the mechanism of how nsP3-fused reporter proteins affects alphavirus replication in specific cells and why temperature can reverse this phenotype is not clear and requires further investigation.

Temperature shift assay using WT CHIKV-D-Luc-SGR or WT and mutant ONNV confirmed the effect of temperature on replication. However, the phosphorylation of eIF2α between CHIKV SGR and ONNV infection seems contradictory (Fig. 5.4C and 5.6C). Although much more genome replication for CHIKV SGR at 28°C, I did not observe a concomitant increase in eIF2α phosphorylation; on the contrary, an increase in eIF2α phosphorylation at 37°C was seen, even though its genome reduced slightly. In the case of ONNV infection, a reduction in eIF2α phosphorylation when temperature was shifted from 28°C to 37°C and an increase in eIF2α phosphorylation when temperature was shifted from 37°C to 28°C were observed. Data from CHIKV SGR suggested a defect in eIF2α phosphorylation at sub-physiological temperature, while data from ONNV indicated an enhancement of eIF2α phosphorylation at sub-physiological temperature. I assumed that this might be due to the differences between CHIKV SGR and the virus. CHIKV infection induced eIF2α phosphorylation through the PKR activation upon sensing dsRNA and PERK activation in response to ER stress (Rathore et al 2013). Previous work showed that the expression of large amounts of alphavirus

glycoproteins that are post-translationally modified in the ER can lead to ER stress and trigger the unfolded protein response (UPR) (Barry et al 2010). Therefore, it is reasonable to assume that phosphorylation of eIF2α was activated by a combination of viral dsRNA mediated PKR activation and glycoproteins mediated PERK activation, and the latter was able to reverse the defect of eIF2α phosphorylation at sub-physiological temperature. This assumption is supported by the fact that the levels of eIF2α phosphorylation in response to CHIKV SGR replication were significantly lower compared to these in response to ONNV infection at 28°C or 37°C (Fig. 5.4C and 5.6C). Furthermore, this might also shed light on a less pronounced genome enhancement for ONNV in comparison to CHIKV SGR, apart from the previously described defects in virus assembly or release from cells.

To determine if eIF2α phosphorylation was the key mechanism behind temperature variance, ISRIB is utilized to reverse the effect of eIF2α phosphorylation (Sidrauski et al 2015). The data demonstrated that inhibition of eIF2α phosphorylation was not able to recapitulate the effect of lower temperature on replication of CHIKV SGR at 37°C (Fig. 5.8), and did not permit the replication of W220A at 37°C (Fig. 5.9). Therefore, I conclude that although eIF2α phosphorylation was affected by temperature, it is not the key factor that regulates the replication phenotype.

SGs are cytoplasmic, non-membranous aggregates of non-translated mRNPs, which form following eIF2α phosphorylation. I then focused on SG, as formation of SG at lower temperatures was suppressed and delayed (Wheeler et al 2016). Many viruses suppress the formation of SG, indicating the involvement of SG in antiviral activity (Emara & Brinton 2007, Simpson-Holley et al 2011, White & Lloyd 2011, White & Lloyd 2012). Alphaviruses have been shown to induce SG assembly transiently at early time post infection but then regulates SG disassembly as infection proceeded (McCormick & Khaperskyy 2017, McInerney et al 2005, Panas et al 2015, Schulte et al 2016). The alphaviruses inhibit SG formation at late stage by sequestering components of SG, for example G3BP, into membranous granules (Panas et al 2015, Panas et al 2012). Recent work in the study of SG composition

during CHIKV infection indicated that nsP3 ADP-ribosylhydrolase activity regulates the disassembly of SG, which transits the bona fide SG (containing initiation factors, SG-related RNA-binding proteins) into condensates that lack translation factors, but contain G3BP and other SG-associated RNA binding proteins (Jayabalan et al 2021). Despite huge differences in composition, two known components of SG, G3BP1/2 are required for alphavirus replication (Kedersha et al 2016, Tourriere et al 2003). Although SG formation induced by $NaAsO_2$ were inhibited at lower temperature, ONNV infection induced G3BP-positive granules at both 28°C and 37°C, and surprisingly these G3BP-positive granules differ significantly in sizes and numbers. In trying to understand why smaller and more numerous G3BP-positive granules might promote genome replication at lower temperature, the mean surface area and volume of G3BP-positive granules per cell was calculated. To do this, the G3BP-positive granules were assumed as spherical and the following parameters were used: at 28°C the mean cross area of G3BP-positive granules was 0.5 μm^2 (radius 0.4 μm) and the number of G3BP-positive granules per cell were 65; at 37°C the mean cross area of G3BP-positive granules was 1.6 μm^2 (radius 0.7 μm) and the number of G3BP-positive granules per cell were 29. Using these parameters, I determined that the mean surface area of G3BP-positive granules was 123 μm^2 per cell and the mean volume of G3BP-positive granules was 1.6 μm^3 per cell at 28°C, whereas at 37°C the mean surface area of G3BP-positive granules was 178 μm^2 per cell and the mean volume of G3BP-positive granules was 41.6 μm^3. As can be calculated, the mean volume of G3BP-positive granules at 37°C was 26 times compared to it at 28°C. A possible explanation might be that at lower temperature, the bona fide large SG assembly induced by ONNV infection was inhibited and resulted in formation of smaller G3BP-positive granules. However, those bona fide SG can be assembled transiently (although difficult to be detected) at 37°C, but their translation initiation factors were rapidly disassembled by nsP3 ADP-ribosylhydrolase activity and a large portion of them resolve to G3BP-positive granules. This is consistent with the recent work, arguing that about 27% of nsP3-positive cells had canonical SG (Jayabalan et al 2021). This assumption can also be supported by the fact that (1)

these G3BP-positive granules at either temperature don't contain translation initiation factors as detected; and (2) a portion of G3BP-positive granules at 37°C were still sensitive to CHX, which is an indicator of canonical SG. Further research on the different compositions of G3BP-positive granules at physiological and sub-physiological temperatures might be performed via enriching larger complexes of G3BP-positive granules and purification of G3BP-positive granules through immunoprecipitation (Wheeler et al 2017).

Chapter 6: Ablation of nsP3-interacting cold shock proteins enhances alphavirus replication at early time points

6.1 Introduction

Cold shock proteins are among the most evolutionarily conserved proteins (Jones & Inouye 1994, Wolffe 1994, Wolffe et al 1992), with defined characteristic of one or more CSD. Upon a sudden temperature downshift, mammalian cells exhibit a cold shock response and cold shock proteins are largely synthesized to overcome the deleterious effects of the temperature change. Previous work showed that YB1 (Y-box binding protein-1) interacts with SINV nsP3 and forms complexes (Gorchakov et al 2008). To further investigate the role of nsP3 in the enhancement of alphavirus replication at sub-physiological temperature, I interrogated the dataset for the presence of cold shock proteins interacting with nsP3 and identified UNR (upstream of N-RAS) and SRSF5 (Serine and Arginine Rich Splicing Factor 5) in the mass spectrometry work (Fig. 6.1) (Gao 2018). Based on those work, I interrogated the effects of the three cold shock proteins (YB1, UNR and SRSF5) in alphavirus replication. YB1 is encoded by the gene YBX1, and inside cells it forms RNA-protein complexes and modulates the expression of many target genes, thereby participating in cellular reprograming (Kang et al 2014, Kossinova et al 2017). The UNR gene was initially identified as a regulator of N-Ras expression (Boussadia et al 1997, Jeffers et al 1990), but later it was discovered to encode a protein possessing 5 CSD and undergoes alternative splicing (Doniger et al 1992, Jacquemin-Sablon et al 1994), and was then renamed cold shock protein containing E1 (CSDE1). UNR/CSDE1 binds to single strand DNA or RNA (Ferrer et al 1999, Triqueneaux et al 1999), and regulates translation and mRNA stability by working with the polypyrimidine-tract-binding protein (Mitchell et al 2001, Sawicka et al 2008). The generation of UNR or YB1 knockout mice indicated their essential roles in mouse development. SRSF5 is a member of the serine/arginine-rich family of pre-mRNA splicing factors and constitute part of the spliceosome (Chen et al 2018b, Kim et al 2016), which processes RNA binding and protein binding.

Accession	Description	Abundance Ratio: (TST-WT) / WT	Abundance Ratio: (TST-PV) / WT	Abundance Ratio: (TST-WT) / (TST-PV)
Q9H307	Pinin	100	100	0.064
Q53G35	Phosphoglycerate mutase (Fragment)	100	100	0.042
Q3ZBS7	Uncharacterized protein	100	100	0.089
A0A024RDE5	Ras-GTPase activating protein SH3 domain-binding protein 2, isoform CRA_a	10.171	14.304	0.711
Q59EK7	CS0DF038YO05 variant (Fragment)	3.444	34.751	0.099
A0A024R0E2	Cold shock domain containing E1, RNA-binding, isoform CRA_a	3.028	18.168	0.167

Figure 6.1 Excerpts of proteins interacting with CHIKV nsP3 by mass spectrometry.

Picture is taken from (Gao 2018). Red rectangles indicate cold shock proteins SRSF5 and UNR respectively.

To explore the effect of the three cold shock proteins in alphavirus replication, I generated cell lines in which expression of the cold shock protein was ablated by shRNAs. I initially selected RD cells for ablation of the cold shock proteins as they support high levels of replication for CHIKV SGR and ONNV as well as exhibit clear and typical SG. The lentiviruses were used to transduce the shRNAs into RD cells to generate stable cell clones, in which expression of the cold shock proteins was ablated.

By introducing a luciferase reporter system and use of the YB1 knockout cells, YB1 has been shown to bind to DENV 3'-UTR and mediates antiviral effects (Paranjape & Harris 2007). Here I use the previously described CHIKV-D-Luc-SGR reporter

system and tested the replication of WT and mutants in the cold shock protein ablated RD cells as well as the RD-shCTL (control shRNA RD cells) cells. During transfection and replication of CHIKV-D-Luc-SGR, puromycin was removed as it might have an effect on translation (Pestka 1971). Here AUD mutant R243A/K245A was also tested as it showed a similar replication phenotype. Replication of WT and the AUD mutants (W220A and R243A/K245A) from the cold shock protein ablated RD cell lines and the RD-shCTL cells at 28°C or 37°C indicates impact of the cold shock proteins on alphavirus replication.

The effect of the cold shock proteins was also investigated in the context of ONNV (with a ZsGreen reporter), a reporter system indicating genome replication during virus infection. This is especially helpful in replication measurement of the AUD mutants, as no ZsGreen expression means no virus production for the AUD mutants, saving extensive labor from quantification of virus production by plaque assay. Therefore, I infected WT and mutant ONNV in the cold shock protein ablated RD cells as well as the RD-shCTL cells to explore whether replication defects of the AUD mutants can be recovered at 37°C. I also investigated growth curve of replication and virus production for WT ONNV, to shed light on the effects of the cold shock proteins in virus replication and production.

Some of the cold shock proteins are involved in the formation of SG. For example, YB1, a known component of SG, possess the ability for self-assembly (Kedersha & Anderson 2007). In human sarcoma cells, YB1 activates G3BP1 mRNA and thus regulates G3BP1 expression and the following nucleation of SG (Somasekharan et al 2015). UNR has also been identified as a component of SG (Youn et al 2018). Therefore, the effect of the cold shock proteins on SG formation was investigated in the cold shock protein ablated RD cells as well as the RD-shCTL cells at 28°C or 37°C. Differences in the formation of SG might indicate a role of the cold shock proteins in antiviral activities.

6.2 Results

6.2.1 Generation of cold shock proteins ablated RD cell lines

As RD cells are human-derived, each of the shRNAs targeting YB1, UNR or SRSF5 from human genes was selected and ligated with the backbone of pMKO.1-TRC (shRNA expression). Lentiviruses expressing each of the shRNAs were generated by transfection and transduced into RD cells under the puromycin selection. As expected, YB1, UNR or SRSF5 were efficiently ablated in RD cells at 28°C or 37°C (Fig. 6.2). Interestingly, after incubating at 28°C for 24 h, protein expression of YB1, UNR or SRSF5 were not much higher at 28°C than 37°C (Fig. 6.2).

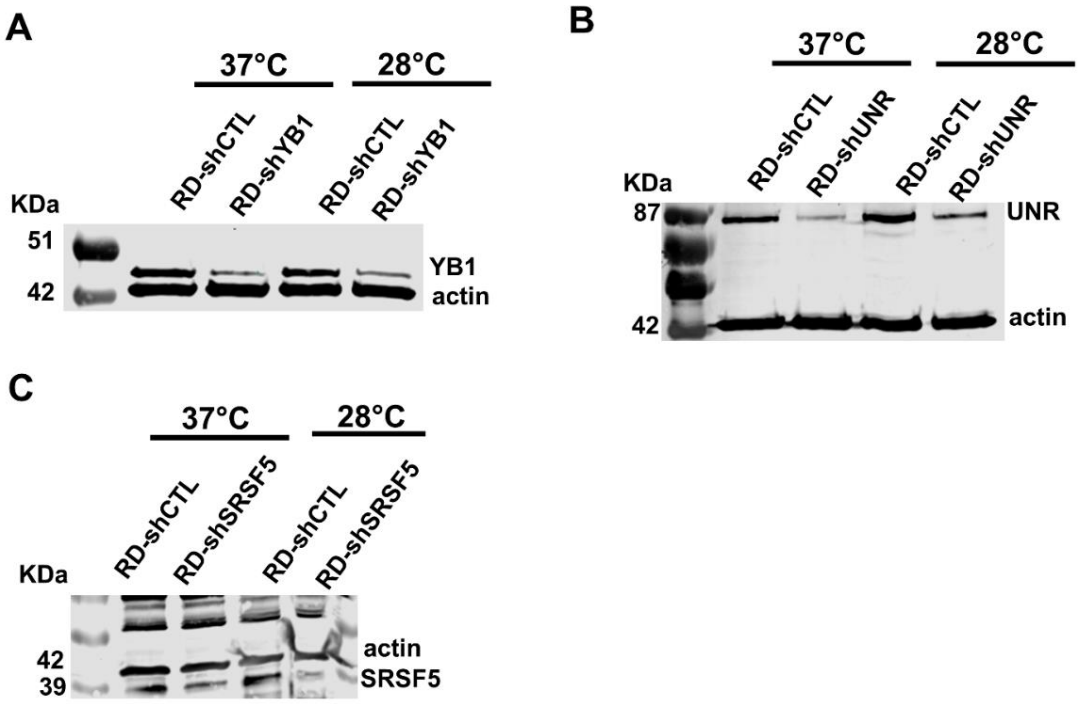

Figure 6.2 Generation of cold shock proteins ablated RD cell lines.

Each of the shRNAs targeting human YB1, UNR or SRSF5 genes was designed and ligated with the backbone of pMKO.1-TRC. The lentiviruses pCAG-HIVgp, pCMV-VSV-G-RSV-rev and pLKO.1-TRC-shRNA (shCTL, shYB1, shUNR or shSRSF5) were co-transfected into HEK293T cells. Supernatants containing lentiviruses were collected at 48 and 72 hpt. RD cells were then transduced with each of the lentiviruses in the presence of 8 µg/ml polybrene, which were then under puromycin selection. The cells were then incubated at 37°C until mock transduced cells were completely dead. These cold shock protein ablated RD cells were incubated at 28°C or 37°C and protein expression of YB1 (A), UNR (B) and SRSF5 (C) at the two temperatures were verified by western blotting.

6.2.2 Replication of WT and mutant CHIKV-D-Luc-SGR in the cold shock protein ablated RD cell lines

To explore if the cold shock proteins play a role in the replication phenotype of the AUD mutants, WT, AUD mutants (W220A and R243A/K245A) and GAA were transfected into the cold shock protein ablated RD cells and incubated at 28°C or 37°C. In order to clearly show the replication differences at various time points, these are shown on separate graphs in Figure 6.3. A significant increase in replication for WT, W220A or R243A/K245A but not for GAA at 12 hpt in the cold shock protein ablated cells compared to the RD-shCTL cells at 28°C was observed. However, WT showed a significant reduction in replication at 37°C (Fig. 6.3B), whereas W220A and R243A/K245A exhibited a significant increase in replication at 12 hpt in the cold shock protein ablated RD cells compared to the RD-shCTL cells at 37°C (Fig. 6.3B). To note, although the AUD mutants showed significant increase in replication at 37°C, they were still much lower compared to WT, suggesting the replication defects of the AUD mutants cannot be recovered by ablating expression of the cold shock proteins. Interestingly, increased replication for WT, W220A or R243A/K245A in cold shock protein ablated cells compared to RD-shCTL cells at 24 hpt, at 28°C or 37°C (Fig. 6.3 A and B right panel) was not observed. Most of them showed no apparent difference in replication, apart from significant reduced replication for WT in the cold shock protein ablated cells compared to RD-shCTL cells at 24 hpt at 37°C (Fig. 6.3 B left three). All together, these data suggest that ablation of cold shock proteins increase CHIKV replication at early time points but not at late time points.

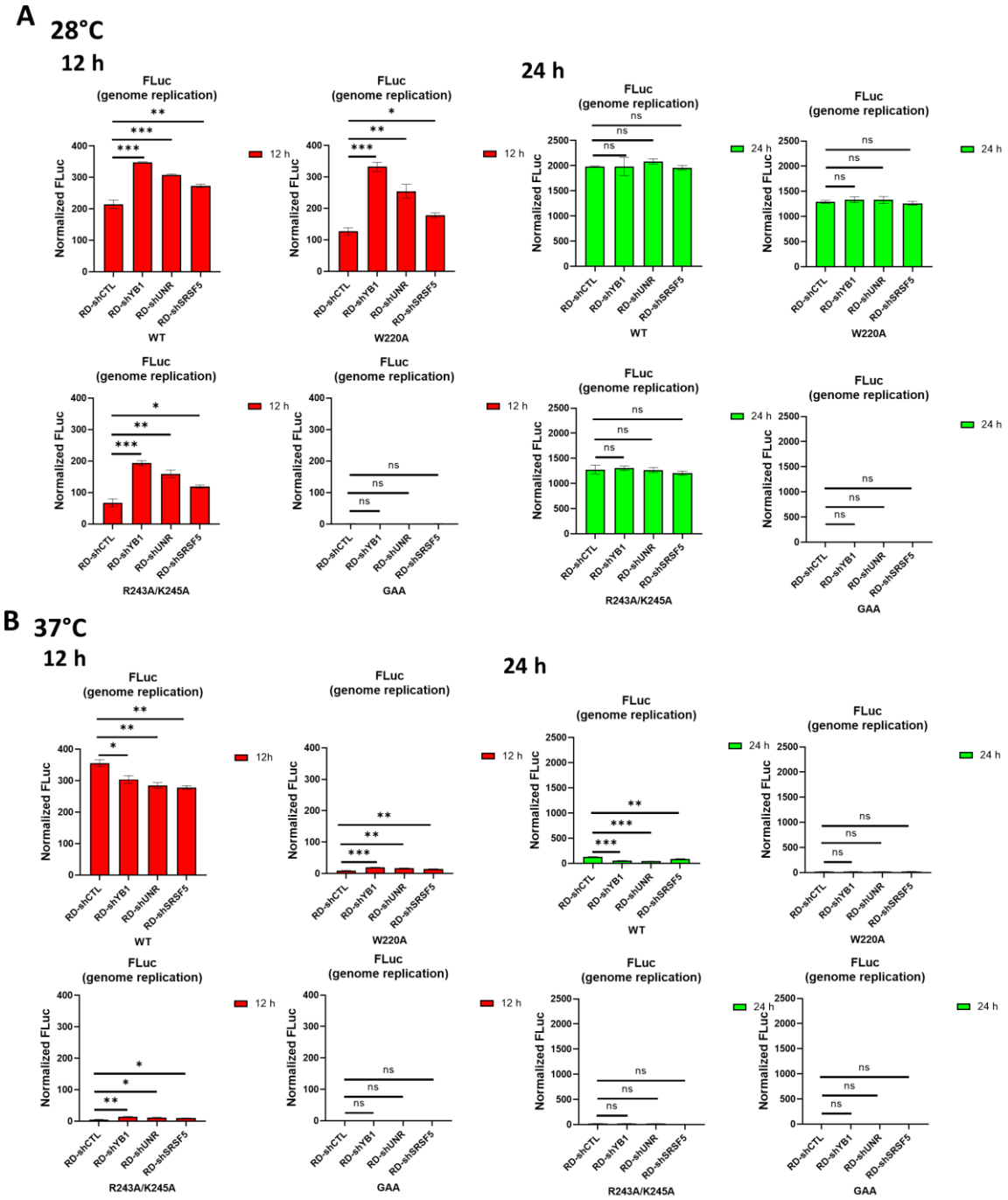
A
28°C
12 h
24 h
FLuc
(genome replication)
Normalized FLuc
RD-shCTL
RD-shYB1
RD-shUNR
RD-shSRSF5
WT
W220A
R243A/K245A
GAA
12 h
24 h
B
37°C
12h

Figure 6.3 Replication of WT and mutant CHIKV-D-Luc-SGR at 28°C or 37°C in the cold shock protein ablated RD cell lines.

The cold shock protein ablated RD cells were seeded into 24 well plates without puromycin. The next day, cells were transfected with WT and mutant CHIKV-D-Luc-SGR RNA and incubated at 37°C or 28°C. Cells were collected at indicated time points. FLuc activities were measured and normalized to their respective 4 h values at 28°C (A) or 37°C (B), and thus values represent fold-change compared to those 4 h values. ns ($P>0.05$), * ($P<0.05$), ** ($P<0.001$), *** ($P<0.001$) compared to their FLuc activities in RD-shCTL at 12 or 24 hpt respectively. Data are displayed as the means ±S.E. of two experimental replicates.

6.2.3 Replication of WT and mutant ONNV in the cold shock protein ablated RD cell lines at 28°C or 37°C

To further explore the possible effect of the cold shock proteins on replication phenotype of the AUD mutants during infection, the cold shock protein ablated RD cells were infected with WT, W220A and R243A/K245A ONNV at an MOI of 0.1 and incubated at 28°C or 37°C. Cells were fixed with 4% paraformaldehyde at 48 hpi and ZsGreen expression representing genome replication was quantified and normalized by IncuCyte. Interestingly, similar levels of ZsGreen expression for WT, W220A or R243A/K245A in the cold shock protein ablated RD cells compared to the RD-shCTL cells at 28°C (Fig. 6.4A) were observed. However, at 37°C, WT ONNV lysed a large majority of cold shock protein ablated RD cells whereas it only lysed a less majority of the RD-shCTL cells, indicating that ablation of the cold shock proteins had an early effect on virus production (Fig. 6.4B). To note, consistent with the results of AUD mutants in CHIKV-D-Luc-SGR, ablation of the cold shock proteins failed to recover replication defects of the AUD mutants in ONNV (Fig. 6.4B). Although WT ONNV lysed more cold shock protein ablated RD cells than the RD-shCTL cells at 48 hpi at 37°C, they exhibited indistinguishable ZsGreen expression when normalized to cells (Fig. 6.4C), suggesting a similar maximum replication capacity between the cold shock protein ablated RD cells and the RD-shCTL cells.

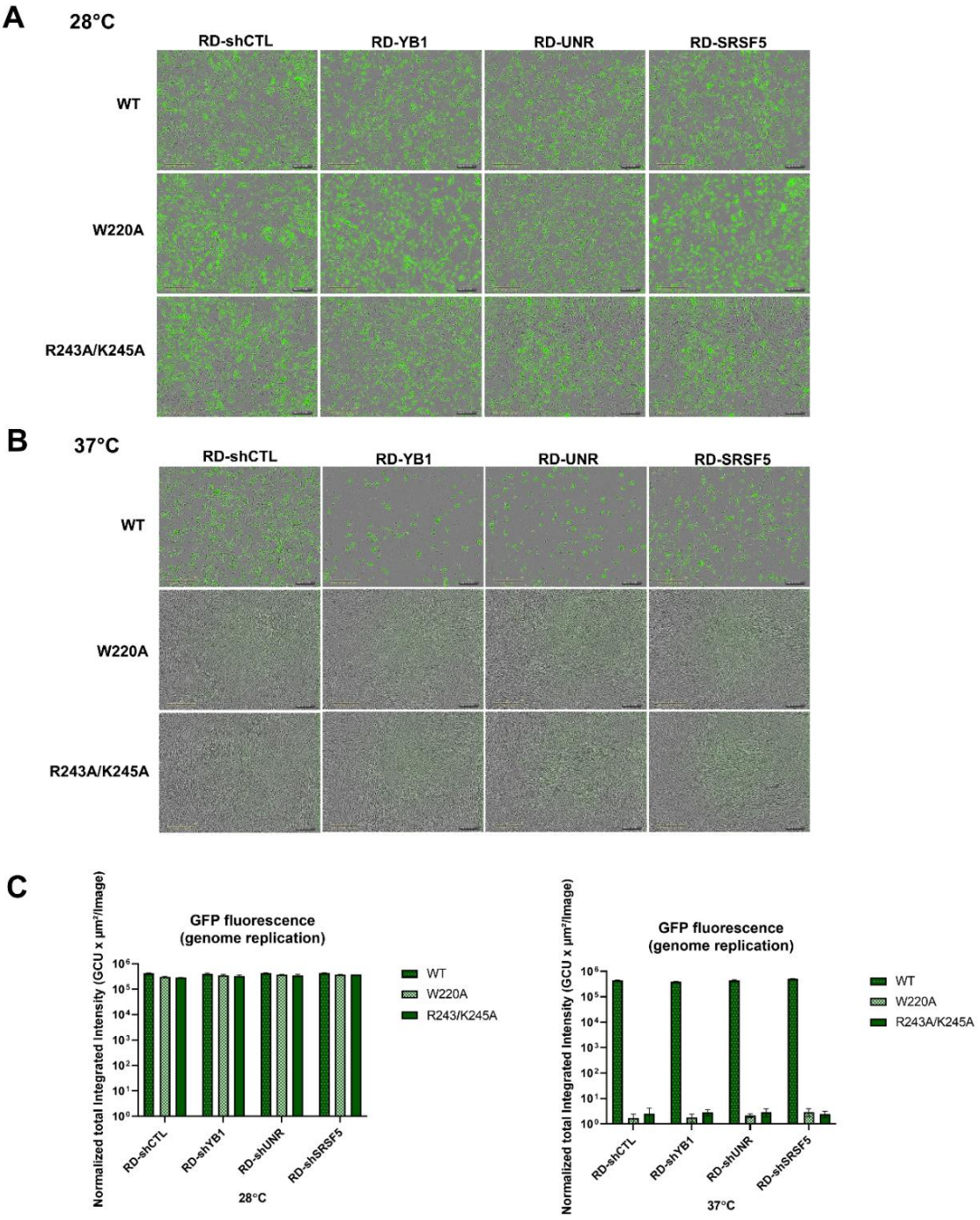
A
28°C
RD-shCTL
RD-YB1
RD-UNR
RD-SRSF5
WT
W220A
R243A/K245A
B
37°C
RD-shCTL
RD-YB1
RD-UNR
RD-SRSF5
WT
W220A
R243A/K245A
C
GFP fluorescence
(genome replication)
Normalized total Integrated Intensity (GCU x µm²/Image)
RD-shCTL
RD-shYB1
RD-shUNR
RD-shSRSF5
28°C
WT
W220A
R243/K245A
GFP fluorescence
(genome replication)
Normalized total Integrated Intensity (GCU x µm²/Image)
RD-shCTL
RD-shYB1
RD-shUNR
RD-shSRSF5
37°C
WT
W220A
R243A/K245A

Figure 6.4 Replication of WT and mutant ONNV in the cold shock protein ablated RD cell lines at 28°C or 37°C.

(A and B) ZsGreen expression of WT and mutant ONNV at 28°C or 37°C in the cold shock protein ablated RD cell lines. The cold shock protein ablated RD cells were seeded into 12 well plates without puromycin. The next day, cells were infected with WT and mutant ONNV at an MOI of 0.1 and incubated at 37°C or 28°C. Cells were fixed with 4% paraformaldehyde at 48 hpi and ZsGreen expression was quantified and normalized by IncuCyte. Data are displayed as the means ±S.E. of three experimental replicates. (C) Normalized ZsGreen expression of WT and mutant ONNV at 28°C or 37°C in the cold shock protein ablated RD cell lines.

6.2.4 Growth curve of replication and virus production of WT ONNV in the cold shock protein ablated RD cell lines and the RD-shCTL cells at 28°C or 37°C

As described before, WT CHIKV-D-Luc-SGR exhibited higher levels of replication at 12 hpt, but similar levels of replication at 24 hpt in the cold shock protein ablated RD cells compared to the RD-shCTL cells at 28°C. I postulated that ablation of the cold shock proteins might have an early effect on replication – enhancing replication at early stage but not at late stage. To test this, the cold shock protein ablated RD cells and the RD-shCTL cells were infected with WT ONNV at an MOI of 0.1 and incubated at 28°C or 37°C. Cells were fixed with 4% paraformaldehyde at 12, 24, 36 and 48 hpi and supernatants were collected for virus titration. As expected, higher levels of ZsGreen expression were detected at 12 or 24 hpi in the cold shock protein ablated cells compared to the RD-shCTL cells at 28°C or 37°C (Fig. 6.5A and B and Fig. 6.6A). However, at later times (36 or 48 hpi), WT ONNV exhibited similar levels of ZsGreen expression in the RD-shCTL cells compared to the cold shock protein ablated RD cells at 28°C, suggesting that ablation of the cold shock proteins only enhances alphavirus replication at early times (Fig. 6.5A and Fig. 6.6A). Consistent with this, WT ONNV induced cytopathic effect (CPE) at 36 hpi and a large majority of the cells were lysed at 48 hpi in the cold shock protein ablated cells at 37°C; however, WT ONNV at 37°C had not yet initiated CPE at 36 hpi and only until 48 hpi a less majority of the cells were lysed in the RD-shCTL cells (Fig. 6.5B). By normalization with cell confluency at 37°C, similar levels of ZsGreen expression for WT ONNV in the cold shock protein ablated cells compared to the RD-shCTL cells were observed, indicating that the highest levels

of replication of WT ONNV was not affected by ablation of the cold shock proteins.In agreement with genome replication, WT ONNV showed more virus production at 12 and 24 hpi, but similar virus production at 36 or 48 hpi in the cold shock protein ablated cells compared to the RD-shCTL cells at 28°C (Fig. 6.6B). At 37°C, virus production for WT ONNV increased from 12-24 hpi and then decreased slightly from 24-48 hpi in the cold shock protein ablated RD cells, whereas it continues increased from 12-48 hpi in the RD-shCTL cells (Fig. 6.6B right panel). These data indicate that virus production was enhanced at early time points (before 24 hpi) but not at late time points (after 24 hpi) by ablation of the cold shock proteins.

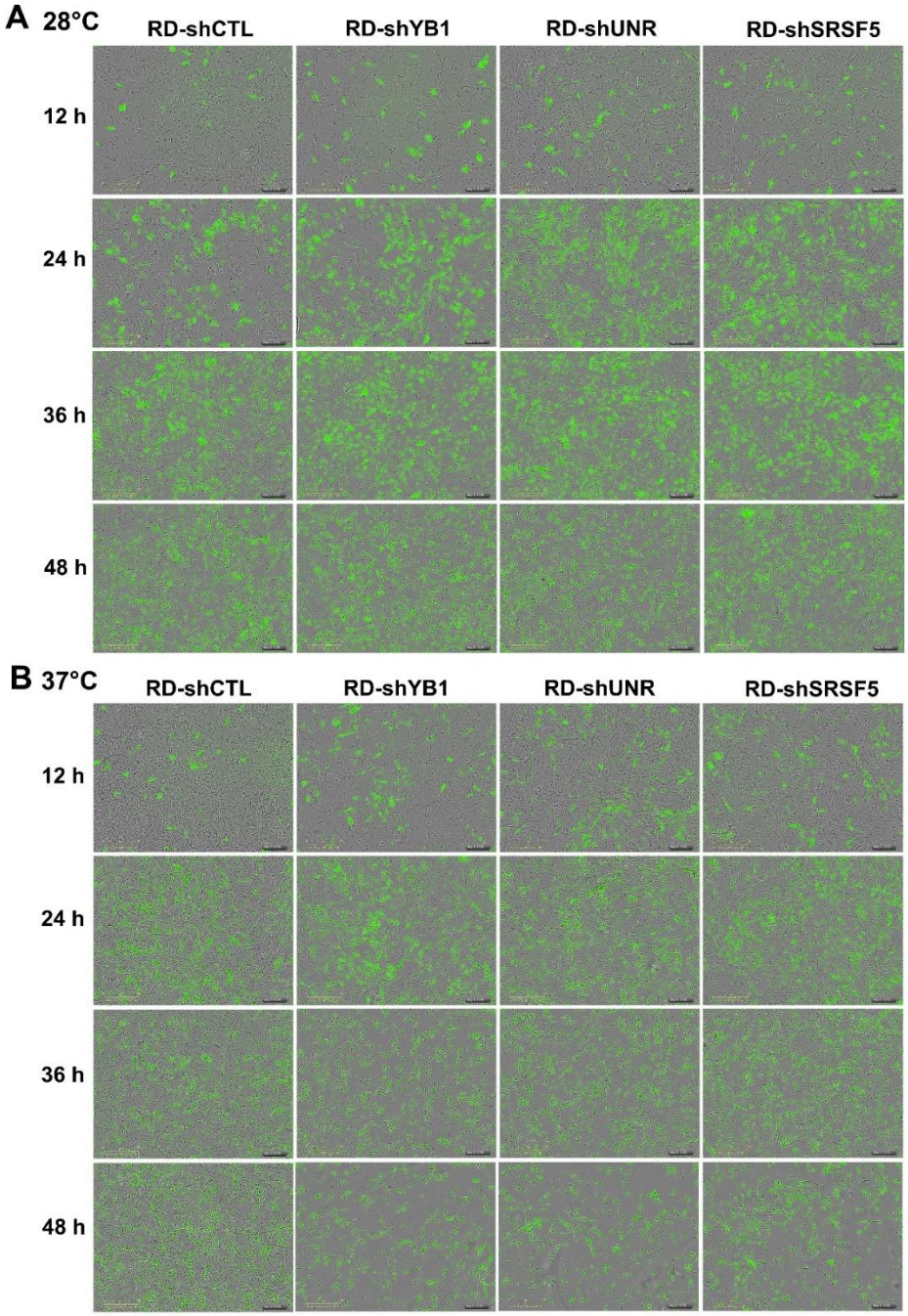

Figure 6.5 Replication of WT ONNV in cold shock protein ablated RD cell lines at different time points at 28°C or 37°C.

The cold shock protein ablated RD cells were seeded into 12 well plates without puromycin. The next day, cells were infected with WT ONNV at an MOI of 0.1 and incubated at 37°C or 28°C. Cells were fixed with 4% paraformaldehyde at indicated time points and ZsGreen expression at 28°C (A) or 37°C (B) was scanned and quantified by IncuCyte. Data are displayed as the means ±S.E. of three experimental replicates.

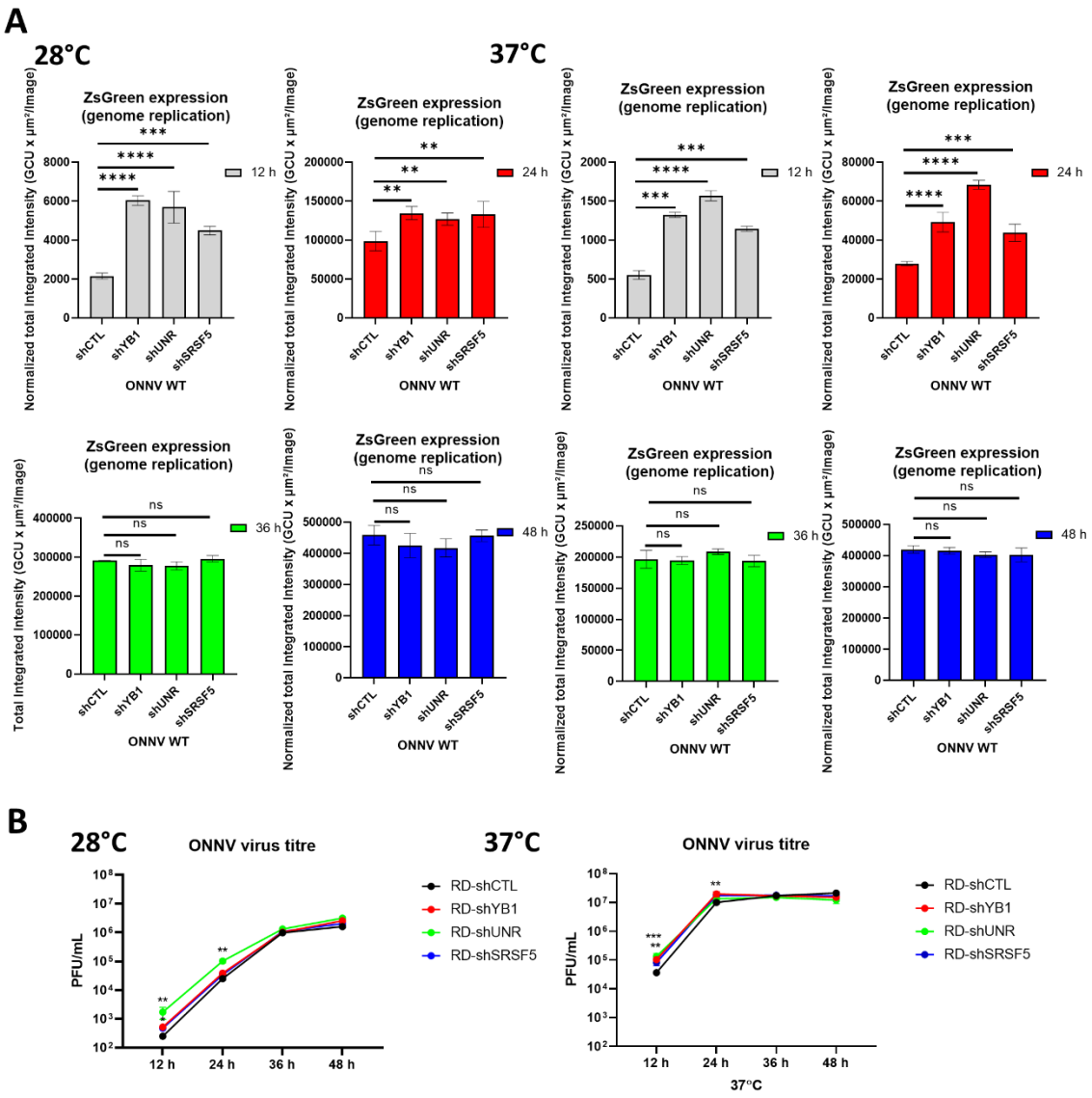

Figure 6.6 Normalized ZsGreen expression and virus production for WT ONNV in the cold shock protein ablated RD cell lines at different time points at 28°C or 37°C.

(A) Normalized ZsGreen expression of WT ONNV at different time points at 28°C or 37°C in the cold shock protein ablated RD cell lines. ZsGreen expression was quantified and normalized with cell confluency by IncuCyte. (B) One step growth curve of WT ONNV in the cold shock protein ablated RD cells at 28°C or 37°C. Supernatants harvested from 28°C or 37°C at indicated time points were titrated by plaque assay on BHK-21 cells at 37°C. ns (P>0.05), * (P<0.05), ** (P<0.01), *** (P<0.001), **** (P<0.0001) compared to replication or virus production of WT ONNV in RD-shCTL cells at each indicated time points. Data are displayed as the means ±S.E. of three experimental replicates.

6.2.5 Effect of ablation of the cold shock proteins on formation of SGs/G3BP-positive granules induced by $NaAsO_2$ or ONNV infection in the cold shock protein ablated RD cells at 28°C or 37°C

YB1 is a known component of SG and possesses the self-assembly of SG (Kedersha & Anderson 2007). It controls G3BP1 expression via activating G3BP1 mRNA and the subsequence nucleation of SG (Somasekharan et al 2015). YB1 was previously reported to interact with SINV nsP3, forming complexes on endosomal membranes as well as nucleus (Gorchakov et al 2008). UNR is also identified as a component of both SG and exosomes (Youn et al 2018). Therefore, I postulate that ablation of the cold shock proteins might have an effect on the formation of SGs/G3BP-positive granules by $NaAsO_2$ or ONNV infection at 28°C or 37°C. As shown in Figure 6.7, SG formation by $NaAsO_2$ at 37°C but not at 28°C in the RD-shCTL cells was observed, which is in agreement with previous results (Fig. 5.11). The assembly of SG by $NaAsO_2$ was also observed at 37°C but not at 28°C in the cold shock protein ablated RD cells (Fig. 6.7), suggesting that removal of these cold shock proteins didn't affect the assembly of SG induced by $NaAsO_2$.

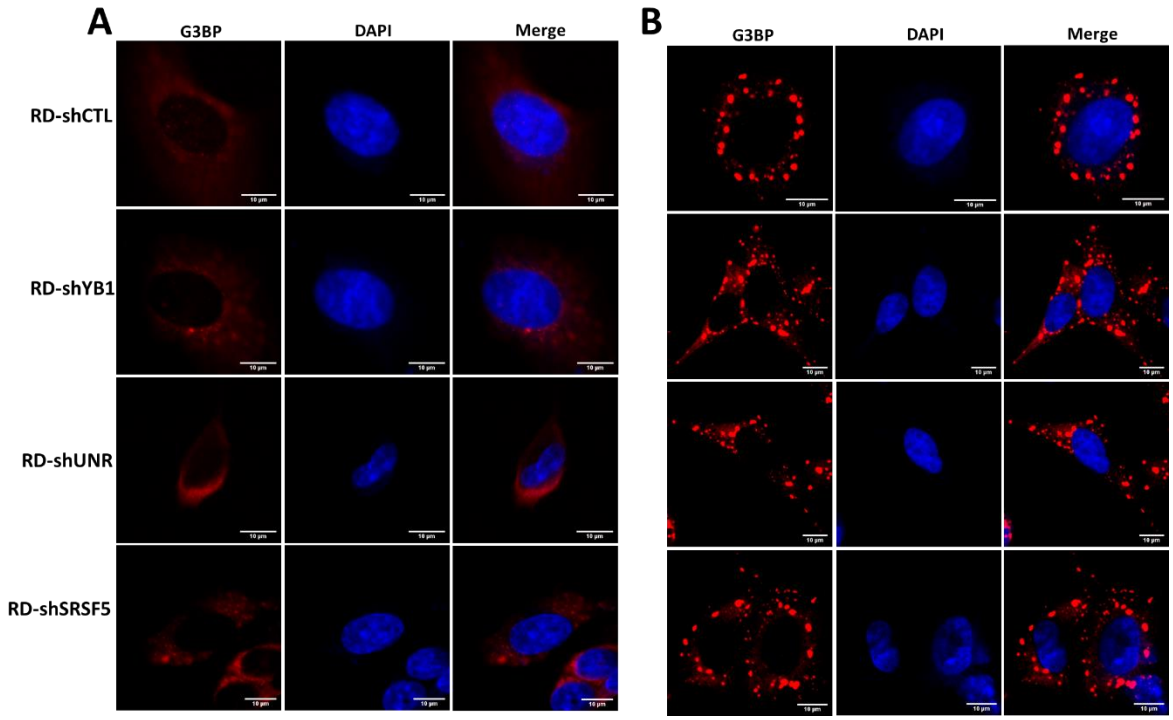

Figure 6.7 Formation of SG induced by $NaAsO_2$ in the cold shock protein ablated RD cells at 28°C or 37°C.

The cold shock protein ablated RD cells and the RD-shCTL cells were incubated at 37°C or 28°C, cells were then treated with 0.5 M $NaAsO_2$ for 1 h prior to fixation. Cells from both temperatures were stained with G3BP antibody (red).

The effect of the cold shock proteins on the formation of G3BP-positive granules induced by ONNV infection at 28°C or 37°C was also investigated. In RD-shCTL cells, SG assembly by ONNV infection was observed at 37°C and 28°C, and in consistence with previous results (Fig. 5.12), larger G3BP-positive granules was observed at 37°C compared to 28°C (Fig. 6.8). The formation of G3BP-positive granules by ONNV infection as well as larger G3BP-positive granules formation at 37°C compared to at 28°C was also observed in the cold shock protein ablated RD cells (Fig. 6.8). The results indicated that ablation of the cold shock protein does not affect the formation of G3BP-positive granules or the size of SG by ONNV infection at 28°C or 37°C. In agreement with the enhanced genome replication at lower temperature as previously described, more dsRNA expression per cell at 28°C compared to 37°C, in either the RD-shCTL cells or the cold shock protein ablated RD cells (Fig. 6.8) was also observed, reassuring that the genome replication of alphavirus was enhanced at sub-physiological temperature.

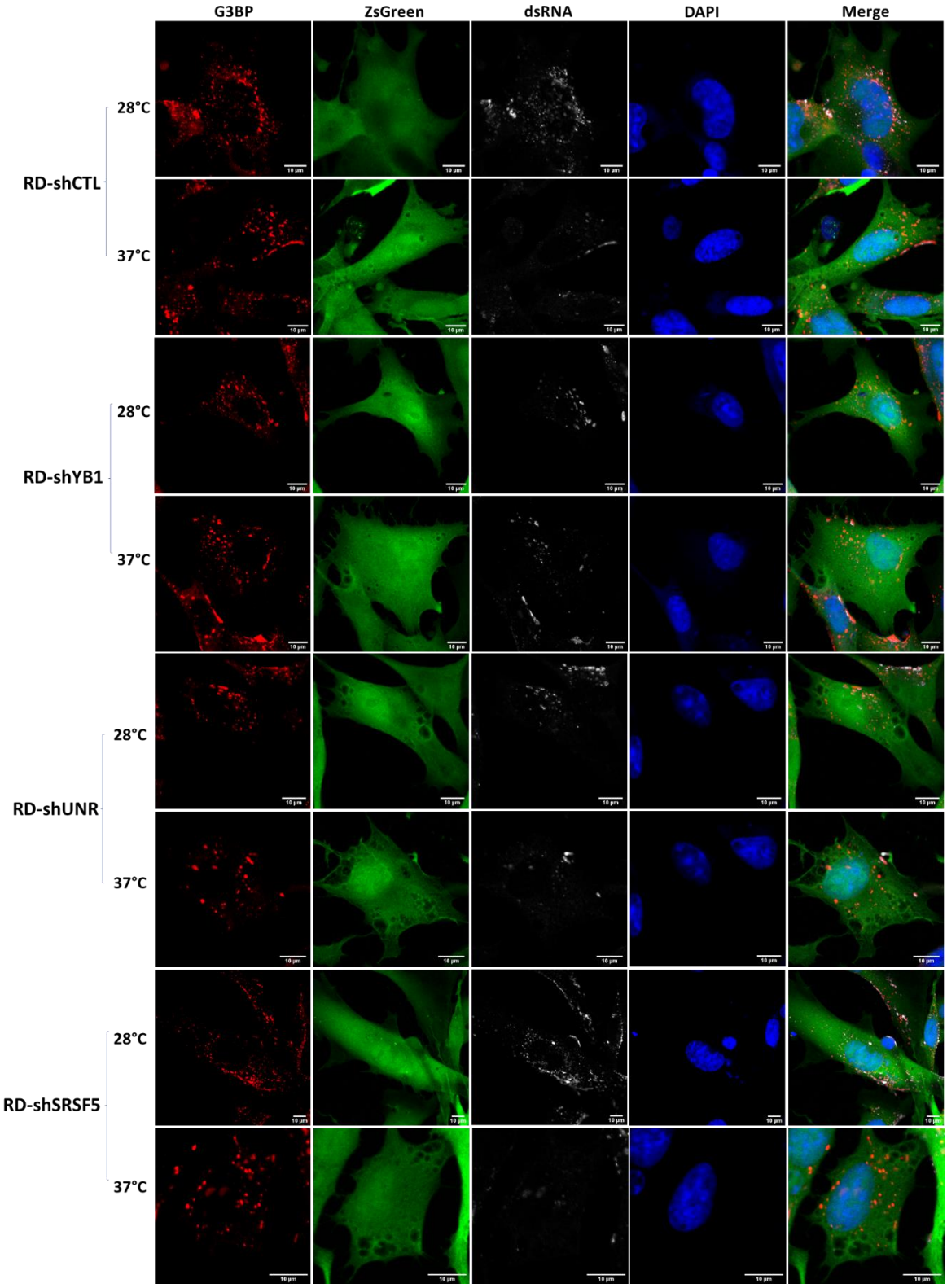
G3BP
ZsGreen
dsRNA
DAPI
Merge
RD-shCTL
28°C
37°C
RD-shYB1
28°C
37°C
RD-shUNR
28°C
37°C
RD-shSRSF5
28°C
37°C

Figure 6.8 Formation of G3BP-positive granules induced by WT ONNV in the cold shock protein ablated RD cells at 28°C or 37°C.

The cold shock protein ablated RD cells or the RD-shCTL cells were infected with WT ONNV at an MOI of 5 and incubated at 37°C or 28°C, cells were then fixed with 4% paraformaldehyde at 8 hpi. Cells from both temperatures were stained with G3BP antibody (red) and dsRNA antibody (gray).

6.3 Discussion

Cold shock proteins are among the most evolutionarily conserved proteins (Jones & Inouye 1994, Wolffe 1994, Wolffe et al 1992), with one or several defined CSD, which possess DNA and RNA binding activities. Indicated by their names, cold shock proteins are largely expressed to overcome the deleterious effects of cold shock. Apart from phosphorylation of eIF2α and SG formation, I also wonder whether cold shock proteins play a role in regulating the replication phenotype of CHIKV SGR and the AUD mutants. Previous work identified YB1 interacting with SINV nsP3 and form complexes, both in nucleus and cytoplasm (Gorchakov et al 2008). With mass spectrometry, our laboratory recently discovered two cold shock proteins interacting with CHIKV nsP3, namely UNR and SRSF5 (Gao 2018). YB1 is involved in diverse cellular functions, including transcription regulation, translation and mRNA stability (Kohno et al 2003). UNR binds to ssDNA or RNA through the CSD(Ferrer et al 1999, Jacquemin-Sablon et al 1994). It also regulates translation and mRNA stability by co-operates with polypyrimidine-tract-binding protein (Mitchell et al 2001, Sawicka et al 2008).SRSF5 is a member of the serine/arginine-rich family of pre-mRNA splicing factors (Kim et al 2016).

YB1 was shown to bind to DENV 3'-UTR and mediate antiviral effects by translation suppression of the viral RNA (Paranjape & Harris 2007). Therefore, I assumed that YB1 as well as the other cold shock proteins (UNR and SRSF5) might also functions as antiviral proteins. To further investigate the role of the cold shock proteins in the replication phenotype of CHIKV SGR at different temperatures, first I generated the cold shock proteins ablated RD cells by using lentiviruses containing specific human shRNAs and selected by puromycin. The

observation of enhanced genome replication at 12 hpt but not at 24 hpt for WT and mutant CHIKV-D-Luc-SGR in the cold shock protein ablated RD cells compared to RD-shCTL cells at 28°C suggested a role of suppressing genome replication at early time points for the cold shock proteins. This can also be supported by the fact that WT CHIKV-D-Luc-SGR exhibited lower replication at 12 hpt at 37°C in the cold shock protein ablated RD cells compared to the RD-shCTL cells, as the peak replication had been bought forward in the cold shock protein ablated RD cells. To note, although replication of the AUD mutants was enhanced at 37°C in the cold shock protein ablated RD cells, they were still much lower compared to WT, suggesting that the three cold shock proteins are not the key factor to determine the replication phenotype of the AUD mutants.

The assumption of the cold shock proteins function as antiviral proteins and enhance replication at early but not late stages was also supported in the context of ONNV (Fig. 6.4). Consistent with observation from replication of the AUD mutants in CHIKV-D-Luc-SGR at 37°C, mutant ONNV were not able to initiate replication in the cold shock protein ablated RD cells, reassuring that the cold shock proteins were not the key factor regulating the replication phenotype of the AUD mutants. In the growth curve of replication and virus production of WT ONNV in the cold shock protein ablated RD cells and RD-shCTL cells, WT ONNV exhibited enhanced replication and virus production at early time points (12 and 24 hpi) but not at late time points (36 and 48 hpi) in the cold shock protein ablated RD cells compared to RD-shCTL cells at 28°C or 37°C (Fig. 6.5). The data further confirmed the cold shock proteins (YB1, UNR and SRSF5) functions as antiviral proteins and suppress alphavirus replication and production at early time points. In the study of HCV, YB1 acts as both a stimulant and a repressor. The association of HCV NS3/4a with YB1 is required for HCV replication, while knockdown of YB1 increased virus production but impaired virus replication (Chatel-Chaix et al 2011). The mechanism of how alphavirus replication at early stage is suppressed by the cold shock proteins requires further investigation.

Previous work also demonstrated YB1 and UNR are components of SG (Kedersha & Anderson 2007, Keerthikumar et al 2016, Youn et al 2018). By activating mRNA of G3BP1, YB1 controls both G3BP1 expression and the nucleation of SG in human sarcoma cells (Somasekharan et al 2015). The investigation of SGs/G3BP-positive granules formation by $NaAsO_2$ or ONNV infection in the cold shock protein ablated RD cells compared to the RD-shCTL cells at both temperatures demonstrated that with or without these cold shock proteins, the assembly of SG as well as the localization of SG (mostly in cytoplasm) was not much affected, indicating a non-essential role of the cold shock proteins in the formation of SG.

In summary, I explored the function of cold shock proteins interacting with nsP3 on alphavirus replication and production at 28°C or 37°C. I conclude that the cold shock proteins (YB1, UNR or SRSF5) enhanced alphavirus replication and production at early time points, which is not affected by temperature variance. Importantly, induction of the cold shock proteins does not explain the enhanced replication phenotype at sub-physiological temperature.

Chapter 7: Conclusions and future perspectives

Based on our previous work showing that AUD is involved in virus assembly by binding to sub-genomic RNA promoter (Gao et al 2019), the project started in identifying other roles of AUD in alphavirus replication. By using the CHIKV-D-Luc-SGR, I identified three AUD mutants (W220A, D249A and Y324A) replicated poorly in mammalian cells but not in mosquito cells. It was later confirmed that this was not due to mutation reversion or related with RIG-I induced IFNs, but due to temperature variance. Interestingly, WT CHIKV-D-Luc-SGR also exhibited significant higher level of replication (approx. 100-fold) at sub-physiological temperature (28°C) compared to physiological temperature (37°C). The enhanced replication phenotype for WT CHIKV-D-Luc-SGR at sub-physiological temperature was demonstrated not due to the nature of the fused nsP3-reporter protein and was not exhibited by representatives of other arboviruses (Zika and BUNV). However, it remains to be determined whether this phenotype is conserved throughout the entire *Alphavirus* genus. The temperature sensitive replication phenotype of the AUD mutants was later confirmed in the context of infectious CHIKV and ONNV. However, unlike the significant higher level of replication for WT CHIKV-D-Luc-SGR at 28°C, it only exhibited a modest enhancement (2-fold) in replication of WT ICRES-CHIKV and ONNV at sub-physiological temperature, suggesting a defect in virus assembly or release at lower temperature.

My attention then turned to investigate the mechanisms behind temperature variance that determine the enhanced replication phenotype for alphaviruses at sub-physiological temperature. Phosphorylation of eIF2α is a key regulator in translation suppression. It was assumed that translation arrest via the effect of eIF2α phosphorylation might be ablated at lower temperature, which resulted in the enhanced genome replication. However, the data from inhibition of the effect of eIF2α phosphorylation by ISRIB suggested that it was not the key factor in determining the enhanced replication phenotype at sub-physiological temperatures (28°C and 32°C). Following eIF2α phosphorylation, my attention then focused on formation of SG, as no SG were formed at 28°C by treatment with $NaAsO_2$ (Wheeler et al 2016). To my surprise, in contrast to the inability of $NaAsO_2$ to induce SGs at 28°C, ONNV infection was able to induce G3BP-positive granules at

both temperatures, however, they differed significantly in sizes and numbers. The mean cross-sectional area of SG at 28°C was much smaller than 37°C in response to ONNV infection. In further explaining this, by calculation of surface areas and volumes of SGs per cells at two temperatures, I determined a larger surface area and a 26-fold volume of SGs at 37°C compared to 28°C. It might suggest that canonical SG was suppressed in response to ONNV infection at lower temperature but not at 37°C. The role of the cold shock proteins interacting with nsP3 (YB1, UNR and SRSF5) in alphavirus replication was also investigated, and I demonstrated that they were not responsible for the temperature-sensitive replication phenotype of the AUD mutants, but they suppressed alphavirus replication at early time points, which was independent of temperature variance. Building on the findings, this project also proposed many questions that need to be investigated in the future. For example, the inability of the ONNV AUD mutants to replicate at 37°C but not at sub-physiological temperatures (28°C and 32°C) might be correlated with different proteins interacting with AUD at different temperatures. This can be tested by infection of ICRES-CHIKV-nsP3-TST and ICRES-CHIKV in cells at sub-physiological temperatures (28°C and 32°C) or 37°C and different proteins interacting with nsP3 AUD at different temperatures can be determined by mass spectrometry. The phenotype might also be correlated with different RNA-AUD interactions at different temperatures. Our laboratory currently is using the cutting edge iCLIP (individual-nucleotide resolution Cross-Linking and Immunoprecipitation) technology to investigate if there is any difference in RNA binding to AUD in mammalian cells at physiological and sub-physiological temperatures. As the protease activity of nsP2 might play a role in the enhancement of alphavirus replication at sub-physiological temperature (Balistreri et al 2007), a trans-replicase system of independent replication and translation (protease activity is disabled via mutation) plasmids and a separate plasmid expressing protease at different temperatures might shed light on the role of protease in the replication phenotype (Bartholomeeusen et al 2018). The different sizes of G3BP-positive granules at sub-physiological and physiological temperatures suggest different compositions at 28°C or 37°C, and this can be

exploited by enriching G3BP-positive granules using centrifugation and purifying G3BP-positive granules using immunoprecipitation and mass spectrometry (Wheeler et al 2017). To explain the different compositions of G3BP-positive granules at different temperatures, the ADP-ribosylhydrolase activity of macro-domain might play a role. This can be verified by testing the ADP-ribosylhydrolase activity with substrates at physiological (37°C) or sub-physiological temperatures (28°C and 32°C) *in vitro*, or ablating of the ADP-ribosylhydrolase activity by mutation and evaluating the replication in trans-replicase system in mammalian cells at different temperatures.

In conclusion, three CHIKV AUD mutants (W220A, D249A and Y324A) were identified as temperature sensitive mutants. They have the potential to be utilized as vaccines, as they are unable to replication at 37°C. Importantly, the data reported a hitherto unrecognized enhancement of alphavirus genome replication in mammalian cells at sub-physiological temperatures, which might play a role at the early stages of alphavirus transmission to mammalian host via a mosquito bite.

References

Abdelnabi R, Neyts J, Delang L. 2015. Towards antivirals against chikungunya virus. *Antiviral Res* 121: 59-68

Abraham R, Hauer D, McPherson RL, Utt A, Kirby IT, et al. 2018. ADP-ribosyl-binding and hydrolase activities of the alphavirus nsP3 macrodomain are critical for initiation of virus replication. *Proc Natl Acad Sci U S A* 115: E10457-E66

Abraham R, McPherson RL, Dasovich M, Badiee M, Leung AKL, Griffin DE. 2020. Both ADP-Ribosyl-Binding and Hydrolase Activities of the Alphavirus nsP3 Macrodomain Affect Neurovirulence in Mice. *mBio* 11

Abrahamyan LG, Chatel-Chaix L, Ajamian L, Milev MP, Monette A, et al. 2010. Novel Staufen1 ribonucleoproteins prevent formation of stress granules but favour encapsidation of HIV-1 genomic RNA. *J Cell Sci* 123: 369-83

Aggarwal M, Tapas S, Preeti, Siwach A, Kumar P, et al. 2012. Crystal structure of aura virus capsid protease and its complex with dioxane: new insights into capsid-glycoprotein molecular contacts. *PLoS One* 7: e51288

Ahola T, Kaariainen L. 1995. Reaction in alphavirus mRNA capping: formation of a covalent complex of nonstructural protein nsP1 with 7-methyl-GMP. *Proc Natl Acad Sci U S A* 92: 507-11

Ahola T, Karlin DG. 2015. Sequence analysis reveals a conserved extension in the capping enzyme of the alphavirus supergroup, and a homologous domain in nodaviruses. *Biol Direct* 10: 16

Ahola T, Kujala P, Tuittila M, Blom T, Laakkonen P, et al. 2000. Effects of palmitoylation of replicase protein nsP1 on alphavirus infection. *J Virol* 74: 6725-33

Ahola T, Lampio A, Auvinen P, Kaariainen L. 1999. Semliki Forest virus mRNA capping enzyme requires association with anionic membrane phospholipids for activity. *EMBO J* 18: 3164-72

Ahola T, Merits A. 2016. Functions of Chikungunya Virus Nonstructural Proteins In *Chikungunya Virus: Advances in Biology, Pathogenesis, and Treatment*, ed. CM Okeoma, pp. 75-98. Cham: Springer International Publishing

Akhrymuk I, Kulemzin SV, Frolova EI. 2012. Evasion of the innate immune response: the Old World alphavirus nsP2 protein induces rapid degradation of Rpb1, a catalytic subunit of RNA polymerase II. *J Virol* 86: 7180-91

Alto BW, Wiggins K, Eastmond B, Ortiz S, Zirbel K, Lounibos LP. 2018. Diurnal Temperature Range and Chikungunya Virus Infection in Invasive Mosquito Vectors. *J Med Entomol* 55: 217-24

Anderson EC, Catnaigh PO. 2015. Regulation of the expression and activity of Unr in mammalian cells. *Biochem Soc Trans* 43: 1241-6

Arankalle VA, Shrivastava S, Cherian S, Gunjikar RS, Walimbe AM, et al. 2007. Genetic divergence of Chikungunya viruses in India (1963-2006) with special reference to the 2005-2006 explosive epidemic. *J Gen Virol* 88: 1967-76

Arimoto K, Fukuda H, Imajoh-Ohmi S, Saito H, Takekawa M. 2008. Formation of stress granules inhibits apoptosis by suppressing stress-responsive MAPK pathways. *Nat Cell Biol* 10: 1324-32

Ariumi Y, Kuroki M, Kushima Y, Osugi K, Hijikata M, et al. 2011. Hepatitis C virus hijacks P-body and stress granule components around lipid droplets. *J Virol* 85: 6882-92

Ashbrook AW, Burrack KS, Silva LA, Montgomery SA, Heise MT, et al. 2014. Residue 82 of the Chikungunya virus E2 attachment protein modulates viral dissemination and arthritis in mice. *J Virol* 88: 12180-92

Aubry M, Teissier A, Roche C, Richard V, Yan AS, et al. 2015. Chikungunya outbreak, French Polynesia, 2014. *Emerg Infect Dis* 21: 724-6

Balistreri G, Caldentey J, Kaariainen L, Ahola T. 2007. Enzymatic defects of the nsP2 proteins of Semliki Forest virus temperature-sensitive mutants. *J Virol* 81: 2849-60

Barajas D, Jiang Y, Nagy PD. 2009. A unique role for the host ESCRT proteins in replication of Tomato bushy stunt virus. *PLoS Pathog* 5: e1000705

Barkauskaite E, Jankevicius G, Ladurner AG, Ahel I, Timinszky G. 2013. The recognition and removal of cellular poly(ADP-ribose) signals. *FEBS J* 280: 3491-507

Barry G, Fragkoudis R, Ferguson MC, Lulla A, Merits A, et al. 2010. Semliki forest virus-induced endoplasmic reticulum stress accelerates apoptotic death of mammalian cells. *J Virol* 84: 7369-77

Bartel DP. 2004. MicroRNAs: genomics, biogenesis, mechanism, and function. *Cell* 116: 281-97

Bartholomeeusen K, Utt A, Coppens S, Rausalu K, Vereecken K, et al. 2018. A Chikungunya Virus trans-Replicase System Reveals the Importance of Delayed Nonstructural Polyprotein Processing for Efficient Replication Complex Formation in Mosquito Cells. *J Virol* 92

Barton DJ, Sawicki SG, Sawicki DL. 1988. Demonstration in vitro of temperature-sensitive elongation of RNA in Sindbis virus mutant ts6. *J Virol* 62: 3597-602

Berlanga JJ, Ventoso I, Harding HP, Deng J, Ron D, et al. 2006. Antiviral effect of the mammalian translation initiation factor 2alpha kinase GCN2 against RNA viruses. *EMBO J* 25: 1730-40

Bernard E, Solignat M, Gay B, Chazal N, Higgs S, et al. 2010. Endocytosis of chikungunya virus into mammalian cells: role of clathrin and early endosomal compartments. *PLoS One* 5: e11479

Bordeleau ME, Matthews J, Wojnar JM, Lindqvist L, Novac O, et al. 2005. Stimulation of mammalian translation initiation factor eIF4A activity by a small molecule inhibitor of eukaryotic translation. *Proc Natl Acad Sci U S A* 102: 10460-5

Borgherini G, Poubeau P, Staikowsky F, Lory M, Le Moullec N, et al. 2007. Outbreak of chikungunya on Reunion Island: early clinical and laboratory features in 157 adult patients. *Clin Infect Dis* 44: 1401-7

Boussadia O, Amiot F, Cases S, Triqueneaux G, Jacquemin-Sablon H, Dautry F. 1997. Transcription of unr (upstream of N-ras) down-modulates N-ras expression in vivo. *FEBS Lett* 420: 20-4

Boussadia O, Jacquemin-Sablon H, Dautry F. 1993. Exon skipping in the expression of the gene immediately upstream of N-ras (unr/NRU). *Biochim Biophys Acta* 1172: 64-72

Brady OJ, Johansson MA, Guerra CA, Bhatt S, Golding N, et al. 2013. Modelling adult Aedes aegypti and Aedes albopictus survival at different temperatures in laboratory and field settings. *Parasit Vectors* 6: 351

Brandt S, Raffetseder U, Djudjaj S, Schreiter A, Kadereit B, et al. 2012. Cold shock Y-box protein-1 participates in signaling circuits with auto-regulatory activities. *Eur J Cell Biol* 91: 464-71

Breakwell L, Dosenovic P, Karlsson Hedestam GB, D'Amato M, Liljestrom P, et al. 2007. Semliki Forest virus nonstructural protein 2 is involved in suppression of the type I interferon response. *J Virol* 81: 8677-84

Brighton SW. 1984. Chloroquine phosphate treatment of chronic Chikungunya arthritis. An open pilot study. *S Afr Med J* 66: 217-8

Carey DE. 1971. Chikungunya and dengue: a case of mistaken identity? *J Hist Med Allied Sci* 26: 243-62

Carleton M, Lee H, Mulvey M, Brown DT. 1997. Role of glycoprotein PE2 in formation and maturation of the Sindbis virus spike. *J Virol* 71: 1558-66

Castello A, Sanz MA, Molina S, Carrasco L. 2006. Translation of Sindbis virus 26S mRNA does not require intact eukariotic initiation factor 4G. *J Mol Biol* 355: 942-56

Centers for Disease C, Prevention. 2007. Update: chikungunya fever diagnosed among international travelers--United States, 2006. *MMWR Morb Mortal Wkly Rep* 56: 276-7

Chatel-Chaix L, Melancon P, Racine ME, Baril M, Lamarre D. 2011. Y-box-binding protein 1 interacts with hepatitis C virus NS3/4A and influences the equilibrium between viral RNA replication and infectious particle production. *J Virol* 85: 11022-37

Chen KC, Kam YW, Lin RT, Ng MM, Ng LF, Chu JJ. 2013a. Comparative analysis of the genome sequences and replication profiles of chikungunya virus isolates within the East, Central and South African (ECSA) lineage. *Virol J* 10: 169

Chen R, Mukhopadhyay S, Merits A, Bolling B, Nasar F, et al. 2018a. ICTV Virus Taxonomy Profile: Togaviridae. *J Gen Virol* 99: 761-62

Chen R, Wang E, Tsetsarkin KA, Weaver SC. 2013b. Chikungunya virus 3' untranslated region: adaptation to mosquitoes and a population bottleneck as major evolutionary forces. *PLoS Pathog* 9: e1003591

Chen Y, Huang Q, Liu W, Zhu Q, Cui CP, et al. 2018b. Mutually exclusive acetylation and ubiquitylation of the splicing factor SRSF5 control tumor growth. *Nat Commun* 9: 2464

Cherian SS, Walimbe AM, Jadhav SM, Gandhe SS, Hundekar SL, et al. 2009. Evolutionary rates and timescale comparison of Chikungunya viruses inferred from the whole genome/E1 gene with special reference to the 2005-07 outbreak in the Indian subcontinent. *Infect Genet Evol* 9: 16-23

Choi HK, Tong L, Minor W, Dumas P, Boege U, et al. 1991. Structure of Sindbis virus core protein reveals a chymotrypsin-like serine proteinase and the organization of the virion. *Nature* 354: 37-43

Corbet PS, Williams MC, Gillett JD. 1961. O'Nyong-Nyong fever: an epidemic virus disease in East Africa. IV. Vector studies at epidemic sites. *Trans R Soc Trop Med Hyg* 55: 463-80

Couturier E, Guillemin F, Mura M, Leon L, Virion JM, et al. 2012. Impaired quality of life after chikungunya virus infection: a 2-year follow-up study. *Rheumatology (Oxford)* 51: 1315-22

Cristea IM, Rozjabek H, Molloy KR, Karki S, White LL, et al. 2010. Host factors associated with the Sindbis virus RNA-dependent RNA polymerase: role for G3BP1 and G3BP2 in virus replication. *J Virol* 84: 6720-32

Dang Y, Kedersha N, Low WK, Romo D, Gorospe M, et al. 2006. Eukaryotic initiation factor 2alpha-independent pathway of stress granule induction by the natural product pateamine A. *J Biol Chem* 281: 32870-8

Das PK, Merits A, Lulla A. 2014. Functional cross-talk between distant domains of chikungunya virus non-structural protein 2 is decisive for its RNA-modulating activity. *J Biol Chem* 289: 5635-53

Das T, Jaffar-Bandjee MC, Hoarau JJ, Krejbich Trotot P, Denizot M, et al. 2010. Chikungunya fever: CNS infection and pathologies of a re-emerging arbovirus. *Prog Neurobiol* 91: 121-9

Dash PK, Parida MM, Santhosh SR, Verma SK, Tripathi NK, et al. 2007. East Central South African genotype as the causative agent in reemergence of Chikungunya outbreak in India. *Vector Borne Zoonotic Dis* 7: 519-27

de Groot RJ, Rumenapf T, Kuhn RJ, Strauss EG, Strauss JH. 1991. Sindbis virus RNA polymerase is degraded by the N-end rule pathway. *Proc Natl Acad Sci U S A* 88: 8967-71

De I, Fata-Hartley C, Sawicki SG, Sawicki DL. 2003. Functional analysis of nsP3 phosphoprotein mutants of Sindbis virus. *J Virol* 77: 13106-16

De Lamballerie X, Boisson V, Reynier JC, Enault S, Charrel RN, et al. 2008. On chikungunya acute infection and chloroquine treatment. *Vector Borne Zoonotic Dis* 8: 837-9

Delang L, Li C, Tas A, Querat G, Albulescu IC, et al. 2016. The viral capping enzyme nsP1: a novel target for the inhibition of chikungunya virus infection. *Sci Rep* 6: 31819

Delisle E, Rousseau C, Broche B, Leparc-Goffart I, L'Ambert G, et al. 2015. Chikungunya outbreak in Montpellier, France, September to October 2014. *Euro Surveill* 20

Deng J, Harding HP, Raught B, Gingras AC, Berlanga JJ, et al. 2002. Activation of GCN2 in UV-irradiated cells inhibits translation. *Curr Biol* 12: 1279-86

Dever TE. 2002. Gene-specific regulation by general translation factors. *Cell* 108: 545-56

Dickson AM, Anderson JR, Barnhart MD, Sokoloski KJ, Oko L, et al. 2012. Dephosphorylation of HuR protein during alphavirus infection is associated with HuR relocalization to the cytoplasm. *J Biol Chem* 287: 36229-38

Domingo E. 1997. Rapid evolution of viral RNA genomes. *J Nutr* 127: 958S-61S

Doniger J, Landsman D, Gonda MA, Wistow G. 1992. The product of unr, the highly conserved gene upstream of N-ras, contains multiple repeats similar

to the cold-shock domain (CSD), a putative DNA-binding motif. *New Biol* 4: 389-95

Drake JW. 1993. Rates of spontaneous mutation among RNA viruses. *Proc Natl Acad Sci U S A* 90: 4171-5

Dupuis-Maguiraga L, Noret M, Brun S, Le Grand R, Gras G, Roques P. 2012. Chikungunya disease: infection-associated markers from the acute to the chronic phase of arbovirus-induced arthralgia. *PLoS Negl Trop Dis* 6: e1446

Eckei L, Krieg S, Butepage M, Lehmann A, Gross A, et al. 2017. The conserved macrodomains of the non-structural proteins of Chikungunya virus and other pathogenic positive strand RNA viruses function as mono-ADP-ribosylhydrolases. *Sci Rep* 7: 41746

Eckels KH, Harrison VR, Hetrick FM. 1970. Chikungunya virus vaccine prepared by Tween-ether extraction. *Appl Microbiol* 19: 321-5

Edelman R, Tacket CO, Wasserman SS, Bodison SA, Perry JG, Mangiafico JA. 2000. Phase II safety and immunogenicity study of live chikungunya virus vaccine TSI-GSD-218. *Am J Trop Med Hyg* 62: 681-5

Emara MM, Brinton MA. 2007. Interaction of TIA-1/TIAR with West Nile and dengue virus products in infected cells interferes with stress granule formation and processing body assembly. *Proc Natl Acad Sci U S A* 104: 9041-6

Endy TP, Anderson KB, Nisalak A, Yoon IK, Green S, et al. 2011. Determinants of inapparent and symptomatic dengue infection in a prospective study of primary school children in Kamphaeng Phet, Thailand. *PLoS Negl Trop Dis* 5: e975

Esclatine A, Taddeo B, Roizman B. 2004. The UL41 protein of herpes simplex virus mediates selective stabilization or degradation of cellular mRNAs. *Proc Natl Acad Sci U S A* 101: 18165-70

Fehr AR, Channappanavar R, Jankevicius G, Fett C, Zhao J, et al. 2016. The Conserved Coronavirus Macrodomain Promotes Virulence and Suppresses the Innate Immune Response during Severe Acute Respiratory Syndrome Coronavirus Infection. *mBio* 7

Fehr AR, Jankevicius G, Ahel I, Perlman S. 2018. Viral Macrodomains: Unique Mediators of Viral Replication and Pathogenesis. *Trends Microbiol* 26: 598-610

Feijs KL, Forst AH, Verheugd P, Luscher B. 2013. Macrodomain-containing proteins: regulating new intracellular functions of mono(ADP-ribosyl)ation. *Nat Rev Mol Cell Biol* 14: 443-51

Ferrer N, Garcia-Espana A, Jeffers M, Pellicer A. 1999. The unr gene: evolutionary considerations and nucleic acid-binding properties of its long isoform product. *DNA Cell Biol* 18: 209-18

Firth AE, Chung BY, Fleeton MN, Atkins JF. 2008. Discovery of frameshifting in Alphavirus 6K resolves a 20-year enigma. *Virol J* 5: 108

Foy NJ, Akhrymuk M, Akhrymuk I, Atasheva S, Bopda-Waffo A, et al. 2013a. Hypervariable domains of nsP3 proteins of New World and Old World alphaviruses mediate formation of distinct, virus-specific protein complexes. *J Virol* 87: 1997-2010

Foy NJ, Akhrymuk M, Shustov AV, Frolova EI, Frolov I. 2013b. Hypervariable domain of nonstructural protein nsP3 of Venezuelan equine encephalitis virus determines cell-specific mode of virus replication. *J Virol* 87: 7569-84

Frolov I, Hardy R, Rice CM. 2001. Cis-acting RNA elements at the 5' end of Sindbis virus genome RNA regulate minus- and plus-strand RNA synthesis. *RNA* 7: 1638-51

Frolova E, Frolov I, Schlesinger S. 1997. Packaging signals in alphaviruses. *J Virol* 71: 248-58

Frolova EI, Gorchakov R, Pereboeva L, Atasheva S, Frolov I. 2010. Functional Sindbis virus replicative complexes are formed at the plasma membrane. *J Virol* 84: 11679-95

Fros JJ, Domeradzka NE, Baggen J, Geertsema C, Flipse J, et al. 2012. Chikungunya virus nsP3 blocks stress granule assembly by recruitment of G3BP into cytoplasmic foci. *J Virol* 86: 10873-9

Fros JJ, Liu WJ, Prow NA, Geertsema C, Ligtenberg M, et al. 2010. Chikungunya virus nonstructural protein 2 inhibits type I/II interferon-stimulated JAK-STAT signaling. *J Virol* 84: 10877-87

Fros JJ, Major LD, Scholte FEM, Gardner J, van Hemert MJ, et al. 2015. Chikungunya virus non-structural protein 2-mediated host shut-off disables the unfolded protein response. *J Gen Virol* 96: 580-89

Gaedigk-Nitschko K, Schlesinger MJ. 1991. Site-directed mutations in Sindbis virus E2 glycoprotein's cytoplasmic domain and the 6K protein lead to similar defects in virus assembly and budding. *Virology* 183: 206-14

Gandhi NS, Mancera RL. 2008. The structure of glycosaminoglycans and their interactions with proteins. *Chem Biol Drug Des* 72: 455-82

Gao Y. 2018. *Functional analysis of Chikungunya virus non-structural protein 3 alphavirus unique domain*. Dcotorate thesis thesis. University of Leeds, University of Leeds. 185 pp.

Gao Y, Goonawardane N, Ward J, Tuplin A, Harris M. 2019. Multiple roles of the non-structural protein 3 (nsP3) alphavirus unique domain (AUD) during Chikungunya virus genome replication and transcription. *PLoS Pathog* 15: e1007239

Garcia MA, Meurs EF, Esteban M. 2007. The dsRNA protein kinase PKR: virus and cell control. *Biochimie* 89: 799-811

Gardner CL, Burke CW, Higgs ST, Klimstra WB, Ryman KD. 2012. Interferon-alpha/beta deficiency greatly exacerbates arthritogenic disease in mice infected with wild-type chikungunya virus but not with the cell culture-adapted live-attenuated 181/25 vaccine candidate. *Virology* 425: 103-12

Gardner CL, Burke CW, Tesfay MZ, Glass PJ, Klimstra WB, Ryman KD. 2008. Eastern and Venezuelan equine encephalitis viruses differ in their ability to infect dendritic cells and macrophages: impact of altered cell tropism on pathogenesis. *J Virol* 82: 10634-46

George J, Raju R. 2000. Alphavirus RNA genome repair and evolution: molecular characterization of infectious sindbis virus isolates lacking a known conserved motif at the 3' end of the genome. *J Virol* 74: 9776-85

Gerardin P, Barau G, Michault A, Bintner M, Randrianaivo H, et al. 2008. Multidisciplinary prospective study of mother-to-child chikungunya virus infections on the island of La Reunion. *PLoS Med* 5: e60

Gifford GE, Heller E. 1963. Effect of Actinomycin D on Interferon Production by 'Active' and 'Inactive' Chikungunya Virus in Chick Cells. *Nature* 200: 50-1

Gorchakov R, Frolova E, Frolov I. 2005. Inhibition of transcription and translation in Sindbis virus-infected cells. *J Virol* 79: 9397-409

Gorchakov R, Frolova E, Williams BR, Rice CM, Frolov I. 2004. PKR-dependent and -independent mechanisms are involved in translational shutoff during Sindbis virus infection. *J Virol* 78: 8455-67

Gorchakov R, Garmashova N, Frolova E, Frolov I. 2008. Different types of nsP3-containing protein complexes in Sindbis virus-infected cells. *J Virol* 82: 10088-101

Gottesman S. 2018. Chilled in Translation: Adapting to Bacterial Climate Change. *Mol Cell* 70: 193-94

Hahn YS, Grakoui A, Rice CM, Strauss EG, Strauss JH. 1989a. Mapping of RNA-temperature-sensitive mutants of Sindbis virus: complementation group F mutants have lesions in nsP4. *J Virol* 63: 1194-202

Hahn YS, Strauss EG, Strauss JH. 1989b. Mapping of RNA- temperature-sensitive mutants of Sindbis virus: assignment of complementation groups A, B, and G to nonstructural proteins. *J Virol* 63: 3142-50

Halstead SB. 2015. Reappearance of chikungunya, formerly called dengue, in the Americas. *Emerg Infect Dis* 21: 557-61

Hammon WM, Rudnick A, Sather GE. 1960. Viruses associated with epidemic hemorrhagic fevers of the Philippines and Thailand. *Science* 131: 1102-3

Harding HP, Calfon M, Urano F, Novoa I, Ron D. 2002. Transcriptional and translational control in the Mammalian unfolded protein response. *Annu Rev Cell Dev Biol* 18: 575-99

Harding HP, Novoa I, Zhang Y, Zeng H, Wek R, et al. 2000a. Regulated translation initiation controls stress-induced gene expression in mammalian cells. *Mol Cell* 6: 1099-108

Harding HP, Zhang Y, Bertolotti A, Zeng H, Ron D. 2000b. Perk is essential for translational regulation and cell survival during the unfolded protein response. *Mol Cell* 5: 897-904

Hardy RW, Rice CM. 2005. Requirements at the 3' end of the sindbis virus genome for efficient synthesis of minus-strand RNA. *J Virol* 79: 4630-9

Harrison VR, Eckels KH, Bartelloni PJ, Hampton C. 1971. Production and evaluation of a formalin-killed Chikungunya vaccine. *J Immunol* 107: 643-7

Heitmann A, Jansen S, Luhken R, Helms M, Pluskota B, et al. 2018. Experimental risk assessment for chikungunya virus transmission based on vector competence, distribution and temperature suitability in Europe, 2018. *Euro Surveill* 23

Her Z, Malleret B, Chan M, Ong EK, Wong SC, et al. 2010. Active infection of human blood monocytes by Chikungunya virus triggers an innate immune response. *J Immunol* 184: 5903-13

Hetz C. 2012. The unfolded protein response: controlling cell fate decisions under ER stress and beyond. *Nat Rev Mol Cell Biol* 13: 89-102

Hoarau JJ, Jaffar Bandjee MC, Krejbich Trotot P, Das T, Li-Pat-Yuen G, et al. 2010. Persistent chronic inflammation and infection by Chikungunya arthritogenic alphavirus in spite of a robust host immune response. *J Immunol* 184: 5914-27

Holland J, Spindler K, Horodyski F, Grabau E, Nichol S, VandePol S. 1982. Rapid evolution of RNA genomes. *Science* 215: 1577-85

Hyde JL, Chen R, Trobaugh DW, Diamond MS, Weaver SC, et al. 2015. The 5' and 3' ends of alphavirus RNAs--Non-coding is not non-functional. *Virus Res* 206: 99-107

Hyde JL, Gardner CL, Kimura T, White JP, Liu G, et al. 2014. A viral RNA structural element alters host recognition of nonself RNA. *Science* 343: 783-7

Ivashkiv LB, Donlin LT. 2014. Regulation of type I interferon responses. *Nat Rev Immunol* 14: 36-49

Jackson RJ, Hellen CU, Pestova TV. 2010. The mechanism of eukaryotic translation initiation and principles of its regulation. *Nat Rev Mol Cell Biol* 11: 113-27

Jacquemin-Sablon H, Triqueneaux G, Deschamps S, le Maire M, Doniger J, Dautry F. 1994. Nucleic acid binding and intracellular localization of unr, a protein with five cold shock domains. *Nucleic Acids Res* 22: 2643-50

Jayabalan AK, Adivarahan S, Koppula A, Abraham R, Batish M, et al. 2021. Stress granule formation, disassembly, and composition are regulated by alphavirus ADP-ribosylhydrolase activity. *Proc Natl Acad Sci U S A* 118

Jeffers M, Paciucci R, Pellicer A. 1990. Characterization of unr; a gene closely linked to N-ras. *Nucleic Acids Res* 18: 4891-9

Jones JE, Long KM, Whitmore AC, Sanders W, Thurlow LR, et al. 2017. Disruption of the Opal Stop Codon Attenuates Chikungunya Virus-Induced Arthritis and Pathology. *mBio* 8

Jones PG, Inouye M. 1994. The cold-shock response--a hot topic. *Mol Microbiol* 11: 811-8

Jones PH, Maric M, Madison MN, Maury W, Roller RJ, Okeoma CM. 2013. BST-2/tetherin-mediated restriction of chikungunya (CHIKV) VLP budding is counteracted by CHIKV non-structural protein 1 (nsP1). *Virology* 438: 37-49

Kaariainen L, Ahola T. 2002. Functions of alphavirus nonstructural proteins in RNA replication. *Prog Nucleic Acid Res Mol Biol* 71: 187-222

Kaariainen L, Sawicki D, Gomatos PJ. 1978. Cleavage defect in the non-structural polyprotein of Semliki Forest virus has two separate effects on virus RNA synthesis. *J Gen Virol* 39: 463-73

Kallio K, Hellstrom K, Balistreri G, Spuul P, Jokitalo E, Ahola T. 2013. Template RNA length determines the size of replication complex spherules for Semliki Forest virus. *J Virol* 87: 9125-34

Kam YW, Lee WW, Simarmata D, Harjanto S, Teng TS, et al. 2012. Longitudinal analysis of the human antibody response to Chikungunya virus infection:

implications for serodiagnosis and vaccine development. *J Virol* 86: 13005-15

Kang S, Lee TA, Ra EA, Lee E, Choi H, et al. 2014. Differential control of interleukin-6 mRNA levels by cellular distribution of YB-1. *PLoS One* 9: e112754

Karo-Astover L, Sarova O, Merits A, Zusinaite E. 2010. The infection of mammalian and insect cells with SFV bearing nsP1 palmitoylation mutations. *Virus Res* 153: 277-87

Karpe YA, Aher PP, Lole KS. 2011. NTPase and 5'-RNA triphosphatase activities of Chikungunya virus nsP2 protein. *PLoS One* 6: e22336

Karpf AR, Blake JM, Brown DT. 1997a. Characterization of the infection of Aedes albopictus cell clones by Sindbis virus. *Virus Res* 50: 1-13

Karpf AR, Lenches E, Strauss EG, Strauss JH, Brown DT. 1997b. Superinfection exclusion of alphaviruses in three mosquito cell lines persistently infected with Sindbis virus. *J Virol* 71: 7119-23

Katsafanas GC, Moss B. 2007. Colocalization of transcription and translation within cytoplasmic poxvirus factories coordinates viral expression and subjugates host functions. *Cell Host Microbe* 2: 221-8

Kedersha N, Anderson P. 2002. Stress granules: sites of mRNA triage that regulate mRNA stability and translatability. *Biochem Soc Trans* 30: 963-9

Kedersha N, Anderson P. 2007. Mammalian stress granules and processing bodies. *Methods Enzymol* 431: 61-81

Kedersha N, Chen S, Gilks N, Li W, Miller IJ, et al. 2002. Evidence that ternary complex (eIF2-GTP-tRNA(i)(Met))-deficient preinitiation complexes are core constituents of mammalian stress granules. *Mol Biol Cell* 13: 195-210

Kedersha N, Cho MR, Li W, Yacono PW, Chen S, et al. 2000. Dynamic shuttling of TIA-1 accompanies the recruitment of mRNA to mammalian stress granules. *J Cell Biol* 151: 1257-68

Kedersha N, Ivanov P, Anderson P. 2013. Stress granules and cell signaling: more than just a passing phase? *Trends Biochem Sci* 38: 494-506

Kedersha N, Panas MD, Achorn CA, Lyons S, Tisdale S, et al. 2016. G3BP-Caprin1-USP10 complexes mediate stress granule condensation and associate with 40S subunits. *J Cell Biol* 212: 845-60

Kedersha N, Stoecklin G, Ayodele M, Yacono P, Lykke-Andersen J, et al. 2005. Stress granules and processing bodies are dynamically linked sites of mRNP remodeling. *J Cell Biol* 169: 871-84

Kedersha NL, Gupta M, Li W, Miller I, Anderson P. 1999. RNA-binding proteins TIA-1 and TIAR link the phosphorylation of eIF-2 alpha to the assembly of mammalian stress granules. *J Cell Biol* 147: 1431-42

Keerthikumar S, Chisanga D, Ariyaratne D, Al Saffar H, Anand S, et al. 2016. ExoCarta: A Web-Based Compendium of Exosomal Cargo. *J Mol Biol* 428: 688-92

Kendall C, Khalid H, Muller M, Banda DH, Kohl A, et al. 2019. Structural and phenotypic analysis of Chikungunya virus RNA replication elements. *Nucleic Acids Res* 47: 9296-312

Khan AH, Morita K, Parquet MDC, Hasebe F, Mathenge EGM, Igarashi A. 2002. Complete nucleotide sequence of chikungunya virus and evidence for an internal polyadenylation site. *J Gen Virol* 83: 3075-84

Kielian M, Chanel-Vos C, Liao M. 2010. Alphavirus Entry and Membrane Fusion. *Viruses* 2: 796-825

Kim DY, Firth AE, Atasheva S, Frolova EI, Frolov I. 2011. Conservation of a packaging signal and the viral genome RNA packaging mechanism in alphavirus evolution. *J Virol* 85: 8022-36

Kim HR, Lee GO, Choi KH, Kim DK, Ryu JS, et al. 2016. SRSF5: a novel marker for small-cell lung cancer and pleural metastatic cancer. *Lung Cancer* 99: 57-65

Kim WJ, Back SH, Kim V, Ryu I, Jang SK. 2005. Sequestration of TRAF2 into stress granules interrupts tumor necrosis factor signaling under stress conditions. *Mol Cell Biol* 25: 2450-62

Kim WJ, Kim JH, Jang SK. 2007. Anti-inflammatory lipid mediator 15d-PGJ2 inhibits translation through inactivation of eIF4A. *EMBO J* 26: 5020-32

Kimball SR, Horetsky RL, Ron D, Jefferson LS, Harding HP. 2003. Mammalian stress granules represent sites of accumulation of stalled translation initiation complexes. *Am J Physiol Cell Physiol* 284: C273-84

Klimstra WB, Ryman KD, Johnston RE. 1998. Adaptation of Sindbis virus to BHK cells selects for use of heparan sulfate as an attachment receptor. *J Virol* 72: 7357-66

Knight RL, Schultz KL, Kent RJ, Venkatesan M, Griffin DE. 2009. Role of N-linked glycosylation for sindbis virus infection and replication in vertebrate and invertebrate systems. *J Virol* 83: 5640-7

Kohno K, Izumi H, Uchiumi T, Ashizuka M, Kuwano M. 2003. The pleiotropic functions of the Y-box-binding protein, YB-1. *Bioessays* 25: 691-8

Kossinova OA, Gopanenko AV, Tamkovich SN, Krasheninina OA, Tupikin AE, et al. 2017. Cytosolic YB-1 and NSUN2 are the only proteins recognizing specific motifs present in mRNAs enriched in exosomes. *Biochim Biophys Acta Proteins Proteom* 1865: 664-73

Krishna SS, Majumdar I, Grishin NV. 2003. Structural classification of zinc fingers: survey and summary. *Nucleic Acids Res* 31: 532-50

Kuhn RJ, Hong Z, Strauss JH. 1990. Mutagenesis of the 3' nontranslated region of Sindbis virus RNA. *J Virol* 64: 1465-76

Kulasegaran-Shylini R, Thiviyanathan V, Gorenstein DG, Frolov I. 2009. The 5'UTR-specific mutation in VEEV TC-83 genome has a strong effect on RNA replication and subgenomic RNA synthesis, but not on translation of the encoded proteins. *Virology* 387: 211-21

Kumar P, Sweeney TR, Skabkin MA, Skabkina OV, Hellen CU, Pestova TV. 2014. Inhibition of translation by IFIT family members is determined by their ability to interact selectively with the 5'-terminal regions of cap0-, cap1- and 5'ppp-mRNAs. *Nucleic Acids Res* 42: 3228-45

Kummerer BM, Grywna K, Glasker S, Wieseler J, Drosten C. 2012. Construction of an infectious Chikungunya virus cDNA clone and stable insertion of mCherry reporter genes at two different sites. *J Gen Virol* 93: 1991-95

Kuno G, Oliver A. 1989. Maintaining mosquito cell lines at high temperatures: effects on the replication of flaviviruses. *In Vitro Cell Dev Biol* 25: 193-6

Kwon S, Zhang Y, Matthias P. 2007. The deacetylase HDAC6 is a novel critical component of stress granules involved in the stress response. *Genes Dev* 21: 3381-94

Laakkonen P, Ahola T, Kaariainen L. 1996. The effects of palmitoylation on membrane association of Semliki forest virus RNA capping enzyme. *J Biol Chem* 271: 28567-71

Laakkonen P, Auvinen P, Kujala P, Kaariainen L. 1998. Alphavirus replicase protein NSP1 induces filopodia and rearrangement of actin filaments. *J Virol* 72: 10265-9

Laakkonen P, Hyvonen M, Peranen J, Kaariainen L. 1994. Expression of Semliki Forest virus nsP1-specific methyltransferase in insect cells and in Escherichia coli. *J Virol* 68: 7418-25

Lambert N, Strebel P, Orenstein W, Icenogle J, Poland GA. 2015. Rubella. *Lancet* 385: 2297-307

Lanciotti RS, Kosoy OL, Laven JJ, Panella AJ, Velez JO, et al. 2007. Chikungunya virus in US travelers returning from India, 2006. *Emerg Infect Dis* 13: 764-7

Lane WC, Dunn MD, Gardner CL, Lam LKM, Watson AM, et al. 2018. The Efficacy of the Interferon Alpha/Beta Response versus Arboviruses Is Temperature Dependent. *mBio* 9

Langereis MA, Feng Q, van Kuppeveld FJ. 2013. MDA5 localizes to stress granules, but this localization is not required for the induction of type I interferon. *J Virol* 87: 6314-25

Lastarza MW, Grakoui A, Rice CM. 1994a. Deletion and duplication mutations in the C-terminal nonconserved region of Sindbis virus nsP3: effects on phosphorylation and on virus replication in vertebrate and invertebrate cells. *Virology* 202: 224-32

LaStarza MW, Lemm JA, Rice CM. 1994b. Genetic analysis of the nsP3 region of Sindbis virus: evidence for roles in minus-strand and subgenomic RNA synthesis. *J Virol* 68: 5781-91

Lee CHR, Mohamed Hussain K, Chu JJH. 2019. Macropinocytosis dependent entry of Chikungunya virus into human muscle cells. *PLoS Negl Trop Dis* 13: e0007610

Lee RC, Hapuarachchi HC, Chen KC, Hussain KM, Chen H, et al. 2013. Mosquito cellular factors and functions in mediating the infectious entry of chikungunya virus. *PLoS Negl Trop Dis* 7: e2050

Lemant J, Boisson V, Winer A, Thibault L, Andre H, et al. 2008. Serious acute chikungunya virus infection requiring intensive care during the Reunion Island outbreak in 2005-2006. *Crit Care Med* 36: 2536-41

Lemay JF, Lemieux C, St-Andre O, Bachand F. 2010. Crossing the borders: poly(A)-binding proteins working on both sides of the fence. *RNA Biol* 7: 291-5

Leonard VH, Kohl A, Hart TJ, Elliott RM. 2006. Interaction of Bunyamwera Orthobunyavirus NSs protein with mediator protein MED8: a mechanism for inhibiting the interferon response. *J Virol* 80: 9667-75

Lescar J, Roussel A, Wien MW, Navaza J, Fuller SD, et al. 2001. The Fusion glycoprotein shell of Semliki Forest virus: an icosahedral assembly primed for fusogenic activation at endosomal pH. *Cell* 105: 137-48

Leung AKL, McPherson RL, Griffin DE. 2018. Macrodomain ADP-ribosylhydrolase and the pathogenesis of infectious diseases. *PLoS Pathog* 14: e1006864

Li G, Rice CM. 1993. The signal for translational readthrough of a UGA codon in Sindbis virus RNA involves a single cytidine residue immediately downstream of the termination codon. *J Virol* 67: 5062-7

Li W, Li Y, Kedersha N, Anderson P, Emara M, et al. 2002. Cell proteins TIA-1 and TIAR interact with the 3' stem-loop of the West Nile virus complementary minus-strand RNA and facilitate virus replication. *J Virol* 76: 11989-2000

Li YG, Siripanyaphinyo U, Tumkosit U, Noranate N, A An, et al. 2013. Chikungunya virus induces a more moderate cytopathic effect in mosquito cells than in mammalian cells. *Intervirology* 56: 6-12

LibreTexts. 2021. Pathogen Recognition.

Lindquist JA, Brandt S, Bernhardt A, Zhu C, Mertens PR. 2014. The role of cold shock domain proteins in inflammatory diseases. *J Mol Med (Berl)* 92: 207-16

Lindquist ME, Lifland AW, Utley TJ, Santangelo PJ, Crowe JE, Jr. 2010. Respiratory syncytial virus induces host RNA stress granules to facilitate viral replication. *J Virol* 84: 12274-84

Liu LN, Lee H, Hernandez R, Brown DT. 1996. Mutations in the endo domain of Sindbis virus glycoprotein E2 block phosphorylation, reorientation of the endo domain, and nucleocapsid binding. *Virology* 222: 236-46

Liu N, Brown DT. 1993. Phosphorylation and dephosphorylation events play critical roles in Sindbis virus maturation. *Virology* 196: 703-11

Liu SY, Sanchez DJ, Aliyari R, Lu S, Cheng G. 2012. Systematic identification of type I and type II interferon-induced antiviral factors. *Proc Natl Acad Sci U S A* 109: 4239-44

Lopez S, Yao JS, Kuhn RJ, Strauss EG, Strauss JH. 1994. Nucleocapsid-glycoprotein interactions required for assembly of alphaviruses. *J Virol* 68: 1316-23

Low WK, Dang Y, Schneider-Poetsch T, Shi Z, Choi NS, et al. 2005. Inhibition of eukaryotic translation initiation by the marine natural product pateamine A. *Mol Cell* 20: 709-22

Lu L, Han AP, Chen JJ. 2001a. Translation initiation control by heme-regulated eukaryotic initiation factor 2alpha kinase in erythroid cells under cytoplasmic stresses. *Mol Cell Biol* 21: 7971-80

Lu YE, Eng CH, Shome SG, Kielian M. 2001b. In vivo generation and characterization of a soluble form of the Semliki forest virus fusion protein. *J Virol* 75: 8329-39

Lu YE, Kielian M. 2000. Semliki forest virus budding: assay, mechanisms, and cholesterol requirement. *J Virol* 74: 7708-19

Lulla A, Lulla V, Merits A. 2012. Macromolecular assembly-driven processing of the 2/3 cleavage site in the alphavirus replicase polyprotein. *J Virol* 86: 553-65

Lulla A, Lulla V, Tints K, Ahola T, Merits A. 2006. Molecular determinants of substrate specificity for Semliki Forest virus nonstructural protease. *J Virol* 80: 5413-22

Lulla V, Karo-Astover L, Rausalu K, Merits A, Lulla A. 2013a. Presentation overrides specificity: probing the plasticity of alphaviral proteolytic activity through mutational analysis. *J Virol* 87: 10207-20

Lulla V, Kim DY, Frolova EI, Frolov I. 2013b. The amino-terminal domain of alphavirus capsid protein is dispensable for viral particle assembly but regulates RNA encapsidation through cooperative functions of its subdomains. *J Virol* 87: 12003-19

Lulla V, Sawicki DL, Sawicki SG, Lulla A, Merits A, Ahola T. 2008. Molecular defects caused by temperature-sensitive mutations in Semliki Forest virus nsP1. *J Virol* 82: 9236-44

Lumsden WH. 1955. An epidemic of virus disease in Southern Province, Tanganyika Territory, in 1952-53. II. General description and epidemiology. *Trans R Soc Trop Med Hyg* 49: 33-57

Lusa S, Garoff H, Liljestrom P. 1991. Fate of the 6K membrane protein of Semliki Forest virus during virus assembly. *Virology* 185: 843-6

Luscher B, Butepage M, Eckei L, Krieg S, Verheugd P, Shilton BH. 2018. ADP-Ribosylation, a Multifaceted Posttranslational Modification Involved in the Control of Cell Physiology in Health and Disease. *Chem Rev* 118: 1092-136

Malet H, Coutard B, Jamal S, Dutartre H, Papageorgiou N, et al. 2009. The crystal structures of Chikungunya and Venezuelan equine encephalitis virus nsP3 macro domains define a conserved adenosine binding pocket. *J Virol* 83: 6534-45

Malone RW, Homan J, Callahan MV, Glasspool-Malone J, Damodaran L, et al. 2016. Zika Virus: Medical Countermeasure Development Challenges. *PLoS Negl Trop Dis* 10: e0004530

Mancini EJ, Clarke M, Gowen BE, Rutten T, Fuller SD. 2000. Cryo-electron microscopy reveals the functional organization of an enveloped virus, Semliki Forest virus. *Mol Cell* 5: 255-66

Marissen WE, Lloyd RE. 1998. Eukaryotic translation initiation factor 4G is targeted for proteolytic cleavage by caspase 3 during inhibition of translation in apoptotic cells. *Mol Cell Biol* 18: 7565-74

Martin JL, McMillan FM. 2002. SAM (dependent) I AM: the S-adenosylmethionine-dependent methyltransferase fold. *Curr Opin Struct Biol* 12: 783-93

Martinez MG, Snapp EL, Perumal GS, Macaluso FP, Kielian M. 2014. Imaging the alphavirus exit pathway. *J Virol* 88: 6922-33

Matsuki H, Takahashi M, Higuchi M, Makokha GN, Oie M, Fujii M. 2013. Both G3BP1 and G3BP2 contribute to stress granule formation. *Genes Cells* 18: 135-46

Mazroui R, Sukarieh R, Bordeleau ME, Kaufman RJ, Northcote P, et al. 2006. Inhibition of ribosome recruitment induces stress granule formation independently of eukaryotic initiation factor 2alpha phosphorylation. *Mol Biol Cell* 17: 4212-9

Mbaika S, Lutomiah J, Chepkorir E, Mulwa F, Khayeka-Wandabwa C, et al. 2016. Vector competence of Aedes aegypti in transmitting Chikungunya virus: effects and implications of extrinsic incubation temperature on dissemination and infection rates. *Virol J* 13: 114

McClain DJ, Pittman PR, Ramsburg HH, Nelson GO, Rossi CA, et al. 1998. Immunologic interference from sequential administration of live attenuated alphavirus vaccines. *J Infect Dis* 177: 634-41

McCormick C, Khaperskyy DA. 2017. Translation inhibition and stress granules in the antiviral immune response. *Nat Rev Immunol* 17: 647-60

McEwen E, Kedersha N, Song B, Scheuner D, Gilks N, et al. 2005. Heme-regulated inhibitor kinase-mediated phosphorylation of eukaryotic translation initiation factor 2 inhibits translation, induces stress granule formation, and mediates survival upon arsenite exposure. *J Biol Chem* 280: 16925-33

McInerney GM, Kedersha NL, Kaufman RJ, Anderson P, Liljestrom P. 2005. Importance of eIF2alpha phosphorylation and stress granule assembly in alphavirus translation regulation. *Mol Biol Cell* 16: 3753-63

McInerney GM, Smit JM, Liljestrom P, Wilschut J. 2004. Semliki Forest virus produced in the absence of the 6K protein has an altered spike structure as revealed by decreased membrane fusion capacity. *Virology* 325: 200-6

McPherson RL, Abraham R, Sreekumar E, Ong SE, Cheng SJ, et al. 2017. ADP-ribosylhydrolase activity of Chikungunya virus macrodomain is critical for virus replication and virulence. *Proc Natl Acad Sci U S A* 114: 1666-71

Mehrabi M, Hosseinkhani S, Ghobadi S. 2008. Stabilization of firefly luciferase against thermal stress by osmolytes. *Int J Biol Macromol* 43: 187-91

Melancon P, Garoff H. 1987. Processing of the Semliki Forest virus structural polyprotein: role of the capsid protease. *J Virol* 61: 1301-9

Mercer J, Helenius A. 2009. Virus entry by macropinocytosis. *Nat Cell Biol* 11: 510-20

Mi S, Durbin R, Huang HV, Rice CM, Stollar V. 1989. Association of the Sindbis virus RNA methyltransferase activity with the nonstructural protein nsP1. *Virology* 170: 385-91

Mi S, Stollar V. 1991. Expression of Sindbis virus nsP1 and methyltransferase activity in Escherichia coli. *Virology* 184: 423-7

Mitchell SA, Brown EC, Coldwell MJ, Jackson RJ, Willis AE. 2001. Protein factor requirements of the Apaf-1 internal ribosome entry segment: roles of polypyrimidine tract binding protein and upstream of N-ras. *Mol Cell Biol* 21: 3364-74

Moller-Tank S, Kondratowicz AS, Davey RA, Rennert PD, Maury W. 2013. Role of the phosphatidylserine receptor TIM-1 in enveloped-virus entry. *J Virol* 87: 8327-41

Montero H, Rojas M, Arias CF, Lopez S. 2008. Rotavirus infection induces the phosphorylation of eIF2alpha but prevents the formation of stress granules. *J Virol* 82: 1496-504

Morazzani EM, Wiley MR, Murreddu MG, Adelman ZN, Myles KM. 2012. Production of virus-derived ping-pong-dependent piRNA-like small RNAs in the mosquito soma. *PLoS Pathog* 8: e1002470

Mordecai EA, Cohen JM, Evans MV, Gudapati P, Johnson LR, et al. 2017. Detecting the impact of temperature on transmission of Zika, dengue, and chikungunya using mechanistic models. *PLoS Negl Trop Dis* 11: e0005568
Mourya DT, Mishra AC. 2006. Chikungunya fever. *Lancet* 368: 186-7
Mukhopadhyay S, Zhang W, Gabler S, Chipman PR, Strauss EG, et al. 2006. Mapping the structure and function of the E1 and E2 glycoproteins in alphaviruses. *Structure* 14: 63-73
Mulvey M, Brown DT. 1995. Involvement of the molecular chaperone BiP in maturation of Sindbis virus envelope glycoproteins. *J Virol* 69: 1621-7
Nallagatla SR, Hwang J, Toroney R, Zheng X, Cameron CE, Bevilacqua PC. 2007. 5'-triphosphate-dependent activation of PKR by RNAs with short stem-loops. *Science* 318: 1455-8
Nallagatla SR, Toroney R, Bevilacqua PC. 2011. Regulation of innate immunity through RNA structure and the protein kinase PKR. *Curr Opin Struct Biol* 21: 119-27
Neuvonen M, Kazlauskas A, Martikainen M, Hinkkanen A, Ahola T, Saksela K. 2011. SH3 domain-mediated recruitment of host cell amphiphysins by alphavirus nsP3 promotes viral RNA replication. *PLoS Pathog* 7: e1002383
Nickens DG, Hardy RW. 2008. Structural and functional analyses of stem-loop 1 of the Sindbis virus genome. *Virology* 370: 158-72
Ohn T, Kedersha N, Hickman T, Tisdale S, Anderson P. 2008. A functional RNAi screen links O-GlcNAc modification of ribosomal proteins to stress granule and processing body assembly. *Nat Cell Biol* 10: 1224-31
Onomoto K, Jogi M, Yoo JS, Narita R, Morimoto S, et al. 2012. Critical role of an antiviral stress granule containing RIG-I and PKR in viral detection and innate immunity. *PLoS One* 7: e43031
Ou JH, Strauss EG, Strauss JH. 1981. Comparative studies of the 3'-terminal sequences of several alpha virus RNAs. *Virology* 109: 281-9
Owen KE, Kuhn RJ. 1996. Identification of a region in the Sindbis virus nucleocapsid protein that is involved in specificity of RNA encapsidation. *J Virol* 70: 2757-63
Panas MD, Ahola T, McInerney GM. 2014. The C-terminal repeat domains of nsP3 from the Old World alphaviruses bind directly to G3BP. *J Virol* 88: 5888-93
Panas MD, Schulte T, Thaa B, Sandalova T, Kedersha N, et al. 2015. Viral and cellular proteins containing FGDF motifs bind G3BP to block stress granule formation. *PLoS Pathog* 11: e1004659
Panas MD, Varjak M, Lulla A, Eng KE, Merits A, et al. 2012. Sequestration of G3BP coupled with efficient translation inhibits stress granules in Semliki Forest virus infection. *Mol Biol Cell* 23: 4701-12
Panning M, Grywna K, van Esbroeck M, Emmerich P, Drosten C. 2008. Chikungunya fever in travelers returning to Europe from the Indian Ocean region, 2006. *Emerg Infect Dis* 14: 416-22
Paranjape SM, Harris E. 2007. Y box-binding protein-1 binds to the dengue virus 3'-untranslated region and mediates antiviral effects. *J Biol Chem* 282: 30497-508

Paredes AM, Brown DT, Rothnagel R, Chiu W, Schoepp RJ, et al. 1993. Three-dimensional structure of a membrane-containing virus. *Proc Natl Acad Sci U S A* 90: 9095-9

Paucker K, Boxaca M. 1967. Cellular resistance to induction of interferon. *Bacteriol Rev* 31: 145-56

Paul D, Bartenschlager R. 2013. Architecture and biogenesis of plus-strand RNA virus replication factories. *World J Virol* 2: 32-48

Pehrson JR, Fuji RN. 1998. Evolutionary conservation of histone macroH2A subtypes and domains. *Nucleic Acids Res* 26: 2837-42

Peranen J, Rikkonen M, Liljestrom P, Kaariainen L. 1990. Nuclear localization of Semliki Forest virus-specific nonstructural protein nsP2. *J Virol* 64: 1888-96

Pestka S. 1971. Inhibitors of ribosome functions. *Annu Rev Microbiol* 25: 487-562

Pfeffer M, Kinney RM, Kaaden OR. 1998. The alphavirus 3'-nontranslated region: size heterogeneity and arrangement of repeated sequence elements. *Virology* 240: 100-8

Picard-Jean F, Brand C, Tremblay-Letourneau M, Allaire A, Beaudoin MC, et al. 2018. 2'-O-methylation of the mRNA cap protects RNAs from decapping and degradation by DXO. *PLoS One* 13: e0193804

Pohjala L, Barai V, Azhayev A, Lapinjoki S, Ahola T. 2008. A luciferase-based screening method for inhibitors of alphavirus replication applied to nucleoside analogues. *Antiviral Res* 78: 215-22

Pohjala L, Utt A, Varjak M, Lulla A, Merits A, et al. 2011. Inhibitors of alphavirus entry and replication identified with a stable Chikungunya replicon cell line and virus-based assays. *PLoS One* 6: e28923

Porta J, Jose J, Roehrig JT, Blair CD, Kuhn RJ, Rossmann MG. 2014. Locking and blocking the viral landscape of an alphavirus with neutralizing antibodies. *J Virol* 88: 9616-23

Powers AM, Brault AC, Shirako Y, Strauss EG, Kang W, et al. 2001. Evolutionary relationships and systematics of the alphaviruses. *J Virol* 75: 10118-31

Powers AM, Brault AC, Tesh RB, Weaver SC. 2000. Re-emergence of Chikungunya and O'nyong-nyong viruses: evidence for distinct geographical lineages and distant evolutionary relationships. *J Gen Virol* 81: 471-9

Powers AM, Logue CH. 2007. Changing patterns of chikungunya virus: re-emergence of a zoonotic arbovirus. *J Gen Virol* 88: 2363-77

Prado Acosta M, Geoghegan EM, Lepenies B, Ruzal S, Kielian M, Martinez MG. 2019. Surface (S) Layer Proteins of Lactobacillus acidophilus Block Virus Infection via DC-SIGN Interaction. *Front Microbiol* 10: 810

Prow NA, Tang B, Gardner J, Le TT, Taylor A, et al. 2017. Lower temperatures reduce type I interferon activity and promote alphaviral arthritis. *PLoS Pathog* 13: e1006788

Putics A, Filipowicz W, Hall J, Gorbalenya AE, Ziebuhr J. 2005. ADP-ribose-1"-monophosphatase: a conserved coronavirus enzyme that is dispensable for viral replication in tissue culture. *J Virol* 79: 12721-31

Qin Q, Hastings C, Miller CL. 2009. Mammalian orthoreovirus particles induce and are recruited into stress granules at early times postinfection. *J Virol* 83: 11090-101

Rabouw HH, Langereis MA, Anand AA, Visser LJ, de Groot RJ, et al. 2019. Small molecule ISRIB suppresses the integrated stress response within a defined window of activation. *Proc Natl Acad Sci U S A* 116: 2097-102

Rack JG, Perina D, Ahel I. 2016. Macrodomains: Structure, Function, Evolution, and Catalytic Activities. *Annu Rev Biochem* 85: 431-54

Ramsey J, Chavez M, Mukhopadhyay S. 2019. Domains of the TF protein important in regulating its own palmitoylation. *Virology* 531: 31-39

Randall RE, Goodbourn S. 2008. Interferons and viruses: an interplay between induction, signalling, antiviral responses and virus countermeasures. *J Gen Virol* 89: 1-47

Rathore AP, Haystead T, Das PK, Merits A, Ng ML, Vasudevan SG. 2014. Chikungunya virus nsP3 & nsP4 interacts with HSP-90 to promote virus replication: HSP-90 inhibitors reduce CHIKV infection and inflammation in vivo. *Antiviral Res* 103: 7-16

Rathore AP, Ng ML, Vasudevan SG. 2013. Differential unfolded protein response during Chikungunya and Sindbis virus infection: CHIKV nsP4 suppresses eIF2alpha phosphorylation. *Virol J* 10: 36

Ray S, Catnaigh PO, Anderson EC. 2015. Post-transcriptional regulation of gene expression by Unr. *Biochem Soc Trans* 43: 323-7

Reikine S, Nguyen JB, Modis Y. 2014. Pattern Recognition and Signaling Mechanisms of RIG-I and MDA5. *Front Immunol* 5: 342

Reineke LC, Kedersha N, Langereis MA, van Kuppeveld FJ, Lloyd RE. 2015. Stress granules regulate double-stranded RNA-dependent protein kinase activation through a complex containing G3BP1 and Caprin1. *mBio* 6: e02486

Reineke LC, Lloyd RE. 2015. The stress granule protein G3BP1 recruits protein kinase R to promote multiple innate immune antiviral responses. *J Virol* 89: 2575-89

Renault P, Josseran L, Pierre V. 2008. Chikungunya-related fatality rates, Mauritius, India, and Reunion Island. *Emerg Infect Dis* 14: 1327

Renault P, Solet JL, Sissoko D, Balleydier E, Larrieu S, et al. 2007. A major epidemic of chikungunya virus infection on Reunion Island, France, 2005-2006. *Am J Trop Med Hyg* 77: 727-31

Reyes-Sandoval A. 2019. 51 years in of Chikungunya clinical vaccine development: A historical perspective. *Hum Vaccin Immunother* 15: 2351-58

Rezza G, Nicoletti L, Angelini R, Romi R, Finarelli AC, et al. 2007. Infection with chikungunya virus in Italy: an outbreak in a temperate region. *Lancet* 370: 1840-6

Roberts GC, Stonehouse NJ, Harris M. 2019. The Chikungunya virus nsP3 macro domain inhibits activation of the NF-κB pathway. *bioRxiv*

Roberts GC, Zothner C, Remenyi R, Merits A, Stonehouse NJ, Harris M. 2017. Evaluation of a range of mammalian and mosquito cell lines for use in Chikungunya virus research. *Sci Rep* 7: 14641

Robin S, Ramful D, Zettor J, Benhamou L, Jaffar-Bandjee MC, et al. 2010. Severe bullous skin lesions associated with Chikungunya virus infection in small infants. *Eur J Pediatr* 169: 67-72

Robinson MC. 1955. An epidemic of virus disease in Southern Province, Tanganyika Territory, in 1952-53. I. Clinical features. *Trans R Soc Trop Med Hyg* 49: 28-32

Rojas M, Arias CF, Lopez S. 2010. Protein kinase R is responsible for the phosphorylation of eIF2alpha in rotavirus infection. *J Virol* 84: 10457-66

Ross RW. 1956. The Newala epidemic. III. The virus: isolation, pathogenic properties and relationship to the epidemic. *J Hyg (Lond)* 54: 177-91

Rozanov MN, Koonin EV, Gorbalenya AE. 1992. Conservation of the putative methyltransferase domain: a hallmark of the 'Sindbis-like' supergroup of positive-strand RNA viruses. *J Gen Virol* 73 (Pt 8): 2129-34

Rupp JC, Jundt N, Hardy RW. 2011. Requirement for the amino-terminal domain of sindbis virus nsP4 during virus infection. *J Virol* 85: 3449-60

Rupp JC, Sokoloski KJ, Gebhart NN, Hardy RW. 2015. Alphavirus RNA synthesis and non-structural protein functions. *J Gen Virol* 96: 2483-500

Russo AT, White MA, Watowich SJ. 2006. The crystal structure of the Venezuelan equine encephalitis alphavirus nsP2 protease. *Structure* 14: 1449-58

Rwaguma EB, Lutwama JJ, Sempala SD, Kiwanuka N, Kamugisha J, et al. 1997. Emergence of epidemic O'nyong-nyong fever in southwestern Uganda, after an absence of 35 years. *Emerg Infect Dis* 3: 77

Ryman KD, Gardner CL, Burke CW, Meier KC, Thompson JM, Klimstra WB. 2007. Heparan sulfate binding can contribute to the neurovirulence of neuroadapted and nonneuroadapted Sindbis viruses. *J Virol* 81: 3563-73

Ryman KD, White LJ, Johnston RE, Klimstra WB. 2002. Effects of PKR/RNase L-dependent and alternative antiviral pathways on alphavirus replication and pathogenesis. *Viral Immunol* 15: 53-76

Salonen A, Ahola T, Kaariainen L. 2005. Viral RNA replication in association with cellular membranes. *Curr Top Microbiol Immunol* 285: 139-73

Sanchez-Aparicio MT, Ayllon J, Leo-Macias A, Wolff T, Garcia-Sastre A. 2017. Subcellular Localizations of RIG-I, TRIM25, and MAVS Complexes. *J Virol* 91

Saraste J, Kaaiainen L, Soderlund H, Keranen S. 1977. RNA synthesis directed by a temperature-sensitive mutant of Semliki Forest virus. *J Gen Virol* 37: 399-406

Sawicka K, Bushell M, Spriggs KA, Willis AE. 2008. Polypyrimidine-tract-binding protein: a multifunctional RNA-binding protein. *Biochem Soc Trans* 36: 641-7

Sawicki DL, Perri S, Polo JM, Sawicki SG. 2006. Role for nsP2 proteins in the cessation of alphavirus minus-strand synthesis by host cells. *J Virol* 80: 360-71

Sawicki DL, Sawicki SG. 1985. Functional analysis of the A complementation group mutants of Sindbis HR virus. *Virology* 144: 20-34

Sawicki DL, Sawicki SG. 1993. A second nonstructural protein functions in the regulation of alphavirus negative-strand RNA synthesis. *J Virol* 67: 3605-10

Sawicki SG, Sawicki DL, Kaariainen L, Keranen S. 1981. A Sindbis virus mutant temperature-sensitive in the regulation of minus-strand RNA synthesis. *Virology* 115: 161-72

Schilte C, Staikowsky F, Couderc T, Madec Y, Carpentier F, et al. 2013. Chikungunya virus-associated long-term arthralgia: a 36-month prospective longitudinal study. *PLoS Negl Trop Dis* 7: e2137

Schnierle BS. 2019. Cellular Attachment and Entry Factors for Chikungunya Virus. *Viruses* 11

Scholte FE, Tas A, Albulescu IC, Zusinaite E, Merits A, et al. 2015. Stress granule components G3BP1 and G3BP2 play a proviral role early in Chikungunya virus replication. *J Virol* 89: 4457-69

Scholte FE, Tas A, Martina BE, Cordioli P, Narayanan K, et al. 2013. Characterization of synthetic Chikungunya viruses based on the consensus sequence of recent E1-226V isolates. *PLoS One* 8: e71047

Schuffenecker I, Iteman I, Michault A, Murri S, Frangeul L, et al. 2006. Genome microevolution of chikungunya viruses causing the Indian Ocean outbreak. *PLoS Med* 3: e263

Schulte T, Liu L, Panas MD, Thaa B, Dickson N, et al. 2016. Combined structural, biochemical and cellular evidence demonstrates that both FGDF motifs in alphavirus nsP3 are required for efficient replication. *Open Biol* 6

Schwartz O, Albert ML. 2010. Biology and pathogenesis of chikungunya virus. *Nat Rev Microbiol* 8: 491-500

Sergon K, Njuguna C, Kalani R, Ofula V, Onyango C, et al. 2008. Seroprevalence of Chikungunya virus (CHIKV) infection on Lamu Island, Kenya, October 2004. *Am J Trop Med Hyg* 78: 333-7

Shin G, Yost SA, Miller MT, Elrod EJ, Grakoui A, Marcotrigiano J. 2012. Structural and functional insights into alphavirus polyprotein processing and pathogenesis. *Proc Natl Acad Sci U S A* 109: 16534-9

Shirako Y, Strauss JH. 1994. Regulation of Sindbis virus RNA replication: uncleaved P123 and nsP4 function in minus-strand RNA synthesis, whereas cleaved products from P123 are required for efficient plus-strand RNA synthesis. *J Virol* 68: 1874-85

Shirako Y, Strauss JH. 1998. Requirement for an aromatic amino acid or histidine at the N terminus of Sindbis virus RNA polymerase. *J Virol* 72: 2310-5

Sidrauski C, Acosta-Alvear D, Khoutorsky A, Vedantham P, Hearn BR, et al. 2013. Pharmacological brake-release of mRNA translation enhances cognitive memory. *Elife* 2: e00498

Sidrauski C, McGeachy AM, Ingolia NT, Walter P. 2015. The small molecule ISRIB reverses the effects of eIF2alpha phosphorylation on translation and stress granule assembly. *Elife* 4

Silva LA, Dermody TS. 2017. Chikungunya virus: epidemiology, replication, disease mechanisms, and prospective intervention strategies. *J Clin Invest* 127: 737-49

Simmons DT, Strauss JH. 1972a. Replication of Sindbis virus. I. Relative size and genetic content of 26 s and 49 s RNA. *J Mol Biol* 71: 599-613

Simmons DT, Strauss JH. 1972b. Replication of Sindbis virus. II. Multiple forms of double-stranded RNA isolated from infected cells. *J Mol Biol* 71: 615-31

Simpson-Holley M, Kedersha N, Dower K, Rubins KH, Anderson P, et al. 2011. Formation of antiviral cytoplasmic granules during orthopoxvirus infection. *J Virol* 85: 1581-93

Sissoko D, Malvy D, Ezzedine K, Renault P, Moscetti F, et al. 2009. Post-epidemic Chikungunya disease on Reunion Island: course of rheumatic manifestations and associated factors over a 15-month period. *PLoS Negl Trop Dis* 3: e389

Smith AE, Helenius A. 2004. How viruses enter animal cells. *Science* 304: 237-42

Smith JA, Schmechel SC, Raghavan A, Abelson M, Reilly C, et al. 2006. Reovirus induces and benefits from an integrated cellular stress response. *J Virol* 80: 2019-33

Solignat M, Gay B, Higgs S, Briant L, Devaux C. 2009. Replication cycle of chikungunya: a re-emerging arbovirus. *Virology* 393: 183-97

Somasekharan SP, El-Naggar A, Leprivier G, Cheng H, Hajee S, et al. 2015. YB-1 regulates stress granule formation and tumor progression by translationally activating G3BP1. *J Cell Biol* 208: 913-29

Sourisseau M, Schilte C, Casartelli N, Trouillet C, Guivel-Benhassine F, et al. 2007. Characterization of reemerging chikungunya virus. *PLoS Pathog* 3: e89

Spuul P, Balistreri G, Kaariainen L, Ahola T. 2010. Phosphatidylinositol 3-kinase-, actin-, and microtubule-dependent transport of Semliki Forest Virus replication complexes from the plasma membrane to modified lysosomes. *J Virol* 84: 7543-57

Spuul P, Salonen A, Merits A, Jokitalo E, Kaariainen L, Ahola T. 2007. Role of the amphipathic peptide of Semliki forest virus replicase protein nsP1 in membrane association and virus replication. *J Virol* 81: 872-83

Srivastava SP, Kumar KU, Kaufman RJ. 1998. Phosphorylation of eukaryotic translation initiation factor 2 mediates apoptosis in response to activation of the double-stranded RNA-dependent protein kinase. *J Biol Chem* 273: 2416-23

Staikowsky F, Talarmin F, Grivard P, Souab A, Schuffenecker I, et al. 2009. Prospective study of Chikungunya virus acute infection in the Island of La Reunion during the 2005-2006 outbreak. *PLoS One* 4: e7603

Steel JJ, Franz AW, Sanchez-Vargas I, Olson KE, Geiss BJ. 2013. Subgenomic reporter RNA system for detection of alphavirus infection in mosquitoes. *PLoS One* 8: e84930

Strauss JH, Strauss EG. 1994. The alphaviruses: gene expression, replication, and evolution. *Microbiol Rev* 58: 491-562

Sumpter R, Jr., Loo YM, Foy E, Li K, Yoneyama M, et al. 2005. Regulating intracellular antiviral defense and permissiveness to hepatitis C virus RNA replication through a cellular RNA helicase, RIG-I. *J Virol* 79: 2689-99

Sun S, Xiang Y, Akahata W, Holdaway H, Pal P, et al. 2013. Structural analyses at pseudo atomic resolution of Chikungunya virus and antibodies show mechanisms of neutralization. *Elife* 2: e00435

Suomalainen M, Liljestrom P, Garoff H. 1992. Spike protein-nucleocapsid interactions drive the budding of alphaviruses. *J Virol* 66: 4737-47

Suopanki J, Sawicki DL, Sawicki SG, Kaariainen L. 1998. Regulation of alphavirus 26S mRNA transcription by replicase component nsP2. *J Gen Virol* 79 (Pt 2): 309-19

Suzuki Y, Minami M, Suzuki M, Abe K, Zenno S, et al. 2009. The Hsp90 inhibitor geldanamycin abrogates colocalization of eIF4E and eIF4E-transporter into stress granules and association of eIF4E with eIF4G. *J Biol Chem* 284: 35597-604

Teijaro JR. 2016. Type I interferons in viral control and immune regulation. *Curr Opin Virol* 16: 31-40

Thomas S, Rai J, John L, Schaefer S, Putzer BM, Herchenroder O. 2013. Chikungunya virus capsid protein contains nuclear import and export signals. *Virol J* 10: 269

Tomar S, Hardy RW, Smith JL, Kuhn RJ. 2006. Catalytic core of alphavirus nonstructural protein nsP4 possesses terminal adenylyltransferase activity. *J Virol* 80: 9962-9

Toribio R, Diaz-Lopez I, Boskovic J, Ventoso I. 2016. An RNA trapping mechanism in Alphavirus mRNA promotes ribosome stalling and translation initiation. *Nucleic Acids Res* 44: 4368-80

Torii S, Orba Y, Sasaki M, Tabata K, Wada Y, et al. 2020. Host ESCRT factors are recruited during chikungunya virus infection and are required for the intracellular viral replication cycle. *J Biol Chem* 295: 7941-57

Torres M, Akhtar S, McKenzie EA, Dickson AJ. 2021. Temperature Down-Shift Modifies Expression of UPR-/ERAD-Related Genes and Enhances Production of a Chimeric Fusion Protein in CHO Cells. *Biotechnol J* 16: e2000081

Tourriere H, Chebli K, Zekri L, Courselaud B, Blanchard JM, et al. 2003. The RasGAP-associated endoribonuclease G3BP assembles stress granules. *J Cell Biol* 160: 823-31

Triqueneaux G, Velten M, Franzon P, Dautry F, Jacquemin-Sablon H. 1999. RNA binding specificity of Unr, a protein with five cold shock domains. *Nucleic Acids Res* 27: 1926-34

Trobaugh DW, Gardner CL, Sun C, Haddow AD, Wang E, et al. 2014. RNA viruses can hijack vertebrate microRNAs to suppress innate immunity. *Nature* 506: 245-8

Truant AL, Hallum JV. 1977. A persistent infection of baby hamster kidney-21 cells with mumps virus and the role of temperature-sensitive variants. *J Med Virol* 1: 49-67

Tsetsarkin K, Higgs S, McGee CE, De Lamballerie X, Charrel RN, Vanlandingham DL. 2006. Infectious clones of Chikungunya virus (La Reunion isolate) for vector competence studies. *Vector Borne Zoonotic Dis* 6: 325-37

Tuittila M, Hinkkanen AE. 2003. Amino acid mutations in the replicase protein nsP3 of Semliki Forest virus cumulatively affect neurovirulence. *J Gen Virol* 84: 1525-33

Tuittila MT, Santagati MG, Roytta M, Maatta JA, Hinkkanen AE. 2000. Replicase complex genes of Semliki Forest virus confer lethal neurovirulence. *J Virol* 74: 4579-89

Utt A, Das PK, Varjak M, Lulla V, Lulla A, Merits A. 2015. Mutations conferring a noncytotoxic phenotype on chikungunya virus replicons compromise enzymatic properties of nonstructural protein 2. *J Virol* 89: 3145-62

Utt A, Quirin T, Saul S, Hellstrom K, Ahola T, Merits A. 2016. Versatile Trans-Replication Systems for Chikungunya Virus Allow Functional Analysis and Tagging of Every Replicase Protein. *PLoS One* 11: e0151616

Vanlandingham DL, Hong C, Klingler K, Tsetsarkin K, McElroy KL, et al. 2005. Differential infectivities of o'nyong-nyong and chikungunya virus isolates in Anopheles gambiae and Aedes aegypti mosquitoes. *Am J Trop Med Hyg* 72: 616-21

Vasiljeva L, Merits A, Golubtsov A, Sizemskaja V, Kaariainen L, Ahola T. 2003. Regulation of the sequential processing of Semliki Forest virus replicase polyprotein. *J Biol Chem* 278: 41636-45

Vazeille M, Moutailler S, Coudrier D, Rousseaux C, Khun H, et al. 2007. Two Chikungunya isolates from the outbreak of La Reunion (Indian Ocean) exhibit different patterns of infection in the mosquito, Aedes albopictus. *PLoS One* 2: e1168

Ventoso I, Sanz MA, Molina S, Berlanga JJ, Carrasco L, Esteban M. 2006. Translational resistance of late alphavirus mRNA to eIF2alpha phosphorylation: a strategy to overcome the antiviral effect of protein kinase PKR. *Genes Dev* 20: 87-100

Vihinen H, Ahola T, Tuittila M, Merits A, Kaariainen L. 2001. Elimination of phosphorylation sites of Semliki Forest virus replicase protein nsP3. *J Biol Chem* 276: 5745-52

ViralZone. 2017. alphavirus virion. In *Swiss Institute of Bioinformatics*

Volk SM, Chen R, Tsetsarkin KA, Adams AP, Garcia TI, et al. 2010. Genome-scale phylogenetic analyses of chikungunya virus reveal independent emergences of recent epidemics and various evolutionary rates. *J Virol* 84: 6497-504

Wahlberg JM, Boere WA, Garoff H. 1989. The heterodimeric association between the membrane proteins of Semliki Forest virus changes its sensitivity to low pH during virus maturation. *J Virol* 63: 4991-7

Wang YF, Sawicki SG, Sawicki DL. 1991. Sindbis virus nsP1 functions in negative-strand RNA synthesis. *J Virol* 65: 985-8

Wang YF, Sawicki SG, Sawicki DL. 1994. Alphavirus nsP3 functions to form replication complexes transcribing negative-strand RNA. *J Virol* 68: 6466-75

Weaver SC. 2006. Evolutionary influences in arboviral disease. *Curr Top Microbiol Immunol* 299: 285-314

Weaver SC. 2014. Arrival of chikungunya virus in the new world: prospects for spread and impact on public health. *PLoS Negl Trop Dis* 8: e2921

Weaver SC, Winegar R, Manger ID, Forrester NL. 2012. Alphaviruses: population genetics and determinants of emergence. *Antiviral Res* 94: 242-57

Weber C, Berberich E, von Rhein C, Henss L, Hildt E, Schnierle BS. 2017. Identification of Functional Determinants in the Chikungunya Virus E2 Protein. *PLoS Negl Trop Dis* 11: e0005318

Weber C, Konig R, Niedrig M, Emmerich P, Schnierle BS. 2014. A neutralization assay for chikungunya virus infections in a multiplex format. *J Virol Methods* 201: 7-12

Weber F, Dunn EF, Bridgen A, Elliott RM. 2001. The Bunyamwera virus nonstructural protein NSs inhibits viral RNA synthesis in a minireplicon system. *Virology* 281: 67-74

Weger-Lucarelli J, Aliota MT, Kamlangdee A, Osorio JE. 2015a. Identifying the Role of E2 Domains on Alphavirus Neutralization and Protective Immune Responses. *PLoS Negl Trop Dis* 9: e0004163

Weger-Lucarelli J, Aliota MT, Wlodarchak N, Kamlangdee A, Swanson R, Osorio JE. 2015b. Dissecting the Role of E2 Protein Domains in Alphavirus Pathogenicity. *J Virol* 90: 2418-33

Wek RC. 1994. eIF-2 kinases: regulators of general and gene-specific translation initiation. *Trends Biochem Sci* 19: 491-6

Wek SA, Zhu S, Wek RC. 1995. The histidyl-tRNA synthetase-related sequence in the eIF-2 alpha protein kinase GCN2 interacts with tRNA and is required for activation in response to starvation for different amino acids. *Mol Cell Biol* 15: 4497-506

Welch WJ, Sefton BM. 1979. Two small virus-specific polypeptides are produced during infection with Sindbis virus. *J Virol* 29: 1186-95

Weston JH, Welsh MD, McLoughlin MF, Todd D. 1999. Salmon pancreas disease virus, an alphavirus infecting farmed Atlantic salmon, Salmo salar L. *Virology* 256: 188-95

Wheeler JR, Jain S, Khong A, Parker R. 2017. Isolation of yeast and mammalian stress granule cores. *Methods* 126: 12-17

Wheeler JR, Matheny T, Jain S, Abrisch R, Parker R. 2016. Distinct stages in stress granule assembly and disassembly. *Elife* 5

White CL, Thomson M, Dimmock NJ. 1998. Deletion analysis of a defective interfering Semliki Forest virus RNA genome defines a region in the nsP2 sequence that is required for efficient packaging of the genome into virus particles. *J Virol* 72: 4320-6

White JP, Cardenas AM, Marissen WE, Lloyd RE. 2007. Inhibition of cytoplasmic mRNA stress granule formation by a viral proteinase. *Cell Host Microbe* 2: 295-305

White JP, Lloyd RE. 2011. Poliovirus unlinks TIA1 aggregation and mRNA stress granule formation. *J Virol* 85: 12442-54

White JP, Lloyd RE. 2012. Regulation of stress granules in virus systems. *Trends Microbiol* 20: 175-83

WHO. 2006. Outbreak news. Chikungunya and dengue, south-west Indian Ocean. *Wkly Epidemiol Rec* 81: 106-8

Wielgosz MM, Huang HV. 1997. A novel viral RNA species in Sindbis virus-infected cells. *J Virol* 71: 9108-17

Williams MC, Woodall JP. 1961. O'nyong-nyong fever: an epidemic virus disease in East Africa. II. Isolation and some properties of the virus. *Trans R Soc Trop Med Hyg* 55: 135-41

Wimalasiri-Yapa B, Stassen L, Hu W, Yakob L, McGraw EA, et al. 2019. Chikungunya Virus Transmission at Low Temperature by Aedes albopictus Mosquitoes. *Pathogens* 8

Wintachai P, Wikan N, Kuadkitkan A, Jaimipuk T, Ubol S, et al. 2012. Identification of prohibitin as a Chikungunya virus receptor protein. *J Med Virol* 84: 1757-70

Wolffe AP. 1994. Structural and functional properties of the evolutionarily ancient Y-box family of nucleic acid binding proteins. *Bioessays* 16: 245-51

Wolffe AP, Tafuri S, Ranjan M, Familari M. 1992. The Y-box factors: a family of nucleic acid binding proteins conserved from Escherichia coli to man. *New Biol* 4: 290-8

Wu SR, Haag L, Sjoberg M, Garoff H, Hammar L. 2008. The dynamic envelope of a fusion class II virus. E3 domain of glycoprotein E2 precursor in Semliki Forest virus provides a unique contact with the fusion protein E1. *J Biol Chem* 283: 26452-60

Yap ML, Klose T, Urakami A, Hasan SS, Akahata W, Rossmann MG. 2017. Structural studies of Chikungunya virus maturation. *Proc Natl Acad Sci U S A* 114: 13703-07

Yazdani R, Kaushik VV. 2007. Chikungunya Fever. *Rheumatology (Oxford)* 46: 1214-5; author reply 15

Yoneyama M, Kikuchi M, Matsumoto K, Imaizumi T, Miyagishi M, et al. 2005. Shared and unique functions of the DExD/H-box helicases RIG-I, MDA5, and LGP2 in antiviral innate immunity. *J Immunol* 175: 2851-8

Yoo JS, Takahasi K, Ng CS, Ouda R, Onomoto K, et al. 2014. DHX36 enhances RIG-I signaling by facilitating PKR-mediated antiviral stress granule formation. *PLoS Pathog* 10: e1004012

Youn JY, Dunham WH, Hong SJ, Knight JDR, Bashkurov M, et al. 2018. High-Density Proximity Mapping Reveals the Subcellular Organization of mRNA-Associated Granules and Bodies. *Mol Cell* 69: 517-32 e11

Zeller H, Van Bortel W, Sudre B. 2016. Chikungunya: Its History in Africa and Asia and Its Spread to New Regions in 2013-2014. *J Infect Dis* 214: S436-S40

Zhang R, Earnest JT, Kim AS, Winkler ES, Desai P, et al. 2019. Expression of the Mxra8 Receptor Promotes Alphavirus Infection and Pathogenesis in Mice and Drosophila. *Cell Rep* 28: 2647-58 e5

Zhang R, Kim AS, Fox JM, Nair S, Basore K, et al. 2018a. Mxra8 is a receptor for multiple arthritogenic alphaviruses. *Nature* 557: 570-74

Zhang W, Mukhopadhyay S, Pletnev SV, Baker TS, Kuhn RJ, Rossmann MG. 2002. Placement of the structural proteins in Sindbis virus. *J Virol* 76: 11645-58

Zhang Y, Burkhardt DH, Rouskin S, Li GW, Weissman JS, Gross CA. 2018b. A Stress Response that Monitors and Regulates mRNA Structure Is Central to Cold Shock Adaptation. *Mol Cell* 70: 274-86 e7

Zhu GF, Liu ZH, Wang J. 1984. Improved technic for dengue virus micro cell culture. *Chin Med J (Engl)* 97: 73-4

Appendix

Replicons and Virus	
Mutants	Backbone
WT	CHIKV-D-Luc-SGR, CHIKV-nsP3-mCherry-FLuc-SGR, CHIKV-FLuc-SGR, ICRES, ONNV-2SG-ZsGreen
T218A	CHIKV-D-Luc-SGR
M219A	CHIKV-D-Luc-SGR
W220A	CHIKV-D-Luc-SGR, ICRES, pcDNA 3.1 (+), ICRES, ONNV-2SG-ZsGreen
P221A	CHIKV-D-Luc-SGR
C246A	CHIKV-D-Luc-SGR
D249A	CHIKV-D-Luc-SGR, ICRES, pcDNA 3.1 (+), ICRES, ONNV-2SG-ZsGreen
A251Q	CHIKV-D-Luc-SGR
Y324A	CHIKV-D-Luc-SGR, ICRES, pcDNA 3.1 (+), ICRES, ONNV-2SG-ZsGreen
GAA	CHIKV-D-Luc-SGR
Constructs	
Plasmids for lentiviruses	pCAG-HIVgp, pCMV-VSV-G-RSV-rev, pLKO.1-TRC-shCTL, pLKO.1-TRC-shYB1, pLKO.1-TRC-shUNR, pLKO.1-TRC-shSRSF5

Appendix Table 9.1 List of constructs generated and used in this study.

Mutants		Q5 site-directed mutagenesis for CHIKV SGR
T218Q	Forward	ATACATCAAATGTGGCCAAAGCAAACAGAG
	Reverse	CTCCGCCATATCCACAGCCGTCT
M219Q	Forward	ATACATACTCAATGGCCAAAGCAAACAGAG
	Reverse	CTCCGCCATATCCACAGCCGTCT
W220A	Forward	ATACATACTATGGCCCCAAAGCAAACAGAG
	Reverse	CTCCGCCATATCCACAGCCGTCT
P221A	Forward	ATACATACTATGTGGGCCAAGCAAACAGAG
	Reverse	CTCCGCCATATCCACAGCCGTCT
C246A	Forward	CAGAAAGCCCCGGTGGATGATGCAGAC
	Reverse	CCTGATCGATTCAATACTTTCCCCCAG
D249A	Forward	CCGGTGGCCGATGCAGACGCATCATC
	Reverse	GCATTTCTGCCTGATCGATTCAATAC
A251Q	Forward	CCGGTGGATGATCAAGACGCATCATC
	Reverse	GCATTTCTGCCTGATCGATTCAATAC
Y324A	Forward	CGCGTAAGTCCAAGGGAAGCTAGATCT
	Reverse	AGATCTAGCTTCCCTTGGACTTACGCG
Mutants		**PCR for ONNV AUD**
W220A	Forward	TATACCATGGCACCTAAACAAACTGAAGCCAACG
	Reverse	TATCTCTGCCATATCTACAGCAG
R243A/K245A	Forward	GAGTCCGTCGCACAAGCATGTCCCGTAGACGACGC
	Reverse	TATGCTCTCCCCCAGAGCATATAG
D249A	Forward	CCCGTAGCCGACGCCGACGCCTCATTC
	Reverse	ACATTTTTGCCTGACGGACTCTATGCTC

Y324A	Forward	CCGAGAACGGCCAGGCCTGCGGACGAAATC
	Reverse	GCTCACTCGAGACGGTACATTG
siRNA		**PCR**
YB1	Forward	CCGGCCAGTTCAAGGCAGTAAATATCTCGAGATATTTA CTGCCTT GAACTGGTTTTTG, 5' Phosphate
	Reverse	AATTCAAAAACCAGTTCAAGGCAGTAAATATCTCGAGAT ATTTAC TGCCTTGAACTGG, 5' Phosphate
UNR	Forward	CCGGGTTAACCTCTTACGGATTTATCTCGAGATAAATC CGTAAGA GGTTAACTTTTTG, 5' Phosphate
	Reverse	AATTCAAAAAGTTAACCTCTTACGGATTTATCTCGAGAT AAATCC GTAAGAGGTTAAC, 5' Phosphate
SRSF5	Forward	CCGGCGGATGCACACCGACCTAAATCTCGAGATTTAG GTCGGTGT GCATCCGTTTTTG, 5' Phosphate
	Reverse	AATTCAAAAACGGATGCACACCGACCTAAATCTCGAGA TTTAGGT CGGTGTGCATCCG, 5' Phosphate
mCherry fragment		**PCR**
mCherry	Forward	CGAGGAGGATAACATGGCC
	Reverse	GTTCCACGATGGTGTAGTCC
Sequencing for AUD reversion in CHIKV SGR	Forward	TGGATGAGCACATCTCCATAGAC
Sequencing for CHIKV whole genome		**PCR**
ICRES-CHIKV-1	Forward	CTGTGTACGTGGACATAGACGC
	Reverse	GTTCAGCCCCACCAACAG
ICRES-CHIKV-2	Forward	CCATTTGTGATCAAATGACCGGC
	Reverse	CCCACCAGTACCAGTCCTG
	Forward	GCTGGTGAGGGCAGAGAG

ICRES-CHIKV-3	Reverse	CCCGCTGTTTCGAGGATAGG
ICRES-CHIKV-4	Forward	CAATAATGGCGGGCATCTGC
	Reverse	GAGGGTTAGCGGCGTTG
ICRES-CHIKV-5	Forward	GCCTTCGTAGGACAGGTCAC
	Reverse	GTCAGTGACGTGATTGTACTCGC
ICRES-CHIKV-6	Forward	GTGTTCTTCGTTTCCCCTCCC
	Reverse	GCATGCTGCCACTGCG
ICRES-CHIKV-7	Forward	CGGCGCCTGTGTACTC
	Reverse	CGCCGATGAAGGCCG
ICRES-CHIKV-8	Forward	GCCAGCCGAGTGCTG
	Reverse	GCCGCTGTCCCCTGGTTTGCC
ICRES-CHIKV-9	Forward	CGCGCAGATACCCGTG
	Reverse	GAGCCACCGCAATTACACTTG
ICRES-CHIKV-10	Forward	CCCCAGACACCCCTGATC
	Reverse	CGCCGCCCCACATAAATG
ICRES-CHIKV-11	Forward	CGTCATCCCGTCTCCGTAC
	Reverse	CTTGTACGCGGAATTCGGC
ICRES-CHIKV-12	Forward	AGCCAGCAAGAAAGGCAAGTG
	Reverse	CATCTCCTACGTCCCTGTGG
Sequencing for ONNV all nsPs		**PCR**
ONNV-1	Forward	GCTGACAGCGCGTTTTTGAAG
	Reverse	CATTAGGAAGCCGTCGGC
ONNV-2	Forward	GGGCTGTGTTCAACAGACC
	Reverse	GCCTGCGGTGTCAGTACTAAG

ONNV-3	Forward	CAAGTGGCTCTTGAGCAAAGC
	Reverse	GGCTGTTACAGGCAGTGTACAC
ONNV-4	Forward	CTGGTAACCAGGCATGACTTGG
	Reverse	CTCCTGGTCTATTGTCCCAGTG
ONNV-5	Forward	GGAGTGGGAAGCTGAACACG
	Reverse	CTAGTGGCCTGTCCTGCATAC
ONNV-6	Forward	GATGCTAGGGGGGGACTC
	Reverse	GCTCACTCGAGACGGTACATTG
ONNV-7	Forward	GTCGTACGCGTTCACCCAG
	Reverse	GTCCGTCAGCTCTTCCACTTC
ONNV-8	Forward	GGAGCTAGCACACCGATCG
	Reverse	CCCTTATAGGGCTTGAGGCG
ONNV-9	Forward	CCAACTGTGGCATCCTACCAAG
	Reverse	GCGCCTTTACTGACACTACTGC
ONNV-10	Forward	CTGACCGCCATGATGTTGCTAG
	Reverse	GGTACTCGGTGAACACGCG

Appendix Table 9.2 List of oligonucleotide primers used in this study.

'Forward' and 'Reverse" indicate forward primer and reverse primer, respectively.